DOCTOR OF PHILOSOPHY

Gully dynamics evolution under environment change pressures

Olivier, George

Award date:
2024

Awarding institution:
Coventry University
Stellenbosch University

GULLY DYNAMICS EVOLUTION UNDER ENVIRONMENTAL CHANGE PRESSURES

By

George Olivier

PhD

July 2024

GULLY DYNAMICS EVOLUTION UNDER ENVIRONMENTAL CHANGE PRESSURES

By

George Olivier

A thesis submitted in partial fulfilment of the University's requirements for the Degree of Doctor of Philosophy

July 2024

Stellenbosch
UNIVERSITY
IYUNIVESITHI
UNIVERSITEIT

Gully dynamics evolution under environmental change pressures

by
George Olivier

Dissertation presented for the degree of Doctoral of Science in the Faculty of Science at Stellenbosch University

Supervisor: Dr Willem de Clercq
Supervisor: Dr Marco Van De Wiel
Co-supervisor: Dr Jana Fried
Administrative co-supervisor: Dr Eric Mashimbye

March 2024

DECLARATION

By submitting this research dissertation electronically, I declare that the entirety of the work contained therein is my own, original work, that I am the sole author thereof (save to the extent explicitly otherwise stated), that reproduction and publication thereof by Stellenbosch University will not infringe any third party rights and that I have not previously in its entirety or in part submitted it for obtaining any qualification. Although Dr E Mashimbye is listed as a co-supervisor in this study, his role was administrative in nature. As such, he was not involved in conceptualising or directing the research. He also did not read the dissertation.

The nature and scope of my contribution to each thesis chapter were as follows:

Chapter	Nature of contr bution	The extent of contribution (%)
Chapter 1	This chapter was written by me. Suggestions were made regarding content by my supervisors and co-supervisor.	George Olivier 100%
Chapter 2	This chapter was published in Earth Surface Processes and Landforms. See Section 1.6 for exact publication details. Data capture was completed by me whereafter co-authors (SU and CU supervisor), provided comments and suggestions regarding conceptualisation, figures, and data interpretation.	George Olivier 80% Marco Van De Wiel 10% Willem de Clercq 10%
Chapter 3	This chapter was published in Earth Surface Processes and Landforms. See Section 1.6 for exact publication details. Data capture and model setup and run were completed by me, whereafter co-authors (SU and CU supervisor), provided comments and suggestions regarding conceptualisation, figures, and data interpretation.	George Olivier 85% Marco Van De Wiel 10% Willem de Clercq 5%
Chapter 4	This chapter was currently in review at Catena. See Section 1.6 for more detail regarding the submission status. Conceptualisation, data capture, model setup, and run were completed by me. Co-authors provided comments and suggestions regarding figures and data interpretation. Data regarding benchmarks methods were shared by Carlos and Miguel.	George Olivier 80% Marco Van De Wiel 10% Carlos Castillo 5% Miguel Vallejo-Orti 5%
Chapter 5	This chapter is formatted for submission as a journal article. The article is co-authored by my academic supervisors and co-supervisor. Conceptualisation was determined by Marco, Jana, and me. Site selection, data gathering, and analysis were completed by me, with directive feedback from my supervisors and co-supervisor.	George Olivier 80% Marco Van De Wiel 10% Willem de Clercq 5% Jana Fried 5%
Chapter 6	The last chapter, summarising, and synthesising findings, was written by me, with feedback in the form of comments from my supervisors (SU and CU) and co-supervisor.	George Olivier 100%

Promotor – Stellenbosch University (SU): Dr WP de Clercq

Promotor – Coventry University (CU): Dr MJ Van De Wiel

Co- promotor – Coventry University (CU): Dr J Fried

SUMMARY

Gully erosion is a severe land degradation process, primarily impacting land resources on-site and water resources off-site. When active in a catchment, it can be the dominant driver of soil loss, causing significant environmental and socio-economic consequences. However, other soil erosion mechanisms remain at the forefront of research, which contributed to our inability to assess gully erosion on a catchment to regional scale. The current capability to model gully erosion on larger geographic extents remains limited due to the complexity of interactions of control factors and various sub-processes driving gully expansion. In this study, an approach to apply local case studies to inform on regional gully severity is introduced to address modelling shortcomings, and an initial scaled framework is provided, which could be implemented for future regional scale investigations and monitoring. South Africa has a long history of erosion problems and has been considered an area with high gully incidence. The "hotspot" perception, coupled with the diverse climatic and geo-environmental attributes exhibited in South Africa, motivated the use as the focal region for this study.

Local case study sites were used to extract physiographic properties and gully severity to produce a susceptibility map for South Africa. Additional local sites were selected across the E-W climate gradient of South Africa to assess gully severity and to isolate climate and land use controls of gully erosion to provide clues on how environmental change may influence future gully erosion. The findings from the susceptibility map, which used secondary data from the literature, converged with the findings from primary data derived from sites located across the climate gradient of South Africa. Gully erosion severity increases eastwards towards the Grassland biome, in which gullying is most severe. Here, gully erosion resulted in soil losses of up to 17 t ha^{-1} $y^{-1,}$ which exceeds the baseline limit (27 times more) and is almost twice the sustainable limit calculated for South Africa when the upper thresholds for both these limits are used. Perceptions from landowners/ -users/ and -managers mostly align with gully concerns from the field sites, showing that their appraisals are concurrent with local gully severity. Remediation efforts are ongoing at several sites; however, measures focus on gully headcuts and do not consider vegetation establishment. Vegetation is considered critical, especially for long-term success rates of mitigation, and could be a reason for the lack of successful mitigation. The poor success rate is also disconcerting, as climate change will likely exacerbate gully erosion in South Africa.

Although climate change is predicted to increase gully erosion due to larger storm magnitudes, the data presented here indicates that rainfall intensity is likely to play a secondary role in exacerbating gully erosion. Rainfall variability may be the principal driver of gully erosion. If climate change increases the frequency of El Niño Southern Oscillation events, gully erosion severity may increase and even reactivate previously stabilised gullies due to more intense rainfalls after periodic droughts. Continuous assessment and monitoring of gully extents are crucial to assessing where gullies are of concern and whether there is a change in severity. Manually digitising gullies or solely relying on fieldwork will not sufficiently address a need for monitoring via temporal data. Semi-automated detection strategies which are scaleable and transferrable would enable the extraction of gully dimensions unbiasedly and would allow to quantitively assess gully expansion (or contraction) by subtracting polygon- or raster-based output.

A semi-automated approach that uses gully morphology to extract gully dimensions is developed and tested with datasets from South Africa, Namibia, Spain, and Australia. Initial assessment shows positive results, accurately predicting > 75.4% of the gullied area when scaling between small gullies (planimetric area of 1619 m^2) to large gullies (planimetric area of 70246 m^2). Regarding transferability to benchmark areas where other land uses were practised and where different spatial resolution data were used as input, the variance between 1.4% and 14.8% was determined, with producer accuracies above 84.5% and 70.6%. The semi-automated method has some shortcomings, with the requirement for manually digitising gully headcuts being the most pertinent.

As a framework, regional assessments and monitoring should implement a scaled approach. The initial step should produce a susceptibility map using key variables associated with gullying. Following that, more computationally intensive detection strategies could be implemented, constrained to areas of most concern defined by susceptibility. Lastly, representative field sites can be identified from the detected gullies, where primary data can be retrieved to quantify gully processes, severity, and implications. Continued work is required to refine this framework, for example, refining semi-automated approaches to increase accuracy and increasing localised field sites in different geo-environments to improve trend analysis and better our understanding of how various controls interact to steer gully evolution. Lastly, this new information should yield data that can be used to build and calibrate models; such gully evolution modelling currently needs to

be improved and is pivotal to further our understanding of how gully networks will react to climate and land-use changes.

KEYWORDS

gully erosion, soil loss, susceptibility, automated detection, climate change, environmental change, El Niño, South Africa.

OPSOMMING

Donga erosie lei tot ernsitge grond verlies, en het veral ‘n impak op grond hulpbronne waar erosie plaasvind, asook water hulpbronne elders in die opvangsgebied. In opvangsgebiede waar donga erosie aktief is, kan dit lei tot ernstige omgewings- en sosio-ekonomiese gevolge. Ander vorms van grond erosie bly egter aan die voorpunt van navorsing, wat ‘n rol gespeel het in die huidige onvermoë om donga erosie op groter skaal te analsieer. Ons vermoë om donga erosie suksesvol te modelleer is ook tans beperk, meerendeels as gevolg van komplekse interaksie tussen faktore wat dit dryf, asook verskeie sub-prosesse wat aanleiding gee tot die evolusie daarvan. Plaaslike gevallestudies word gebruik op ‘n streekskaal, om aan die terkortkominge van modelering, inligting te verskaf oor verspreiding van donga ersosie. ’n Initiële raamwerk word ook aanbeveel vir toekomstiges analises en monitering van donga erosie op streekskaal. Suid-Afrika het 'n lang geskiedenis van probleme wat geassosieer word met erosie, en word beskou as ‘n area met n hoë voorkoms van dongas. Hierdie “hotspot”-persepsie, tesame met die diverse klimaat- en geo-omgewingskenmerke wat in Suid-Afrika voorkom, was die motivering om dit as die fokus area te gebruik vir hierdie studie.

Plaaslike gevallestudies was gebruik om die fisiografiese eienskappe en die graad van donga erosie te kombineer om ‘n donga vatbaarheidskaart vir Suid-Afrika te produseer. Bykomende plaaslike gevallestudies was ook gekies langs die Oos-Wes klimaatgradiënt van Suid-Afrika om die erns van donga erosie in Suid-Afrika te ondersoek. Die areas was strategies gekies om sodoende klimaat en landgebruik faktore wat dongas dryf te isoleer, om meer te leer van moontlike toekomstige veranderinge rakende klimaats- en landgebruiks-veranderinge. Bevindinge van die vatbaarheidskaart, wat sekondêre inligting gebruik, en die plaaslike gevallestudies, wat primêre inligting produseer het, stem ooreen met waar donga erosie die grootste probleem is. Die intensiteitsgraad van dongas neem ooswaarts toe in die rigting van die Grasveld bioom. Hier lei donga erosie tot 17 t ha^{-1} j^{-1}, wat die basisvlak oorskry (27 keer meer) en byna twee keer die volhoubare limiet is wat vir Suid-Afrika bereken is wanneer die boonste drempels vir beide hierdie limiete gebruik word. Persepsies van grondeienaars, -gebruikers, en -bestuurders, stem meestal ooreen met wat in die veld bepaal is, wat n aaanduiding is dat hul persepsies in lyn plaaslike erosie vlakke. Remediëringspogings is aan die gang op verskeie gevallestudie areas; strategie fokus egter op die initlële inkloof area waar die donga begin. Strategië fokus op fisiese grondwerk en neem nie plantegroei in ag nie. Plantegroei word as krities beskou, veral vir suksesvolle langtermyn

rehabilitasie en kan 'n rede wees vir die gebrek aan suksesvolle remediering. Die swak sukseskoers is ook problematies, veral omdat klimaatsverandering waarskynlik donga erosie in Suid-Afrika sal vererger.

Alhoewel klimaatsverandering voorspellings toon dat dongas erosie sal verhoog as gevolg van groter stormsterktes, dui die data wat hier aangebied word dat reënvalintensiteit waarskynlik 'n sekondêre rol sal speel in die verergering van donga erosie. Die wisslevalligheid van reënval sal waarskynlik die hoofdrywer van donga erosie wees. As klimaatsverandering die frekwensie van El Niño Suidelike Ossillasie-gebeurtenisse verhoog, kan die intensiteit van donga erosie toeneem en selfs stabiele dongas heraktiveer as gevolg van meer intense reënval na periodieke droogtes. Deurlopende assessering en monitering van dongas is krities om te bepaal waar donga erosie begin toeneem. Om dongas met per hand te teken vanaf fotos of uitsluitlik op veldwerk staat te maak, sal nie monitering van dongas op grootskaal kan aanspreek nie. Semi-outomatiese strategiee om dongas te identifiseer word benodig, verkieslik metodes wat op verskillende skale asook in kontrasterende omgewings toegepas kan word. Sulke metodes sal ons in staat stel om donga afmetings op n onvooroordeelde manier te doen, en sodoende donga uitbreiding (of inkrimping) kwantitief te evalueer.

Semi-outomatiese benadering word hier ontwikkel wat op die morfologie van dongas gebaseer is. Die metode is in Suid-Afrika ontwikkel, en getoets op dongas van verskeie skale en omgewings in Suid-Afrika, Namibië, Spanje en Australië. Aanvanklike assessering toon positiewe resultate, en voorspel dongas met groottes tussen klein- (planimetriese oppervlakte van 1619 m^2) en groot-skaal (planimetriese oppervlakte van 70246 m^2) met akkuraatheid wat 75.4% oorskry. Wanneer die metode getoets word op dongas met verskillende omgewingskarakteristieke, en vergelyk word met metodes wat spesifiek in daardie areas onwikkel was, is ‘n variansie tussen 1.4% en 14.8% bepaal. Die semi-outomatiese metode het 'n paar tekortkominge, met die mees beduidenste een die handmatige identifiesering van donga se inkerwingspunt waar die donga begin.

‘n Raamwerk om dongas op n streekskaal te evalueer en monitor word voorgestel. Die raamwerk se aanvanklike stap bestaan uit die produsering van n vatbaarheidskaart wat faktore wat dongas dryf te gebruik as insette. Daarna kan ‘n semi-automaties strategie geimplementeer word, wat tien teen een meer rekenaar intensiewe prosesse sal bevat, om dongas te karteer. Die semi-automatiese strategie kan beperk word tot hoë donga vatbaarheidsareas. Laastens kan verteenwoordigende

plaaslike gevallestudies identifiseer word vanaf die gekarteerde dongas, waar primêre data ingewin kan word rakende intensiteit, prosesse, en gevolge van donga erosie.

Verdere werk word vereis om die stappe binne hierdie raamwerk te verfyn, bv., die verfyning van semi-outomatiese benaderings om akkuraatheid te verhoog en om meer plaaslike gevalle studies te identifissser sodat n beter verspreiding van donga voorkoms in verkeie geo-omgewingsfaktore bepaal kan word. Hierdie verspreiding kan gebruik word om beter tendense vas te stel, asook hoe om die verskeie kombinasies van dryf faktore van dongas, die evolusie daarvan beinvloed. Laastens, kan die inligting wat ingewin word, gebruik word vir die ontwikkeling van modelle, asook die kalibrasie van moderlingsbevindinge. Met hierdie modelle kan ons begrip verbeter rakende hoe klimaat- en land gebruiks-veranderinge, donga evolusie kan beinvloed.

TREFWOORDE

Donga erosie, grondverlies, omvatbarheid, automatiese kartering, klimaatsverandering, land gebruiksverandering, El Niño, Suid Afrika.

ACKNOWLEDGEMENTS

I sincerely thank:

- My family, especially Nicolette, for her love, support, and understanding when I had to spend precious family time in front of a laptop, in the field in some remote parts, or 13300km away at Coventry University. It is time that I will not get back, but it made me realise how remarkable my young family is. I hope we will continue to make many special memories together, some of them as memorable as the "*boot storie*" that can be used as nighttime stories for John George and soon-to-arrive Nicolette Elizabeth.

- My supervisors, Marco Van de Wiel, Dr Willem de Clercq and Jana Fried, for providing guidance and insight, for their patience and belief in me, and for providing opportunities to travel, which provided good learning experiences and networking opportunities that can further my career.

- My colleagues, especially Alex Kisters at the Earth Sciences department for allowing me time away from the normal grind to pursue this Ph.D. project, their encouragement and interest throughout my journey.

- All the participants and gatekeepers, thank you for your willingness and time to partake in this research project and for allowing access to gully sites of interest for measurements and observations related to gully erosion.

- The CGA at Stellenbosch University for delivering upon all my data requests; sometime on short notice.

- Jay L Roux from the University of the Free State that also provided access to his data.

- Adriaan van Niekerk from Stellenbosch University who introduced the concept of Height Above Nearest Drainage

- Matthias Vanmaercke from KU Leuven for a helpful communication regarding gully erosion rates and RDN.

- Coventry University PRP panels throughout the PhD process, in particular Bastien Dieppois for his advice and willingness to help.

- Coventry University for the for the Collaborative Research Grant, and funding to allow me to travel to and spend time at Coventry University campus.

- The National Research Foundation of South Africa through the AUDA-NEPAD SANWATCE WARFSA Aligned Research Grants Programme for providing funds for 2 years of the PhD project.

- The British Society of Geomorphology for providing funding through a grant (BSG-2023-14) to proceed with additional fieldwork.

CONTENTS

TABLES

FIGURES

ACRONYMS AND ABBREVIATIONS

A^a	Average accuracy
A^p	Production accuracy
A^u	User accuracy
AD	Anno Domini
AHP	Analytical Hierarchy Process
CD: NGI	Chief Directorate of National Geospatial Information, Department of Rural Development and Land Reform
COVID-19	Corona Virus 2019
DEM	Digital Elevation Model
dGPS	Differential Global Positioning System
DJI	Da-Jiang Innovations
E_o	Over prediction error
E_u	Under prediction error
E_{tot}	Total prediction error
EC	Eastern Cape
EGU	European Geosciences Union
ENSO	El Niño Southern Oscillation
ESRI	Environmental Systems Research Institute, Inc.
EXTERRA	Extra Terra
FR	Frequency Ratio
FR^^	Normalised Frequency Ratio
FS	Free State
GDP	Gross Domestic Product
GEOBIA	Geographic Object-Based Image Analysis
gHAND	Gully Height Above Nearest Drainage model
GIS	Geographical information systems
GSI	Gully Susceptibility Index
HAND	Height Above Nearest Drainage
KZN	KwaZulu-Natal
MAR	Mean Annual Rainfall
MCDM	Multi-Criteria Decision Making
NC	Northern Cape
NGO	Non-governmental organisation

QGIS	Quantum Geographic Information System
RDN	Rainy Day Normal
RGB	Red Green Brown
RUSLE	Revised Universal Soil Loss Equation
SPI	Stream Power Index
SPOT-5	Satellite pour l'Observation de la Terre 5
SRTM	Shuttle Radar Topography Mission
TWI	Total Wetness Index
UAV	Unmanned Aerial Vehicle
US	United States
WC	Western Cape

CHAPTER 1: INTRODUCTION TO THIS THESIS

1.1 INTRODUCTION

Soil erosion is recognised as a primary cause of land degradation and is projected to increase in most climate zones in the world (Eekhout & de Vente, 2022). Hence, addressing soil erosion and the rehabilitation of eroded and degraded lands have found inclusion in numerous policy frameworks, for example, the Land Degradation Neutrality framework (Cowie et al., 2018), which is part of the United Nations Sustainable Development Goals 15 (United Nations, 2015) and the European Union Soil Strategy for 2030 (European Commission, Directorate-General for Environment, 2021a) that is part of the European Commission Biodiversity Strategy for 2030 (European Commission, Directorate-General for Environment, 2021b). The implementation of these policies is further justified by the impacts and costs of soil erosion which have been approximated to lead, for example, to a loss of 33.7 million tons of agricultural food production globally, an equivalent of eight billion US (United States) dollars lost to the global GDP (Sartori et al., 2019).

Although gully erosion, a form of channelised water erosion, typically occupies less than 5% of the landscape, it has been demonstrated to be the dominant form of soil loss in a catchment when active (Poesen, 2018). At the catchment level, up to 94% of soil losses have been attributed to gully erosion processes (Bennett et al., 2000; Poesen et al., 2003). Looking at one source of soil loss from gully erosion, a global review of the effects of gully headcut retreat recorded volumetric soil losses of up to 4.74E+4 m^3 y^{-1} (Vanmaercke et al., 2016). Other sources such as gully wall and floor would hence further add to the global soil loss volume that is occurring due to gully erosion but are not captured in Vanmaercke et al's (2016) estimate. Considering the percentage of soil losses attributable to gully erosion, it is a primary geomorphic process driving the degradation of land and water resources, therefore holding significant socio-economic and sustainability consequences (Kuhn et al., 2023) A better understanding of gully erosion causes, processes and impacts is therefore of great importance, and has been recognised as such in the academic literature.

Castillo & Gómez (2016) conducted a comprehensive review of gully erosion studies spanning almost a century. They found gully erosion studies transcending politically drawn country

boundaries, permeating into different land uses and climates (the polar climate is the only climatic region in which gully erosion studies were lacking). South Africa was considered a "hotspot" of gully erosion in this review. The "hotspot" classification, coupled with the climatic and geo-environmental diversity associated with the 1.22 million km^2 country, motivated the use of South Africa as a focal region for this study.

The consequences of gully erosion in South Africa are only communicated occasionally in published literature, but both on- and off-site impacts have been reported (Table 1.1). On-site impacts are primarily associated with land resources and are bound to a local scale, affecting the inter-gully area (Poesen et al., 2003). Reported on-site impacts in South Africa include a reduction in soil quality lowering crop yields (Talbot, 1947), reduced animal productivity (per. comms., F. Loock, 2022), in some cases, livestock deaths from falling into large gullies (pers. comms., community meeting, 2022), and an increase in costs (time and monetary) due to mitigation works (per. comms., F. Loock, 2022). Additionally, on-site impacts have been found to affect infrastructure, for example, damaging fence lines on farms (Keay-Bright & Boardman, 2006), and threatening, but also leading to the destruction of houses and roads in the former communal areas (Morokong & Blignaut, 2019; pers. comms., community meeting, 2022).

Gullies increase the hillslope-channel connectivity, resulting in off-site impacts which mostly affect water resources, thus operating at a catchment scale (Poesen et al., 2003). Reported off-site impacts in South Africa, include the siltation of channels (Talbot, 1947) and reducing reservoir capacity, therefore, the life span of dams (Le Roux, 2018), which can aggravate drought effects and access to water.

Table 1.1. On- and off-site impacts of gully erosion and gully control factors (South Africa and globally derived).

Gully erosion control and driving factors
Local
Rock type
Soil
- Structure
- Chemistry
- Biological
Rainfall
Groundwater
Temperature
Topography
- Slope
- Upslope drainage area

Rainfall
Groundwater
Snowmelt
Temperature
Vegetation cover
Anthropogenic activities
- Agricultural land-use (change) practices
- Agricultural intensification
- Deforestation
- Overgrazing
- Land abandonment
- Road construction
- Policy

Global

Climate change
- Rainfall
- Temperature

Gully erosion impacts

On-site

Removal of fertile topsoil
Loss in water holding capacity of soil
Decrease in agricultural production
Increase in agricultural cost
- Labour costs, for example, filling of gullies
- Transport cost, for example, due to dissected fields

Prevents erecting infrastructure or damages erected structures

Off-site

Siltation of reservoirs
Surface water pollution
Increase risk of flooding
Negative impact on aquatic ecosystem health
Changes in stream morphology

Although contemporary gully erosion is evident in South Africa (Grellier et al., 2014; Grenfell et al., 2014; Seutloali et al., 2014), it is not a recent phenomenon and has a long past. For example, the impacts associated with gullying ("evil of sluits") in the Karoo during the early 1900s were presented by Rowntree (2014) in the form of published articles by farmers and agricultural officers; Talbot (1947) found widespread gullying in the Swartland wheat belt after surveying aerial photographs from 1938; and severe gullying occurred in the establishment of the homelands in the 1960s (Hoffman & Ashwell, 2001). Despite the longstanding knowledge that gullies occur in South Africa, Liggit & Fincham (1988) concluded in the 1980s that there was a severe lack of research on this critical sediment resource. Although the increase of gully erosion studies since 1988 is evident, there remains an urgent need to investigate gully erosion

in South Africa, especially since field sites in the country tend to be confined to certain areas (Chapter 2).

1.2 GULLY EROSION

1.1.1. A gully or not

Since the publication of Poesen et al. (2003), which this study considers to be a landmark review paper on gully erosion, a significant increase in gully erosion research occurred (Castillo & Gómez, 2016). However, varying definitions (to some extent also terminology) of gullies in literature persist, leading to what Bennett & Wells (2019) termed disciplinary fragmentation, which inhibits the advancement of our understanding of gully erosion. As presented in Castillo & Gómez, 2016, different regional terminologies are used to refer to gullies:

- Gully is used most frequently in the literature at the global scale (for example, Castillo & Gómez, 2016, Bartley et al., 2020; Vanmaercke et al., 2021)
- Donga in certain African countries (for example, Lyons et al., 2013 in South Africa, Avakoudjo et al., 2021 in Burkina-Faso, and Prah, 1989 in Lesotho)
- Sluit or sloot occasionally used in South Africa (Rowntree, 2013; Chapter 2)
- Lavaka in Madagascar (for example, Wells et al., 1991)
- Cárcava in Spain and Mexico (for example, Franco-Ramos et al., 2022)
- Ravine in France (for example, Larue, 2005)
- Wadi in Arabic (for example, Abuzied & Pradhan, 2021)
- Voçoroca in Brazil (for example, Bouramtane et al., 2022)
- Barranco in Argentina (for example, Ries & Marzolff, 2003)

In addition to the numerous terms used to refer to gully erosion, several definitions are used. The definitions mainly identifies thresholds to differentiate between rills and (permanent) gullies, initially qualitatively: an erosive feature too large for a prairie dog to jump across, used by the United States Soil Conservation Service (Fullen & Catt, 2004, cited in Thwaites et al., 2021) and later more quantitatively, for example, a threshold of 929 cm^2 (one square foot), which represents a channel that cannot be easily obliterated by conventional tillage (Hauge, 1977). Minimum depth thresholds, to distinguish gullies from rills, have also been introduced, for example, 0.3 m (Handbook, 2008 in Thwaites et al., 2022), 0.5 m (Imeson & Kwaad, 1985;

Foster, 1986; Douglas-Mankin et al., 2020), or 0.6 m (Brice, 1966). Foster (1986) described another category of gully, called an "ephemeral" gully, which exhibits size threshold limits between rills and permanent gullies. These ephemeral gullies are typically found in agricultural fields in valley bottoms, within swales (Foster, 1986; Casalí et al., 2006; Capra, 2013), linear landscape elements such as ploughed contours and tillage tracks (Casalí et al., 2006; Douglas-Mankin et al., 2020), and can be easily obliterated by tillage (Capra, 2013). Yet confusingly, Poesen et al. (2003) defined an ephemeral gully as consisting of a minimum area of 929 cm^2. Douglas-Mankin et al. (2020) describe a more recent threshold, between 150 cm^2 and 10000 cm^2 to distinguish between a rill and an ephemeral gully.

Bennett & Wells (2019) argued that the disciplinary fragmentation within gully erosion research mainly originates from the defined thresholds primarily adjudged from an agricultural practice perspective, *viz*. conventional tillage. Yet, gully erosion is not only associated with agricultural fields, with many geomorphic studies investigating gully erosion in other land-uses or land-covers, for example, cities (Carvalho Junior et al., 2010; Imwangana et al., 2015), natural grassland (Grellier et al., 2012; Le Roux et al., 2022), rangelands (Boardman et al., 2003; Koci et al., 2020), and forests (Parkner et al., 2007; Katz et al., 2014). To establish a definition that could be used in different fields, thus without conventional tillage being the discriminatory factor for setting thresholds, Bennett & Wells (2019) distinguished between "*field*" and "l*andscape*" gullies. Field gullies are defined as "*gullies that are relatively small in size compared with the geomorphic setting in which they are found or the landscape unit of interest... and by definition, would include all gullies in association with agricultural landscapes*" (Bennett & Wells, 2019:48), whilst landscape gullies are defined as "*gullies that are relatively large in size, such that these erosional features would dominate the local geomorphic landscape in which they occur or the landscape scale of interest*" (Bennett & Wells, 2019:48). Thwaites et al. (2021) extended the work by Bennett & Wells (2019) to address the disciplinary fragmentation due to varied definitions and terminology, and dedicated an article towards providing a detailed framework to describe and classify gullies in a standardised manner, which includes a generic gully definition:

"*A gully is a persistent, incised erosion feature with walls and/or head scarp on average > 0.5 m deep (or that cannot generally be removed by conventional tillage methods for Field Gullies) and cannot be defined as a stream channel (first order or greater). The feature erodes residual*

soils, unconsolidated materials and saprolite, but not solid bedrock. Mass-movement dominates the erosion process within the void, and it has multiple modes of expansion. It always includes extension by headward retreat into an otherwise undissected land surface by way of a clearly-defined head scarp or head wall. It has erosional side walls of at least moderately steep gradient (~30°; ~60%), and gully walls are dominantly bare soil materials with a distinct break of slope from the uneroded land surface, that exhibit erosion by means of mass movement, with or without sapping by seepage. The feature overall is typically driven by ephemeral flows associated with direct rainfall into the gully and in the gully catchment. Alluvial gullies, however, are commonly affected by backwater – by floodwaters from the stream/river they adjoin. The active sediment source is predominantly from within the gully as a clear, bounded, internal erosional zone" (Thwaites et al., 2021:116).

Although the definition captures much more detail than previous attempts and mostly agrees with the ideas from Bennet & Wells (2019), some aspects remain arguable. Some studies implement a stream order to distinguish between streams and gullies, although this is more commonly used in gully detection techniques to semi-automatically map gullies, for example, Johansen et al. (2012) define gullies as being allocated a stream order ≤ 3. However, this depends on the spatial resolution of the Digital Elevation Model (DEM) due to its association with flow accumulation. In older gullies, headcut retreat may become negligible, mostly stabilising or kept in check by agricultural activities, with gully extension and sediment mainly derived at gully walls (Martínez-Casasnovas et al., 2003). More importantly, the definition neglects smaller gullies, those that fall into the "ephemeral" class. It is reasonable to assume that Bennett & Wells (2019) intended to include smaller gullies below the 0.5 m threshold of Thwaites et al. (2021), irrespective of whether they occur in an agricultural field or another land-use, under the "field" gully definition. Additionally, not all gullies have an abrupt headcut as some are more gradual in slope (Oostwoud Wijdenes et al., 1999), which has further implications for the definition. The gully will thus start to occur somewhere downstream, probably when it reaches 0.5 m in depth, but then is "headless" and, therefore, not a gully under the definition of Thwaites et al. (2021).

A more simplistic definition was derived to characterise a gully for use throughout this study, nevertheless, one that captures the most pertinent aspects as defined by Thwaites et al. (2021). Accordingly, a gully is defined as a clearly defined erosive channel scoured into sediments and

unconsolidated rocks by concentrated surface- or subsurface water flow (as also indicated by Schumm et al., 1984; Kirkby & Bracken, 2009) that is predominantly driven by ephemeral flow directly related to rainfall, and the primary source of expansion, and the dominant source of sediment is from mass wasting processes within or in proximity to the erosive channel.

1.1.2. Gully erosion processes

Gully erosion can result from different geomorphic processes such as surface slips or subsurface pipes but often arise from a knickpoint on the topography (Figure 1.1). Fluvial erosion is initially the primary driving force of gully development (Morgan, 1995). When confined water flow exceeds the critical shear strength of a soil, the gully floor is scoured as soil particles are entrained, resulting in the deepening of the gully (Bocco, 1991). However, once the main gully landform elements form, namely the gully headcut and walls (Figure 1.2 a, b), the principal sediment source originates from mass wasting events (Thwaites et al., 2021) (Figure 1.2b, c, d). The mass wasting events can occur at the gully headcut, linearly expanding the gully headward (Piest et al. 1975; Collison, 2001; Vandekerckhove et al. 2003) (Figure 1.2a), or sidewalls, causing lateral growth (Piest et al. 1975; Martínez-Casasnovas et al. 2003; Chaplot et al., 2011) (Figure 1.2 c, d, e, f). Numerous processes interact to lead to eventual mass wasting (falling, slumping, sliding, creep) *viz*. channel scour, jet flow and plunge pool erosion, back trickle, tension cracks, fluting, and subsurface flow (sapping, piping, tunneling) (see Figure 1.2 for examples of gully processes).

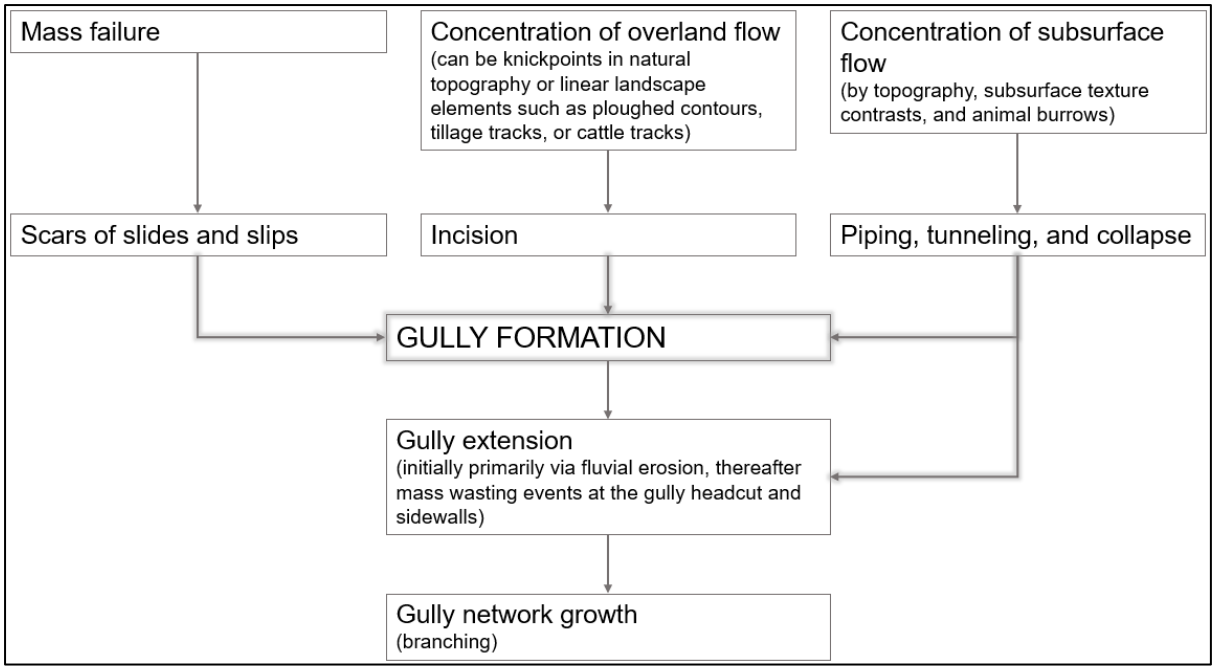

Figure 1.1 Schematic showing point of gully initiation and growth processes (modified from Bergsma et al., 2006).

Figure 1.2 Examples of active gully processes (all examples photos from South Africa): a) an active headcut showing recent collapse close to the Ofcolaco, Limpopo (24°10'1.85"S 30°34'30.78"E); b) gully

deepening from renewed scour of an existing gully floor resulting in the formation of a headcut close to Riebeek Kasteel, Western Cape (33°16'58.80"S 18°45'43.24"E); c) undercutting of a gully wall from inner gully flow close to Montagu, Western Cape (33°44'51.73"S 20°38'53.88"E); d) tension cracks forming at a gully headcut close to Nqanqarhu, Eastern Cape); e) gully wall with a pipe outlet (the collapsed pipe roof is also evident) close to Riebeek Kasteel, Western Cape; f) gully widening from overflow resulting in the formation of fluting close to Sinxago, Eastern Cape (28°38'1.68"E 28°38'1.68"E) (photographs by George Olivier).

Although confined water flow results in the deepening of the gully, it can cause gully sidewalls to become undercut, especially along the outer bend of a gully channel (like a cut bank of a meandering river) (Simon et al., 2000) (Figure 1.2c). When the overhang can no longer support itself, it collapses in a mass wasting event. Similar mass wasting events also occur at the gully headcut when it becomes undercut, although the undercutting mechanism is different (Figure 1.3). When concentrated runoff flows over the gully headcut, jet flow may occur, which scours the gully floor of the headcut to form a plunge pool (Guo et al., 2021). The vortex flow within the plunge pool continues to enlarge the plunge pool, undercutting the gully headcut (Guo et al., 2021). In addition, back trickle from water flowing over the gully headcut further accentuates the undercut (Ireland et al., 1939). As the undercut enlarges due to plunge pool development, the overhung soil mass will not be able to support itself and will collapse when a critical threshold is reached, *viz*., a mass wasting event.

Tension cracks can occur at both the gully headcuts and walls due to tensile strains on the soil due to being undercut (Oostwoud Wijdenes et al., 1999). Typically, tension cracks run parallel to the gully headcut or wall and can accelerate mass wasting events because these cracks increase through flow as concentrated runoff enters the cracks, promoting undercut enlargement and piping (Collison, 2001) (Figure 1.2d). Piping is a form of subsurface erosion controlled by soil properties (primarily by textural differences causing permeability contrasts and dispersivity), leading to gully enlargement when collapse of its roof occurs in proximity to the gully headcut or wall (Figure 1.2e). Groundwater sapping can, similarly to through flow, also lead to undercut expansion and the development of pipes, encouraging mass wasting and expediting gully erosion (Hagerty, 1991).

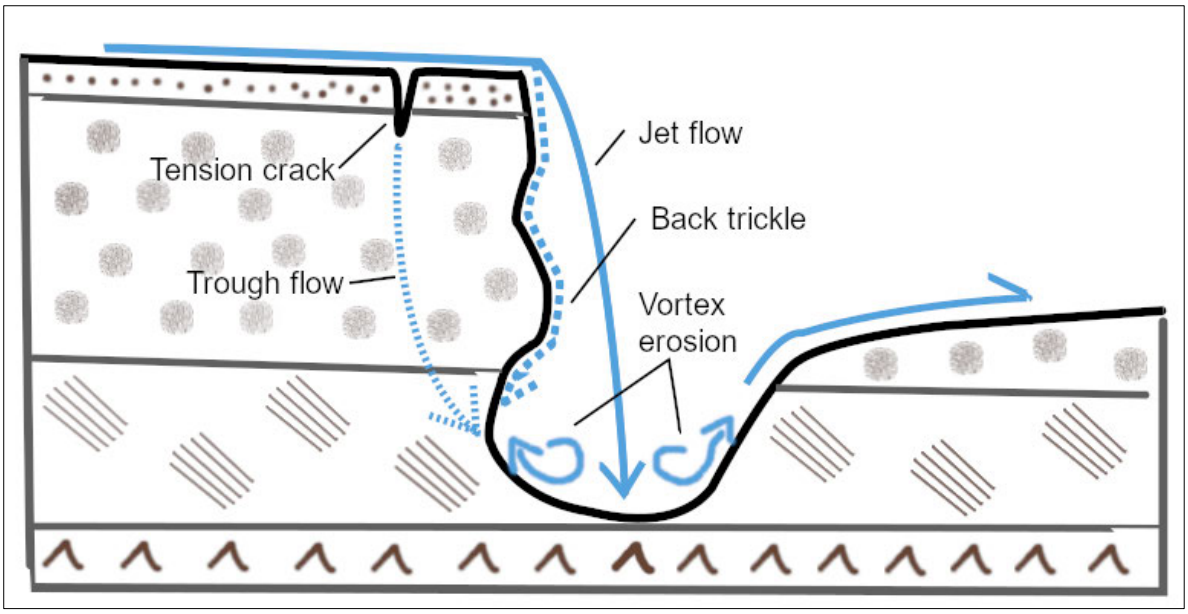

Figure 1.3 Diagram depicting the gully processes contributing to a headcut becoming undercut leading to an eventual mass wasting event (Graphic by George Olivier).

At gully headcuts and sidewalls where undercutting, tension cracks, and groundwater seepage are less prominent, runoff and splash erosion from rainfall often lead to fluting (Brooks et al., 2009) (Figure 2f). The flutes, elongated grooves that taper towards the top (Bergsma et al., 1996), form due to preferential erosion of less cohesive soils on the face of a gully headcut and sidewall (Vandekerckhove et al., 2000) (Figure 1.2f). Carving of the flutes leads to gully expansion (Brooks et al., 2009), but more rapid growth occurs from the destruction of flutes in mass wasting events when a critical threshold is reached (Vandekerckhove et al., 2000; Shit & Maiti, 2012).

1.1.3. Factors exerting control over gully erosion

A diverse number of factors (Table 1) control the magnitude and frequency of gully processes and, therefore, the rate of gully expansion. These controlling factors, either local or global, determine the erodibility and/ or affecting concentrated surface or sub-surface water flow triggering gully processes.

The physical, chemical, biological intrinsic properties determine the stability of soils and control how prone soils are to erosion (Laker, 2004). Physical properties of soil, viz., unconsolidated colluvium (Botha et al., 1994; Rienks et al., 2000) or alluvium (Brooks et al., 2007; Shellberg et al., 2016), structureless soil, and loosely packed loess have been associated

with gully erosion due to the low resistance to detachment of soil aggregates. Rock type of the parent material of a soil exerts a strong influence on intrinsic physical and chemical soil properties enhancing or detracting soil susceptibility to gully erosion (Laker, 2004). High gully occurrence is found in soil derived from mudrock and shale due to piping resulting from contrasting texture (Beckedahl, 1996; Le Roux & Sumner, 2012; Van Zijl et al., 2013). Prevalent gully erosion has been reported in soils with clay mineralogy that enhances dispersion such as those with high exchangeable sodium derived from marlstones (Ramezanpour et al., 2010) and mudrock (Laker, 2004; Le Roux & Sumner, 2012).

Climatic characteristics exert control over gully erosion on a local and global scale due to their impact on concentrated surface and sub-surface water flow (Anderson et al., 2021). On a local scale, gully erosion has been associated with rainfall intensity, antecedent soil moisture, groundwater, snowmelt, and freeze-thaw (Ionita, 2006; Xu et al., 2019; Anderson et al., 2021). High rainfall intensity events generate erosive concentrated water flows that exceed soil shear strength resulting in soil entrainment, and gullying (Vanmaercke et al., 2016 Anderson et al., 2021). However, prolonged periods of low-intensity rainfall have also been demonstrated to result in gullying (Poesen et al., 1996). Antecedent soil moisture is a critical factor that influences concentrated overland flow occurrence during lower intensity storms, and thus gullying (Castillo et al., 2003). Gully erosion is induced in more extreme climates, for example, through melting snow yielding concentrated run-off on saturated soils. Moreover, freeze-thaw action reduces soil cohesion and promotes piping as thawing topsoil results in subsurface water flow on impermeable frozen subsoil (Ionita, 2006; Xu et al., 2019). On a global scale, gully erosion has been demonstrated to increase up to 300% due to the expected increase in high rainfall intensity events from climate change (Vanmaercke et al., 2016), and possibly also as a result of more extreme temperature fluctuations leading to increased freeze-thaw cycles (Valentin et al., 2005).

Topography plays a role in controlling runoff volume and velocity, strongly influencing gully erosion (Svoray & Markovitch, 2009). Studies have shown that gully headcut position can be explained by the inverse relationship between slope and upslope drainage area of a gully headcut and can be used to identify critical areas vulnerable to gullying (Vandekerckhove et al., 2000; Torri & Poesen, 2014). Areas with steeper slopes or higher intensity rainfall events both require smaller upslope drainage areas to initiate and drive headward erosion. Critical

upslope drainage size for gully erosion is affected by vegetation coverage, the land-use practiced, and the shape of the drainage area of the headcut (Summerfield, 2014; Rossi et al., 2015).

Some research indicated that vegetation is an essential control factor affecting gully erosion, possibly due to its influence on both soil erodibility and concentrated surface and sub-surface water flow generation (Rey, 2003; Frankl et al., 2019). Vegetative growth increases roughness, decreases connectivity, and binds soil by its root architecture to reduce soil erodibility (de Baets et al., 2008). Removing vegetation eliminates these traits making soil more prone to erosion. Rehabilitation strategies using vegetation have successfully reduced or rehabilitated gully erosion (Bartley et al, 2020; Frankl et al., 2021), however this is more challenging in arid regions (Keay-Bright & Boardman, 2007).

Although gully erosion is a natural process, overwhelming evidence suggests that a diverse range of anthropogenic activities can accelerate gully erosion if it results in an increase in soil erodibility, concentrated water flow, or both (Castillo & Gómez, 2016). Reported anthropogenic activities that exacerbate gully erosion are typically associated with the removal of vegetation (mostly the indigenous natural vegetation) in land-use change to establish or expand farming (Ionita et al., 2015; Frankl et al., 2019), overgrazing (often associated with land abandonment) (Boardman et al., 2003), deforestation (Ionita et al., 2015), and fires (Brady, 1993). Impacts on soil properties from human activities from incorrect tillage (Rong et al., 2019) and soil compaction from along footpaths (human and livestock) (Vetter, 2007; Sidle et al., 2019; Nir et al., 2022) and farm roads have been found to induce gullying (Olivier et al., 2018). Incorrect construction or lack of maintenance of gully rehabilitation measures and road culverts have been shown to lead to gully erosion (Seutloali et al., 2016). Governmental and/ or agricultural policies have led to the successful rehabilitation of gullies upon implementation, but also to accelerate gully erosion (Meadows, 2003).

1.3 RESEARCH PROBLEM

Despite the impacts on- and off-site that are associated with gully erosion (Section 1.1), the focus of the scientific community remains centred on other soil erosion processes (Poesen, 2018; also evident from the presentations during the “Soil Erosion, Land Degradation, and Conservation” session at the 2023 European Geosciences Union (EGU) General Assembly).

Approximately 10% of soil erosion studies focuses on gully erosion (Castillo & Gómez, 2016). There has, however, been an increase in gully erosion studies since the IV International Symposium on Gully Erosion hosted in Leuven, Belgium (Castillo & Gómez, 2016). However, knowledge gaps persist (Vanmaercke et al., 2021; Wilkinson et al., 2023), and gully erosion monitoring remains essential to further improve our knowledge from a research perspective as well as a practical land-management and policy perspective (Vanmaercke et al., 2021; Wilkinson et al., 2023).

Monitoring studies on a regional scale would yield the most benefit as they will capture the spatial variability of gully erosion (for example, Mararakanye & Le Roux, 2012; Golosov et al., 2018). However, models and tools that can monitor and predict gully dynamics on large geographic extents remain limited (Poesen, 2018; Vanmaercke et al., 2021). Using local case studies may provide a useful technique to inform on regional gully variability and, moreover, be used to make probable predictions on how gully erosion will be impacted by environmental change.

Identifying local study sites which are representative, without any prior knowledge of gully vulnerability and incidence, may be an arduous task. Implementing a gully susceptibility index could aid in gully site identification. Gully susceptibility indices aggregate a predefined selection of conditioned input maps, which are considered critical gully control factors, and numerous methodologies to combine these inputs have been proposed (Dewitte et al., 2015; Arabameri et al., 2019; Phinzi et al., 2020). Although most susceptibility methods have been demonstrated on catchment scales, upscaling to regional scales is likely (for example, continental gully susceptibility index by De Geeter et al., 2023).

Even though the gully susceptibility index would help identify local gully sites, selection will be improved by adding gully incidence data. The traditional method consists of manually mapping gully erosion scars by interpreting aerial or satellite imagery (Mararakanye & Le Roux, 2012). However, time and labour constraints of this method limit applicability to large geographic extents (even more so for capturing temporal data at these scales). Automated methods would alleviate time and labour pressures and remove potential data bias from user interpretation. Numerous (semi-)automated methodologies using spectral and topographical data have been proposed in the literature (Vrieling et al., 2007; Evan & Lindsay, 2010; Walker et al., 2020) and could provide gully location data constrained to high gully sensitive areas

according to the susceptibility index. Despite numerous (semi-)automated workflows being developed and demonstrated in the literature, clear evidence of their scalability and transferability remains lacking. However, upscaling the workflows is probably due to the distinct morphology of the gully landform.

In conjunction with climate and land use data, selecting sites from the mapped gullies could yield good representative sites. The spatial variability of gullies, from the representative sites, can be coupled with high resolution temporal data of gully erosion to show how control factors impacted historical gully evolution, providing insight into potential future perturbations. At these scales climate becomes critical and long-term data could provide insight into how climate change may impact gully erosion. Additionally, if the spatial application of mitigation measures, for example, contour banks, check dams, leaky dams, gabions, etc., can be captured on a similar regional scale, the efficacy and lifespan mitigation measures can be (quantitatively) evaluated and provide critical information for policy makers and stakeholders.

The following research questions can thus be asked:

1. What is the current level of scientific understanding regarding gully erosion in South Africa, along with the spatial scope of the areas under study?
2. Is it possible to model gully erosion susceptibility on a regional scale, with limited datasets at such extents?
3. Would it be possible to develop a gully detection strategy that is built on limited data input and easily understandable metrics, but remains scalable and transferable to enable use by practitioners?
4. How will gully erosion react to environmental change?
5. What is the land-user and landowner perceptions of gully erosion, and how does it align with findings from remotely sensed data and fieldwork observations?

1.4 AIMS AND OBJECTIVES

The general aim of this study was to conduct a regional scale (in this case a national scale) gully analysis, with a focus on developing methods for such assessments, and using quantitative and qualitive methods to assess the impact of environmental change on gullying.

The following research objectives can be highlighted:

1. Use local study sites to inform on gully erosion over large geographic extents (Chapters 2, 3, 4, and 5).
2. Synthesize gully erosion works in South Africa to intersect views to allow a better understanding of the current state of science in South Africa and to identify broader and local knowledge gaps (Chapter 2).
3. Obtain regional datasets regarding gully control factors to develop and produce a gully susceptibility model for South Africa (Chapter 3).
4. Develop and implement a semi-automatic detection method for South Africa and test this at different geomorphic scales and geo-environments (Chapter 4).
5. Identify sites across the E-W climate gradient of South Africa to isolate land-use and climate as drivers of gully erosion, to assess gullying quantitatively and qualitatively, and to identify possible impacts from environmental change (Chapter 5).

Achieving the aims would yield a novel approach to inform on regional scale gully dynamics in the absence of reliable models on these scales. Sequentially addressing the objectives produces a scalable framework to locate areas that are vulnerable to gully erosion, whereafter gully features can be mapped in areas of concern, and lastly, identify representative gullies to investigate at high resolution (spatially and temporally) to provide quantitative data on expansion rates, which is related to qualitative data to probe how gully dynamics may be affected by future environmental change.

1.5 STUDY AREA DESCRIPTION

South Africa is located on the southern-most tip of Africa, occupying approximately 1.22 million km^2 between 22°S and 35°S and 15°E and 33°E. Although more than 70% of South Africa is covered in sedimentary rock, it has varied and ancient geological formations. In the northeast, the ancient Kaapvaal Craton was accreted from 3.60 Gm - 3.00 Gm, which formed a stable platform onto which various sedimentary and volcanic rocks were deposited (Grab & Knight, 2015). Approximately 2.05 Ma ago, magmas formed the world's most extensive mafic intrusion and large A-type granites (Maier et al., 2013). During the Late Carboniferous period (300 Ma), sedimentary infilling resulted in the formation of the Karoo sedimentary basin, which crops out over approximately half of South Africa (Grab & Knight, 2015). About 183

Ma ago, sedimentary aggradation ceased when volcanic activity resulted in the intrusion of dolerite dykes and sills throughout the Karoo basin (Grab & Knight, 2015).

The Great Escarpment, a semi-continuous mountain parallel to the coastline, separates a narrow coastal region from a vast inland plateau (Moore et al., 2009) (Figure 1.4a). The height of the Great Escarpment varies between approximately 1500 m in the southwest, with its highest point exceeding 3400 m in the western Drakensberg. The inland plateau gradually slopes westwards, from 1500 m to 1000 m altitude (Hoffman & Ashwell, 2001).

Soils in South Africa contain a wide range of properties resulting in 73 defined soil forms. These soils are broadly classified into eight categories according to Fey (2010) (see Table 1.2 for soil concept and World Reference Base classification system comparison). Glenrosa or Mispah and red-yellow apedal soils account for over 50% of soils in South Africa (Land Type Survey Staff, 1972-2006). The former is a lithic soil on convex crests and steep slopes (Fey, 2010a). These young soils are common in South Africa as they are associated with aridity and broken steep slopes, both prevalent in the country's landscape (Fey, 2010a). Red-yellow apedal soils are classified as oxidic due to the uniformity of colour in the B horizon derived from iron oxides (Fey, 2010a). The soils are relatively mature and are widespread, especially in northern South Africa. Duplex soils are frequent in sub-humid and drier parts of South Africa (Fey, 2010a). A marked textural contrast in the B horizon from clay illuviation is characteristic of these soils (Parwada & Van Tol, 2016). Duplex soils often have high dispersibility due to their richness in Na (Fey, 2010). Duplex soils are often derived from the mudrocks and shales in the Karoo basin (Laker, 2004).

Figure 1.4 Site map of the study showing a) elevation (GeoSmart Space, 2020a) and b) rainfall seasons (Schulze & Maharaj, 2006).

Table 1.2 Broad South African soil classes with a short description of soil concept from (Fey, 2010a; Fey, 2010b).

South African soil class	Soil concept	Comparison to World Reference base
Red-yellow apedal soils,	Mostly freely drained, Iron enrichment [residual]; uniform colour with structured B	Ferralsols and Latosols
Plinthic soils (soft B)	Soft B, iron enrichment, mottling, or some cementation	Plinthosols
Glenrosa and Mispah (Inseptic lithic soils)	Young soil on weathered rock	Cambisols and Leptosols
Duplex dominant	Permeable topsoil with marked clay enrichment resulting in contrast texture in subsoil	Stagnosols, Solonchaks and Luvisols
Undifferentiated soils	Variable soil associations	More than one soil form occurs
Ferrihumic horizon (Podzolic soil)	Diagnostic podzol B, metal humate enrichment	Podzols
Grey regic sands (Cumulic soil)	Freely drained, young soil formed on recently deposited colluvial, alluvial, or aeolian sediment	Cambisols Arenosols Fluvisols Luvisols Acrisols Lixisols
Rocky, with little soil	N/A	N/A

Rainfall predominantly occurs in the summer, with 84% of South Africa exhibiting a distinct rain season between November and March (Schulze et al., 2006). In contrast, the southwest consists of a Mediterranean climate with wet winters. The average mean annual rainfall in South Africa is 500 mm (Hoffman & Ashwell, 2001). However, the precipitation is skewed along a W-E climate gradient, generally increasing from west to east (De Wit & Stankiewicz, 2006) (Figure 1.4b). The highest rainfall occurs typically along the eastern parts of the Great Escarpment and the eastern coastal belts (Grab & Knight, 2015). High rainfall areas are sporadic, with 91% of South Africa being classified as drylands (Hoffman & Ashwell, 2001). The climate becomes drier inland, in the rain shadow of the Great Escarpment, with areas with a mean annual rainfall between 0 mm and 200 mm.

The natural vegetation is reflected by the E-W rainfall gradient, consisting of 9 broadly classified biomes (Mucina & Rutherford, 2006). To the west, the unique Fynbos biome, which consists of small shrubs and succulents, is situated within the winter rainfall region, extending partially into the all-year rainfall region. The succulent Karoo and Nama-Karoo biomes cover much of the arid interior of South Africa. In the central plateau, the Grasslands biome dominates, covering 28% of South Africa (Mucina & Rutherford, 2006). The largest biome in South Africa is the Savanna biome (32.1%), which largely borders the Grassland biome, and is found primarily in the northern parts of the country. Where grasses dominate the Grassland biome, the Savanna biome is characterised by a combination of grasses and woody coverage.

The natural vegetation in South Africa has been extensively disturbed to make room for agriculture. Agricultural practices follow the E-W climate gradient and are thus closely related to the different biomes (Hoffman & Ashwell, 2001; Waldner et al., 2017). Grains and fruit are found in the west, transitioning to sheep farming in the arid to semi-arid interior. Cattle and subsistence farming are located in the southern and south-western Grasslands and Savanna in the north. The Grasslands biome in central South Africa is used for grains, while forestry and sugar plantations are found in the humid east. Vegetables are interspersed between these agricultural regions in the south and northeast (Hoffman & Todd, 2000). For a more detailed account of geo-environmental variables in South Africa, see Chapters 2 and 3, in addition to the texts referred to therein.

1.6 RESEARCH METHODOLOGY AND DESIGN

Le Roux & Sumner (2013) proposed a framework for soil erosion of South Africa, implementing different scales and methodologies. Although their study only addresses gully erosion at a catchment scale, the scaled premise they used for a regional-scale investigation is promising. Gully susceptibility modelling and detection strategies are often exclusively applied and are rarely combined (Walker et al., 2020). However, gully susceptibility maps on a regional scale could be used as a tool to constrain the implementation of detection tools, which is likely to be more processing intensive. After detection, smaller local sites could be selected in different geo-environments to study gullies in more detail (Vanmaercke et al., 2021), possibly in-field. Although technological advancements have allowed detailed capture and analysis of gully- and field-scale, fieldwork remains essential to further our understanding of gully erosion (Castillo & Gómez, 2016), which will ultimately help to select optimal mitigation strategies. Additionally, selecting sites on a large geographical extent, along climate gradient, could allow insight into how environmental change could impact gully erosion.

The above scaled framework is implemented to address the study aim. Furthermore, the importance of research impact, as presented by Wilkinson et al. (2023), was considered in founding the aim and objectives for this study. Although numerous gully susceptibility and detection methods have been communicated in literature, they are often complex, for example, machine learning approaches (Pourghasemi et al., 2020) or using obscure spectral statistics to identify gullies (Phinzi et al., 2021). The aim herein is to develop easily understandable tools for each objective, to enhance real-world applications. The project is conducted in four phases (Figure 1.5), and each phase is presented in a standalone chapter.

During phase 1, gully erosion literature was reviewed to identify the state of science in South Africa. The review allowed us to identify: 1) the spatial distribution of case study sites in South Africa; 2) control factors hypothesised to affect gullying; 3) the method; and 4) data implemented in studies. The data gathered helped to conceptualise the project and to recognise appropriate research methods. The precise review strategy, results, and interpretation are presented in Chapter 2.

In phase 2, a gully susceptibility model was developed that blended a statistical overlay and qualitative learning from literature. Data points at the required extent were retrieved and calculated

and combined using map algebra in raster data format. Although it is challenging to validate models on such large scales, especially as there is no single one correct validation method, the model was validated using primary (manually digitised reference data from randomly selected tessellation grids, derived from Google Earth imagery and secondary data that consisted of a published gully inventory derived from SPOT-5 (Satellite pour l'Observation de la Terre 5) imagery in 2012 (Mararakanye & Le Roux, 2012). More detail regarding model development, methods, and validation are presented in Chapter 3.

During phase 3, an experimental gully detection model was developed, focusing on using metrics associated with gullies in the field. Input data was limited to a DEM. The model was tested on gullies on different geomorphic scales in the Tsitsa catchment. Additionally, the model workflow was tested in various geo-environmental sites located in South Africa, Namibia, Spain, and Australia. The model was validated with manually derived reference data, obtained either in-field with a differential Global Positioning System (dGPS) or digitised from remotely sensed imagery. A detailed description of the model workflow and its accuracy metrics are presented in Chapter 4.

In phase 4, study sites were selected across the E-W gradient in an effort to isolate land-use or climate. A triangulation of methods was implemented to comprehensively investigate gully erosion at the various isolated sites to provide insight into how climate change could affect gullying by looking at the past. Stakeholder perceptions to gully erosion were also gauged to learn from local knowledge and assess how their perceptions align with remotely sensed and fieldwork findings. The Corona Virus 2019 (COVID-19) pandemic impacted this part of the study due to government and university restrictions regarding human movement and interaction and institutional closures. Furthermore, I contracted COVID-19 resulting in further delays. There are, thus, some data gaps, although more field sites have been earmarked to be visited after Ph.D. submission. A more detailed description of the methods is presented in Chapter 5.

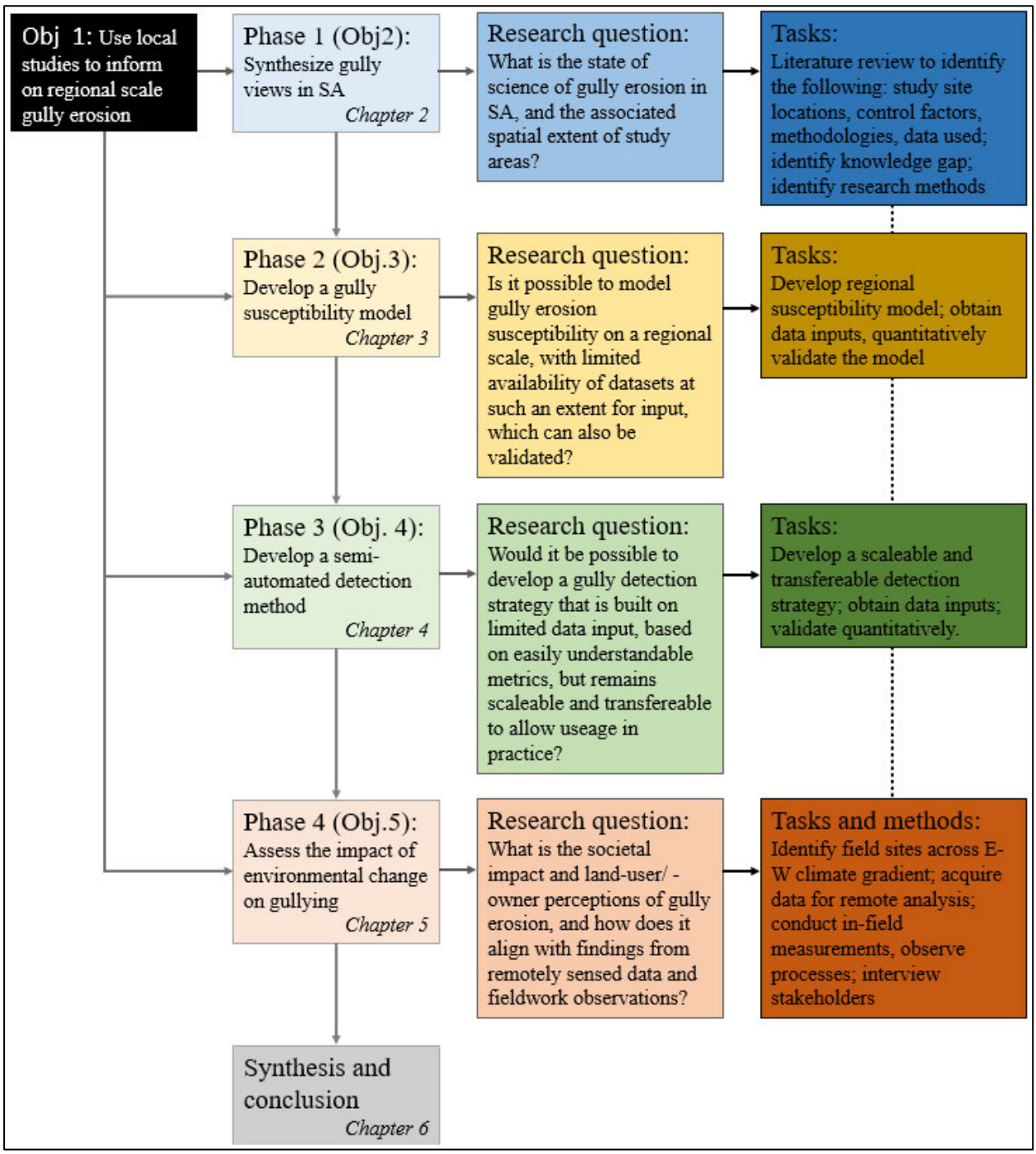

Figure 1.5 Research design, consisting of 4 phases.

1.7 REPORT STRUCTURE AND THESIS FLOW

The article format will be used in this study and comprise of the following articles:

Chapter 2. Intersecting views of gully erosion in South Africa

a. Phase 1: Objectives 1 and 2

b. The chapter was published in Earth Surface Processes and Landforms, a Wiley journal, in 2023 (Olivier G, Van De Wiel MJ & De Clercq WP 2023. Intersecting views of gully erosion in South Africa. *Earth Surface Processes and Landforms* 48(1), 119-142; **https://doi.org/10.1002/esp.5525**). The chapter herein differs from the published version due to minor edits relating to comments received from my PhD Viva on 17 November 2023.

Chapter 3. Predicting gully erosion susceptibility in South Africa by integrating literature directives with regional spatial data

a. Phase 2: Objective 1 and 3

b. The chapter was published in Earth Surface Processes and Landforms, a Wiley journal, in 2023 (Olivier G, Van De Wiel MJ & De Clercq WP 2023. Predicting gully erosion susceptibility in South Africa by integrating literature directives with regional spatial data. *Earth Surface Processes and Landforms* 48(14), 2661-2681; **https://doi.org/10.1002/esp.5653**). The chapter herein differs from the published version due to minor edits relating to comments received from my PhD Viva on 17 November 2023.

Chapter 4. Giving gully detection a HAND – testing the scalability and transferability of a semi-automated object-orientated approach to map gullies

a. Phase 3: Objective 1 and 4

b. An original workflow was presented at the 2020 European Geosciences Union (EGU) General Assembly. The workflow was re-engineered as it did not scale or transfer well to other study sites. The re-engineered workflow, presented in the chapter, was published in Catena, an Elsevier journal (Olivier G, Van De Wiel MJ & De Clercq WP 2024. Giving gully detection a HAND – testing the scalability and transferability of a semi-automated object-orientated approach to map gullies. *Catena* 236,107706; **https://doi.org/10.1016/j.catena.2023.107706**.. The published article is an updated version which includes more sites compared to the chapter presented herein.

Chapter 5. Historical evolution of gullies – Impact of climate and land-use

a. Phase 4: Objective 1 and 5

b. The chapter was presented at the 2023 EGU General Assembly.

The following chapter, Chapter 2, consists of article 1, and is a systematic review of gully erosion in South Africa. The chapter uses the works of Moon & Dardis (1988) "Geomorphology of Southern Africa", as a landmark text to investigate whether gully erosion, which Liggit & Fincham (1989) identified as a neglected geomorphic process in South Africa, has received increase research attention. Numerous reviews have been published (for example, Poesen et al., 2003; Valentin et al., 2005; Kirkby & Bracken, 2009; Capra, 2013; Torri & Poesen, 2014; Vanmaercke et al., 2016), but a review focusing on a specific country remains scarce. The country-specific focus is used to explore literature by intersecting the views regarding gully erosion in South Africa. The work concludes by identifying some local (South Africa) and global (international) research gaps.

In Chapter 3, a regional/ national gully susceptibility model is developed and implemented in South Africa. Instead of using a gully inventory map, which is often done for susceptibility models using statistics or machine learning approaches, a learning from literature approach was used as an input for the model. A triple validation process is undertaken, making use of primary and secondary data.

In Chapter 4, a methodology is developed to map gullies semi-automatically. Although semi-automated gully mapping methods have been published using spectral, topographic, or a combination of data types, they are rarely tested outside the region where it was developed. The detection strategy is based on the distinct landform elements of a gully, i.e., sharp slopes associated with gully walls that surround a gently sloped gully floor. The semi-automated method is tested on gullies of various geomorphic sizes (small-scale to colossus-scale) and geo-environments (including South Africa, Namibia, Spain, and Australia.

In Chapter 5, the impact of land-use and climate are isolated to infer how environmental change may impact gully erosion. Areas of similar land-use were selected across the E-W climate gradient of South Africa to isolate climate, whilst different land-uses within the confines of the same study site were selected to isolate land-use. A triangulation of methods (remote sensing, field measurements and observations, and interviews) are used to investigate the impact of each control factor comprehensively.

Chapter 6 is the concluding chapter. The work is summarised to discuss how the general aim was addressed and how it fits within the current state of science. It concludes by providing recommendations for future research.

CHAPTER 2: INTERSECTING VIEWS ON GULLY EROSION IN SOUTH AFRICA

2.1 ABSTRACT

Gully erosion is an environmental problem recognised as one of the worst land degradation processes worldwide. Insight into regional gully perturbations is required to combat the serious on- and off-site impacts of gullying on a catchment management scale. In response, we intersect different perspectives on gully erosion-specific views in South Africa, a country that exhibits various physiographic properties and spans 1.22 million km^2. While the debate surrounding gully origin continues, there is consensus that anthropogenic activities are a major contemporary driver. The anthropogenic impact caused gullying to transcend climatic, geomorphic, and land-use boundaries, although it becomes more prominent in central to eastern South Africa. Soil erodibility plays a crucial role in what extent gully erosion severity is attained from human impact, contributing to the east-west imbalance of erosion in South Africa. Soil erosion rates from gullying and badlands are limited but suggest that it ranges between 30 t ha^{-1} y^{-1} and 123 t ha^{-1} y^{-1} in the more prominent areas. These soil loss rates are comparable to global rates where gullying is concerning; moreover, they are up to four orders of magnitude higher than the estimated baseline erosion rate. On a national scale, the complexity of gullying is evident by different temporal timings of (re)activation or stabilising and different evolution rates. Continued efforts are required to understand the intricate interplay of human activities, climate, and preconditions determining soil erodibility. In South Africa, more medium- to long-term studies are required to understand better how changing control factors affect gully evolution. More research is needed to implement and appraise mitigation measures, especially using indigenous knowledge. Establishing (semi)-automated mapping procedures would aid in gully monitoring and assessing the effectiveness of implemented mitigation measures. More urgently, the expected changes in climate and land-use necessitate further research on how environmental change affects short-term gully erosion dynamics.

2.2 INTRODUCTION

Numerous literature reviews are written on gully erosion to synthesise our understanding of this process (for example, Poesen et al., 2003; Valentin et al., 2005; Kirkby & Bracken, 2009; Capra, 2013; Torri & Poesen, 2014; Vanmaercke et al., 2016), but rarely do such reviews focus on a specific country (for example, Abdulfatai et al., 2014; Bocco & Oliva, 1992). A country-specific focus is expected to present the national dimension of the phenomenon. Although findings are characteristic to the country, intersecting views on gully erosion at these scales would benefit our conceptual understanding of gullying at regional scales by 1) introducing different perspectives from dispersed studies and 2) providing insight into how contrasting human perturbations and physiographic properties impact gully dynamics and evolution. Advancing conceptual understanding at regional scales is essential to develop predictive tools and devise adequate mitigation and rehabilitation strategies at a catchment management scale (Vanmaercke et al., 2021).

This review focuses on South Africa. The country occupies a large extent (approximately 1.22 million km^2), exhibiting various, sometimes unique, physiographic properties, land-use, and socio-economic circumstances. Published literature approximates that 50% to 70% of the South African landscape is susceptible to erosion (Garland et al., 2000; Le Roux et al., 2008), especially water erosion (Laker, 2004). Nationally, soil loss is estimated as 12.6 t ha^{-1} y^{-1}, although this is skewed towards the east, where rates exceeding 50 t ha^{-1} y^{-1} become prevalent (Le Roux et al., 2008).

Compelling evidence suggests that human activities amplified preconditions prone to soil erosion, including gully erosion, (for example, Talbot 1947; Hoffman & Todd, 2000; Kakembo & Rowntree, 2003; Compton et al., 2010; Parwada & Van Tol, 2016) resulting in the east-west imbalance in South Africa. Soil erosion in the Karoo (see orientation Figure 2.1) and western South Africa has been attributed to the influence of colonial farming methods, especially intensification (Talbot, 1947; Boardman et al., 2003; Meadows, 2003). It is, however, in the east where the displacement of persons to the former homelands under a previous political regime is argued to have resulted in severe erosion, including gullying, due to population and economic pressures in an environment favourable to erosion (Shackleton, 1993; Hoffman & Todd, 2000; Fox & Rowntree, 2001; Hoffman & Ashwell, 2001; Meadows, 2003). Preconditions here consist of sloping topography and soils inherently susceptible to erosion, such as those derived from mudrock

and shales (especially from the Beaufort and Ecca groups, that provide dispersive soils with weak aggregate stability (Laker, 2004). Observations indicate that communal areas in the former homelands are more likely to be degraded compared to commercial farms, even when in proximity (Kakembo & Rowntree, 2003; Mararakanye & Sumner, 2017).

Figure 2.1 An orientation map of South Africa showing the location of the former homelands, Karoo, the Swartland region and the position of the Great Escarpment, the Sneeuberg, and the Cape Fold mountains (data sourced from Mucina & Rutherford, 2006; Burger, 2013; Khuthadzo, 2019; and Centre for Geographical Analysis at Stellenbosch University).

Problems with soil erosion in South Africa are not a recent phenomenon. One of the earliest directorates against soil erosion was established in 1682 (Verster et al., 2009). However, despite gully erosion being a common landscape feature (King, 1963) (Figure 2.2, 1.2), Liggit & Fincham (1989) found that gully erosion research was neglected and in urgent need to be studied. To investigate whether this research gap has been addressed, we review gully erosion specific research in South Africa, using the landmark text "Geomorphology of Southern Africa" (Moon & Dardis, 1988) as the starting point. We aim 1) to examine case study sites from the literature to determine

the state of gully erosion in South Africa based on contextualizing gully soil loss rates and analysing the impact of driving factors on temporal gully dynamics; 2) to identify research gaps that require further attention.

Figure 2.2 Examples of gully morphology in different biomes and land-uses in South Africa: a) Gully along a drainage line with agricultural fields to the left and natural fynbos to the right close to Riebeek Kasteel, Western Cape; b) gully headcut eroding around a check dam wall on a mixed rangeland farm in the Karoo close to Graaff Reinet, Eastern Cape; c) gully headcut found in a communal grazing area of the former homelands in the Grasslands close to Sinxago, Eastern Cape; d) a sinuous gully channel found on a private game reserve in the Savanna region close to Hoedspruit, Limpopo (photos: G. Olivier).

2.3 REGIONAL CONTEXT IN SOUTH AFRICA

The mean annual rainfall in South Africa exhibits a strong W-E climate gradient (De Wit & Stankiewicz, 2006), generally increasing from west to east (Figure 2.4), coupled with distinct rainfall seasons (Figure 2.4). South Africa is mostly arid in the west except for a constricted area in the southwest. Towards the east, sub-humid to humid regions are found where mean annual

rainfall exceeds 1000mm (Schulze et al., 2006). The Rainy Day Normal (RDN), calculated from 10' resolution long-term (1961-1990) climate data from New et al. (2002) by:

$$RDN = \frac{MAR}{ARD} \quad \text{Equation 2.1}$$

where RDN is Rainy Day Normal;

MAR represents the mean annual rainfall;

ARD is the number of annual rain days

Figure 2.3 Rainfall variation in South Africa, showing a W-E climate gradient (for mean annual rainfall (Schulze et al., 2006) and Rainy Day Normal (derived from New et al., 2002). Summer rainfall dominates South Africa, although winter and all-year rainfall regions present towards the E and SE (rainfall seasonality data from Schulze & Maharaj, 2006.

High rainfall intensity events increase the chance of large volumes of water to collect as concentrated flow along pathways (Anderson et al., 2021). Gullying can be induced if runoff

reaches a critical threshold (Poesen et al., 2003), activating various processes. These processes include fluvial scour that deepens the gully floor and undercuts gully sidewalls, waterfall erosion that leads to plunging pool development at the gully headcut, and fluting, all of which may lead to mass wasting events in the gullied domain. By means of RDN, rainfall intensity was strongly correlated with gully headcut retreat in a global study (n = 724) by Vanmaercke et al. (2016).

In the South African context, gully susceptibility may therefore be interpreted to increase with RDN towards the east but also be susceptible in a confined area within the winter rainfall region in the west. However, the interpretation needs to be mindful that there are other controls affecting runoff volume and flow intensity, which work in conjunction with rainfall intensity to influence gully erosion susceptibility. These include soil moisture (Schoener & Stone, 2019), catchment size and shape (Rossi et al., 2015), slope (Torri & Poesen, 2014), surface roughness, and vegetative cover (Torri & Poesen, 2014).

Topographically, South Africa has a narrow coastal region, separated from the inland plateau by the Great Escarpment (Moore et al., 2009) (Figure 2.1 and 2.5a), with its highest point in the western Drakensberg. Steep to very steep slopes (> 20%) are located along the escarpment, the Cape Fold mountains, KwaZulu-Natal, and the eastern parts of the Eastern Cape (Figure 2.5a, b). However, these strongly sloping areas are not the most susceptible to gullying. Instead, gullies are prominent features on concave mid-slopes, foot slopes, and valley floors (Flügel et al., 2003; Kakembo et al., 2009; Compton et al., 2010; Le Roux & Sumner, 2012), and it is these topographic positions that have higher gully susceptibility due to larger magnitudes of concentrated overland flow collecting where material is available for removal.

The Karoo basin occupies approximately two-thirds of South Africa and consists of sedimentary strata deposited from the Carboniferous to Jurassic periods (Figure 2.5c), known as the Karoo Supergroup (Soeder & Borglum, 2019). As parent material, the sedimentary Ecca (early to mid-Permian period) and Beaufort (mid-Permian to early Triassic period) groups of the Karoo Supergroup have specifically been shown to produce soil susceptible to gullying (Laker, 2004). These soils are often highly dispersive and duplex due to the inherited clay mineralogy (Parwada & Van Tol, 2016) and silica content (Laker, 2004). Duplex soils have a marked texture contrast between the A and B horizons (See Figure 2.5d for spatial soil distribution in South Africa and Table 1.2 for a comparison between South African soil classes and the World Reference Base classification system). When free water accumulates at the less permeable subsoil, water can

disperse and remove soil, resulting in piping (Van Zijl & Ellis., 2013). Once soil pipes collapse, renewed gullying can occur (Faulkner, 2006). Dispersive soils in South Africa are not only confined to the duplex soils from the Karoo Supergroup but have also been found in other strata belonging to the Cape Supergroup and the Cretaceous Uitenhage Group (Bell & Maud, 1994).

Figure 2.4 Geo-environmental maps of South Africa: a) topography (GeoSmart Space, 2020a); b) slope (derived from topographical data from GeoSmart Space, 2020a); c) generalised rock type (Burger, 2013); d) generalised soil classification (Land Type Survey Staff, 1972-2006); e) biomes (Mucina & Rutherford, 2006); f) simplified land-use/ cover (Department of Environment, Forestry, & Fisheries, 2018).

In terms of land-use and land-cover, degraded grasslands are predicted to be most affected by erosion (Le Roux et al., 2008). Hoffman & Todd (2000) found communal land tenure (often situated on grasslands; Figure 2.1, 2.5e, f) associated with significantly higher soil degradation values than commercial farming areas. Heavy soil degradation indices were also captured for parts

of the Karoo, especially in the confines of the Orange River (Hoffman & Todd, 2000). These areas in South Africa will therefore have a high prevalence of gullying. The savanna region in the northern parts of South Africa also may be susceptible to gullying, as high soil degradation values were found (Hoffman & Todd, 2000), although Le Roux et al. (2008) indicate questionable soil loss here due to the protective effect of canopy cover over erodible soils.

For a more detailed account of geo-environmental variables in South Africa, see Moon and Dardis (1988), Johnson et al. (2006), Mucina & Rutherford (2006), Schulze et al. (2007), Fey (2010a), Holmes (2012), Grab & Knight (2015), Holmes & Boardman (2018), and Department of Environment, Forestry, & Fisheries (2021).

2.4 METHODS

2.4.1 Literature search

Google Scholar and Scopus were used to build a database of gully erosion research in South Africa. The keywords used included “gully”, “donga”, “sluit” (a term occasionally used for gullies in South Africa), and “sloot” (Afrikaans terminology used for gullies). Each of the abovementioned terms was searched individually and combined with “erosion”. The keyword search was applied to all search fields, but the search was explicitly limited to South Africa and excluded other southern African countries. In addition, the search was limited to English and Afrikaans texts and was completed on 2 October 2022.

After applying the above search criteria, papers featuring gully erosion as part of their research aim (based on the title and information attained from abstracts) were incorporated into a database. Hereafter the database was expanded by a backward and forward reference search, adding relevant works missed during the keyword search as well as papers with a broader scope yet still addressing gully erosion in South Africa. The backward reference search consisted of examining the reference lists of the papers in the database. Scopus was used to conduct a forward reference search to identify studies that cited papers in the database. The resulting database was divided into two parts: 1) “DONGA”: papers consisting of gully-specific studies, i.e., where gullies were explicitly studied, and 2) “EXTERRA”: broader scope erosion or land degradation studies that were identified from the forward and backward reference searches and deemed contextually relevant.

2.4.2 Key gully characteristics sourced directly from papers

The articles in the literature database were analysed to identify the key characteristics of gully erosion in South Africa.

Factors hypothesised to have led to gully origin, and control factors of contemporary gullying processes were captured for both the EXTERRA and DONGA sections. Where multiple papers authored by the same researchers investigated the same study site, gully origin and control factors were captured once and were only edited if additional factors were identified in the subsequent work. If the same site was studied by different researchers, it was considered a new appraisal, and all gully origin and control factors were captured. Specific land-use and physiographic properties were noted from study site descriptions and the discussion sections to be used as supplementary contextual information to the control factors. The academic background of the first author of these papers was determined by using the Google and Google Scholar search engines and the search functionality within ResearchGate to investigate any potential bias towards gully causality and academic orientation.

Additional information was captured for articles in the DONGA database. The title and stated aim/s of these articles were used to organise articles into meaningful categories relating to study type: 1) Causal factors, processes, and impacts; 2) methods; 3) evolution; 4) qualitative; 5) morphometry; 6) quantify soil loss; 7) review; 8) gully control; and 9) multiple. The mode of study was categorised according to 1) Remote sensing; 2) field survey; 3) literature; 4) workshops or interviews; and 5) experimental. The geographical location of gully sites in the DONGA section was captured by a singular point coordinate (x, y). In cases where coordinates were not provided, an approximate geographical location was derived using place names provided in the site description. The methodological approach implemented at these locations was captured, in addition to the spatial and temporal scale and soil loss data (including rate and bulk density figures). Where gully erosion rates were reported per gullied area or combined with inter-gullied erosion, it was recalculated to a gully erosion rate per catchment area to make it comparable to other findings.

2.5 RESULTS

2.5.1 Meta-analysis of papers

A total of 82 publications were retrieved from search results, 53 of which were classified as DONGA studies (47 research papers, five M.Sc. theses and one conference abstract) and 30 (29 research papers and one Ph.D. thesis) as EXTERRA. Until 2011, DONGA research remained mostly constant at one to two publications per year, but it has increased over the last decade (Figure 2.6). However, several papers of these newer present new findings from continued research at the earlier sites, for example, in the Sneeuberg (Boardman et al., 2003; Keay-Bright & Boardman, 2007; Boardman et al., 2015; Favis-Mortlock et al., 2018), the Sandspruit catchment (Olivier et al., 2016; Olivier et al., 2018), and near Potshini village (Chaplot et al., 2011; Grellier et al., 2012; Chaplot, 2013; Podwojewski et al., 2020; Chaplot & Mutema, 2022). The Eastern Cape and KwaZulu-Natal received the most research attention, with 23 and 12 different gully sites respectively, while the North West and Gauteng had none (Figure 2.7).

Figure 2.5 Timeline of South African gully erosion research publications in the DONGA database and cumulative number of case studies. Bar colours indicate the study type of manuscripts in the DONGA database.

Figure 2.6 Location of gully study sites investigated in South Africa (n=49) overlaying the national gully inventory mapped by Mararakanye & Le Roux (2012). Gully study sites that reported soil loss (excluding sediment yield) are symbolised with red circles that are proportional to the magnitude of soil loss from gullying.

Causal factors, processes, and impacts are frequently used for DONGA studies (n = 16; Table 2.1), with an emphasis on gully origin (Cobban & Weaver, 1993; Boardman et al., 2003; Lyons et al., 2013; Rowntree, 2013) and contemporary driving factors (Le Roux & Sumner, 2012; Chaplot, 2013; Mararakanye & Sumner, 2017). Several papers implemented *Multiple* study types (n = 13), which also had a strong *Causal factor, processes, and impacts* component (41%; Table 2.1). *Methodological* approaches (n = 7) consisted of assessing gully risk (Watson and Ramokgopa, 1997) and evaluating new detection methods related to spectral properties (Mararakanye & Nethengwe, 2012; Makaya et al., 2019b), vegetation indices (Taruvinga, 2008; Phinzi & Ngetar, 2017; Phinzi et al., 2021) and DEM (Olivier et al., 2022). Larger temporal scale studies investigated gully *Evolution* (n = 4), mainly in arid regions, providing context relating to the influence of connectivity cycles on gully channel migration (Grenfell et al., 2014; Manjoro et al., 2012; Pulley et al., 2018).

The Sneeuberg area was the focus of three *Review* papers. Two of these papers evolved from a long-term project by Boardman et al. (2003) and a third by Rowntree (2013), who assessed published reports from farmers and agricultural extension officers between 1889 and 1910. *Qualitative* work (n = 3) consisted of descriptive work (Dardis & Beckedahl, 1988) and classification procedures (Flügel et al., 1999; Olivier et al., 2016). Morphometry studies (n = 3) include an enormous effort by Mararakanye & Le Roux (2012), who manually mapped and measured gully features on a national scale in South Africa. The least common study types are the *Quantification of soil loss* (n = 2) and *gully control* (n = 2), although they form a key combination of *Multiple* studies (Table 2.1).

Table 2.1 Number of gully erosion studies by category.

DONGA studies (n = 53)	
Category	**Number**
Causal factors, processes, and impacts	16
Multiple	13
Methods (identification and/ or prediction)	7
Evolution	4
Morphometry	3
Review	3
Qualitative	3
Gully control	2
Quantify soil loss	2
Category combinations within "Multiple" (in %)	
Category	**%**
Causal factors, processes, and impacts	41.4
Quantify soil loss	24.1
Qualitative	13.8
Gully control	10.3
Morphometry	10.3

In the combined DONGA and EXTERRA groups, gully controlling and driving factors were explored by first authors with a variety of academic backgrounds (Table 2.2). Most first authors are in Geography (27.5%) and Geo-Informatics (15%) disciplines. The controlling and driving factors identified by the different academic groups are not limited to the lead researcher's academic background but span a broader scope (Table 2.2). Anthropogenic activities were identified as the primary cause and driver of gullying, irrespective of the first author's academic background (Table 2.2).

Table 2.2 Academic background of first authors researching gully erosion in South Africa, and dominant controlling and driving factors of gullying identified in their papers (n = first authors of papers presenting controlling and driving factors of gullying).

Academic background	Controlling and driving factors				
	Anthropogenic	Topography	Geology	Climate	Soil
Geography (n = 11)	9	3	8	2	6
Geo-Informatics (n = 6)	5	5	1	2	1
Soil Science (n = 4)	2		1	1	4
Geomorphology (n = 4)	4	1		1	
Geography and environmental (n = 3)	3	1		2	2
Physical geography (n = 3)	1		1	1	
Geology (n = 2)	1			1	
Hydrology (n = 2)	1	1		1	1
Ecology (n = 3)	3	1		1	
Agriculture (n = 1)	1	1	1	1	
Archaeology (n = 1)	1				

2.5.2 Applied techniques

Nearly 60% of DONGA studies used at least one remotely sensed product (Table 2.3). Initially, aerial imagery was mainly implemented sequentially to investigate gullying on long temporal scales at high- to medium spatial resolutions (Liggit & Fincham, 1989; Garland and Broderick 1992, Brady, 1993; Morel, 1998). From 2012, satellite imagery became more prominent and more often used for mapping purposes from single acquisition dates (Le Roux & Sumner, 2012; Mararakanye & Le Roux, 2012; Mararakanye & Nethengwe, 2012). As a result, spatial coverage increased compared to aerial imagery, albeit at medium spatial resolution only. More recently, the advancements in Geographic Information System (GIS) environments allowed the integration of several remotely sensed data sets in a singular environment (Kakembo et al., 2009; Grellier et al., 2012; Olivier, 2013; Seutloali et al., 2016; Mararakanye & Sumner, 2017, Olivier et al., 2018; Makaya et al., 2019b; Le Roux & Van der Waal, 2020; Bernini et al., 2021). Introducing more variables restricted the studies to shorter temporal scales but allowed more complex efforts to understand gully occurrence (Mararakanye & Le Roux, 2012; Mararakanye & Nethengwe, 2012; Le Roux & Sumner, 2012; Olivier et al., 2016; Seutloali et al., 2016; Bernini et al., 2021).

Topographic variables are frequently combined with imagery in a GIS environment (Kakembo et al., 2009; Grellier et al., 2012; Olivier, 2013; Seutloali et al., 2016; Mararakanye & Sumner, 2017, Olivier et al., 2018; Makaya et al., 2019b). Although other physiographic factors were used less often initially, more recently, it has been used more prominently, for example, geological (Le Roux & Sumner, 2012; Mararakanye & Sumner, 2017; Bernini et al., 2021), soil (Seutloali et al., 2016; Mararakanye & Sumner, 2017), land-use/ cover (Le Roux & Sumner, 2013; Du Plessis et al., 2020; Bernini et al., 2021), climate (Mararakanye & Sumner, 2017), and vegetation data (Mararakanye, 2015; Bernini et al., 2021). Topographic variables were mainly derived from single-date DEMs and applied as a general exploratory measure to derive causes of gully occurrence. Slope gradient was widely used (Kakembo et al., 2009; Olivier et al., 2016; Seutloali et al., 2016), primarily as classes to determine where gully features were located and were not specifically related to gully morphology features, for example, gully head, floor, or outlet. Other commonly used topographic indices include contributing catchment area above gully heads (Grellier et al., 2012; Mararakanye & Sumner, 2017), curvature (Chaplot, 2013; Bernini et al.; 2021), Stream Power Index (SPI) (Kakembo et al., 2009; Chaplot, 2013; Mararakanye, 2015; Mararakanye & Sumner, 2017) and Topographic Wetness Index (Chaplot, 2013; Mararakanye, 2015; Mararakanye & Sumner, 2017). More specific uses of DEMs and topographic variables, such as soil loss quantification from DEM-of-Difference (Flügel et al., 1999) or investigating gully wall retreat (Chaplot, 2013; Podwojewski et al., 2020), were rare.

Field surveys often augmented remote sensing studies, for example, morphological measurements by Boardman et al. (2003, Grellier et al. (2012), and Seutloali et al. (2016), more detailed surveying by Brady (1993) and Grenfell et al. (2014), and detailed soil analysis by Du Plessis et al. (2020), or as a minimum ground truthing (Table 2.3). Field surveys remain a valuable technique and are used by several research efforts as their main investigative means (Botha et al., 1994; Rienks et al., 2000; Keay-Bright & Boardman, 2009; Manjoro et al., 2012; Manjoro et al., 2017). Most field surveys were conducted on singular field visits, except for a long-term project in the Sneeuberg, Eastern Cape (Keay-Bright & Boardman, 2009 to Favis-Mortlock et al., 2018).

Field surveys consisted primarily of observations and morphological measurements. Morphological measurements ranged from basic depth measurements (Dardis & Beckedahl, 1988) to more complex measurements that estimated volumetric soil loss or gullies extent (for example, Manjoro et al., 2012, Grellier et al., 2012 and Makaya et al., 2019b). Novel specialised techniques

such as using a cell phone clinometer to measure local gradient (Favis-Mortlock et al., 2018) and in-depth soil analysis to determine its influence on gullying (Rienks et al., 2000; Du Plessis et al., 2020) remained scarce.

The use of existing literature (Watson & Ramokgopa, 1997; Boardman et al., 2010; Rowntree, 2013), interviews (Keay-Bright & Boardman, 2007), and experimental work (Chaplot et al., 2011) were less common as the primary technique or as supportive for remotely sensed studies (Table 2.3).

Table 2.3 Techniques used in gully erosion research in South Africa coupled with temporal (short term < 5 years, medium term 5 to 15 years, and long-term >15 years) and spatial resolution (high < 2m, medium 2 to 15m, and coarse >15m).

DONGA studies (n = 53)		**Spatial resolution**[†]			
Category	**Number**	**< 2m**	**2 – 15m**	**>15m**	**Unknown**
Remote sensing	31				
- Aerial photography	9				
< 5 years		2	1		
< 5 – 15 years			1		
> 15 years		2	3		
- Satellite imagery (RGB and/ or spectral)	7				
< 5 years			6		1
< 5 – 15 years					
> 15 years					
- Digital Elevation Models	2				
< 5 years		1		1	
< 5 – 15 years					
> 15 years					
- Combination of remotely sensed data sets[†]	14				
< 5 years		5	5	1	1
< 5 – 15 years		1			
> 15 years		1			
Field Survey	14				
< 5 years	10				
< 5 – 15 years	1				
> 15 years	3				
Literature	5				
Workshop and/ or Interview	1				
Experimental	1				

Techniques combined with remote sensing techniques (in %)	
Category	**%**
- Field Survey	48.3
- Ground truth	41.4
- No additional techniques	6.9
- Experimental	3.4

† Highest spatial resolution spatial dataset was selected

2.5.3 Analysis of literature findings

2.5.3.1 Soil loss from gully erosion

Soil loss rates from gully erosion were reported for ten sites and varied by five orders of magnitude (10^{-3} to 10^{2} t ha^{-1} y^{-1}; Table 2.4). Measurement techniques differed at each gully site. Olivier et al. (2018) extrapolated a soil loss rate of 0.003 t ha^{-1} y^{-1} from the soil accumulation in sediment traps along the flow paths of gully floors. Schmiedel et al. (2017) made morphological measurements and combined them with shape observations to estimate a soil loss rate of 3 t ha^{-1} y^{-1}. Favis-Mortlock et al. (2018) derived soil loss rates of 45 t ha^{-1} y^{-1} and 123 t ha^{-1} y^{-1} from erosion pins at various badland sites in proximity. Headward erosion was assessed by Grellier et al. (2012) from a time series of aerial imagery and fieldwork to calculate soil loss as 25.7 t ha^{-1} y^{-1}. Chaplot et al. (2011), Chaplot (2013), and Chaplot & Mutema (2022) estimated soil loss rates between 2.3 t ha^{-1} y^{-1} and 4.8 t ha^{-1} y^{-1} from gully walls from rainfall experiments and erosion pins installed on sidewalls, respectively.

Soil loss rates from gully erosion contributed an average of 122% compared to the soil loss risk map from Le Roux et al. (2008) (Table 2.4). The highest values were obtained from badlands (Favis-Mortlock et al., 2018), whilst the lowest rate occurred from rates extrapolated from sediment traps (Olivier et al., 2018).

No clear trend exists between gullied area and the soil loss rate calculated (Figure 2.8a), which could be attributed to the source of measurement (gully floor, plots in badlands, gully walls, and gully headcut) of a constrained dataset. Similarly, no correlation was found between gullied area and the corresponding Revised Universal Soil Loss Equation (RUSLE)-predicted soil loss rate (Figure 2.8b). Although RUSLE does not adequately model gully erosion (Van Zyl, 2007; Capra, 2013) due to its inability to account for mass wasting and sub-surface processes, it could nonetheless be expected that a higher likelihood of gullying would occur where high soil losses were modelled. The coarse resolution of the national RUSLE prediction (250 m) coupled with its sensitivity to slope as a predictor variable may be reasons for the absence of correlation. Gullied area and measurement time (Figure 2.8c) also show no trend, probably because the measurement time corresponds to the aims of the study rather than the size of the gully under investigation.

Table 2.4 Soil loss caused by gully erosion, listed in order of longitude and compared to a national erosion risk map produced for South Africa by Le Roux et al. (2008).

Author	Centroid polygon		Province†	Gullied area (ha) [catchment area (ha)]	Survey method	Measured from	Measurement time (y)	Bulk density (g cm^{-3})	Gully soil loss rate (t ha^{-1} y^{-1})	RUSLE predicted soil loss (t ha^{-1} y^{-1}) ¶	% Gully soil loss compared to RUSLE
	x (dd)	y (dd)									
Olivier et al., 2018, 2019	18.76	-33.28	WC	2.01 [128.92]	Field	Gully floor	0.5	N/A	0.003	4.15	0.07
Schmiedel, et al., 2017	19.07	-31.26	NC	0.14 [33.6]	Field	Volume	50	1.5	3	15.55	57.88
Favis-Mortlock et al., 2018 ‡	24.56	-31.67	EC	2 x 0.0032 [?]	Field	Badlands	16	1.7	123 §	84.21	146.06
Favis-Mortlock et al., 2018	24.56	-31.7	EC	2 x 0.0032 [?]	Field	Badlands	16	1.7	93 §	14.61	636.55
Favis-Mortlock et al., 2018	24.57	-31.68	EC	2x 0.0016 [?]	Field	Badlands	16	1.7	59 §	78.51	75.15
Favis-Mortlock et al., 2018	24.57	-31.69	EC	2x 0.0016 [?]	Field	Badlands	16	1.7	92 §	166.37	55.30
Favis-Mortlock et al., 2018	24.58	-31.70	EC	2x 0.0016 [?]	Field	Badlands	16	1.7	45 §	38.72	116.22
Grellier et al., 2012 #	29.35	-28.81	KZN	0.37 [3.5]	Field, aerial	Headcut	64	1.4	25.7	43.59	58.96
Chaplot, 2013	29.36	-28.82	KZN	30.72 [?]	Field	Gully wall	1	0.92-1.55	2.3	163.94	1.40
Chaplot et al., 2011, 2022	29.36	-28.53	KZN	0.0001 [?]	Field	Gully wall	N/A	1.3	4.8	6.57	73.06

† WC, NC, EC, and KZN denote Western Cape, Northern Cape, Eastern Cape, and KwaZulu-Natal respectively

‡ The erosion rates reported by Favis-Mortlock et al. (2018) forms part of a long-term project investigating land degradation in the Karoo, EC. The soil loss rates for these study sites have been reported previously (Keay-Bright & Boardman, 2009; Boardman et al., 2015) and only the most recent soil loss rate was reported for each site in this paper.

§ 2 plots combined and averaged

Soil loss reported for 15 gully heads of the same gully network and therefore soil loss was averaged

¶ Derived from Le Roux et al., 2008

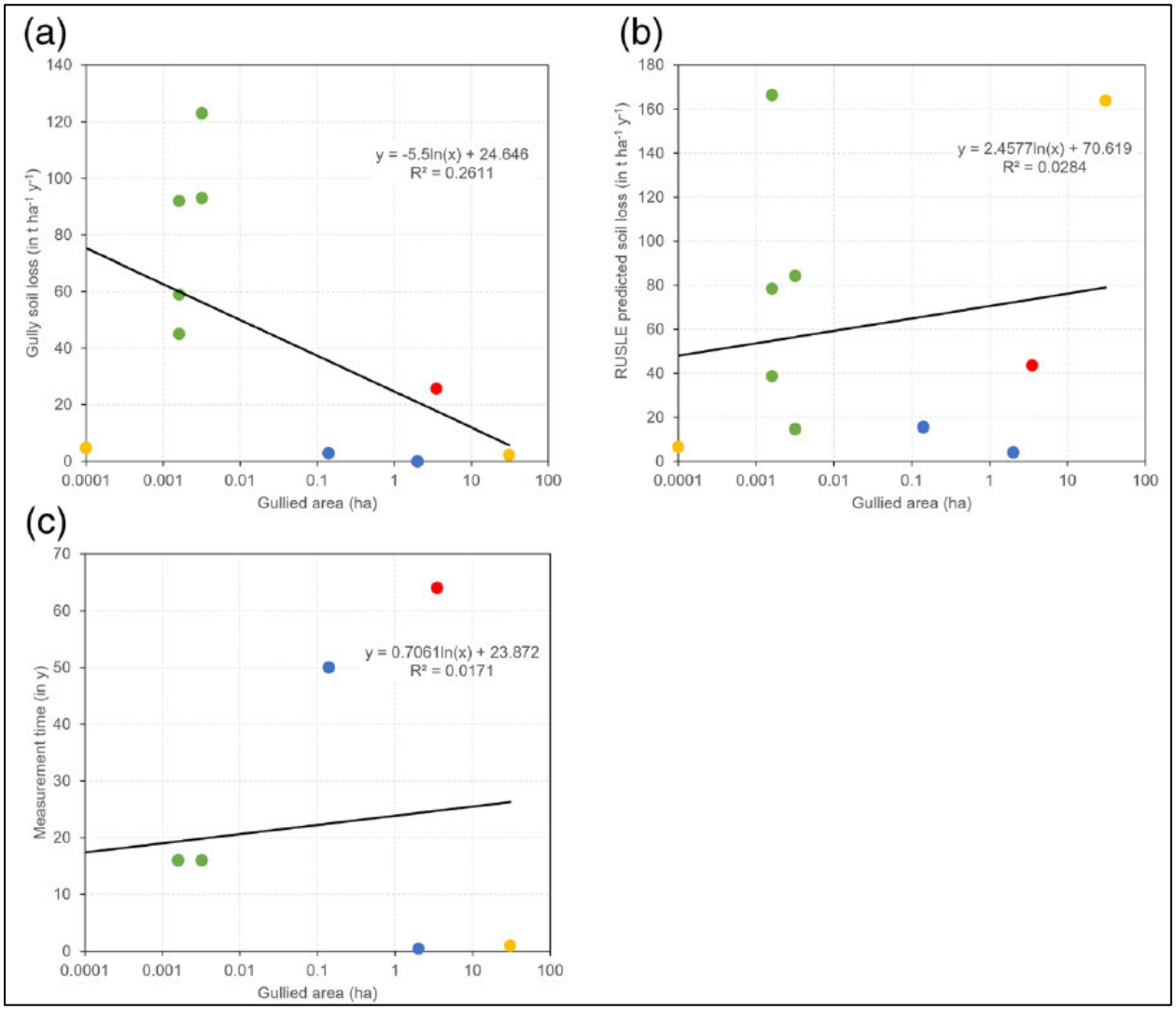

Figure 2.7 Relationship between catchment area and soil loss from gully erosion. Symbol colours denote location of the soil loss measurement: blue: gully floors (n = 2); yellow: gully walls (n = 2); red: gully headcut (n = 1); and green: badlands (n = 5).

2.5.3.2 Temporal gully evolution

Gully activity and extent changes were reported on medium- (5 - 10 years) to long-term (>10 years) time scales for 16 studies (Figure 2.9). The heterogeneous nature of gully erosion in South Africa is evident from the different timings of erosion episodes at various geographical locations and the episodic activation stabilisation cycles for the same gullies (Marker, 1988; Kakembo & Rowntree, 2003; Sonneveld et al., 2005; Grellier et al., 2012).

The temporal variations in gully erosion were attributed to a diverse range of anthropogenic factors and climate (Figure 2.9). Farming intensity was associated with severe gullying in the western

parts of South Africa (Talbot, 1947; Meadows, 2003) and the central Karoo (Keay-Bright & Boardman, 2006; Favis-Mortlock et al., 2018). However, the extent of gully features reduced in both regions from the 1940s due to land management strategies (Meadows, 2003; Keay-Bright & Boardman, 2006), although soil loss from gully channel tributaries of badlands in the Karoo was still alarming (Favis-Mortlock et al., 2018). Cyclical gully erosion occurred due to anthropogenic stressors, such as population pressure (Marker, 1988; Grellier et al., 2012), overgrazing (Grellier et al., 2012), and land abandonment (Vetter, 2007; Kakembo & Rowntree, 2003; Kakembo et al., 2009), along with natural factors such as rainfall intensity (Kakembo & Rowntree, 2003) and the cyclical nature of seasonal rainfall (Dollar & Rowntree, 1995). Although remediation strategies in the western Eastern Cape and KwaZulu-Natal remain scarce in published literature, natural factors (Sonneveld et al., 2005) and political policy (Seutloali et al., 2017) were associated with lowering gully severity.

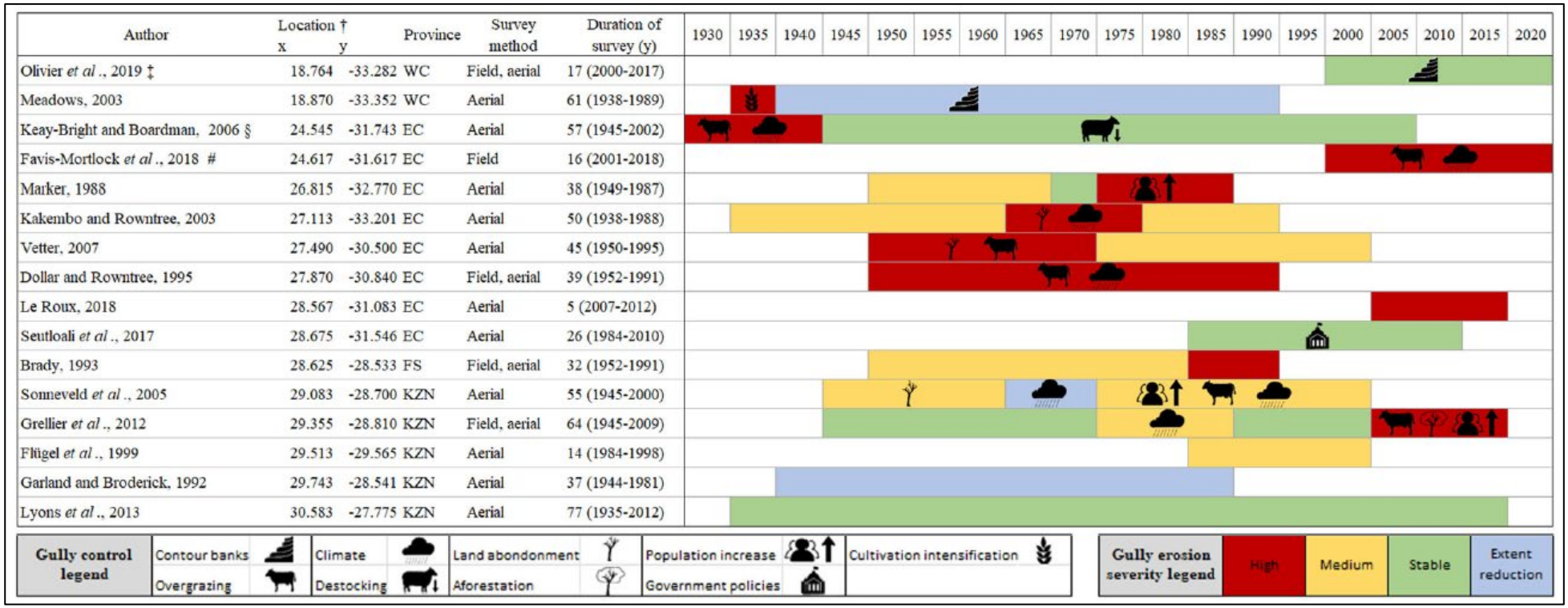

† Location of studies are ordered according to province and longitude; WC, EC, FS, and KZN denote Western Cape, Eastern Cape, Free State, and KwaZulu-Natal respectively.
‡ Olivier et al. (2018, 2019) were used to identify gully evolution at this gully site. Only the most recent paper was named in this table.
§ Keay-Bright & Boardman (2006) forms part of a long-term monitoring project in the Karoo, Eastern Cape. Only the most recent paper reporting on remote valley bottom gullies was included in this table.
# Favis-Mortlock et al. (2018) forms part of a long-term monitoring project in the Karoo, Eastern Cape. Only the most recent paper reporting on erosion pin data for the badlands site was name in this table.

Figure 2.8 Gully evolution in South Africa according to medium term (>5 years) and long term (>10 years) observational and measurement-based research. Locations are ordered according to longitude (Figure after Castillo & Gómez, 2016).

2.5.3.3 Factors driving gully origin

The DONGA and EXTERRA studies hypothesised various natural and anthropogenic causes of gully origin and contemporary gully erosion (Figures 2.10, 2.11). Natural causes of gully origin were related to intrinsic properties and external climate forcing.

Lithological controls were demonstrated in the Highveld (Tooth et al., 2004) and KwaZulu-Natal (Bernini et al., 2021). In the Highveld, gully genesis was proposed from floodplain abandonment resulting from rivers breaching downstream dolerites (Tooth et al., 2004). In KwaZulu-Natal, the late Quaternary Masotcheni formation exhibits various cut and fill features associated with gully erosion, providing evidence of non-anthropogenic gully origin (Botha et al., 1994). The susceptibility to gullying was suggested to be a result of the unconsolidated nature of deposited colluvium, variable dispersibility (Rienks et al., 2000), and thin soils found upslope (Temme et al., 2008). In the Karoo, a more arid setting, gullying was determined to be a cyclical process related to slope and episodic, high-intensity rainfall events (Grenfell et al., 2014). Lyons et al. (2013) proposed climate change associated with the Medieval Climate Anomaly and Little Ice Age (between AD 900 - 1800) as the driver of gully origin.

However, anthropogenic activities leading to gully origin have also been firmly advocated, especially in the Karoo. The occupation of European settlers and a change to farming land-use with subsequent activities such as movement via wagon, kraaling (the practice of bringing stock that roamed free during the day to an enclosure, also known as a kraal, at night for watering and safety from predators), overgrazing, and the draining of wetlands for cultivation have been strongly presented as initiating gully erosion in the late 19th and early 20th century (Neville et al., 1994; Boardman et al., 2010).

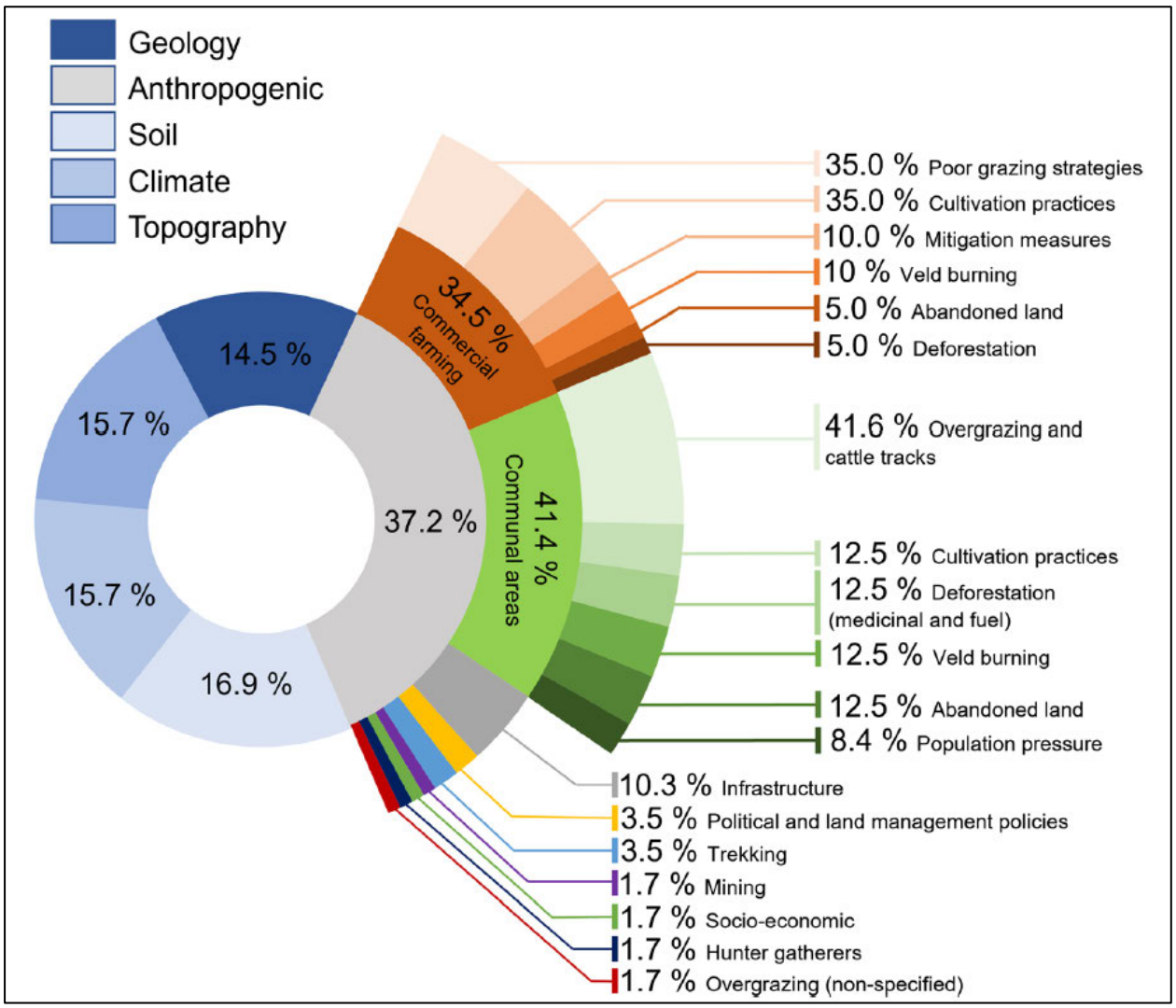

Figure 2.9 Controlling and driving factors of gully erosion in South Africa from short-, medium-, and long-term studies extracted from the DONGA and EXTERRA groups.

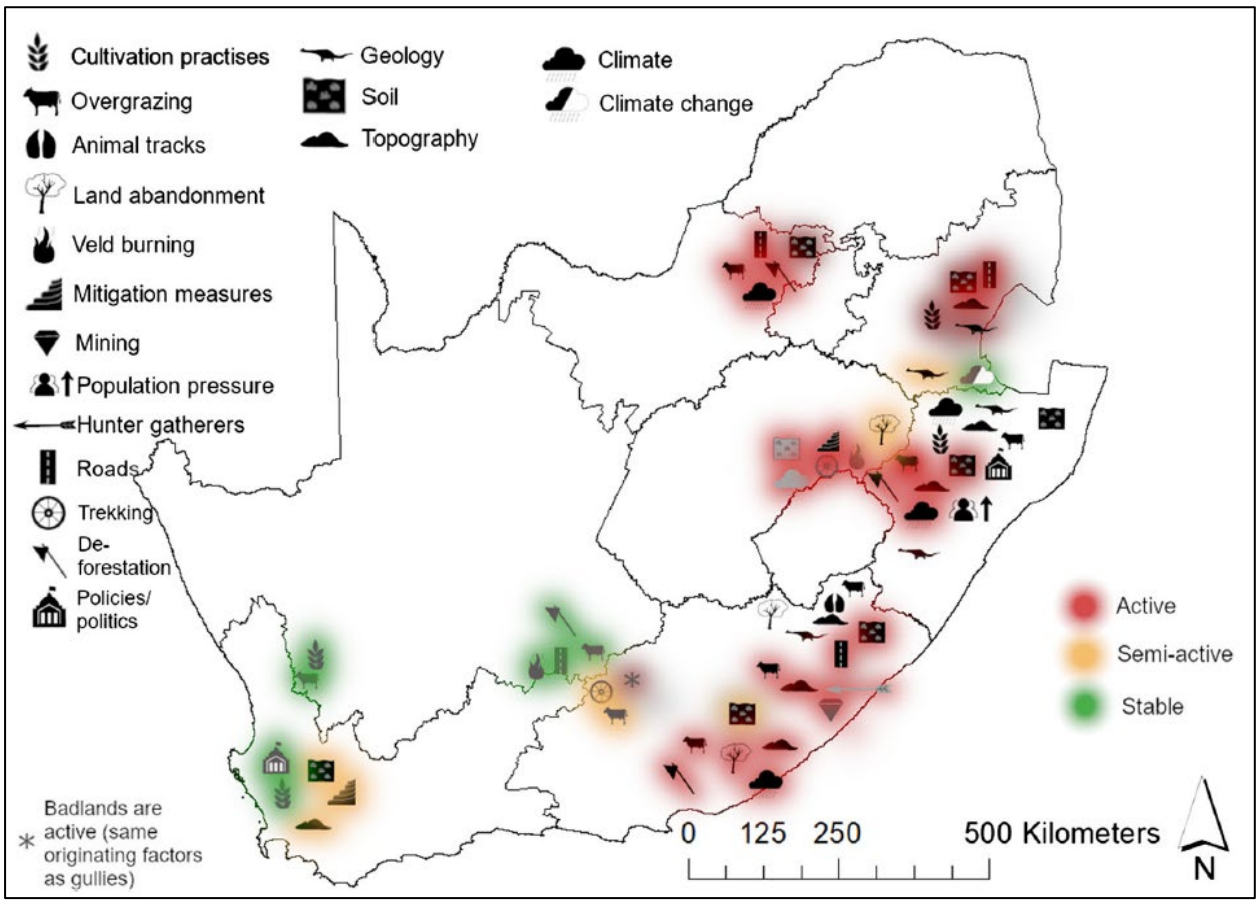

Figure 2.10 Driving and control factors from the DONGA and EXTERRA groups (excluding national studies as these do not have a x, y coordinate) plotted according to its study locality. Grey symbols indicate factors that lead to gully origin; black symbols indicate contemporary driving factors. The severity of gully erosion was extracted from literature at each location and mapped according to colour symbology: red highlighted symbols depict sites where gully erosion is active, orange highlights where semi-active, and green highlights show gullies that have stabilised. Where no gully activity information was apparent, the symbology was not highlighted (white background).

2.5.3.4 Factors driving (and rehabilitating) contemporary gully erosion

According to the DONGA and EXTERRA studies, contemporary gully erosion also has a strong anthropogenic impression (Figures 10, 11). Overgrazing on commercial and communal land has the highest incidence of gully association among farming-related activities. Contour banks were shown to successfully rehabilitate gully erosion, although it has the potential to incur gullying (Olivier et al., 2018). Governmental policies had contrasting effects as they resulted in the reduction of gully extent in the Western Cape (Meadows, 2003) and stabilising gullies in the Eastern Cape (Seutloali et al., 2017), but the more murky, inhumane policies that included the

formation of, and the displacement of people to the former homelands resulted in the acceleration of gully erosion (Meadows, 2003; Hoffman & Todd, 2000). Impervious surfaces such as roads and incorrect positioning of culverts have also been shown to induce gully erosion (Beckedahl & Dardis, 1988; Seutloali et al., 2016). Mining and anthropogenic activities pre-dating European colonisation have been less advocated as causes of gully erosion (Hanvey & Dardis, 1991).

Although anthropogenic activities are the main component accelerating contemporary gully erosion, the inherent preconditions of an area set the potential to erode (Liggit & Fincham, 1989). Inherent controlling factors, soil, geology, and topography have been identified to work synchronously with anthropogenic activities (Figures 10, 11). The lithological properties of the Masotcheni formation, *viz*. deep and loosely consolidated colluvium, exhibiting high relative sodium content compared to other exchange cations, and often being capped by duplex soils, were found to yield contemporary gullying (Rienks et al., 2000). Duplex soils, especially those derived from the mudstones and shales of the Beaufort and Ecca groups, show a high predisposition to gullying and are often dissected with large gullies (Laker, 2004; Le Roux & Sumner, 2012; Le Roux et al., 2022). Clay accumulates in the B horizon in these duplex soils, resulting in a sharp contrast in texture between the top- and sub-soil (Parwada & Van Tol, 2016). The permeability difference in the soil matrix causes free water to accumulate in the subsoil, where soil can disperse along the hydraulic gradient to an outlet, resulting in piping (Beckedahl, 1996). Subsequent piping can induce severe gullying, extending existing gullies laterally and linearly via slumping (Brady, 1993), forming perpendicular tributary gullies (Le Roux et al., 2022), or new discontinuous gullies that can form parallel to existing gullies in the catchment (Beckedahl & Dardis, 1988). Soil dispersibility was also associated with gullying in the Western Cape (Olivier et al., 2013). However, no pipes were evident, and the extent of gullying was much less severe compared to areas with duplex soils in the east of South Africa.

Rock hardness has also been shown to influence gullying. In rivers, breaching of dolerite barriers has been shown to result in gullying on the floodplain of meandering rivers (Tooth et al., 2004). Where dolerite dykes are exposed on gully floors due to active incision, the resistance of dolerite to fluvial erosion may cause regenerative gullying of the gully floor downstream (Le Roux et al., 2022). Dardis & Beckedahl (1991) found that the longitudinal morphology of rock-incised gullies is influenced by the hardness of lithology, becoming V-shaped with increasing hardness. Interestingly, gullies that have incised through soil to reach bedrock have been found not to

become narrower or V-shaped but instead become more stable (Boardman & Foster, 2008) or continue to extend laterally, sometimes to extraordinary widths (Le Roux et al., 2022).

Few studies have reported severe gully erosion on steep slopes (Makaya et al., 2019a), with most authors identifying a preferential zone for gully erosion on footslopes and valley bottoms (Keay-Bright & Boardman, 2007; Le Roux & Sumner, 2012; Kakembo et al., 2009). The hardness of lithologies of the underlying bedrock was also attributed to influence gully dynamics (Dardis & Beckedahl, 1991).

Climate was identified as a driver of contemporary gully erosion in the form of intense rainfall (Kakembo & Rowntree, 2003), rainfall variance (Dollar & Rowntree, 1995; Grenfell et al., 2014), and the increase in annual rainfall (Grellier et al., 2012). The impact of rainfall on gullying is complex and cannot be looked at in isolation, for example, an increase in rainfall may lead to heightened gully activity (Grellier et al., 2012) but may also smooth gully scars and allow regeneration of vegetation that can inhibit gully erosion (Laker, 2004; Sonneveld et al., 2005). Drought was also associated with gullying as it reduces vegetative cover (Boardman et al., 2003; Sonneveld et al., 2005), and is often followed by heavy rainfall (Laker, 2004). Clear evidence of climate change resulting in contemporary gully erosion has not yet been presented, but Meadows (2003) indicated that relic gullies in the Swartland, Western Cape, may be reactivated due to more intense rainfall events occurring earlier in the wet season. Similarly, Boardman et al. (2017) anticipated that more intense rainfall might exceed anthropogenic activities as the driver of gully erosion in the Karoo.

Although several researchers name mitigation measures found at their study sites (Table 2.5), the implementation and appraisal of the effectiveness and service life thereof are rare in published literature in South Africa. In the Sneeuberg area of the Karoo, the removal of grazing on badlands alone did not yield significant vegetation increase to allow successful reclamation as vegetation and seedlings suffer in this harsh environment (Keay-Bright & Boardman, 2007). Also in the Karoo, Schmiedel et al. (2017) experimented with a more elaborate study involving check dams, geotextiles, and revegetation. Despite positive feedback, soil aggradation and an increase in vegetative cover, the cost was high, deeming mitigation efforts unsustainable without aid from government policy.

Table 2.5 Gully mitigation measures reported in South Africa.

Area	Approximate date of installation	Contemporary gully activity	Rehabilitation methods													
			Revegetation	Reducing stock numbers	Check dams	Increasing water holes	Contour banks	Fencing	Geotextile	Gully fill	High-density grazing	Reintegration of stock	Rotational cultivation	Stone slopes	Tillage/ mulching
Swartland, WC	1940s	Semi-active/ stable			x	x	x			x		x	x		x
Namakwa district, NC ‡	2011	Stable	x		x				x						
Sneeuberg, EC	-	Semi-active §	x	x				x			x				
Broader Karoo, EC §	1900s	Stable	x	x			x	x						x	

† WC, NC, and EC denote Western Cape, Northern Cape, and Eastern Cape respectively
‡ Experimental study on Avontuur in the Northern Cape investigating the effectiveness of rehabilitation methods
§ Badlands remain active (little remediation work has focussed on them)
# Focus was mostly in Sneeuberg area (Graaff Reinet, Wellwood, and Cranemere; See Rowntree, 2013)

2.6 DISCUSSION

2.6.1 Perspectives on gullying

The nature of gully genesis, i.e. human influence as opposed to changes in the natural environment, is still debated in South Africa, as in many other parts of the world (Stankoviansky, 2003; Parkner et al., 2007; Dotterweich et al., 2014; Shellberg et al., 2016). Different synopsis for gully origin is valid due to varying physiographic and climatic properties. Origin studies in South Africa, however, mainly provide a localised narrative and should be expanded regionally to strengthen our understanding of gully evolution; moreover, further investigations in areas with conflicting origins of gullies in proximity, such as the Sneeuberg (Grenfell et al., 2012; Boardman, 2014) are needed.

Despite the different views on the origins of gullies, there is overwhelming evidence - irrespective of the authors' academic background - that contemporary gully erosion in South Africa is accelerated by anthropogenic activities (similar to global findings in a review from Castillo & Gómez, 2016). The anthropogenic impact in South Africa is highlighted by a 100-fold increase in soil erosion for the Orange River catchment (77% of South Africa) between 1939 and 1969 compared to the Holocene (Compton et al., 2010). The removal of vegetation from poor grazing strategies, including overgrazing, is the predominant factor resulting in gullying in South Africa, regardless of land tenure. Intensification of cultivation and burning, both associated with commercial farming practices and communal areas, are also main drivers. The positioning of roads and road culverts is the main non-farming anthropogenic factor accelerating gully erosion.

While land susceptibility and climatic perturbations alone have rarely been advocated as accelerating gullying in South Africa, it does affect the potential for erosion, constraining or enhancing gully severity once the gully process begins. Land susceptibility, especially with regards to rock type (sedimentary strata of Elliot group and the Tarkastad and Adelaide subgroups of the Beaufort formation) and soil (dispersive, duplex, and poorly consolidated deep soils), is likely a key contributor to the W-E imbalance of erosion in South Africa, with higher gully severity in central to eastern parts of the country. However, detailed analysis of soil as an individual causal factor in gully erosion in South Africa remains scarce. In all likelihood, soil is understudied and thus under-represented in the importance of driving gully erosion (Figure 2.10).

Although human activities mainly cause accelerated gully erosion, human intervention has also successfully rehabilitated previously gullied areas (Garland & Broderick, 1992; Meadows, 2003). Gully mitigation measures have mostly been initiated by government actors, with private undertakings being seemingly more limited. In South Africa, there is currently no agreement on how, and occasionally even if, gullies should be rehabilitated. Examples include Pulley et al. (2018), that argues that human mitigation interference should be minimised as gullies may evolve into wetlands, and contrasting attitudes toward short-term high-density grazing (Keay-Bright & Boardman, 2007; Orr et al., 2008; Bennetto, 2019). Nonetheless, it is the authors' opinion that favourable perceptions of gully erosion are the minority, and acceptable solutions to mitigate gullying should be sought. Research focussing on gully rehabilitation and mitigation measures in South Africa remains scarce (Keay-Bright & Boardman, 2007; Schmiedel et al., 2017), mainly consisting of mere mentions of efforts employed.

2.6.2 Regional trends

Gully erosion in South Africa is a highly complex and variable phenomenon in its spatial occurrence, temporal (re)activation and stabilising cycles, and the interplay of anthropogenic and natural driving factors. Gully occurrence in South Africa, like global findings (Castillo & Gómez, 2016), is not confined to specific preconditions, land-use, or tenure. Unexpectedly, in nature and wildlife reserves where attempts are made to restore land to its original state, gullying continues to be stubbornly active (Brady, 1993; M Fitchet, professional game ranger, personal communication, November 2021). The lag time, found between the moment the main driver of gullying is neutralised to gully stability, remains poorly understood. Keay-Bright & Boardman (2007) made a similar finding when grasses on the interfluves of badlands showed little response to destocking. Sequential erosion rates may be one way to monitor and compare sites from different geographic locations.

Few study sites in South Africa explicitly present gully erosion rates, although the W-E spread portrays important differences in gully severity. To provide a comparative measure of gully intensity in South Africa, we compare gully activity (Table 5) with two soil loss thresholds (Mcphee & Smithen, 1984; Reinwarth et al., 2019), a modelled soil loss rate on a national scale (Le Roux & Sumner, 2013) and global gully data that shares geomorphic similarity to the research site of interest (Figure 2.12). The two thresholds consist of sustainable soil loss tolerance estimated

between 5 t ha^{-1} y^{-1} to 10 t ha^{-1} y^{-1} (Mcphee & Smithen, 1984) and a natural baseline calculated as 0.01 t ha^{-1} y^{-1} to 0.64 t ha^{-1} y^{-1} (Reinwarth et al., 2019).

In the Swartland, western South Africa, gully erosion is currently stable after intense gullying in the 1930s. The triggering and stabilising of gully erosion were strongly influenced by human activities, driven by policies and politics. In the 1930s, cultivation intensification linked to the Wheat Importation Restrictions Act (1930) and incorrect farming methods, such as ploughing up and down the slope, caused severe gully erosion (Meadows, 2003). By the 1990s, however, gully extent had reduced by 85% (Morel, 1998). Although a reduction in annual rainfall may also have promoted a decrease in gully activity (Morel, 1998), the reduction was mostly attributed to soil conservation measures proposed by Talbot (1947). With the help of government subsidies, 25000 km of contour banks were constructed (Meadows, 2003), which Steudel et al. (2015) demonstrated would inhibit erosion (for other soil conservation methods, see Talbot, 1947).

Stability was later confirmed by Olivier et al. (2018; 2019), who found active gully processes, but no evident increase in extent and a negligible 0.003 t ha^{-1} y^{-1} soil loss rate. The rate is significantly lower than the national soil loss prediction (Le Roux & Sumner, 2013) and the natural baseline (Reinwarth et al., 2019) described in South Africa (Figure 2.12a). Compared to similar global geomorphic sites, the soil loss in the Swartland is appreciably lower, for example, soil loss measured in a discontinuous gully (0.1 t ha^{-1} y^{-1} New South Wales, Australia by Crouch, 1990) and where soil conservation methods were successfully implemented (5 t ha^{-1} y^{-1} to 2 t ha^{-1} y^{-1} and in Wisconsin, USA by Trimble, (1999) (Figure 2.12a). If the Swartland case study can be considered representative of the western Western Cape, the current gully evolutionary trend is stabilisation.

In the Karoo, gully origin narratives differ, but human influence has been advocated more strongly (Boardman et al., 2003; Keay-Bright & Boardman, 2007; Rowntree, 2013). For example, in a long-term localised study in the Sneeuberg, vegetation disturbance from the occupation and farming practices of European settlers was argued as the leading cause of gully development (Boardman et al., 2003; Boardman, 2014). Covering a more extensive area by reviewing published material from farmers in an agricultural journal, Rowntree (2013) made a similar finding of gully origin in the Karoo.

Gullies, including badlands, were deemed to have formed prior to 1945, mostly from overgrazing (Keay-Bright & Boardman, 2006). Although active gullies were found, valley-bottom gullies were deemed stable from a temporal aerial photograph analysis (Keay-Bright & Boardman, 2006). Similar Karoo gullies elsewhere were estimated to produce soil loss well below the sustainable tolerance (Schmiedel et al., 2017). Likewise, Rowntree & Foster (2012) found soil loss from gullies to be negligible, primarily acting as conduits for hillslope and badland sources from the 1940s. Contrastingly to the valley bottom gullies, estimations from badlands indicate continued high soil losses of up to 123 t ha^{-1} y^{-1} from the long-term study in the Sneeuberg by Boardman and colleagues (Favis-Mortlock et al., 2018) (Figure 2.12a). European badlands have more severe soil loss levels, likely due to higher rainfall and being a different typology, for example, 200 t ha^{-1} y^{-1} and 302 to 455 t ha^{-1} y^{-1} reported in France (Bufalo & Nahon, 1992) and Spain (Martínez Casasnovas & Poch, 1998) (Figure 2.12a) respectively. If the above work is representative of the greater Karoo, the contemporary evolutionary stage of gullying is mature. Upslope badlands are a continued source of severe erosion, while inactive valley bottom gullies provide effective connectivity pathways for sediment.

Towards the east, in the Grasslands biome situated in the eastern Eastern Cape and KwaZulu-Natal, the common impression is that the former homelands, an area under communal tenure, are heavily degraded, accompanied by a high gully incidence. Studies in this database, especially the map produced by Mararakanye & Le Roux (2012) and the national review of Hoffman & Todd (2000), confirm this impression. Degradation and gullying are proposed to have accelerated due to the apartheid government, which forcibly removed persons and located them in homelands (Hoffman & Ashwell, 2001). The relocation of a large number of persons to a confined area resulted in high anthropogenic pressures (Meadows, 2003) in a region that exhibits preconditions suited to erosion. Sumner (1957; in Laker, 2004) indicated that organic matter is the only aspect related to the structure of soils overlaying the Beaufort and Ecca groups and that any structural integrity is lost when this organic matter is removed.

With an increase in population, organic matter would have been lost from deforestation for fuel (Grellier et al., 2012) and overgrazing (Dollar & Rowntree, 1995). Overgrazing has a dual effect due to animals removing vegetation by feeding and compacting soil along their trackways, augmenting gully development at sidewalls and headcuts. The compaction can cause fluvial incision or bank gullying due to an increase in surface runoff or cause soil cracking as vegetative

growth is retarded, leading to slumping at gully sidewalls or headcuts (Brady, 1993). Abandoned cultivated fields in homelands do not show the same vegetation rebound as in the Mediterranean countries (Cerqueira et al., 2022), and bare soil is left unprotected with mitigation structures, such as contour banks, not being preserved and cattle free to graze (Kakembo & Rowntree, 2003). Land susceptibility to gully erosion here is high due to duplex soils with high dispersion capacity (for example, communal areas in the Tsitsa in the Eastern Cape in Le Roux et al., 2022) and deep unconsolidated colluvium and re-eroded material (for example, in the Mkomazi catchment in KwaZulu-Natal in Flügel et al., 2003). Gully occurrence is thus high, often having very large dimensions and can be located in proximity (Mararakanye & Le Roux, 2012; Le Roux et al., 2022).

Soil loss from gullying measured in the communal areas in the former homelands situated in KwaZulu-Natal varied from 2.3 t ha^{-1} y^{-1} to 25.7 t ha^{-1} y^{-1}, contributing between 1.40% and 73.03% (Table 5) of the soil loss predicted by Le Roux et al. (2008). These estimates, however, are only partial as they either focus on gully wall retreat (Chaplot et al., 2011; Chaplot, 2013) or headward retreat (Grellier et al., 2012). A more accurate estimation could therefore be closer to 30 t ha^{-1} y^{-1}, which is three times the sustainable soil loss rate for South Africa.

The communal land tenure in South Africa is distinct and has few comparable global data points (Figure 2.12a). However, the headward retreat rates from Grellier et al. (2012) can be compared to a global headward retreat dataset compiled by Vanmaercke et al. (2016) (Figure 2.12b). The comparison shows that soil loss from headward retreat in the communal areas of the former homelands in South Africa plots in the upper quartile range of global data, signifying its severity. The current evolutionary trend is that gully erosion in the former homelands is severely active.

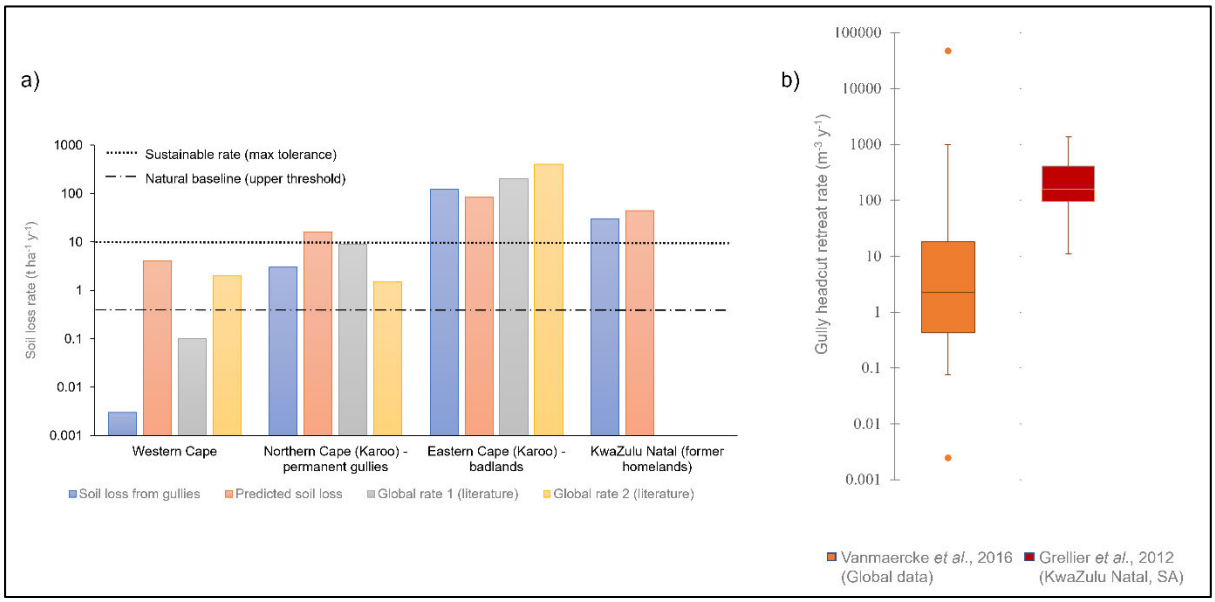

Figure 2.11 Contextual soil loss rates from gully erosion in South Africa: a) Soil loss rate from gully sites with predicted soil loss at the site from Le Roux et al. (2008) and two global sites with similar gully type or landscape, with natural baseline rate (Reinwarth et al., 2019) and sustainable rate (Mcphee & Smithen, 1984) for reference; b) Boxplot indicating global gully headcut retreat rates from Vanmaercke et al. (2016) in orange (n = 672) and KwaZulu-Natal gully headcut retreat rates from Grellier et al. (2016) in red (n = 15).

2.6.3 Gaps in gully research, in South Africa and beyond

Knowledge gaps in South Africa gully research with global relevance include 1) the impact of environmental change on gullying; 2) quantifying sediment yield from gullying; 3) how subsurface flow architecture influences gully occurrence; and 4) the implementation of gully mitigation measures to assess efficacy and service life thereof.

Gully erosion is expected to increase under climate change conditions (Poesen, 2018), globally and in South Africa. This assumption is highlighted by a global study that calculated headcut retreat to increase up to 300% (Vanmaercke et al., 2016). In South Africa, similar predictions have been implied: Meadows (2003) warned that relic gullies in the Swartland may be reactivated, while Boardman et al. (2017) indicated that climate change (essentially an increase in RDN) may overtake anthropogenic activities as the main driving factor of gully erosion in the Karoo. In addition, land-use changes that have been shown to cause gully erosion (Galang et al., 2007; Li et al., 2021) may further exacerbate gully erosion with climatic changes. Thus, there is an urgent need for computational gully erosion models to allow comprehensive investigations into gully

erosion dynamics, including assessing the impacts of environmental change conditions on gully erosion. However, model development and field data collection must complement each other to achieve simulation results that can be calibrated and validated.

Establishing reliable models will also help to determine sediment yield from gully erosion (Poesen, 2018), a parameter that is scarce in global gully erosion literature (Castillo & Gómez, 2016). Most sediment yield models overlook gullying as they cannot predict the range of subprocesses related to gullying (Poesen, 2018). Estimating sediment yield from gullying is thus often addressed separately. Different methodologies, albeit contentious, are often used, for example, Le Roux (2018) used an estimation of connectivity of gullies from a gully inventory in the Tsitsa catchment in South Africa, while Flügel et al. (2003) followed an evolution modelling approach (developed by Sidorchuk, 1999) of a representative gully in the Nzinga catchments in South Africa, while Ndombda et al. (2009) used a delivery ratio founded on gully morphology and age in Nyumba Ya Mungu catchment in Tanzania. Further research is required to improve our understanding to build toward successful, validated modelling of sediment yield: for example, measuring controls on gully connectivity, establishing soil loss sediment yield ratios for different environments, identifying locations and causes of temporary sediment stores, and elucidating the magnitude of storm events that would flush the sediment stores.

The role of piping in gullying is still poorly understood (Castillo & Gómez, 2016), hampering modelling of gully erosion and estimations of sediment yield. Numerous gully erosion studies worldwide report piping as a process affecting gullying. However, few of these studies investigate the mechanisms and contribution of piping towards gully evolution in detail (Bernatek-Jakiel & Poesen, 2018), despite some of the worst eroded areas in Europe (Faulkner, 2006) and South Africa (Le Roux et al., 2022) being affected by piping. In South Africa, a rare detailed study was conducted in the Eastern Cape and KwaZulu-Natal by Beckedahl (1996), but this impressive work should be continued and expanded to other regions. Particular attention for future research should be given to quantifying the impact of piping on new gully formation and expansion. The longevity of the impacts of piping should also be investigated, as Vanderkerckhove et al. (2000) found that piping-induced gullying diminishes after a certain period, but in a more humid setting in South Africa, it seems to be a continued source of expansion (Brady, 1993; Le Roux et al., 2022).

Additionally, dispersive soils in which piping occurs may reduce the effectiveness of gully rehabilitation measures commonly used to promote infiltration (Frankl et al., 2016). Gully

rehabilitation has been undertaken in several countries (for example, Pathak et al*.,* 2006; Rey and Labonne, 2015; Wilkinson et al., 2022; Yang et al., 2019). However, the long-term efficacy thereof (most studies are short-term) and the impacts on sediment yield reduction (very few studies measure this) are still poorly understood globally (Bartley et al., 2020). Further research is required to establish "best practice" guidelines to identify the optimal zones (above the gully catchment vs inter-gully applications; or a combination of both) and type of application for each zone (structures, revegetation, or both), the expected life expectancy, and the potential impact on sediment yield for specific environments and gully types.

Such guidelines would help identify whether, for example, successful rehabilitation strategies applied at the Burdekin catchment in Australia (Wilkinson et al., 2022) can be transferred to the Tsitsa catchment in South Africa. There is a morphological difference in size, shape, and geo-environmental setting (see Brooks et al., 2009 and Le Roux et al**.,** 2022). In terms of application, Van Zijl & Ellis (2013) caution against the use of commonly applied rehabilitation methods such as contouring and check dams (as was used effectively in the Swartland; see Morel, 1998) in dispersive soils. These structures will promote free water accumulation in the soil, accelerating piping-induced gullying. However, Frankl et al. (2016) showed that check dams could be used successfully (and promote more acceptance) if one additionally inserts a vertical geomembrane to create a sub-surface dam. In South Africa, the focus should be on applying acceptable rehabilitation techniques that promote indigenous vegetation, local knowledge, and involvement. The severely degraded homelands that are located on dispersive soils, where some of the most extensive gullying occurs in South Africa, need the most urgent attention to see if and how these gullies can be rehabilitated. Continued research should also be afforded to the Karoo, where badlands remain severely active and revegetation (identified as the main parameter in gully rehabilitation for long-term gully control; Frankl et al., 2021) struggles (Keay-Bright & Boardman, 2007). Piloting fast-growing, drought-tolerant spekboom (in various forms, *viz*. seedlings and sprouts) in these areas where revegetation is problematic could be investigated (Panter & Ruwanza, 2019). Although valley bottom gullies are considered stable, primarily acting as conduits for hillslope sources (Rowntree, 2013), rehabilitation efforts should also continue here, to trap sediment and water, to reduce sediment yield and allow water to infiltrate that will hopefully promote easier revegetation.

Two South African-specific shortcomings include the lack of research on ephemeral gullying and investigating gullying in homelands that exhibit varying geo-environmental variables. Gully research in South Africa exclusively focusses on large permanent gullies. In other parts of the world, ephemeral gullying has been shown to produce up to 94% of soil loss within agricultural catchments (Poesen et al., 2003); there is thus a need to see how this finding compares to South Africa. Future studies could be aimed at finding the geographical location and estimated soil loss of such gullies in South Africa, especially in major agricultural regions.

Although much research has been done on degradation, most gully erosion research focusses on the eastern Eastern Cape and KwaZulu-Natal. Research needs to be expanded to other former homeland areas that are situated on different lithologies to enquire whether communal tenure, in general, is associated with gullying or only where land susceptibility to erosion is high. Research considering multiple sites in former designated homeland areas should preferably combine quantitative and qualitative methodologies to incorporate local knowledge and ensure that suitable sites are compared.

2.6.4 Proposed methodological approaches and technology for expanding gully research

Despite an increase in gully erosion specific studies since 1988, they remain limited and sparse (n = 53), nucleated around areas in the Karoo and former homelands in the Eastern Cape and KwaZulu-Natal. Gully erosion should become wider studied, expanding to other environments and regions not yet studied. Most studies have focussed on *Causal factors, processes, and impacts*. This focus should remain, especially when new environments are investigated. Preferably this should be completed in conjunction with the quantification of soil loss and focusing on more long-term studies (>10 years), which have been lacking in South Africa. An increase in the quantification of gullying will result in more data points, which can be analysed to find trends of gully occurrence and environmental variables (like Figure 8). Aerial imagery, which in South Africa can be relatively easily obtained and mostly has a high temporal and spatial resolution, should be reinstituted.

By using aerial imagery, baseline long-term retreat rates can be calculated, quantifying soil loss (for example Grellier et al., 2012). Extrapolations can also be made with regards to factors causing gullying, although care must be taken as aerial imagery only yields a snapshot of change that occurred since the previous image. It would be useful to couple this with qualitative methods such

as interviews (Keay-Bright & Boardman, 2007), workshops (Hoffman & Todd, 2000), or participatory mapping that may highlight evolutionary gully changes between imagery snapshots. Alternatively, the combination with high-temporal resolution satellite imagery (for example, Sentinel-2), although a lower spatial resolution than the aerial imagery, may yield interesting results with regard to inter-seasonal erosion. The focus, however, will be compelled to be on large permanent gullies due to the spatial resolution of Sentinel-2.

Unmanned Aerial Vehicles (UAVs) can offer a higher spatial resolution cost-effectively and be employed to survey gullies temporally but have been limited to work by Grellier et al. (2012) and Le Roux et al. (2022) in South Africa. Internationally, UAVs have been shown to be a valuable tool for investigate gully erosion from its imagery (Kariminejad et al., 2019), derived Structure from Motion DEMs (D'Oleire-Oltmanns et al., 2012; Koci et al., 2017), and when combined with other remotely sensed data sets (Wang et al., 2016) or terrestrial imagery (Stöcker et al., 2015). The application of UAV technology in South Africa should be explored further to understand the temporal evolution of gullies and event-driven erosion from repeat imagery. The possibility of using UAVs as a community science project should be probed as farmers start incorporating UAVs in farming. If successful, the community science project would allow inter-annual frequency imagery and possibly insight into seasonal gully evolution.

Repeat UAV imagery can also be used to monitor gullies, especially in areas with high gully susceptibility, and to assess the effectiveness of any rehabilitation methods. However, assessing repeat images will require mapping manually or semi-automatically. Generating a semi-automated methodology would be beneficial as it could yield fast and repeatable mapping, irrespective of the user. However, the heterogeneity of the spectral reflectance of gullies (King et al., 2005) may inhibit detection from RGB or multispectral imagery, having additional complexity if repeat imagery is captured during different seasons. A gully's distinct morphology can be successfully used for the successful detection of gullies (Castillo et al., 2007; Olivier et al., 2022) and thus applied to UAV-generated DEMs. Further testing of this is, however, required. In South Africa, these methods can be applied to environments exhibiting different geo-environmental properties, for example, along the E-W climate gradient of South Africa, to test the accuracy and transferability of semi-automated detection methods.

Long-term data, coupled with inter-annual data from remote sensing or qualitative work, would provide better insight into the dynamics of gully perturbations. This improved understanding could

be used to investigate the modelling of gully erosion in South Africa, an endeavour that has rarely been attempted. Innovative gully modelling approaches were used by Flügel et al. (2003) and Le Roux (2018) to account for gully sediment yield. Both models are good approximations, but the model of Le Roux (2018) is static, while Flügel et al. (2003) use the approach from Sidorchuk (1999) that proposes the gully process is of high frequency and soil loss initially, whereafter it dissipates and stabilises. Neither model can account for the cyclical nature of gullying captured in temporal studies in South Africa (Figure 8). We thus require models that can predict gully evolution and estimate soil loss, considering the cyclical nature thereof, as well as the impact of inherent control factors such as dolerite intrusions, soil dispersibility, and changes in inter-annual vegetative cover.

2.6.5 Limitations of intersecting views of gullying

This paper reviewed gully erosion in South Africa with a focus on gully-specific studies. More general soil erosion research was used for contextual purposes only. The core DONGA database consisted of 53 papers, with few retrieved white papers or governmental research institutional additions. Although limited in scope, we believe that the database provided a good representation of the current state of gully erosion in South Africa. Unfortunately, certain areas are most likely underrepresented in the gully erosion database, for example, the Free State – although gullying does occur here as per the national gully map of South Africa (Mararakanye & Le Roux, 2012) and as shown by a mapping procedure for soil erosion, which included specific symbology for active and inactive gullying (Thwaites, 1986).

2.7 CONCLUSION

In this review, we intersected perspectives of fragmented gully erosion-specific studies in South Africa to provide insight into a national dimension of the phenomena. Gully erosion in South Africa transcends climatic, geomorphic, and land-use boundaries. Regionally, gullies are at various stages of evolution, with different temporal timings of (re)activation or stabilising. Anthropogenic factors appear to be the principal cause of regional evolutionary changes.

Sites depicting soil loss rates from gullying are sparse and scattered in South Africa. Although we can make inferences from the existing sites, expansion to areas with limited coverage is required. From the sites reporting on soil loss rates from gully erosion, it was evident that human interference

can cause but also halt and reverse gully erosion. Moreover, contemporary gully erosion remains a concern in the Karoo and is alarming in communal areas in KwaZulu-Natal. In these communal areas, displaced persons are forced to live from the soil while facing glaring population pressure. The physiographic properties of the region are prone to erosion, resulting in human interference exacerbating gullying. The implementation of mitigation and rehabilitative measures here is urgent, but we need to augment methods with indigenous knowledge to ensure cost-effectiveness and acceptability. Rehabilitation measures should also be site-specific and should be designed to account for local perturbations that are driving gullying – the measures implemented in the Swartland may not necessarily be good or acceptable to communal areas.

The identified South African-specific research gaps include a paucity of sites exploring medium- to long-term soil rates and related triggering events South Africa. While "old" technology, such as historical aerial imagery, could be utilised, newer technologies, such as Sentinel-2 and UAV imagery, should be adopted more readily. Another shortcoming, most likely due to the scale of imagery used in South Africa, is the disregard for ephemeral gully research. In numerous countries (European, Asian, and American), ephemeral gullying is an important sediment source that reduces agricultural production capacity; it is, therefore, important to probe this finding in regions of South Africa. Identifying the geographic location and severity of this type of gully erosion requires immediate attention.

This national scale review also identified research gaps that have global relevance. Firstly, the impact of environmental change on gully erosion has rarely been investigated. Models, supported by accurate and standardised field information, are required to comprehensively assess the implications of environmental change on gully evolution on storm, annual, and decadal timescales. Secondly, the influence of subsurface water flow on gully erosion remains poorly constrained. More work is required here and should be coupled with a strong soil analysis. Incomprehensibly, detailed soil observations and analyses remain scarce in our search for understanding the destruction of our natural resources from gully erosion.

CHAPTER 3: PREDICTING GULLY EROSION SUSCEPTIBILITY IN SOUTH AFRICA BY INTEGRATING LITERATURE DIRECTIVES WITH REGIONAL SPATIAL DATA

3.1 ABSTRACT

Gully erosion has been identified as a severe land degradation process with environmental and socio-economic consequences. Identifying areas susceptible to gully erosion will aid in developing strategies to inhibit future degradation. Various approaches have been implemented to predict and map gully erosion susceptibility but are mostly restricted to small geographical extents due to process limitations. Here we introduce a novel method that predicts gully erosion susceptibility on a regional-/ national-scale (1.22 million km^2) by synthesising literature directives with a statistical approach. Findings from a literature review were used to extract physiographic properties associated with gully erosion that was conditioned to characterise susceptibility by using the Frequency Ratio model. The conditioned physiographic properties were aggregated by a weighted overlay procedure using an aggregation of controlling factors derived from the literature review as a weighting system. The Gully Susceptibility Index (GSI) model was validated against a published gully inventory map (n=163019) and randomly generated 1 km^2 tesselation zones from which primary validation data was derived. Although uncertainties within the modelling procedure exist (for example, gully site distribution, the spatial resolution of input data, and determination of gully points), the validation shows that the GSI model is generally robust, identifying areas of contrasting susceptibilities. Furthermore, findings converge with other susceptibility metrics, which have been derived by different methodologies. Since empirical gully erosion research has been conducted worldwide, this model could be applied to regional-scale gully susceptibility modelling assessments (as a solitary method or combined with primary data) in other parts of the world. Additionally, the GSI model can be adopted to model environmental change scenarios.

3.2 INTRODUCTION

Gully erosion is a form of channelised water erosion, which range in size from small drainage patterns on agricultural land that can easily be filled with conventional tillage methods (for example Zhang et al., 2007; Wells et al., 2016), to dramatic landscape scars several meters in depth and width (for example Hudec et al., 2005; Brooks et al., 2007) (Figure 1). Irrespective of their appearance, gullying has been shown to be the dominant erosive form when active in a catchment (Wu et al., 2008; Shellberg & Brooks, 2012), comprising up to 94% of total soil loss when considering world data (Bennett et al., 2000; Poesen et al., 2003). Soil loss incurred from gully erosion affects land and water resources resulting in environmental and socio-economic pressures.

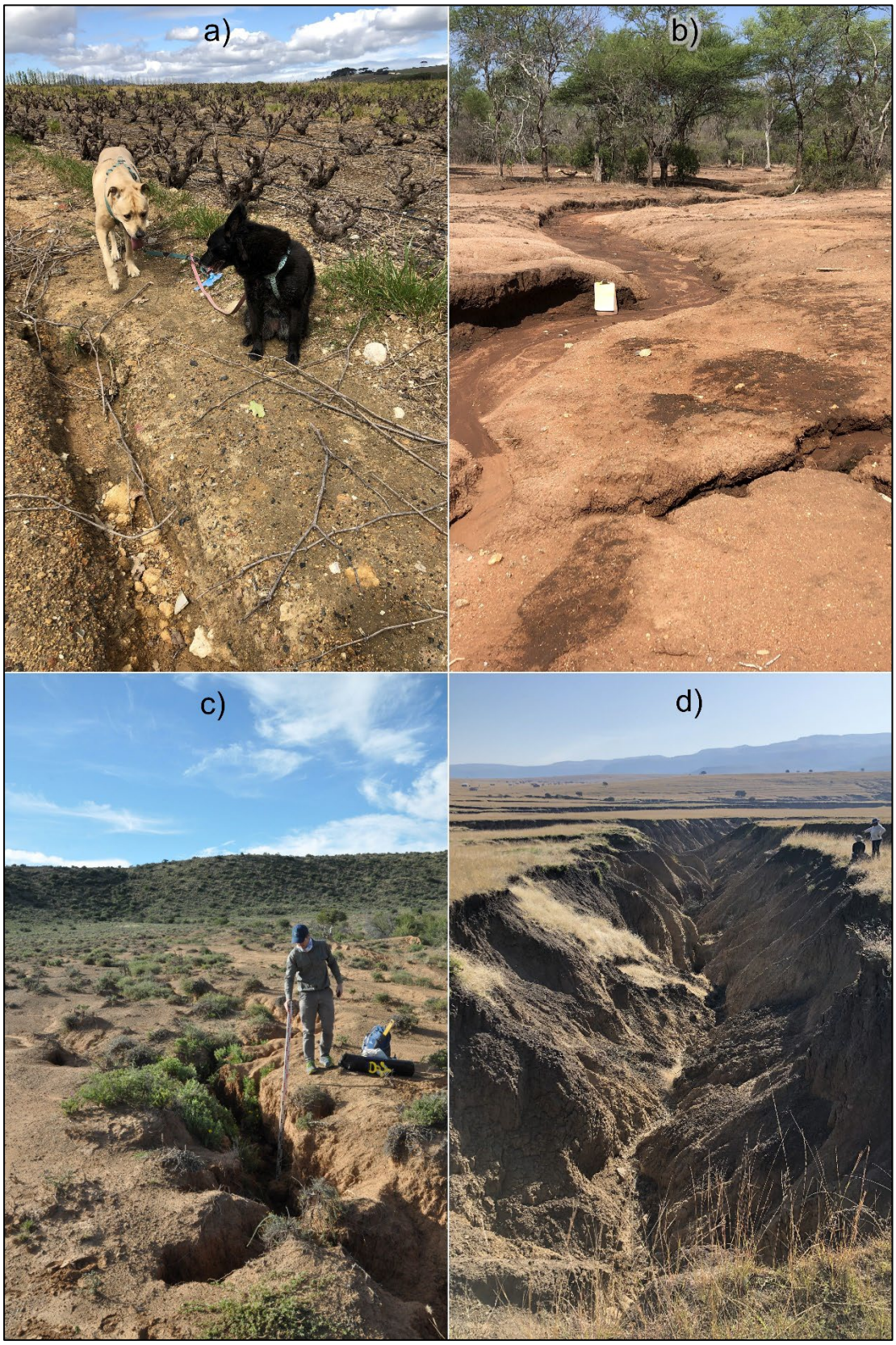

Figure 3.1 Examples of gullies found in different land-uses and varying levels of magnitude in South Africa: a) a gully in proximity to a bush vine vineyard in the Cape Winelands, Stellenbosch; b) a sinuous gully on a private

game reserve in the Savanna biome in the Lowveld, close to Ofcolaco; c) a deep narrow gully found on rangeland in the Karoo, close to Graaff Reinet; d) a mother gully found in the Grasslands biome where communal tenure is practiced, close to Nqanqrhu (photographs by George Olivier [a,b,d] and Marco Van De Wiel [c]).

Mapping gully features can show the distribution thereof and be used to indicate vulnerability to gullying (Vanmaercke et al., 2021). Large gully inventories from manual mapping (gully location mapping) are scarce due to the labour-intensive workflow (Mararakanye & Le Roux, 2012), while results are influenced by image resolution and interpretation of the cartographer. Mapping gully susceptibility provides an indirect means to assess vulnerability and can overcome the limitations associated with manual mapping. A susceptibility index considers critical control factors associated with gully erosion to estimate the probability of future gullying and does not directly map the gully perimeter. Nevertheless, such a map should identify gully-prone areas where mitigation and rehabilitation works can be focused (Le Roux & Van der Waal, 2020).

Gully susceptibility mapping makes use of conditioned factor maps as input. Determining the input factors is critical as it needs to represent the factors, which can work independently or synergistically, to control gullying. Lithology, soil, rainfall, topography, and anthropogenic influences should be considered as they are the main factors exerting a control over gully processes (Poesen et al., 2003; Valentin et al., 2005; Castillo & Gómez, 2016) due to their capacity to increase soil erodibility and /or concentrated surface or sub-surface water flow (Patton & Schumm, 1975; Nordström, 1988; Bocco, 1991). The rock type of parent material can exert an influence on the physical and chemical properties of a soil, controlling erodibility (Laker, 2004) that affects gully susceptibility (Rienks et al., 2000), morphology (Imeson & Kwaad, 1980; Shellberg & Brooks, 2012), and the dominant erosive process (Bernatek-Jakiel & Poesen, 2018). Rainfall characteristics exert a control over gullying (Vanmaercke et al., 2016) due to its impact on concentrated surface and sub-surface water flow, while the distribution of rainfall also impacts antecedent soil moisture affecting the erodibility of a soil (Anderson et al., 2021). Topography directs water flow from rainfall, therefore, regulating the volume and velocity of concentrated flow, affecting gully susceptibility (Parkner, et al., 2006; Gómez-Gutiérres et al., 2015; Rossi et al., 2015). Overwhelming evidence suggests that anthropogenic activities are accelerating gully erosion (Castillo & Gómez, 2016; Olivier et al., 2023a). Human influences that expose gully-prone pre-conditions and/ or increase concentrated overland flow, include land-use change to farming (Boardman et al., 2003; Zucca et al., 2006), commercial farming intensification (cultivated and

rangelands) (Talbot, 1947; Shellberg & Brooks, 2012), population pressure in communal areas resulting in deforestation and overgrazing (Grellier et al., 2012; Le Roux & Sumner, 2012), abandonment of cultivated fields (Kakemo & Rowntree, 2003; Lesschen et al., 2008). Infrastructure and movement corridors have also led to gullying, for example, roads including road culverts (Moeyersons et al., 2015; Seutloali et al., 2016), and footpaths (both from animal and humans) (Le Roux & Sumner, 2012; Nir et al., 2021).

Lithology (Dewitte et al., 2015; Saha et al., 2020; Azedou et al., 2021) and soil (Shit et al., 2015; Rahmati et al., 2016; Domazetović et al., 2019) classification maps are frequently used as input factor maps. Topographical factors are generally used as multiple inputs consisting of first (slope and aspect) and second order terrain derivatives (curvature). Additionally, terrain derived hydrological parameters such as stream density, distance to stream, contributing drainage area, SPI, and Total Wetness Index (TWI) (see Lucà et al., 2011; Dewitte et al., 2015; Gómez-Gutiérrez et al., 2015; Rahmati et al., 2016; Rahmati et al., 2017; Garosi et al., 2018; Domazetović et al., 2019; Saha et al., 2020; Azedou et al., 2021). Anthropogenic activities are mostly represented by land-use/ land-cover maps (Lucà et al., 2011; Rahmati et al., 2017; Azedou et al., 2021). Rainfall and climate inputs are rarely used as inputs (Arabameri et al., 2019; Nhu et al., 2020) because there is generally not enough climatic variability within the geographical extent in which gully susceptibility mapping is applied to justify inclusion.

Several methods exist to aggregate the conditioned factor maps to produce gully susceptibility maps. These mapping procedures can be divided into three broad categories (Arabameri et al., 2020): 1) Multi-Criteria Decision Making (MCDM), 2) statistical methods, and 3) machine learning. MCDM includes Analytical Hierarchy Procedure (AHP) (Arabameri et al., 2019; Domazetović et al., 2019; Makaya et al., 2019). Statistical methods include approaches such as the certainty factor, linear or logistic regression, frequency ratio, weight of evidence, and index of entropy (Lucà et al., 2011, Conoscenti et al., 2014; Dube et al., 2014; Dewitte et al., 2015, Rahmati et al., 2016, Garosi et al., 2018, Zabihi et al., 2018). Machine learning algorithms include procedures such as Support Vector Machine, random forest, Naïve Bayes, artificial neural networks, maximum entropy, classification and regression trees (Taruvinga, 2008; Eustace et al., 2011; Garosi et al., 2019; Hosseinalizadeh et al., 2019; Phinzi et al., 2020; Pourghasemi et al., 2020; Saha et al., 2020). Despite an increase in global gully erosion research, and thus an increase in associated sites where gullying is investigated (Castillo & Gómez, 2016), using existing

literature as a directive to predict gully susceptibility has not been tested to the authors' knowledge. Gullying erosion research sites from literature can be used to train data and compile a factorial database from expert analysis of the main causes of gullying, which can be used as a standardised weighting scale. Furthermore, findings regarding the severity of activity can be implemented as an additional scalable weight. Gully susceptibility modelling from literature directives has the potential to be used as standalone input on a regional scale, depending on the distribution of gully erosion sites in the research area of interest. The impact of climate and rainfall becomes significant at such scales (Vanmaercke et al., 2016), and warrants inclusion, which may also benefit modeling efforts to test gully susceptibility to climate change. Additionally, data mined from literature can be supplementary, and used as additional data points, when conducting a high-resolution analysis on a smaller geographical extent. Data from literature can be readily combined with existing approaches, *viz*. MCDM, statistical approaches, or machine learning.

In this study we test the applicability of using data mined from gully erosion research sites in published literature as training data points to map gully susceptibility on a national scale in South Africa. The mined data will be used to condition input in conjunction with the Frequency Ratio statistic and as weights to aggregate the conditioned inputs to produce the gully susceptibility map.

Our research aims to: 1) capture local physiographic properties associated with gullying from published case studies (land-use/ land-cover, geology, soil, topography) and combine it with global factors (climate) to predict gully susceptibility on a national scale; 2) to validate these findings with an existing gully inventory map for South Africa (Mararakanye & Le Roux, 2012), in addition to fifteen randomly selected zones, each consisting of a singular susceptibility class, $1km^2$ in extent. If successful, this gully susceptibility mapping procedure should be transferrable to other countries even if different geomorphic and physiographic conditions exist and geographic extents vary, provided gully case studies have been conducted there previously.

3.3 METHODS

3.3.1 Study area

South Africa is located on the southern-most tip of Africa between 22°S and 35°S and 15°E and 33°E and is approximately 1.22 million km^2 in extent. Erosion in South Africa is not a recent phenomenon, with King (1963) remarking that gullies are prominent landscape features in the country. Mararakanye & Le Roux (2012) mapped gully features larger than 10 m in dimension from SPOT-5 imagery, finding gullies to be widespread across the region (Figure 2). They found gullies to be prevalent in the Karoo (northern Eastern Cape and southeastern Northern Cape), former homelands areas (eastern Eastern Cape, central North West, northern and southwestern KwaZulu-Natal, south-eastern and north-eastern Limpopo, and along the provincial border of the Free State with the Eastern Cape and KwaZulu-Natal), and in the Grasslands biome in the Free State along the Lesotho border (See Figures 3.2 for mapped gullies, 3a for the geographical extent of the Karoo and former homelands, and 3.3d for the biome classification map). Scattered gullying also occurs in the Western Cape (Fynbos and Karoo biomes), Mpumalanga (Grasslands biome; Figure 3.3d), and the rest of the Northern Cape (Karoo biome) (See figures 3.2 and 3.3d).

Figure 3.2 Mapped gully features in South Africa from SPOT-5 imagery by Mararakanye & Le Roux (2012), overlaid with gully research sites.

Figure 3.3 Study area map: a) introductory map showing areas and lithology locations commonly referred to in text (data sourced from Mucina & Rutherford, 2006; Burger, 2013; Khuthadzo, 2019; and Centre for Geographical Analysis at Stellenbosch University); b) topography (GeoSmart Space, 2020a); c) mean annual rainfall (Schulze & Maharaj, 2006); and d) biomes found in South Africa (Mucina & Rutherford, 2006).

Many of the gullies can be considered as "old". In the Swartland region, Talbot (1947) investigated severe erosion and gullying due to the intensification of cultivation in the 1930s. Gully networks in the Karoo, have mainly been attributed to ox wagon trackways that were developed in the late 19th century (Neville *et* al., 1994), a change to European farming systems, and intensification on rangelands leading to overgrazing in the late 19th and early 20th century (Keay-Bright & Boardman, 2007; Rowntree, 2013). In the former homelands, severe land degradation, including gullying, occurred from population pressures in an environment susceptible to erosion (Hoffman & Ashwell, 2001). Gully erosion, mostly in the north-east of South Africa, has been argued to have an even earlier origin, emerging from climatic disturbances (Temme *et* al., 2008; Lyons et al., 2013).

A recent review by Olivier et al. (2023a) showed contemporary gullying to be a continued concern in South Africa. Gully erosion rates of up to 25.7 t ha^{-1} y^{-1} (Grellier et al., 2012) are documented, which increases to up to 123.7 t ha^{-1} y^{-1} (Favis-Mortlock et al., 2018) when badlands are included. These contemporary erosion rates exceed the upper limits of the South African baseline (0.64 t ha^{-1} y^{-1} by Reinwarth et al., 2019) and sustainable threshold (10 t ha^{-1} y^{-1} by Mcphee & Smithen, 1984) rates established for the country. Currently, contemporary gullying in South Africa, as in the rest of the world, is driven by a complex synergistic relationship between human and natural controls (Castillo & Gómez, 2016; Olivier et al., 2023a).

South Africa exhibits a diversity of natural controls. South Africa has marked rainfall regions, which are dominated by a large summer rainfall region, apart from a winter rainfall region in the west and an all-year winter rainfall region in the SW Cape (Schulze & Maharaj, 2006). Mean annual rainfall exhibits a W-E climate gradient (De Wit & Stankiewicz, 2006), generally increasing from west to east (Figure 3.2c). Arid regions with a mean annual rainfall below 200mm are found in the west, becoming sub-humid to humid in the east where mean annual rainfall can exceed 1000mm (Schulze et al., 2006). The natural vegetation is reflected by the E-W rainfall gradient, consisting of 9 broadly classified biomes (Mucina & Rutherford, 2006) (Figure 3.2b). To the west, the unique Fynbos biome, which consists of small shrubs and succulents, is situated within the winter rainfall region, extending partially into the all-year rainfall region. The succulent Karoo and Nama-Karoo biomes cover much of the arid interior of South Africa, which transitions to the Albany Thicket biome that gives way to Grasslands in the east. To the northeast the Karoo biomes changes to Savanna. The forest biome is interspersed in the all-year rainfall region and the humid east, with the Indian Ocean Coastal Belt biome found on the eastern coastal area.

The natural vegetation in South Africa has been extensively disturbed to make room for agriculture. The agricultural regions closely follow the biomes (Hoffman & Ashwell, 2001; Waldner et al., 2017) (Figure 3.2c). Grains and fruit are found in the west, which transitions to sheep farming in the arid to semi-arid interior. Cattle farming and subsistence farming are found in the southern and south-western Grasslands and Savanna in the north. The Grasslands biome in central South Africa is used for grains, while forestry and sugar plantations are found in the humid east. Vegetables are found interspersed between these agricultural regions in the south and northeast (Hoffman & Tod, 2000).

South Africa has a narrow coastal region, separated from a vast plateau by the Great escarpment (Moore et al., 2009), which is at its highest in the western Drakensberg range (Figure 3.2a). The inland plateau gradually slopes downwards from 1500 m in the east to 1000 m in the west (Hoffman & Ashwell, 2001) and comprises of a sedimentary basin (Moore et al., 2009), with scattered mafic intrusions. The Bushveld Complex is situated in the northeast and comprises of the world's largest mafic intrusion (Maier et al., 2013). Felsic intrusions are also common in the north-east and forms part of the roof structure of the Bushveld Complex (Van Tongeren & Mathez, 2015). Carbonate rich rocks are less common, although a large sequence is found in central north of South Africa.

Soils in South Africa contain a wide range of properties resulting in 73 defined soil forms. These soils are broadly classified into eight categories (Fey, 2010a, b) (Table 1.2 for soil concept and World Reference Base classification system comparison). Duplex soil, often derived from mudrocks in the Karoo basin, has a marked texture contrast in the soil profile. The texture contrast of duplex soil results in permeability differences, which have been demonstrated to be susceptible to erosion (Parwada & Van Tol, 2016; Podwojewski et al., 2020). Glenrosa and Mispah soils are abundant in South Africa. These soils are lithic with distinguishable parent material visible in the B horizon. Lithic type soils have been associated with erosion in South Africa, not due to its common occurrence, but by its position on convex crests and mid-slopes (Fey, 2010a). Structureless red-yellow apedal soil is largely found in the arid north.

3.3.2 Literature directives

Google Scholar and Scopus were used to build a database of gully erosion research in South Africa. The textbook "Geomorphology of Southern Africa" (Moon and Dardis, 1988) was used as the landmark text from which the search started. The keywords used in the search included "gully", "donga", "sluit" (a term occasionally used for gullies in South Africa, and "sloot" (Afrikaans terminology used for gullies). The abovementioned terms were searched individually and combined with the word "erosion". The keyword search was applied to all search fields, but the search was limited to South Africa, excluding other southern African countries. The search was limited to English and Afrikaans texts and was completed on 10 March 2023.

After applying the above search criteria, publications featuring gully erosion as part of their research aim (based on the title and information attained from abstracts) were incorporated into a

database. Hereafter the database was expanded by a backward and forward reference search, adding relevant works missed during the keyword search, including published research with a broader scope that addressed gully erosion. During the backward reference search the reference lists of publications in the database were examined. Scopus was used to conduct a forward reference search to identify studies that cited research works from the database.

The database was used to compile factors indicated to have led to gully formation and controlling factors that played a role in contemporary gullying processes. Several published papers investigated the same area of interest. In cases where one or more of the same researchers were involved in the authorship, gully origin and controlling factors were captured once and edited only if additional factors were identified in the subsequent work. If different researchers investigated the same area of interest, it was considered a new appraisal, and all gully origin and controlling factors were captured.

The location of each gully erosion site was identified from coordinates, maps, and place names provided in the study location descriptions of the papers in the database. A single (x, y) coordinate point, placed at the main gully headcut, was assigned to represent each gully site. The placement of the point at the main gully headcut was derived semi-automatically from a manually digitised polygon of the gully feature. Semi-automated mapping methods of gullies are rarely tested outside the area where they are developed. Therefore, the challenges to upscale and transfer semi-automated mapping methods remain poorly understood. We thus opted to manually digitise gullies to achieve high data accuracy. A single user digitised the gully features on a scale of 1:2000 in Quantum Geographic Information System (QGIS) 3.16.16 using Google Earth images imported as XYZ tiles.

In studies investigating a plot or singular gully network, the whole gully network was digitised. The gully with the largest planimetric area was selected as the representative gully and digitised in study areas consisting of catchment scale extents. The main gully headcut point was derived from the digitised gully network. The mapped polygon was converted to points, spaced at 1 m intervals. The furthest point from the gully outlet, digitised as the line perpendicular to flow where the gully expires, was deemed the main gully headcut location. A sensitivity analysis was conducted by digitising two gullies driven by contrasting processes (subsurface vs surface) five times to assess planimetric areal and gully headcut position changes.

The level of activity at each gully research site was discerned and classified as stable, partially active, or active. The publications were used to extract activity severity information, but where the text refrained from reporting it, the level of activity was determined from Google Earth imagery. The most recent clear image available from Google Earth was compared to a clear historical image acquired ten years prior (or as close to ten years as possible). Gullies were labelled as stable when no extent changes were evident. A gully was classified as partially active when no gully headcut changes were evident and changes to gully wall expansion were limited to 5% of gully length, or depositional features within the confines of the gully were discernable. Gullies with more extensive lateral and linear growth were classed as active.

3.3.3 Susceptibility modelling

Based on the database and a recent literature review of gully erosion in South Africa (Olivier et al., 2023a), five broad categories were identified to include in the susceptibility model, namely: topography, soil, geology, climate, and anthropogenic activities. Seven control factor datasets were selected to represent these five broad categories, all of which were limited to national extents (where spatial resolution is not indicated, the dataset consisted of vector data) (Table 3.1).

Human activities were indicated as a critical driver of gully erosion worldwide (Castillo & Gómez, 2016). In South Africa, the political past has significantly impacted erosion distribution (Hoffman & Ashwell, 2001; Olivier et al., 2023). To spatially accommodate the historical narrative of gullying, a regional agricultural zonal map derived from 1978 data (Khuthadzo, 2019) was implemented as a factor map (Figure 3.4b). Furthermore, a generalised land-use/land-cover class map with a spatial resolution of 30 m (Department of Forestry, Fisheries, & the Environment, 2016) was used to represent contemporary anthropogenic coverage (Figure 3.4a).

Figure 3.4 Factor maps representing anthropogenic factors used in the weighted overlay procedure: a) Land-use/ cover map from 2014 (Department of Forestry, Fisheries, & the Environment, 2021); b) an agricultural zonal map derived from 1978 data (Environmental Systems Research Institute, 2021).

Table 3.1 Specific control factor datasets used per broad category, including its native spatial resolution and source, in addition to the weights derived from the literature database that was used in a weighted overlay to produce the final gully susceptibility map.

Broad category	Local/ Global gully control factor dataset	Native spatial resolution†	Source	Literature derived weighting (in %)
Topography	Slope (in %)	20 m	Derived from GeoSmart Space, 2020a	15.7
Geology	General rock type	1:1000000	Burger, 2013	14.5
Soil	Broad soil classification	1:250000	Land Type Survey Staff, 1972-2006	16.9
Climate	Rainy Day Normal	10’	Calculated from New et al., 2002	7.85
	Aridity	0.01’	Council for Scientific & Industrial Research, 2021	7.85
Anthropogenic	Land-use/ -cover	30 m	Department of Forestry, Fisheries, & the Environment, 2021	18.6
	Agricultural regions (1978)	Vector	Environmental Systems Research Institute, 2021	18.6

† For vector data, the scale was added where possible

Climate is represented through two datasets. Firstly, an aridity index was used (spatial resolution of 0.01'; Council for Scientific & Industrial Research, 2021) as a local climatic factor, calculated from annual rainfall and mean annual temperature. Aridity has been associated with gully erosion due to its impact on protective vegetative cover and rainfall variability (Kakembo & Rowntree, 2003). Secondly, RDN was used as a rainfall intensity proxy. Using a global dataset, Vanmaercke et al. (2016) demonstrated a significant correlation between RDN and gully headcut retreat. RDN was calculated from a 10' resolution long-term (1961-1990) climate data from New et al. (2002), according to equation 1 (Figure 3.5).

$$RDN = \frac{MAR}{ARD} \qquad \text{Equation 3.1}$$

where RDN is Rainy Day Normal;

MAR represents the mean annual rainfall;

ARD is the number of annual rain days

Figure 3.5 Climate input for the weighted overlay procedure: a) Rainy Day Normal, which can be used as a proxy for rainfall intensity; b) an aridity index (Council for Scientific and Industrial Research, 2021).

In South Africa, the relationship between parent material and soil characteristics has been demonstrated as a significant impact to gully susceptibility (Laker et al., 2004). Highly dispersive and duplex soils have a propensity towards gullying and are often formed from the shales and mudstones of the sedimentary Ecca (early to mid-Permian period) and Beaufort (mid-Permian to early Triassic period) groups of the Karoo Supergroup. Parent material was incorporated by generally reclassifying the geology (Burger, 2013) to the most prominent rock type (classification scheme shown in APPENDIX A). A broad soil classification from Land Type Survey Staff (1972-2006) was used to represent the soil factor. Although slope and contributing area are commonly used to identify gully headcut location (Torri & Poesen, 2014), the slope-area concept is strongly related to local environmental conditions, therefore not optimal for regional scale studies (Poesen et al., 2003; Vanmaercke et al., 2021). Additionally, De Geeter et al. (2023) demonstrated that coarser spatial resolution DEMs inflate upslope area resulting in poor gully susceptibility modelling performance. We therefore opted for slope as the topographical control factor, since a preferential topographic zone of gully development has been demonstrated on gentler footslopes, often with unconsolidated deposits or erosion-prone soils (Kakembo et al., 2009; Le Roux & Sumner, 2012). The percentage slope was derived in ArcGIS 10.6.1 from a 20 m spatial resolution DEM (GeoSmart Space, 2020a; their DEM is created using aerial photography and supported by SRTM data in low lying areas) (Figure 3.6).

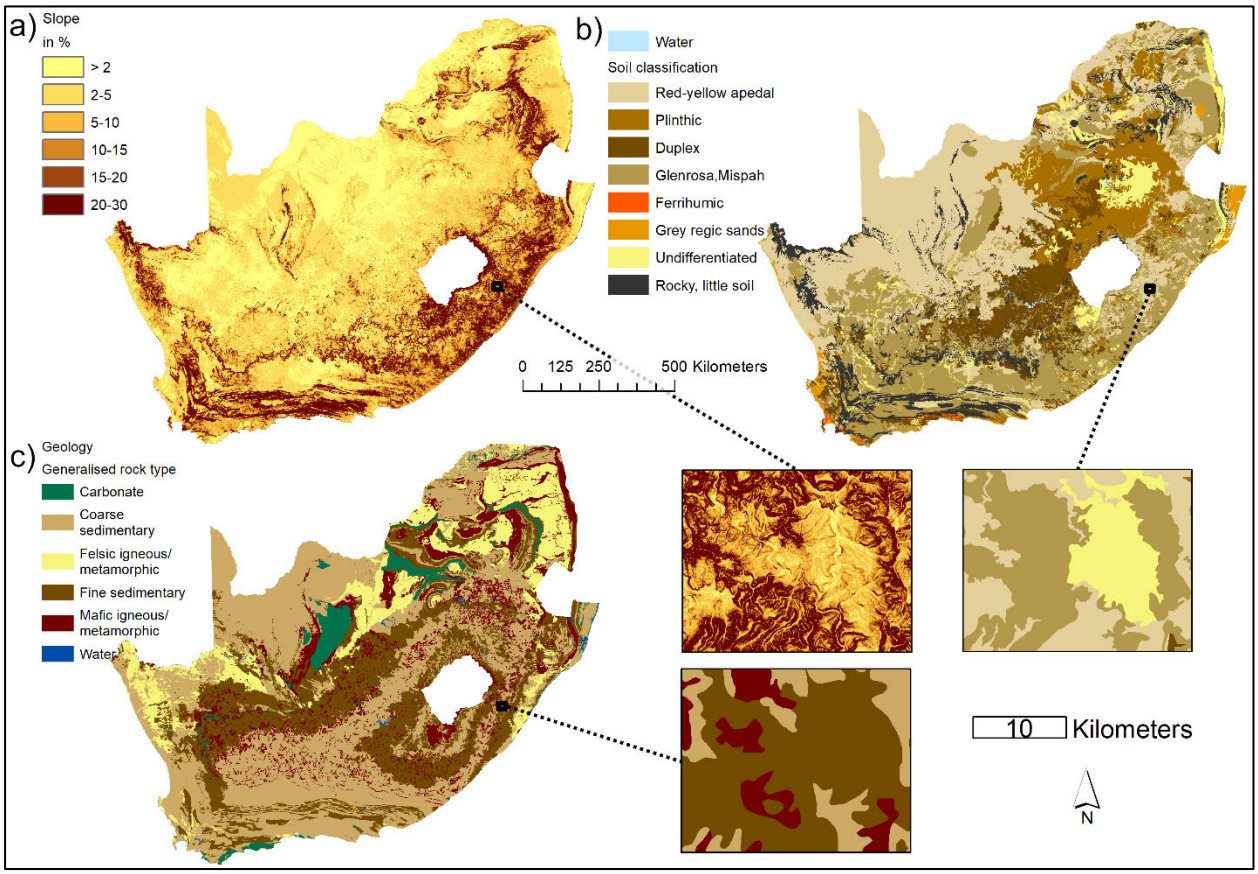

Figure 3.6 Physical precondition factor maps used as input to the weighted overlay model: a) slope (derived from a Digital Elevation Model from GeoSmart Space, 2020a); b) broad soil classification (Land Type Survey Staff, 1972-2006; c) generalised rock type (see APPENDIX A1).

The (x, y) point locations that were semi-automatically determined for each gully site, were overlayed onto the local and global factor maps (Figure 3.4, 3.5, 3.6) to extract the physiographic properties of each gully site. The FR was used to correlate the gully sites (x, y coordinates) with the local and global factors by:

$$FR_i = \frac{\left({}^{G_i}/_{G_{tot}}\right)\times 100}{\left({}^{F_i}/_{F_{tot}}\right)\times 100} \text{ x } Act_i \qquad \text{Equation 3.2}$$

where FR_i is the FR of the i^{th} class of a factor;

G_i is the number of gully sites distributed within the i^{th} class;

G_{tot} is the total gully sites;

F_i is the pixel count in case of raster data or area in case of vector data of the i^{th} class of a factor;

F_{tot} is the total pixel count or area of a factor, dependant of data model and;

Act_i is the average activity of gullies in the i^{th} class quantified according to severity: Stable gullies were scaled as 1, partially active gullies as 1.5, and active gullies as 2.

The FR_i was normalised to a value of one, using:

$$FR^{i\wedge\wedge} = \left(\frac{FR_i - FR_{min}}{FR_{max} - FR_{min}}\right) \quad \text{Equation 3.3}$$

where $FR^{i\wedge\wedge}$ is the normalised FR value of the i^{th} class of a factor;

FR_{min} is the minimum FR_i class score of a factor;

FR_{max} is the maximum FR_i class value of a factor

The closer the $FR^{i\wedge\wedge}$ value is to one, the larger the association with gullying.

The local and global factor maps were prepared for weighted overlay by reclassifying the raster datasets. The reclassification procedure replaced the original factor-class pixel value with the FRi^^ value. Once reclassified, the factor maps were resampled to a common spatial resolution of 10 m. Although 10 m represents a spatial resolution finer than the input raster datasets, a common spatial resolution (denominator) resulted in no new data values being created during the resampling process (Nearest Neighbour technique; Figure 3.7). Additionally, the resampling technique ensured that pixel values aligned spatially. For vector datasets, the FRi^^ values were added to the attribute table and rasterised to a pixel size of 10 m. The 10 m posting is at a much finer spatial resolution than the national vector data was mapped, for example, one can assume a detectable object size of 1000 m, which translates into an estimated spatial resolution of 500 m when considering the geology (Burger, 2013) input map (calculation concept from Tobler, 1987). Although the vector data inputs are coarser when compared to the raster datasets and the accuracy thereof would not be to a 10 m posting, we maintained the output with a 10 m spatial resolution due to two main reasons: 1) we placed more emphasis on having a common scale for the raster data, on ensuring that our calculations do not create new data from interpolations methods (and we do not encounter a loss in training data to the proximity of gully sites), and 2) the classification

of the vector data were further generalised, reducing the importance of exact well-defined boundaries.

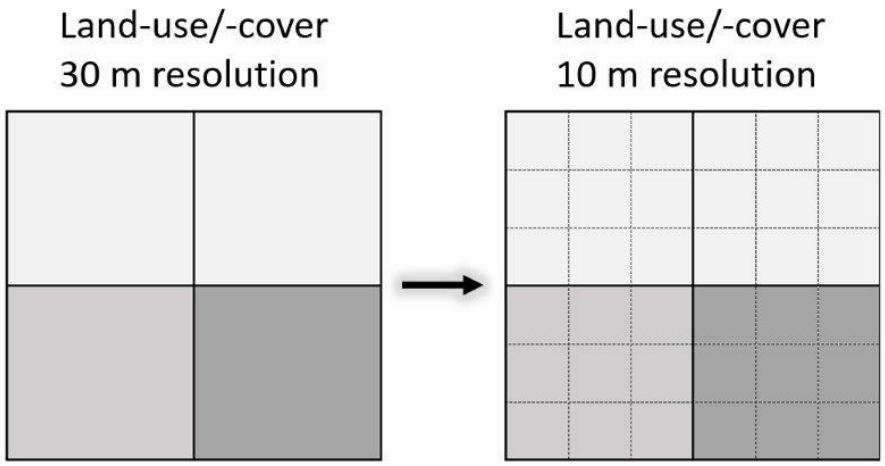

Figure 3.7 Example of resampling raster datasets to a common spatial resolution of 10 m avoiding creating artificial values and ensuring overlay; The shades of grey represent different raster values.

Once the factor maps were conditioned *viz*. rasterised or reclassified and resampled, the gully susceptibility was calculated by a weighted overlay sum from:

$$GSI = \sum_{i=1}^{n}(nGDF_i \times W_i) \qquad \text{Equation 3.4}$$

where GSI is the gully susceptibility value;

i the local and global factors selected for the GSI;

n is the number of global and local factors;

nGDF is the conditioned factor map for i;

FR_{max} is the maximum FR_i class value of a factor

W the weight assigned to i

The weights applied in the final aggregation step correlated to the compilation of control factors from literature (Table 3.1). The GSI output was classified according to the classes derived in De Geeter et al. (2023): Very low (<0.1), low (0.1-0.3), moderate (0.3-0.5), high (0.5-0.7), and very high (>0.7).

3.3.4 Validation

The GSI model was validated using two datasets. Firstly, the GSI model was compared to a published gully inventory map of South Africa (Mararakanye & Le Roux, 2012) produced by digitising gully features from SPOT-5 imagery at a scale of 1:10000 (smallest detectable feature equals 10 m), and secondly, the GSI model was validated against fifteen randomly selected 1 km^2 zones in which primary validation data was captured.

In the first instance, these manually mapped gullies (Mararakanye & Le Roux, 2012; n = 163019) were draped over the GSI modelled raster to calculate the mean GSI value for each gully. The relative gully occurrence was used as an additional accuracy measure by correlating the areal extent of each GSI class with the gullies modelled to have the same mean GSI value by:

$$G_{Ri} = \frac{GSI^{Gi\%}}{GSI^{Ai\%}} \qquad \text{Equation 3.5}$$

G_{Ri} is the relative gully occurrence of the i^{th} GSI class;

$GSI^{Gi\%}$ is the percentage of gullies in the i^{th} GSI class;

$GSI^{Ai\%}$ is the percentage areal coverage of the i^{th} GSI class.

The calculation was compared to a random probability of gully occurrence.

In the second instance, a 1 km^2 hexagon tessellation grid was created for South Africa and overlaid with the GSI model raster. Hexagons with 90% coverage of a particular GSI class were extracted, and three hexagon sites were randomly selected for each GSI class. Gully features within each site were manually digitised at a scale of 1:2000 from Google Earth imagery (smallest detectable feature equals 2 m) imported as XYZ tiles in QGIS 3.16.16 (available from: https://mt1.google.com/vt/lyrs=y&x={x}&y={y}&z={z}) to produce a higher accuracy validation dataset compared to the national inventory map. Gully density in terms of planimetric area and gully headcuts were calculated for each site.

3.4 RESULTS

3.4.1 Mapped gullies

A total of 60 gully locations are mapped as points (see APPENDIX B). Several papers present continued findings from the same sites and as such mapped only once (see APPENDIX B). The Eastern Cape and KwaZulu-Natal have the most gully locations, 27 and 19, respectively (Figure 3.2). No papers were found that presented gully erosion research in the Gauteng and North West provinces.

The sensitivity of gully headcut placement was tested on a gully in the Tsitsa catchment (31° 11' 28.62" S; 28° 27' 59.64" E), where sub-surface processes are dominant, and the Sandspruit catchment (33° 25' 55.09" S; 18° 51' 33.78" E), where surface processes dominate. The Tsitsa gully is an order of magnitude larger than the Sandspruit gully, with a mean planimetric area of 13653.8 m^2 and 5584.1 m^2, respectively. The standard deviation varies between 122.4 m^2 and 125.8 m^2, indicating a percentage difference of less than 1% than the mean for the Tsitsa catchment gully, and 2.3 % lower than the mean for the Sandspruit catchment gully. The distance between the furthest gully headcut points for the Tsitsa gully is 5.1 m, with a minimum bounding geometry of 2.4 m^2. A shorter length of 3.1 m is found between the furthest gully headcut points for the Sandspruit gully, although there is a more extensive lateral spread resulting in a minimum bounding geometry of 3.8 m^2. At both gully locations the gully headcut positions are well within the spatial resolution of the 10 m data sets. Hence, the model results are not sensitive to the manual headcut placement.

3.4.2 Control factors associated with gully erosion susceptibility

Gullies are strongly associated with vegetable farming (FR^^: 1.00) and subsistence areas (FR^^: 0.80) in the agricultural zones, which are used to represent the historical land-use of South Africa (Table 3.2). The small geographic extent of vegetable farming, in addition to the high activity rating, results in vegetable farming having the highest FR^^, even though only one gully is located within it. Most gullies are in the subsistence areas, but due to the larger coverage and lower activity rating, it had a lower FR^^ than vegetable farming. Although a large proportion of gullies are in cattle (25%), sheep (15.0%), and grain (16.7%) farming zones, the prominent geographical extent of those areas reduces the FR^^ to 0.2390 or lower. In the land-use/ -cover dataset, used to relate

gullying to a more contemporary anthropogenic setting, gullies are related to degraded areas (FR^^: 1.00) and bare ground (FR^^: 0.50). Grasslands had a comparable FR^^ to that of bare ground because most gully sites are located within this land-use/ -cover class. Although 20% of gully research sites are located in the Karoo, its FR^^ were between 0.01 to 0.12 due to its extensive geographic coverage.

The strongest correlation between gully occurrence at the 60 sites and rainfall intensity, as represented by RDN, is within an RDN range of eight to twelve. A lower yet still significant correlation is found in lower RDN values between four and eight. Most gullies are mapped in the dry sub-humid and moist sub-humid climate zones, and the strongest FR^^ correlation is found here with values of 0.47 and 1.00, respectively.

In our 60 sites, 80% of gullies are found in sloping areas from 5% to 30% and are also highly active (activity ratings of 1.7 to 1.8). The strongest correlation is found in the 15% to 20% slope class (FR^^: 1.00). In the broad soil class, 43 gullies formed in Glenrosa and/ or Mispah soils. Due to the large proportion of gullies located within the Glenrosa and/ or Mispah soil class, other soil types had a low correlation with gully erosion (up to 0.22). Sedimentary rock is abundant in South Africa (71.7% coverage), and most gully sites (n=42) are found within these lithologies. Gullies are strongly correlated to coarse (FR^^: 1.00) and fine sedimentary rock (FR^^: 0.92), although a significant correlation is also evident with mafic igneous/ metamorphic rock types (FR^^: 0.42).

Table 3.2 Distribution of gully sites according to key physiographic characteristics and the calculated Frequency Ratio (FR) and Normalised FR^^ values.

Factor classification	Class area %	No of study sites	Study sites %	Frequency ratio, FR	Activity	Normalized value, FR^^
Land-use/ -cover						
- Indigenous forest	0.3	0	0	0.00	0.0	0.00
- Thicket/ dense bush	5.7	1	1.7	0.44	1.5	0.04
- Woodland/ open bush	8.7	3	5.0	0.74	1.3	0.07
- Low shrubland	14.4	1	1.7	0.23	2.0	0.02
- Plantations/ woodlots	1.5	1	1.7	2.22	2.0	0.20
- Cultivated commercial annual crops	9.1	0	0	0.00	0.0	0.00
- Cultivated commercial orchards	0.4	0	0	0.00	0.0	0.00
- Cultivated subsistence	1.6	0		0.00	0.0	0.00
- Settlements	2.3	2	3.3	2.15	1.5	0.19
- Wetlands	0.8	0	0	0.00	0.0	0.00
- Grasslands	19.0	35	58.3	5.52	1.8	0.49
- Fynbos	5.6	3	5.0	1.35	1.5	0.12
- Nama Karoo	20.5	8	13.3	1.24	1.9	0.11
- Succulent Karoo	6.1	1	1.70	0.55	2.0	0.05
- Mines	0.3	0	0	0.00	0.0	0.00
- Water	1.7	0	0	0.00	0.0	0.00
- Bare ground	1.2	2	3.3	5.56	2.0	0.50
- Degraded	0.8	3	5.0	11.18	1.7	1.00
Agricultural zones						
- Cattle	22.9	15	25.0	1.75	1.7	0.22
- Diverse	1.8	0	0	0.00	0.0	0.00
- Forestry	1.5	0	0	0.00	0.0	0.00
- Fruit	4.9	1	1.6	0.68	2.0	0.09
- Grains	15.8	10	16.7	1.90	1.8	0.24

- None	2.3	0	0	0.00	0.0	0.00
- Sheep	37.7	9	15.0	0.76	1.9	0.10
- Subsistence	10.9	23	38.3	6.31	1.8	0.80
- Sugar	1.8	1	1.7	1.92	2.0	0.24
- Vegetables	0.4	1	1.7	7.94	2.0	1.00
Rainy Day Normal						
- <4	4.3	0	0.0	0.00	0.0	0.00
- 4-6	25.1	16	26.6	1.91	1.8	0. 69
- 6-8	44.3	22	36.7	1.49	1.8	0. 54
- 8-10	23.2	19	31.7	2.32	1.7	0.84
- 10-12	3.1	3	5.0	2.77	1.7	1.00
- >12	0.1	0	0.0	0.00	0.0	0.00
Aridity index						
- Arid	22.7	2	3.3	0.29	2.0	0.04
- Semi-arid	44.5	11	18.3	0.70	1.7	0.10
- Dry sub-humid	24.9	30	50.0	3.42	1.7	0.47
- Moist sub-humid	7.3	17	28.4	7.32	1.9	1.00
- Humid	0.6	0	0	0.00	0.0	0.00
Slope (in %)						
- <2	29.4	0	0.0	0.00	0.0	0.00
- 2-5	34.9	3	5.0	0.14	1.0	0.02
- 5-10	14.6	14	23.3	2.72	1.7	0.34
- 10-15	6.1	13	21.7	6.39	1.8	0.81
- 15-20	3.8	10	16.7	7.89	1.8	1.00
- 20-30	4.8	11	18.3	6.88	1.8	0.87
- >30	6.4	9	15	4.45	1.9	0.56
Soil						
- Red-yellow apedal	33.8	6	10.0	0.53	1.8	0.12
- Plinthic	11.5	4	6.6	0.87	1.5	0.20
- Duplex dominant	9.8	3	5.0	0.87	1,7	0.19

- Undifferentiated	5.8	1	1.7	0.29	1.0	0.06
- Glenrosa and/or Mispah	28.9	43	71.7	4.46	1.8	1.00
- Ferrihumic horizon	0.2	0	0	0.00	0.0	0.00
- Grey regic sands	1.3	0	0	0.00	0.0	0.00
- Rocky with undifferentiated or little soil	8.5	3	5.0	1.00	1.7	0.22
- Water	0.2	0	0	0.00	0.0	0.00
Rock type						
- Fine sedimentary	25.7	17	28.3	1.99	1.8	0.92
- Coarse sedimentary	46.0	35	58.3	2.15	1.7	1.00
- Mafic igneous/ metamorphic	11.9	4	6.7	0.90	1.6	0.42
- Felsic igneous/ metamorphic	12.7	4	6.7	0.52	1.0	0.24
- Carbonate	3.4	0	0	0.00	0.0	0.00
- Water	0.3	0	0	0.00	0.0	0.00

3.4.3 Gully susceptibility output

According to the GSI using literature directives, 1.8% of South Africa is classified with a very high susceptibility to gullying, and 12.0% is highly susceptible (Figure 3.8; Table 3.3). Overall, GSI increases from the western coast, eastwards to KwaZulu-Natal. The Eastern Cape (43.3% of its area classifies as high to very high GSI) and KwaZulu-Natal (92.1% classifies as moderate to very high GSI) exhibit the most heightened susceptibility to gully erosion. Although the Northern Cape has the lowest GSI (67.6% low to very low GSI), a considerable proportion of the Karoo region is moderately susceptible to gully erosion. The Northern Cape and North West are the provinces with the lowest GSI, with 67.6% and 60.5% of its extent classified as very low to low GSI.

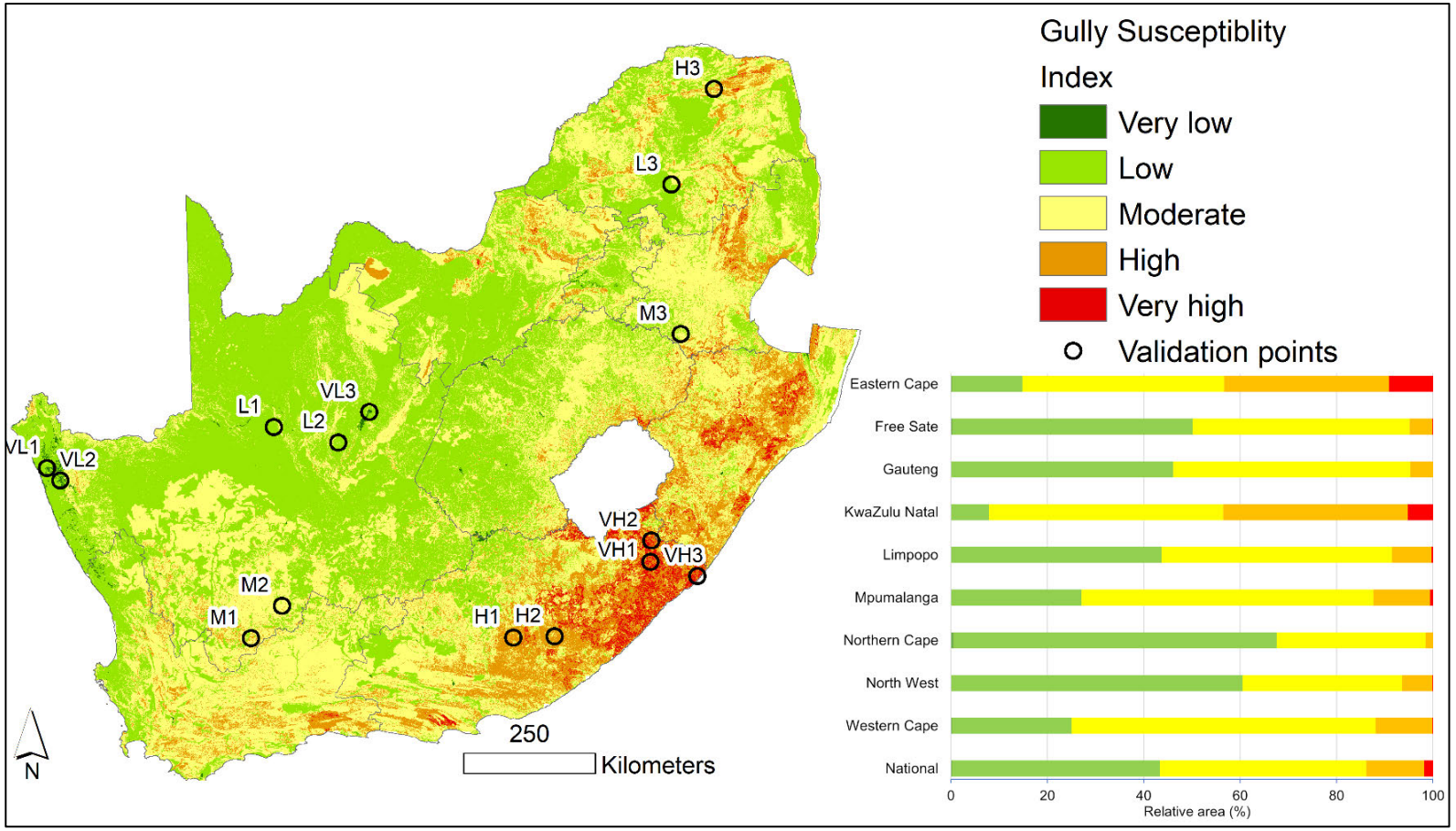

Figure 3.8 Gully susceptibility according to literature directives in South Africa (spatially mapped on the left and in graph format showing relative area on the right). The location of random validation sites is given on the map: VL signifies very low GSI validation sites, V shows low GSI validation areas, M for moderate GSI validation hexagons, H shows the High GSI validation sites, and VH represents the very high GSI validation hexagons. The numbers (1 to 3) following the GSI class show the order of the validation sites for a particular GSI class according to longitude.

Table 3.3 Spatial distribution of the gully susceptibility index (GSI) aggregated for the 9 provinces of South Africa, including a national outlook (Area GSI denotes the areal coverage of each GSI class for the model respectively). The calculated mean GSI for each manually mapped gully by (Mararakanye & Le Roux (2012; n = 160952 [2067 gullies were omitted due to size limitation and NoData values along the South African border and coastline]) is given for each province, including nationally, for each weighted model (denoted as Gully GSI).

Province	Area (km^2)	Gullies (count)	Variable	Very low	Low	Moderate	High	Very high
Eastern Cape	168215		Area GSI	0.2	14.6	41.9	34.2	9.1
		81172	Gully GSI	0.0	19.8	33.8	28.3	18.1
Free State	129806		Area GSI	0.3	49.9	45.0	4.7	0.1
		14211	Gully GSI	0.0	17.0	75.5	7.4	0.1
Gauteng	18015		Area GSI	0.1	46.0	49.2	4.7	0.0
		129	Gully GSI	0.0	30.2	69.0	0.8	0.0
KwaZulu-Natal	92702		Area GSI	0.1	7.8	48.6	38.3	5.2
		25846	Gully GSI	0.0	0.7	42.9	46.6	9.8
Limpopo	125384		Area GSI	0.0	43.7	47.8	8.2	0.3
		3732	Gully GSI	0.0	20.0	71.2	8.8	0.0
Mpumalanga	76257		Area GSI	0.0	27.1	60.6	11.7	0.6
		2568	Gully GSI	0.0	23.9	63.1	12.8	0.2
Northern Cape	372203		Area GSI	0.5	67.1	30.9	1.5	0.0
		18278	Gully GSI	0.1	62.2	37.3	0.4	0.0
North West	104730		Area GSI	0.1	60.4	33.1	6.3	0.1
		797	Gully GSI	0.0	27.9	58.3	13.8	0.0
Western Cape	128708		Area GSI	0.2	24.8	63.1	11.8	0.1
		4219	Gully GSI	0.3	23.9	68.9	6.8	0.1
National	1216020		Area GSI	0.2	43.2	42.8	12.0	1.8
		160952	Gully GSI	0.0	20.2	42.7	25.8	11.3

3.4.4 Gully susceptibility model validation

The mean GSI was calculated for each gully in South Africa (n=160952; 2067 gullies were omitted due to size limitation and NoData values along the South African border and coastline), as mapped by Mararakanye & Le Roux (2012) (Table 3.3). Nationally, 79.8% of the mapped gullies have a mean GSI of moderate or higher. The Eastern Cape and KwaZulu-Natal have the most gullies, also the most mapped gully locations from the literature database. The GSI model

performance is best in these two provinces, with 46.4% to 56.4% of gullies predicted with a high to very high mean GSI, while 99.3% of gullies in KwaZulu-Natal are predicted with a mean GSI of moderate or above. Although gullies in the high to very high classes are limited in the Free State and Limpopo (up to 8.8%), most gullies (80% and 83%) have a mean GSI classification of moderate or higher. The GSI prediction in the Northern Cape was poor, with 62.3% of gullies predicted in the low to very low GSI class.

The relationship between relative gully occurrence and GSI is compared to a random occurrence probability, of which the assumed value is 1 (Figure 3.9). Gullies with a moderate mean GSI converge to the random probability. A strong positive trend is observed nationally for relative gully occurrence and mean gully GSI severity. Low (0.5) to very low (0.09) GSI drops below the random probability of 1, while high (2.1) to very high (6.4) GSI increases above random probability. The positive correlation indicate that the GSI-modelled classifications perform better than a random baseline classification. Interprovincially, the correlation between relative gully occurrence and mean GSI gully severity becomes more spread, with the best performance in KwaZulu-Natal. The GSI model performance was worst in the Western Cape, where very low, low, and moderate GSI converge to a random probability, while the high and very high GSI have a classification score lower than a random classification. The low mean GSI classification for gullies in the Northern Cape translates into poor correlation with the higher GSI classes. Still, the large geographic extent of lower GSI prediction in the

province improves prediction, with gullies with a low (0.9) to very low (0.2) mean GSI showing a stronger correlation and modelled below the random baseline.

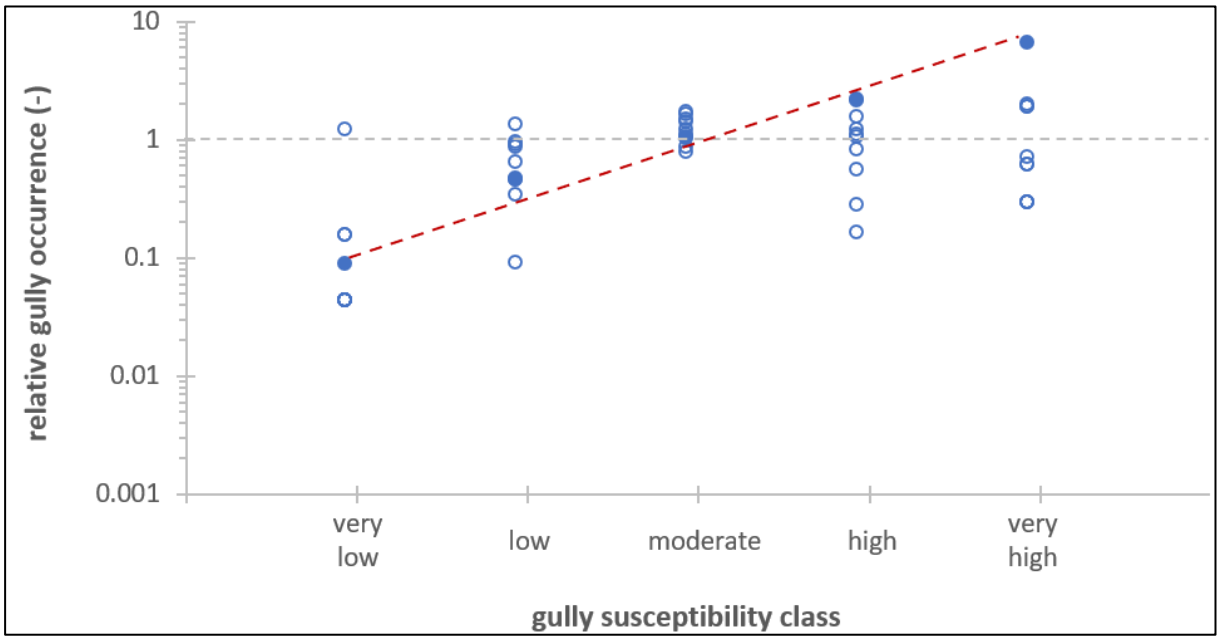

Figure 3.9 Relative gully occurrence per gully susceptibility for the gullies mapped in the national gully inventory map (n = 163019). Non-filled circles denote provincial data, while filled circles denote national data. The horizontal dashed line indicates expected gully occurrence under random distribution, while the red dashed line shows the general trend line.

Fifteen 1 km^2 hexagonal validation areas, three per GSI class, were randomly selected to test the predicted GSI with a high resolution, manually digitised reference dataset (Figure 3.10). A general increasing trend in gully density is noticeable from the low to very high GSI. Gullies are absent in the very low validation zones, and in two of the low GSI classification zones. In the high GSI validation zones, the gully density was comparable to the moderate GSI in two of the areas, while gullies were absent in the third. For the two zones where gully density is similar to the moderate areas (Figure 3.10j, k), the mitigation works in the form of dams and contours are evident. On one of the hillslopes in Figure 3.10k, gully erosion has broken through the contour banks, likely indicative of a higher susceptibility to gullying. At the third validation, aimed for the high GSI, gullies are absent. The GSI model most likely predicted a high GSI for this zone, due to the presence of Glenrosa and/ or Mispah soils, RDN of 4 to 6, and the historical land-use of subsistence farming. The very high validation zones show the highest gully density, up to 171783.5 m/ km^2.

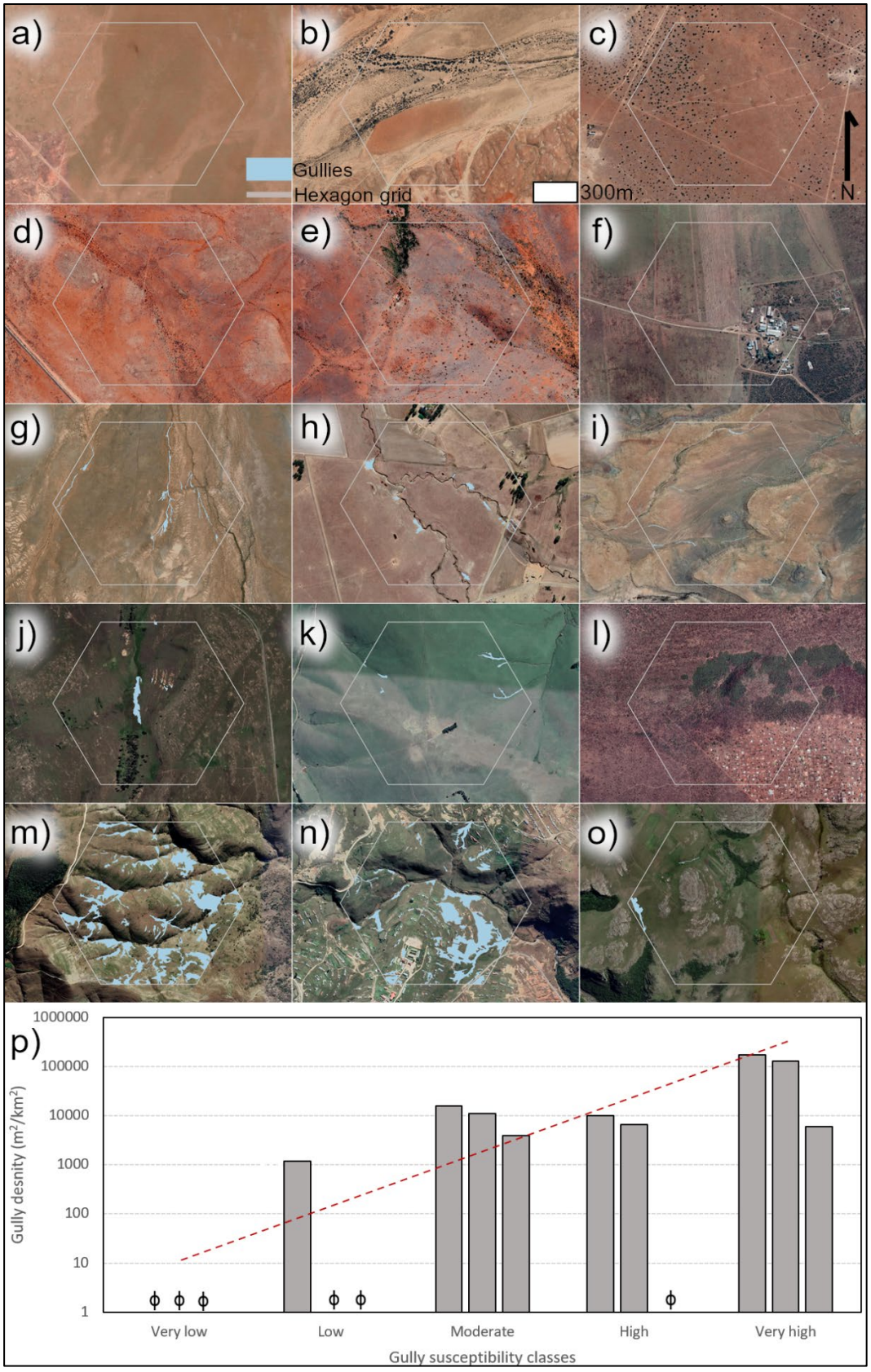

Figure 3.10 The randomly selected 1km^2 hexagon sites used for validation of the GSI model. The first row consists of validation areas that had a 90% or higher very low GSI and is ordered according to longitude: a)

VL1 site, b) VL2 site, c) VL3 site; the second row shows validation areas that had a 90% or higher very low GSI and is ordered according to longitude: d) V1 site, e) V2 site, f) V3 site; the third row represents the validation areas that had a 90% or higher moderate GSI and is ordered according to longitude: g) M1 site, h) M2 site, i) M3 site; the fourth row represents areas of 90% or higher high GSI and is ordered according to longitude: j) H1 site, k) H2 site, l) H3 site; the fifth row consists of the validation areas that had a 90% or higher very high GSI and is ordered according to longitude: m) VH1 site, n) VH2 site, o) VH3 site (see Figure 8 for the geographic location); p) shows gully density of the validation areas according to GSI. The red dashed line shows the general trend line, while ϕ denotes a zero value. Satellite images courtesy of Google Earth.

3.5 DISCUSSION

3.5.1 The spatial relationship between gully controlling factors and literature directives

Regarding the historical land-use dataset, subsistence farming was closely correlated to gully erosion (80%; Table 3.2). Subsistence farming in the historical land-use dataset corresponds to areas of communal land tenure, which has been demonstrated to have high gully incidence (Mararakanye & Le Roux, 2012, Hoffman & Todd, 2000). Although this impact can be considered historical, it remains an area of severe gully erosion (Olivier et al., 2023a). Surprisingly, vegetable farming, a land-use not commonly associated with gully erosion in South Africa, had the highest correlation. The significant association of gullying with vegetable farming is likely due to the small geographical extent of gullying. However, ephemeral gully erosion research has been neglected in South Africa. The possibility therefore exists that this land-use could contribute to gully erosion. As expected, bare ground and degraded regions correlated well with gully erosion, which conforms to other research findings that demonstrated the importance of vegetation as a controlling factor for gullying (Rey, 2004; Zhao et al., 2016). Grasslands also had a good correlation with gully erosion, which has been shown to be prone to gullying, especially where degraded and unimproved land occur (Mararakanye & Le Roux, 2012). Bush encroachment in grasslands, which is a recent phenomenon (Hoffman & Ashwell, 2001), has also been demonstrated to impact gully erosion indirectly (Grellier et al., 2012).

Gully erosion is associated with higher rainfall intensities (Vanmaercke et al., 2016; Anderson et al., 2021), and a higher correlation was found with increasing RDN values for South Africa. There was a poor correlation with semi-arid regions, where research has shown a prevalence towards gullying, mostly due to the impact of rainfall variability on vegetation (Valentin et al.,

2005). Although large proportions of the Karoo were modelled as moderate GSI, the low correlation significantly impacted the prediction in the Northern Cape, where GSI showed poor performance.

In the 60 study sites, 66.7% of gully headcuts were located on slopes <20%. A good correlation is also found between the slope range of 20% to 30% (FR^^: 0.87). Although gullies occur in varied geo-environmental settings, including different slopes (Liggit & Fincham, 1989; Valentin et al., 2005; DeWitte et al., 2015; Mararakanye & Sumner, 2017), our correlation is toward the higher spectrum of slope ranges when compared to other studies in South Africa (for example, Kakembo et al., 2009; Le Roux & Sumner, 2012). Kakembo et al. (2009) and Le Roux & Sumner (2012) conducted a zonal approach investigating the effect of slope gradient on gullying, demonstrating gullying is prevalent in slopes ranging from 8% to 17.5%. The relationship between gullying and slope is complex and hinges upon several variables such as rainfall, upslope drainage, upslope drainage shape, vegetation, land-use, and soil characteristics (Liggit & Fincham, 1989; Laker, 2004; Rossi et al., 2015; Summerfield, 2014; Torri & Poesen, 2014). In South Africa, the most prominent cause resulting in gullies being found in lower slopes can be attributed to the large upslope area that allows an erosive water mass to encounter deep, unstable, often duplex soils derived from mudrocks and shales (Laker, 2004). A plausible reason, however, for our higher slope ranges is caused by the methodology applied to extracting control factor data. An x,y point is placed at the gully headcut interface, where the surrounding hillslope is likely to be steeper than at lower elevations. This point-based methodology is unlike zonal (Kakembo et al., 2009; Le Roux & Sumner, 2012) or field-measurement (Cobban & Weaver, 1993) approaches that consider the entire gully channel.

The steeper slope position identified at the 60 study sites is also likely to have a strong influence on the correlation between gully erosion and soil form. Young soils on weathered rock (i.e., Glenrosa and/ or Mispah), often found on steeper convex slopes (Fey, 2010a), show the best correlation with GSI (71.7%). These soils are predominantly shallow and lithic, with a sandy loam topsoil texture (Van Zijl, 2010), exhibiting a weak structure, resulting in an erodibility rating of medium to high (Crosby et al., 1981 in Kakembo & Rowntree, 2003). Although gully headcuts may have originated or retreated into the steeper young soils, the concentrated flow from the less permeable rocky soils can exacerbate gullying in the lower slopes (Rienks et al., 2000; Laker, 2004). This is especially significant in duplex-dominant soils which show a weak

correlation with gullying according to the GSI model. The low correlation contrasts other works, including on the African continent (Imeson & Kwaad, 1994; Van Zijl et al., 2013; Parwada & Van Tol, 2016; Mararakanye & Sumner, 2017) Europe (Faulkner et al., 2013), the Americas (Wilson et al., 2018), and Australia (Sidle et al., 2019). The predominance of gullying on duplex soils is associated with the abrupt texture contrast between the surface and a subsurface horizon, which typically exhibit dispersive properties (Parwada & Van Tol, 2016). Once the dispersive subsoil is exposed, gullying can become accelerated and more severe (Rienks et al., 2004). Therefore, the low correlation with duplex soil is likely erroneous, and GSI in these areas would have been underpredicted.

Sedimentary rock is abundant on the earth's surface, which could be the reason for the association with gullying in a worldwide review (Castillo & Gómez, 2016) and locally (Olivier et al., 2023a). In South Africa, a strong influence of lithology on gullying has been detected. As parent material, the sedimentary Ecca and Beaufort groups have shown a predisposition towards gullying, primarily due to the formation of duplex and dispersive soils (Laker, 2004).

3.5.2 Model performance and South Africa gully erosion narrative

The GSI model was validated in three ways using two different datasets. Firstly, the GSI model generally performed well when tested against a published national gully inventory for South Africa (Mararakanye & Le Roux, 2012), consisting of 160952 gullies. Secondly, the GSI model showed a distinctly better performance than a random classification model when considering relative gully occurrence and mean gully GSI. Lastly, at fifteen randomly selected gully validation sites, the GSI model showed appropriate susceptibility indicators towards gullying, except for one area that was identified as having a high GSI, despite no gullies being observed. This triple validation shows that the GSI model is generally robust, identifying areas of contrasting susceptibilities. In addition to the validation methodologies, the GSI model broadly converges with other susceptibility metrics, which has been derived by different methodologies. These methods include a qualitative soil degradation assessment derived by Hoffman & Todd (2000), a water erosion risk map produced by Le Roux et al. (2008), and, more recently, a continental gully headcut susceptibility model by De Geeter et al. (2023).

The GSI model shows that 13.8% of South Africa is highly susceptible to gully erosion. However, the risk of gullying is not evenly distributed and is skewed to the east. The higher

skewed risk in the former homeland areas shows that past social injustices continue to have a legacy impact on contemporary gully susceptibility and erosion.

Although large portions of the Karoo are classified with a moderate GSI, gully susceptibility here may be underpredicted, especially in the Northern Cape, where lower GSI classifications were predicted (and GSI performance was poor compared to validation). Several reasons could be attributed to the lower GSI: firstly, the RDN proxy for rainfall intensity; secondly, the historical farming conditioned input factor; and lastly, the slope.

In the first instance, the RDN index serves as a rainfall intensity proxy as a function of mean annual rainfall. Rainfall intensity may not be adequately represented for the Northern Cape due to the low annual rainfall, lowering GSI. Additionally, rainfall variability was not added as a climate metric in the GSI, although it has been demonstrated to be a driver of gully erosion in arid parts of South Africa (Dollar & Rowntree, 1995; Sonneveld et al., 2005). The effect of rainfall variance on gullying is exacerbated when high-intensity rainfall events occur after a drought when vegetation has had limited time to recover. In the Karoo, Keay-Bright & Boardman (2007) demonstrated that vegetation recovery is unlikely in such a harsh environment, which may further contribute to continued gullying. Not including rainfall variance may have further contributed to (artificially) lowering the GSI. In the second instance, the conditioning of the historical farming dataset led to a high gully erosion association with vegetable farming. This association influenced the FR^^ and likely led to the artificial lowering of other classes mainly associated with gullying, such as livestock in the case of the Northern Cape. Lastly, due to the placement of the x,y point at the gully headcut, slope ranges associated with gully erosion in the model were more elevated compared to those reported in the literature (Kakembo et al., 2009; Le Roux & Sumner, 2012). The Northern Cape exhibits mainly moderate to lower slopes (Figure 3.6a), which would have lowered the FR^^ values for the province.

3.5.3 Adoption prospective in other geomorphic and climatic regions

The GSI model, blending literature directives with a statistical approach to model gully susceptibility on a regional scale (in this case national in South Africa), proved successful and robust. There is thus potential to apply this approach using literature at different scales and areas with varying geomorphic environments. The methodology can be used as a standalone

tool to aggregate data mined from a literature review only, as in this study, to conduct a gully susceptibility assessment. Additionally, primary data (for example, a localised study investigating causes of gully erosion) can be merged with the GSI model to provide contextual data for the primary study or provide additional input points to refine the GSI.

Requirements for this methodology implementation to achieve acceptable results regarding GSI are the availability of existing datasets, and the quantity and distribution of research study sites. Existing data sets need to be at a scale (for example, in this study on a national scale) at which susceptibility will be modelled, and output will be affected by accuracy and spatial resolution. Optimally there should be an even distribution of gully research sites from which its locality and local driving and control factors can be extracted, although the GSI models performed well even with scattered datasets in South Africa. Although the GSI model performed well in several underrepresented provinces, it was more successful in the Eastern Cape and KwaZulu-Natal where most gully specific research sites were located.

3.5.4 Limitations and future research

Although the authors took great care in developing a systematic, semi-automated approach to identify the (x, y) coordinate point or each gully, manually digitising the gullies remained an essential initial step. Manually digitising gullies seemingly introduces uncertainties, as it is subjective, resulting in extent differences due to varying interpretations (Vanmaercke et al., 2021). In our case, the same user digitised all gullies, and a sensitivity analysis showed a minor impact within the pixel size of the input datasets. The sensitivity analysis outcome is encouraging, and we consider using a manual approach as an initial step to be valid. However, establishing an automated method for gully headcut identification would be advantageous, as it would remove user bias.

The spatial resolutions of the input datasets introduce further uncertainty. The 20 m DEM would smooth topography and is, therefore, unable to represent larger-scale topographic fluctuations, which may be important to gully initiation and severity. Similarly, RDN, which was used as a proxy for rainfall intensity, was calculated from data with a 10’ resolution. The coarse resolution may be a poor predictor of local extreme rainfall events and the impact of topography on rainfall distribution, which would be important in attaining gully susceptibility. Although

land-cover/ -use suffers from the same resolution limitation, its uncertainties may be less than the two datasets above because it is a discrete data type.

The distribution of gully research sites in South Africa remains sparsely scattered and partially confined to certain areas. The reason for the bias towards certain study areas is not always forthcoming. However, a justifiable assumption can be made that empirical research is more focused on areas where gully erosion is more prevalent. This assumption is evident from the activity weights assigned to gullies.

Despite these limitations, validation data indicate that the GSI model performed well, even in several underrepresented provinces such as the Free State, Limpopo, Mpumalanga, and the Western Cape. Future work can investigate model improvements and further applications.

Conducting work at underrepresented regions in South Africa, including stable gully erosion sites, would provide further insight into regional gully dynamics and yield more distributed data to be used as input, delivering a more precise model. Furthermore, higher-resolution datasets could be generated to refine GSI reductions. Generating a higher-resolution climate dataset to represent rainfall intensity (possibly without reference to mean annual rainfall) may be useful, as it has been shown to be pivotal in gully initiation and expansion (Vanmaercke et al., 2016). Additionally, a South African 2 m DEM (GeoSmart Space, 2020b) exists for a large part of the country, and smaller regional studies can be undertaken to test model accuracy dependency on DEM resolutions. However, the application of how the slope factor should be applied as input needs further testing, for example, a slope-area concept, albeit at high resolution DEM (it has been shown to model gully incision points and therefore potential vulnerability to gullying but shows high variance due to local conditions; Torri & Poesen, 2014), general slope gradient or local slopes (a preferential slope for gully development has been demonstrated in South Africa; Kakembo et al, 2009) and slopes combined with curvature (since curvature provides a measure of slope change and water convergence, which affects erosivity; (Conoscenti et al., 2013).

Currently, the model uses a single point to represent a gully. Additionally, the model presently applies one additional data mined variable from literature, *viz*. activity. Model improvements could be achieved by investigating ways of introducing a gully or gully headcut density metric that replaces the single point or making use of zonal statistics per gully feature instead of points. Furthermore, additional properties could be data mined and used in the model to improve GSI

prediction. We argue against using the age of gullies as a proxy to model severity, as gully activity is non-linear, with varied fluctuations between activity severity during its lifetime (Grellier et al.,2012; Hayas et al., 2017). Capturing data and coupling morphology, gully mechanisms (surface *vs* sub-surface processes as the main driver), and connectivity; moreover, mitigation and rehabilitation measures could be tested for implementation and may produce a more precise model. Mitigation measures may be most beneficial, as mitigation works in South Africa are extensive, for example, Meadows (2003) (having such a dataset for the entire extent of your modelled region could be even more practical). De Geeter et al. (2023) also found poor accuracy in their regional gully susceptibility map, which could be related to the need for a spatial mitigation dataset.

The GSI model could also be extended in scope by adding connectivity and rainfall variability to produce an off-site gully erosion impact map. The output of such a map could be quite different to a susceptibility map, for example, in the Karoo, which consists of a large area with a moderate GSI, that may have a much lower off-site impact due to the tendency of Karoo gullies to meander and flood-out due to rainfall variability (Grenfell et al., 2014; also see Boardman et al., 2017). An off-site impact could be a substantial asset to land managers in identifying high priority areas and mitigation goals.

The GSI model could also be used in conjunction with gully detection methods, for example, constraining semi-automated methods to highly susceptible areas, which can reduce computational time and the geographic extent to which detection methods need to be applied to. Combining these two types of methodologies would produce information regarding gully occurrence and dimensions in susceptible areas spanning different geo-environments. Additionally, if applied temporally, gully erosion rates can be quantified for various gully typologies and geo-environments within susceptible regions., which is continues to be lacking in gully erosion research (Vanmaercke et al., 2021).

Lastly, the GSI model could be tested in modelling different environmental change scenarios by changing RDN and land-cover/ use data. Gully erosion is expected to be impacted by climate change (Vanmaercke et al., 2016) and deriving information regarding gully susceptibility evolution under environmental change is essential for land managers and policymakers. Although the GSI model can produce environmental change outputs, interpretations of such

outputs need to consider that the model is static, thus unable to model positive and negative feedback mechanisms between gullying and environmental change.

3.6 CONCLUSION

Gully erosion has been identified as a severe land degradation process with environmental and socio-economic consequences. Identifying areas susceptible to gully erosion is essential to help the development of strategies to inhibit future degradation. We introduce a novel approach that blends literature directives with statistics to map gully susceptibility on a regional-/ national-scale. The GSI model was validated using an existing, published gully inventory map of South Africa (Mararakanye & Le Roux, 2012) and primary data obtained from randomly allocated 1 km^2 tessellation zones. The GSI model output shows robust performance, even performing well in certain provinces which are underrepresented in gully erosion sites. However, uncertainties remain, which propagate through the execution process. Gully headcut location mapping, increasing the distribution of gully erosion sites, and obtaining higher spatial resolution datasets should be given future attention and could improve prospective future modelling. Despite the uncertainties, the GSI model shows promise due to its validation statistics and convergence with other gully susceptibility metrics derived from different methodologies in South Africa. Due to the empirical research span across the world, the GSI model could be implemented in various countries. Additionally, the GSI model could be used to predict the impact of environmental change on regional gully susceptibility by incorporating RDN inputs for predicted climate change and combining them with expected land-use changes. Lastly, the low data input, simplistic model could be helpful to land managers to effectively identify gully-susceptible areas where costly mitigation works would have the most impact.

CHAPTER 4: GIVING GULLY DETECTION A HAND - TESTING THE SCALABILITY AND TRANSFERABILITY OF A SEMI-AUTOMATED OBJECT-ORIENTATED APPROACH TO MAP PERMANENT GULLIES

4.1 ABSTRACT

Gully erosion can incur on- and off-site impacts with severe environmental and socio-economic consequences. Semi-automated mapping provides a means to map gullies systematically and without bias, providing information on their locations and extents. If used temporally, semi-automated mapping can be used to quantify soil loss and identify soil loss source areas. The information can be used to identify mitigation strategies and test the efficacy thereof. We develop, describe, and test a novel semi-automated mapping workflow, gHAND, based on the distinct topographic landform features of a gully to enhance transferability to different climatic regions. Firstly, topographic heights of a Digital Elevation Model are normalised with reference to the gully channel thalweg to extract gully floor elements, and secondly, slope are calculated along the direction of flow to determine gully wall elements. As the gHAND workflow eliminates the need to define kernel thresholds that are sensitive towards gully size, it is more scalable than kernel-based methods. The workflow is rigorously tested at different gully geomorphic scales, in contrasting geo-environments, and compared to benchmark methods explicitly developed for region-specific gullies. Performance is similar to benchmarks methods (variance between 1.4% to 14.8%) and returned user and producer accuracies above 84.5% and 70.6% for gullies with planimetric area varying between 1421.6 m^2 and 70246 m^2 (situated in contrasting environments). Although the gHAND workflow has limitations, most markedly the requirement of manually digitising gully headcuts, it shows potential to be further developed reliably map gullies of small- to large-scales in different geo-environments.

4.2 INTRODUCTION

Gully erosion is a form of channelised water erosion associated with the severe degradation of land and water resources (Wen et al., 2021; Wilkinson et al., 2015). When gullies are active in a catchment, they can become the dominant erosive force, delivering significant amounts of sediment to the lower catchment (Bennett et al., 2000; Poesen et al., 2003). On-site soil removal and off-site deposition yield significant environmental consequences that limit agricultural potential and production on-site (Xu et al., 2016; Yitbarek et al., 2012), and that translates into water resources (Le Roux, 2018) and aquatic ecosystem pressures off-site (Shellberg, 2021; Wantzen, 2006). Under projected climate change, gully erosion is expected to increase significantly due to an increase in rainfall intensity (Vanmaercke et al., 2016), exacerbating gully-related degradational consequences.

Given the current and future gully erosion threat, there has recently been a significant increase in gully erosion research (Castillo & Gómez, 2016; Peñuela et al., 2023; Rahmati et al., 2022; Setargie et al., 2023; Sun et al., 2022). However, despite the higher research output, there remains a lack of gully occurrence and monitoring datasets at larger scales encompassing a range of geo-environmental regions (Vanmaercke et al., 2021). Establishing such datasets will determine how different control factors impact gully erosion morphology, dynamics, and rates. This, in turn, will help to assess the efficacy of rehabilitation measures and will support the development of gully modelling efforts that can be used to predict gully evolution in changing environments.

Due to time and labour constraints, manually mapped gully inventories covering large scales are rare (for example, Mararakanye & Le Roux, 2012). Usually, these manually captured gully inventories are created as a snapshot in time and not subsequently updated to create a temporal dataset. Additionally, the process is subjective, which may lead to bias and impact upon accuracy (Maugnard et al., 2014). With technological advancements and an increase in the availability of high-resolution (≤2 m) remotely sensed data sets, (semi-)automating mapping procedures can be implemented to address these limitations.

Different methodologies have been applied to semi-automate the mapping process of gully features, for example, using spectral information from satellite imagery (d'Oleire-Oltmanns et al., 2014; Pretorius et al., 2016; Vrieling et al., 2007), DEM (Brecheisen & Richter, 2021;

Castillo et al., 2014; Vallejo-Orti et al., 2019; Walker et al., 2020), or a combination of these data sources (Shruthi et al., 2011). Selecting one data source would be advantageous for creating a low-data-intensive, practical, and transferable semi-automated mapping approach. Topographical input may be more inclined to achieve a practical and transferable approach since gullies have a distinct landform, *viz.*, a persistent elongated erosional feature with an active head scarp and moderately steep to very steep sidewalls (Thwaites et al., 2022). Therefore, DEMs are ideally suited for extraction techniques directly related to gully morphology, making them easily understandable compared to spectral reflectance data derived from different regions of the electromagnetic spectrum. Moreover, using the morphology as a detection guide should enhance the transferability of the approach to regions exhibiting contrasting climates, whereas spectral reflectance may be hindered due to the variance incurred from different vegetation covers, including seasonal changes (Phinzi et al., 2021; Vrieling et al., 2007). Many recent semi-automated research methods try to exploit local terrain differences caused by gullying by calculating differences in topography using pre-determined search window sizes. Evans & Lindsay (2010) used an edge detection method, passing a mean filter subtracted from the DEM, to map gully sidewalls, where the area between the edges was then interpolated. Eustace et al. (2011) calculated slope variance as part of their extensive inputs to detect gully features. Johansen et al. (2012) employed a min/max brightness filter to detect gully edges as the initial step in mapping gullies in their study area. Castillo et al. (2014) calculated a z-score normalisation statistic to identify gully floor and wall elements separately before joining and refining the classification. Francipane et al. (2020), using a roughness index, and Walker et al. (2020), calculating elevation percentiles for various DEM derivatives, employed a similar strategy to identify the gully elements separately. Vallejo-Orti et al. (2019) determined curvature differences within a moving window to identify gully morphology to extract gully features.

Although the approaches to detect the gully landform elements are sound and provide reliable results, determining the optimal window size remains challenging irrespective of the statistic or terrain derivative calculated for input. Using a window size that is too small may result in noise, while using one too large will conceal edge effects (Evans & Lindsay, 2010), showing that such an approach is scale dependent. The scaled sensitivity of the search and filter windows adversely affects the applicability at the catchment to regional scales. Therefore, it would be

helpful to develop a semi-automated method that circumvents defined window sizes to become scale-independent, thus applicable to a range of gully scales.

Implementing Height Above Nearest Drainage (HAND) would overcome the need for implementing window sizes instead using standardised height values. HAND normalises terrain according to drainage, providing local flow path heights to the nearest stream (Nobre et al., 2011). Thus far, HAND has been primarily implemented in flood inundation (Garousi-Nejad et al., 2019; Johnson et al., 2019; Liu et al., 2016) and groundwater (Hamdani & Baali, 2019; Miguez-Macho et al., 2020) research. However, the hydrological normalisation of topography by HAND may also hold the potential to identify gully landform elements, notably the gully floor.

We, therefore, aim to 1) develop a low data-intensive, repeatable, scalable, semi-automated methodology, the Gully HAND (gHAND) workflow, to map permanent gullies, using the HAND model as the primary derivative (which, to the authors' knowledge, has not been used in gully detection strategies; 2) test the scalability of gHAND by mapping gullies of different geomorphic scales in South Africa using a 2 m DEM (GeoSmart Space, 2020b) developed from aerial imagery; 3) test transferability potential by applying gHAND at sites exhibiting different geo-environmental conditions and where different DEM products are available; and 4) benchmark against other semi-automated mapping methods.

4.3 METHODS

4.3.1 Study area

4.3.1.1 Regional setting of development sites and evaluating of scalability

The Tsitsa catchment was used for the initial development of gHAND and to test the scalability thereof. The Tsitsa River is approximately 200km long (Le Roux, 2018), with its confluence in steep topography into the Mzimvubu River. Upstream of the confluence, undulating plains are found, whereafter the catchment becomes steeper again as the river approaches the Drakensberg. The aerial extent of the Tsitsa catchment is approximately 4927 km^2, located between 30° 46' 51" S and 31° 29' 15" S latitude and 27° 56' 13" E and 29° 13' 43" E longitude (Figure 4.1a). The climate is sub-humid. Rainfall predominantly occurs in mid to late summer (Schulze & Maharaj, 2006), ranging between 625 mm in the lower plains, and increasing to

1327 mm in the mountainous upper catchment (Le Roux, 2018). The natural vegetation is predominantly from the Grasslands biome region. However, the Savanna biome is also present in the southwestern catchment (Mucina & Rutherford, 2006), where thorny acacia trees have encroached on the grassland area. The main land use in the catchment is communal grazing, with smaller pockets of commercial maize and plantations. The geology is primarily of sedimentary strata, with large parts of the catchments underlaid by the Tarkastad and Adelaide subgroups of the Beaufort formation, and Elliot group (Burger, 2013). The aforementioned sedimentary strata have been linked to derive duplex soils (soils that exhibit a strong texture contrast between surface soil and subsurface soil, mostly from translocation of clay; see Fey, 2010) with high dispersion, closely linked to high erosion susceptibility (Laker, 2004).

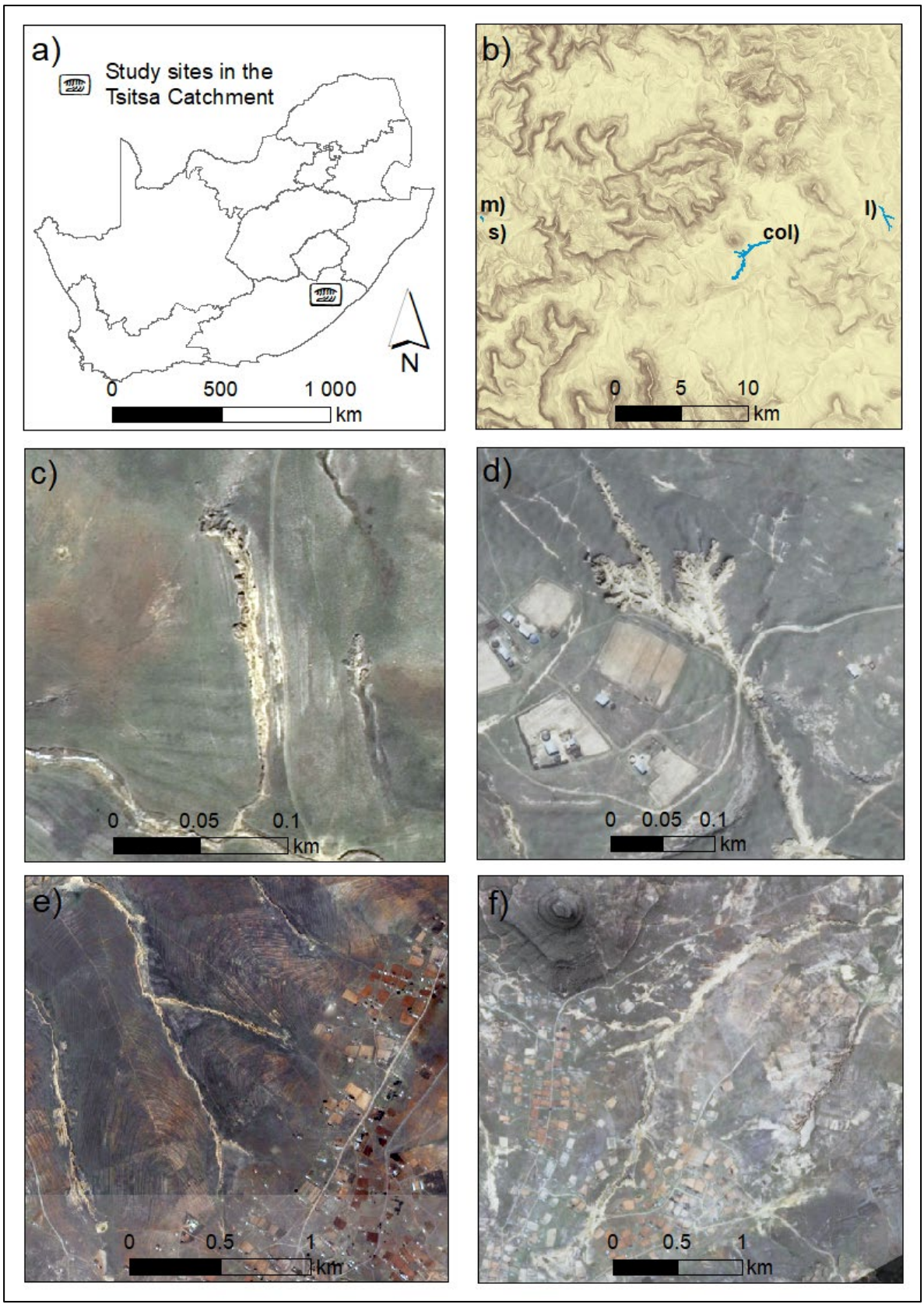

Figure 4.1 Gully sites in the Tsitsa catchment used for testing the scalability of gHAND and evaluate the scalability thereof: **a)** location of the Tsitsa catchment in South Africa; **b)** the position of the four gully sites

overlaid onto a DEM; **c)** small-scale gully (denoted as 's' in panel b); **d)** medium-scale gully (denoted as 'm' in panel b); **e)** large-scale gully (denoted as 'l' in panel b); **f)** colossus-scale gully (denoted as 'col' in panel b) (Aerial imagery is courtesy of Department of Rural Development & Landform, available at http://www.cdngiportal.co.za/cdngiportal/).

Gully erosion is extensive in the Tsitsa, with numerous large gullies (Le Roux et al., 2022). Sub-surface processes predominantly cause gully expansion; slumping results in gullies expanding laterally (Figure 4.2a) and collapsing pipes (Figure 4.3a) and tunnels enlarge gullies both linearly and laterally. Tension cracks that increase throughflow are also present along gully walls and headcuts. However, overland flow processes are also active in the catchments, evident from near-vertical, active gully headcuts (Figure 4.2b) and flute development on sidewalls (Figure 4.2a). Certain large-scale gullies also present meandering morphology (Figure 4.3). A significant collapse, most likely a combination of fluvial scour and sapping, recently occurred on the outer cut bank of the meander of this gully (Figure 4.3b).

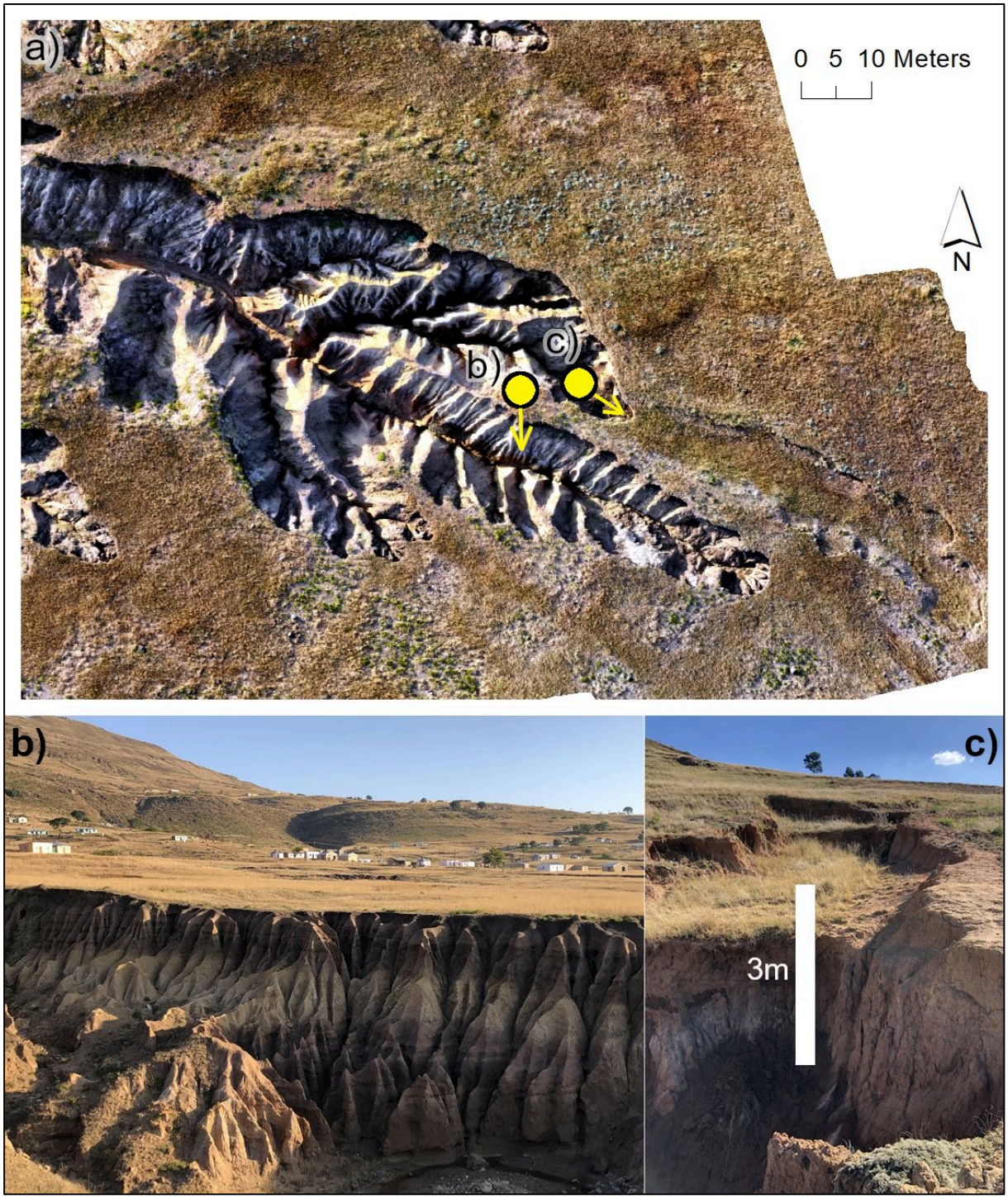

Figure 4.2 Typical large complex gully system in the Tsitsa catchment exhibiting steep gully sidewalls, some of which are fluted, and narrow interfluves between gully channel tributaries: **a)** an aerial photo of the gully taken by a DJI Mavic 3 Unmanned Aerial Vehicle; **b)** shows a V-shape channel formed by slumping sidewalls from subsurface flow processes nearer the photographer. Recent slumps can be seen with soil still having grass coverage. Further downstream of the gully headcut, surface flow processes are evident from the fluting sidewalls (position and direction of photo denoted as b in panel

a); **c)** an active, near-vertical gully headcut found downstream of a shallow, grass-covered gully channel (position and direction of photo denoted as c in panel a).

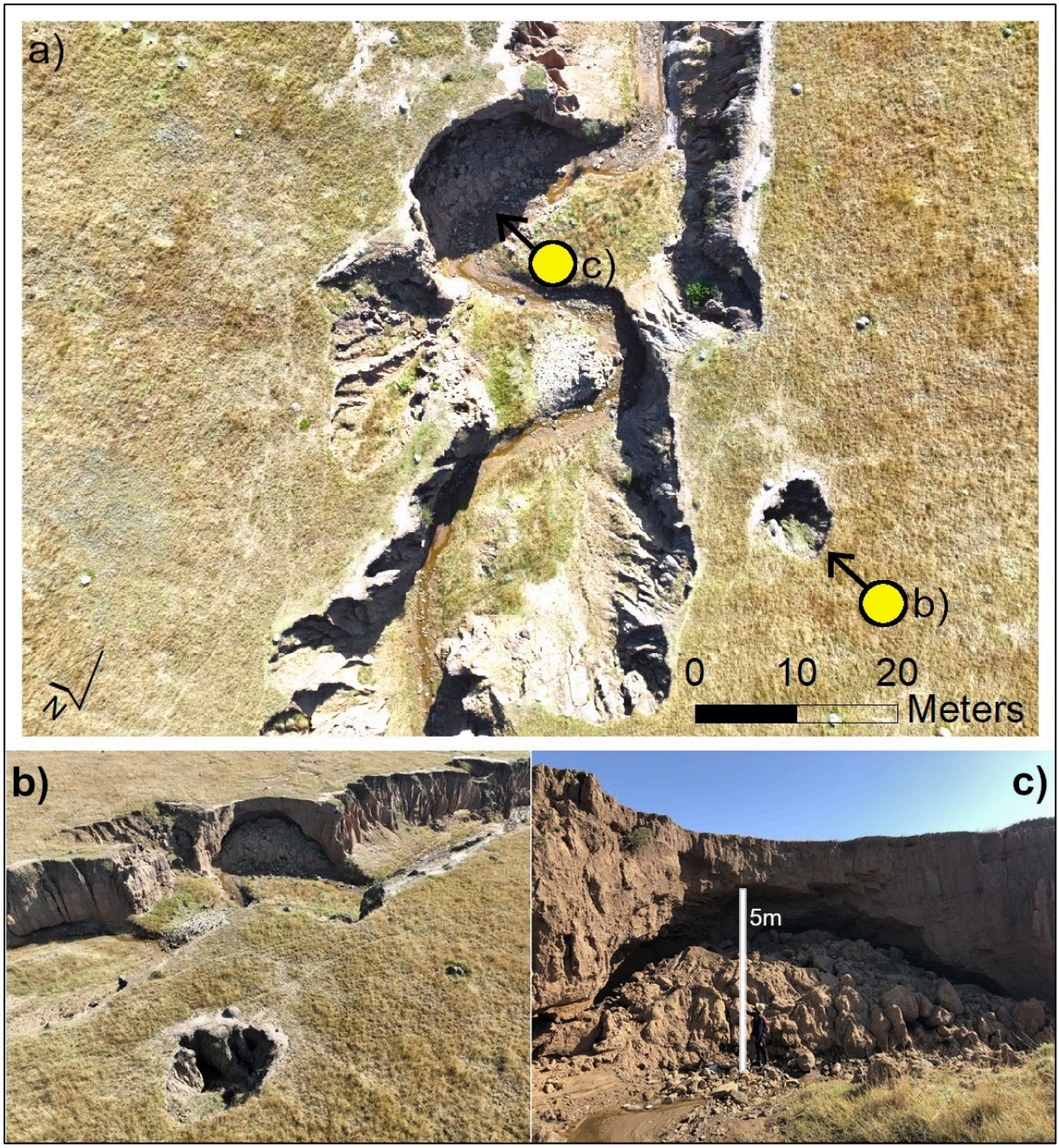

Figure 4.3 An extensive gully system in the Tsitsa catchment that shows river-like morphology with actively eroding cut bank, with deposition occurring at point bar: **a)** an aerial photo of the gully taken by a DJI Mavic 3 Unmanned Aerial Vehicle; **b)** the collapse of a large sub-surface pipe is evident in the foreground, which is connected to the gully at a large outlet at the gully wall-gully floor interface. Significant deposits can be seen at the outer meander wall (position and direction of photo denoted as b in panel a); **c)** the significant collapse from scour resulting in undercutting of the gully wall at the outer meander gully wall, in addition to grass coverage on the deposited soil at the inner meander bend in the foreground (position and direction of photo denoted as c in panel a).

Four gully sites (Table 4.1), increasing in geomorphic scale, were selected to develop gHAND methodology and evaluate scalability. All four gullies are continuous and situated in communal grazing areas surrounded by gentle slopes. The small-scale gully (planimetric area < 2500 m^2; Figure 4.1c; 31° 11’ 37” S, 28° 28’ 25” E) has an N-to-S orientation and is 183.3 m in length with a planimetric gullied area of 1619.0 m^2 and a maximum width of 18 m. The gully consists of a singular gully headcut, although protruding lobes are found along sidewalls. The medium-scale gully (planimetric area between 2500 m^2 and 25000 m^2; Figure 4.1d; 500 m west of the small-scale gully) is near the small-scale gully and features an N-to-S orientation. A road dissects the gully, whereafter it widens up to 54 m upstream and consists of multiple gully headcuts. The length along the major drainage axis is 430.9 m, and the composite gullied area has a planimetric area of 12135.6 m^2.

The large-scale (planimetric area between 25000 m^2 and 250000 m^2; Figure 4.1e; 31° 11’ 59” S, 28° 47’ 21” E) gully has an S-to-N orientation, with a maximum width of 37 m. The gully length along its major drainage axis is 2142.8 m, and the total planimetric gullied area is 70246.7 m2. The gully has two major tributaries but also features shorter branches that are broad and numerous renewed headcuts along knickpoints in the existing gully floor. The colossus-scale gully (planimetric area >250000 m^2; Figure 4.1f; 30° 13’ 46” S, 28° 40’ 06” E) has an SW-to-NE orientation. The gully is one of the largest in the world, and twice the size of the largest gully documented in peer-reviewed literature, according to Le Roux et al. (2022), who manually mapped this gully via UAV. The gully is 5113.2 m long along its major drainage axis and has a planimetric area of 425403.7 m^2, exhibiting widths up to 210 m. There will be discrepancies between the morphometric measurements of Le Roux et al. (2022) and those presented here, since Le Roux et al. (2022) used UAV imagery with a 0.1 m spatial resolution obtained from September 2018, while we used the 2015 aerial imagery with a 2 m spatial

resolution (GeoSmart Space, 2020b). The gully is complex, showing various active surface processes (fluvial scour, undercutting from confined surface flow, plunge pools at near-vertical gully headcuts, and extensive fluting) and sub-surface processes (including piping), most of which lead to catastrophic mass failures (Le Roux et al., 2022). Furthermore, the gully exhibits a meandering morphology in the lower reaches, with active erosion at the cut bank and depositional point bars.

Table 4.1 Gully characteristics.

Site	DEM type	Scale	Orientation	Environment	Length along main channel (in m)	Maximum width (in m)	Planimetric area (in m^2)
Scalability testing							
Tistsa catchment	Surface	Small	North to South	Communal grazing, sub-humid	183.3	18	1619.0
Tsitsa catchment	Surface	Medium	North to South	Communal grazing, sub-humid	430.9	54	12135.6
Tsitsa catchment	Surface	Large	South to North	Communal grazing, sub-humid	2142.8	37	70246.7
Tsitsa catchment	Surface	Colossus	Southwest to Northeast	Communal grazing, sub-humid	5113.2	210	425403.7
Transferability testing							
Herbert catchment, Australia	Terrain	Small	East to West	Grazing, wet tropics	202.7	13	1530.1
Montagu, South Africa	Surface	Medium	West to East	Game reserve, arid	487.5	17	5188.3
Cordoba, Spain	Surface	Medium	Northeast to Southwest	Intensive grain, Mediterranean	662.0	20	14067.5
Krumhuk, Namibia	Surface	Large	North to South	Cattle farm, arid	698.3	152	66019.3

4.3.1.2 Regional setting of sites testing transferability

Four additional gully sites were selected to test the transferability of gHAND (Table 4.1; Figure 4.4). Site selection was made according to data availability, whether the site exhibited a contrasting climate compared to the Tsitsa catchment, and preferably where gully detection approaches based on topographical attributes were applied previously. In Australia, a continuous gully was selected in the Herbert catchment near Innot Springs (Figure 4.4c; 17 43" 16' S, 145 11' 1" E; the gully is in the Great Barrier Reef catchment, where Walker et al., 2020 conducted a semi-automated detection approach, although our gully is located approximately 200 km north of the Walker et al, 2020 study site). The gully is located on native pasture in a catchment that experiences strong seasonal rainfall patterns (Bartley et al., 2003). The gully has a linear morphology with a singular headcut and has a planimetric area of 1530.1 m^2. For further information regarding the environmental setting, see Bartley et al. (2003).

A continuous gully was selected at Krumhuk, Namibia (Figure 4.4e; 22° 44' 03" S, 17° 05' 46" E; same gully as Vallejo-Orti et al., 2019) found on a commercial cattle farm, in an arid region that features densely populated shrubs. The gully morphology is different from the other test sites, which are mostly linear. The gully at Krumhuk exhibits extensive lateral erosion of the sidewalls in the form of rills and smaller gullies, lowering the slope of the historical short sharp sloped gully walls. The channel widths extend up to 152 m wide (Vallejo-Orti et al., 2019), but the landscape seems to be transitioning to a badlands landform, losing the original distinct channel. For further information regarding the environmental setting and gully characteristics, see Vallejo-Orti et al. (2019).

In South Africa, a discontinuous gully was selected in a conservation area in the semi-arid Karoo (Figure 4.4d; 33° 40' 52" S, 20° 36' 35" E; same gully as Olivier et al., 2022) with a mean annual rainfall of 135 mm (Schulze et al., 2006). The gully has two morphologically different gully channels that join and wane into a deposition zone. The northern gully leg is a narrow, meandering channel consisting of active cut banks and deposition dominant point bars, whilst the southern branch is broad and straight. The gully is the widest at one of the meanders in the northern leg (17.3 m) and has a planimetric area of 5188.3 m^2.

In Córdoba, Spain, which exhibits a Mediterranean climate, a continuous gully (Figure 4.4b; 37° 49' 09" N, 4° 35' 39" W; same gully as Castillo et al., 2014) along a drainage line of an

extensively agricultural crop farm was selected, with a maximum width of 20 m recorded (Castillo et al., 2014). For further information regarding the environmental setting and gully characteristics, see Castillo et al. (2014).

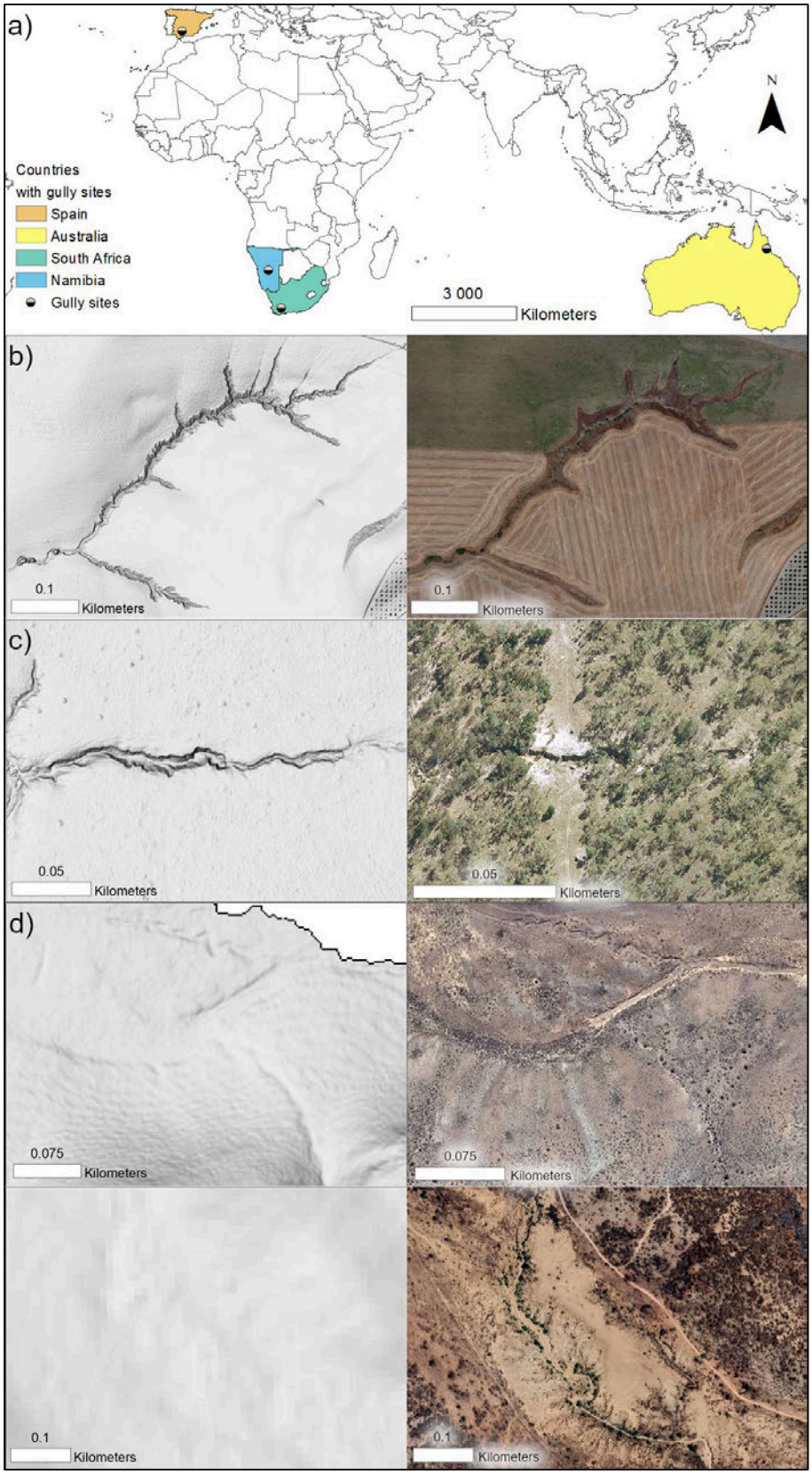

Figure 4.4 Gully locations where the transferability of gHAND method was tested. Gullies are overlaid on a multi-directional hillshade of the DEMs in the first column and imagery in the second column: a) shows

the location of the various test sites where transferability was tested; b) a 0.06 m DEM indicating a gully in Córdoba, Spain (Castillo et al.,2014) and column two shows the satellite imagery showing the gully in Córdoba, Spain, courtesy of Google Earth (21/7/2018); c) 0.5 m DEM showing the gully in the Herbert catchment, Australia (Geoscience Australia National Elevation Data Framework, available at http://www.ga.gov.au/elvis/) and the second column shows an aerial imagery from the gully in the Herbert catchment, Australia (Geoscience Australia National Elevation Data Framework, available at http://www.ga.gov.au/elvis/) captured on the same date as DEM acquisition; d) 2 m DEM depicting the gully close to Montagu, South Africa (GeoSmart Space Pty (Ltd), 2020) and in the second column an aerial image that was used in DEM production (Department of Rural Development & Landform, available at http://www.cdngiportal.co.za/cdngiportal/); e) a 12 m DEM showing a faintly visible gully at Krumhuk, Namibia (Vallejo-Orti et al., 2019) and the second column showing the satellite image depicting the gully on Krumhuk farm in Namibia, courtesy of Google Earth (23/10/2021).

4.3.2 Datasets

In South Africa, GeoSmart Space (2020b) created a 2 m DEM (known as DEMSA2) from aerial imagery (spatial resolution of 0.5 m), augmented by SRTM (Shuttle Radar Topography Mission) data in flatter terrain, covering approximately 96% of the country. The gHAND workflow implemented the 2 m DEM for the sites in the Tsitsa catchment and the testing site in the Karoo (Table 4.2). In addition, the same aerial imagery used as input for creating the 2 m DEM was used as a base map to manually digitise reference gully datasets for both areas.

In the Herbert catchment, Australia, arial flights from 2018 were flown to collect LiDAR data with a target density of 16 points per square meter (Geoscience Australia National Elevation Data Framework, available at http://www.ga.gov.au/elvis/). Aerial imagery from the same flight, supported by a multi-directional hillshade, was used for digitising a reference dataset manually. In Krumhuk, Namibia, a 12 m TanDEM-X was acquired from a TerraSAR-X DLR mission in January 2015 (see Vallejo-Orti et al., 2019 for further detail). In addition, a reference dataset was digitised from 0.5 m Pleiades imagery produced in December 2016. In Córdoba, Spain, a 0.06 m DEM was created using commercial software (Pix4D) from photogrammetric methods (see Castillo et al., 2014 for more detail). A differential dGPS with cm accuracy was used to map the gully perimeter by the change-in-slope criterion. The dGPS points were taken in-field on the date of flight and used as a reference boundary for the gully feature.

Table 4.2 DEM data for all sites.

Site	Company	Parent data from which the DEM is derived	Spatial resolution	Vertical accuracy	Horizontal accuracy	Semi-automated detection method
Córdoba, Spain	Castillo et al., 2014 implemented commercial software Pix4D	Aerial imagery	0.06 m	0.23 m	0.09 m	NorToM (Castillo et al., 2014) and gHAND
Herbert catchment, Australia	LiDAR collected for Reef Trust, by Atlass Aerometrex, with CSIRO as the project manager	LiDAR	0.5 m	0.2 m	0.8 m	gHAND
Tsitsa and Karoo, South Africa	GeoSmart Pty (Ltd)	Primarily aerial imagery	2 m	0.5 m	1 m	gHAND
Krumhuk, Namibia	DLR (German Aerospace Center)	Satellite imagery	12 m	2 m	10 m	IMR, SMPF, and MPCA (Vallejo-Orti et al., 2019) and gHAND

4.3.3 The gHAND procedure

The gHAND workflow combines a raster-based approach (per cell value) with a Geographical Object-Based Analysis Approach (GEOBIA) segmentation (Table 4.3; Figure 4.5). The building blocks for the segmentation approach, used to identify the gully landforms, are created in ArcGIS 10.6.1 (Environmental Systems Research Institute (ESRI), Inc., Redlands, California, United States of America) using raster cells. First, the DEM is hydrologically corrected (Planchon & Darboux, 2002), after which flow direction and a drop raster, essentially a slope calculation along the flow path, are calculated. Next, a multi-directional hillshade technique is incorporated to identify gully headcuts visually, which is the only point where manual input is required in gHAND method. Once identified, the gully headcuts are digitised with a point feature. Finally, the digitised points are used as the origin point of flow, from which HAND can be calculated.

Table 4.3 gHAND procedure.

Process classification	Software application	Step	Output	Description	Environment setting	Tool used
Pixel-based	ArcGIS 10.1.6	1	Conditioned DEM	Fill sinks		Fill (*Spatial analyst)*
		2	Additional flow direction and slope	Calculate the flow direction and Drop Raster slope	Dinf method; include DropRaster as output, which is the slope along the flow path	Flow direction (*Spatial analyst*)
		3	Gullied drainage	Generate a multi-directional hillshade		Open *window analysis*. Select the conditioned DEM and add the hillshade function – select multi-directional
				Digitise gully headcuts as points	Upon completion edit the ID field – Set all to 1	Editor
				Rasterise the digitised points	Set processing extent to DEM (output 1); snap raster to DEM; copy spatial resolution from DEM	Feature to Raster (*Conversion)*
				Reclassify *NoData* to zero values		Reclassify (*Spatial analyst*)
				Calculate the flow direction	D8 method	Flow direction (*Spatial analyst*)
				Calculate the weighted flow accumulation	Use the rasterised gully headcuts (output 2) as weight raster input	Flow accumulation (*Spatial analyst*)
				Create a binary stream network		Reclassify (*Spatial analyst*)
		4	HAND	Calculate the height above nearest drainage	- Stream raster: Output 3 - Surface raster: Output 1	Flow distance (*Spatial analyst*)

					- Flow direction raster: Output 2 (Dinf) - Flow distance type: Vertical - Flow direction type: Dinf	
Object-based	Ecognition Developer 9	5	Generate and classify gully elements	Create meaningful objects from homogenous pixels	Equal weighting for Drop Raster (output 4) and HAND (output 5); Scale parameter: 4, Shape factor: 0.8; Compactness factor: 0.4	Multiresolution segmentation
				Use a threshold approach to identify the gully floor	Use "*Low_HAND*" threshold at image object level	Multi-threshold segmentation
				Remove all objects containing *NoData* values	Use HAND < 0	Assign class
				Merge gully floor elements		Merge region
				Use a threshold approach to identify gully wall candidates	Use "*Heigh_HAND*" and "*Bluff_DropR*" thresholds at image object level	Multi-threshold segmentation
				Combine gully wall candidates		Merge region
				Shrink gully wall elements to off-set overprediction	One iteration	Pixel-based object resizing
				Merge gully wall candidates		Merge region
				Merge gully floor and gull wall candidates		Merge region
		6	Refining gully network	Grow the merged gully candidates	One iteration	Pixel-based object resizing
				Fill any holes found within the classification	Set the area smaller than "*Isle_Hole*" and ensure that the gap is surrounded by gully candidates (relative border = 1)	Assign class

			Smooth gully candidate objects	One iteration (shrink)	Pixel-based object resizing
			Remove any dangling phantom gully branches	Set minimum threshold "*Min_Phan*" with objects below set to unclassified	Assign class
	7	Export gully classification	Save the mapped gully		Export vector layer

2

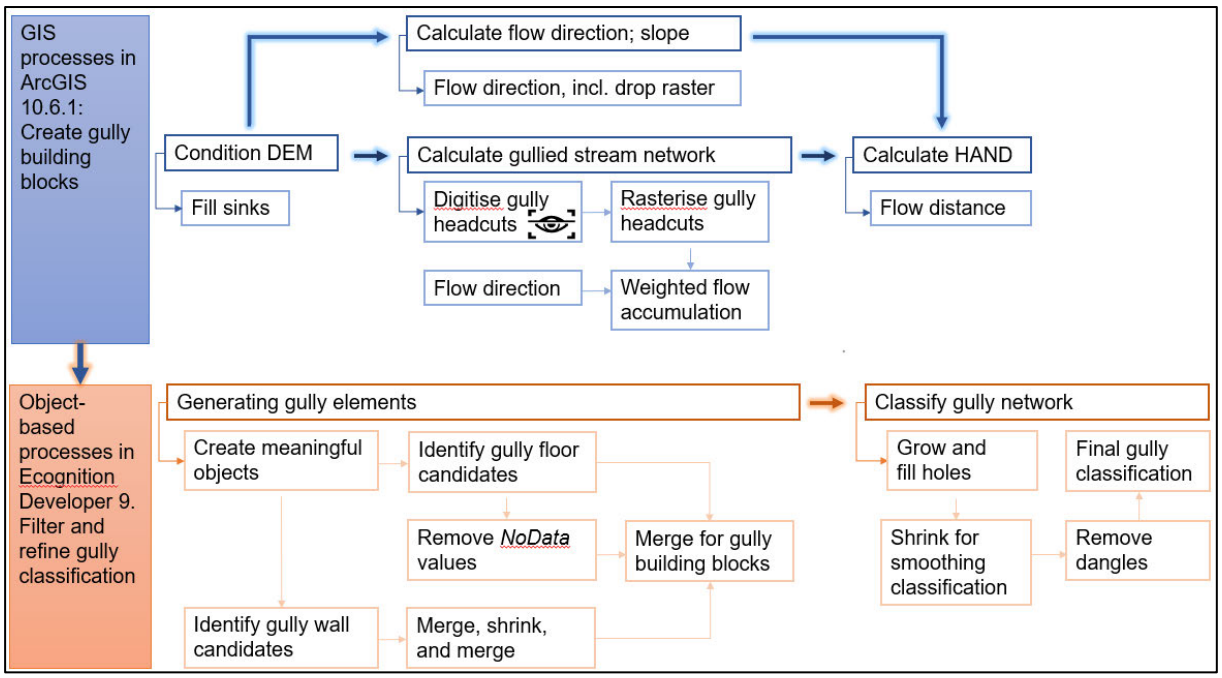

Figure 4.5 The gHAND workflow diagram. The eye symbol shows the timing of manual user input in the workflow. Although user input is required at other timings, mostly threshold definitions, these are required only during the initial setup, whereafter, the model can be simulated automatically for various gullies.

The HAND model normalises the DEM according to its derived drainage network, i.e., a gully channel in this study. The flow path along the channel is assigned a zero value and used as a flat topographic reference from which local heights are calculated (Nobre et al., 2011; Rennó et al., 2008). The gully floor will thus be assigned a zero or near-zero value (Figure 4.6). The near-zero values result from local gully floor topography (influenced by DEM spatial resolution), consequently causing the gully floor not to coincide entirely within the flow path identified by HAND. At the same time, gully wall elements, i.e., the steep slopes in lateral proximity, can be acquired from the drop raster, which is calculated as an optional output during the HAND procedure in ArcGIS 10.6.1 (ESRI Inc., Redlands, CA, USA) (Table 4.2).

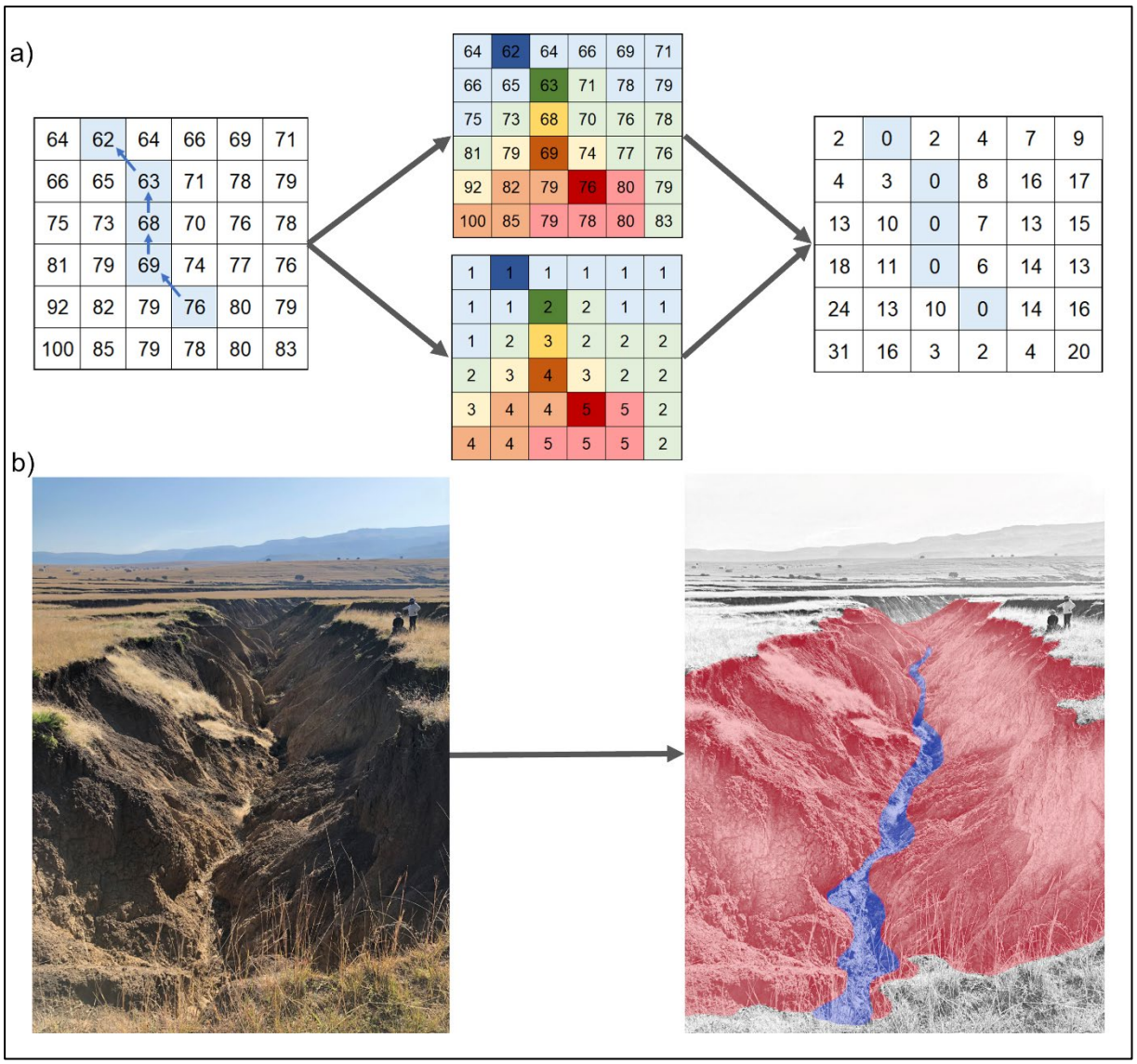

Figure 4.6 Normalising the DEM according to HAND to highlight the distinct morphology of a gully channel: a) raster-based depiction of the HAND calculation (after Nobre et al., 2011). Firstly, the DEM values onto which flow is superimposed according to the D8 method; secondly, a nearest drainage map is created, where each raster cell is associated with the raster cells draining into it; lastly, the HAND normalised raster in which each raster cell exhibits the height to its nearest drainage cell; b) indicating how gHAND method is applied to a gully, where the gully floor is normalised to have zero (or near-zero) values, depicted by blue, while the steep sidewalls can be used by the optional drop-out raster during the HAND calculation process (depicted in red).

The primary building blocks, i.e., HAND and slope, created during the pixel-based approach, are imported into Ecognition 9.1 (Trimble, Munich, Bavaria, Germany) for GEOBIA segmentation to map gully landform elements using objects (Tale 4.2; Figure 4.6). GEOBIA segmentation was selected as it has outperformed exclusive pixel-based approaches in

extracting gully features, because of the ability of the object-orientated approach to extract data regarding shape, proximity, and neighbouring relationships (Francipane et al., 2020). The multi-resolution segmentation process creates objects from a bottom-up approach that groups pixels according to the relative homogeneity within the input variables (Blascke, et al., 2014). The scale parameter controls the allowable variance of homogeneity and is based on a combination of shape and colour properties (in our case the HAND and slope values) and compactness (how closely related the shape is to a circle) (Trimble Germany GmbH, 2023). Larger scale parameters yield larger objects and vice versa (Karydas & Jiang, 2020). Gullies are predominantly linear, following drainage lines, although exceptions such as alluvial amphitheatre gullies also exist (Shellberg & Brooks, 2012; Thwaites et al. 2022). Therefore, a smaller scale parameter was desirable given the 2 m DEM resolution. A trial-and-error calibration was conducted on a medium-scale gully, whereafter a scale parameter of 4 was selected (see APPENDIX C, which showed larger objects resulting in higher overestimation errors). To allow the scale factor to transition with changing spatial resolution, we employed a simple division process:

$$Sf^{\sim} = \frac{Sf}{S_{res}} \quad \text{Equation 5.1}$$

Sf is the original scale factor of four, established for the 2 m DEM;

S_{res} is the spatial resolution of the new input DEM;

$Sf^{\sim}$ is the calculated scale factor to be used during multi-resolution segmentation for the given DEM

A minimum scale factor of 2 was used, however, for coarser spatial resolutions.

More emphasis was placed on shape compared to colour (parameter set to 0.8), and due to the linear shape, the compactness weighting was set to 0.4. The GEOBIA ruleset requires additional thresholds to be set. However, like the scale factor, it is only required during the initial setup, whereafter the ruleset can be applied automatically. The *Low_HAND* threshold, set at 0.5 m conforming to the gully definition of Thwaites et al. (2022), is applied to identify gully floor elements. Gully walls are short steep elements, which Thwaites et al. (2022) define as exhibiting

a minimum slope of 60%. We however opted for a lower slope threshold of 25%, which is more aligned with the threshold that Walker et al. (2020) for their gully detection strategy at DEM resolutions of 1 m (20%). Additionally, the slope was constrained to a HAND depth of 6 m (*Heigh_HAND*), to avoid noise detection caused by steep features on hillslopes. To minimise overprediction due to slope calculation from pixels, gully wall elements were shrunk by one cell. Any holes within the gully map classification with an area smaller than 200 m^2 (*Isle_Hole*) with a HAND depth lower than 6 m were filled if all neighbouring objects were classified as a gully feature. Lastly, all remaining false positives on the hillslope were removed, setting the same size threshold of 200 m^2 (*Min_Phan*).

4.3.4 Limited threshold editing of gHAND

Although we aimed to identify a method that could be scalable and used without editing for a range of gully sizes, we decided to minimally tweak gHAND for the colossus scale gully, to establish whether detection accuracy improvement could be made. Due to the gully dimensions, *Low_HAND* was increased from 0.5 m to 1 m and *Heigh_HAND* was increased from 6 m to 10 m.

4.3.5 Accuracy assessment

The gHAND segmented mapping results were evaluated by measuring the dissimilarity between gHAND-derived and reference polygons (like Castillo et al., 2014) from

$$E_O = \frac{\sum |H_i - r_i|}{R_{Ai}} \quad \text{(Equation 5.2)}$$

$$E_U = \frac{\sum |r_i - H_i|}{R_{Ai}} \quad \text{(Equation 5.3)}$$

$$E_{tot} = |E_o| + |E_u| \quad \text{(Equation 5.4)}$$

E_o is the over-estimation representing the total area of polygon segments derived from gHAND that is outside the perimeter of the reference polygon;

E_u represents the under-estimation of the gHAND mapped polygon by finding the total area of reference polygon segments that exceed the predicted gullied polygon by gHAND;

E_{tot} is the combined error of E_o and E_u;

H_i is the calculated area of the i-th polygon segment mapped by gHAND;

r_i is the area of the i-th reference polygon segment;

R_{Ai} is the total gullied area according to the i-th reference polygon.

Although user (A_u) and producer (A_p) accuracy provide similar information to E_o and E_u, they were included because it is used often calculated in a confusion matrix to assess the accuracy of remotely sensed classification procedures. A_u indicates the likelihood of a mapped feature being correctly detected (related to error of commission), A_p provides the probability that an existing feature will be correctly mapped (related to error of omission). The confusion matrix from which A_u and A_p are derived typically inflate accuracy results in gully erosion research due to the imbalance of gullied and non-gullied areas. (Congalton, 1991; Taruvinga, 2008). To address this over-inflation, an adapted approach is followed herein, based on Vrieling et al. (2007), whereby:

$$A_u = \frac{G_c}{G_t} \quad \text{(Equation 5.5)}$$

$$A_p = \frac{G_c}{G_r} \quad \text{(Equation 5.6)}$$

which is then averaged, to provide an overall accuracy metric calculated as:

$$A_a = \frac{A_u + A_p}{2} \quad \text{(Equation 5.7)}$$

A_u is the adapted user accuracy that provides a measure of how much non-gullied area is mapped as gully by gHAND;

A_p is the adapted producer accuracy that tests how much of the reference gully area is predicted correctly by gHAND;

A_a provides an averaged error;

H_i is the calculated area of the i-th polygon segment mapped by gHAND;

G_c represents true positives, the area correctly mapped as gullies;

G_t is the total area mapped as a gully;

G_r is the total gullied area according to the reference dataset.

Besides the quantitative evaluation of the gHAND detection method, a qualitative assessment was conducted visually by the same operator to identify areas of poor classification. The qualitative assessment helps to understand areas of poor prediction, possibly improving future prediction efforts using gHAND.

4.3.6 Parameter sensitivity analysis

A second evaluation tested the sensitivity towards the digitised gully headcuts, because – as the only non-automated step in gHAND – this step might be prone to subjective user judgements. This sensitivity analysis thus established the robustness against subtle differences in user judgement. The sensitivity towards the placement of the digitised point representing the gully headcut was tested by moving it by 2 m, 5 m, 10 m, and 20 m, respectively, in the four cardinal directions. See APPENDIX D. The sensitivity was tested on a small-scale gully in the Tsitsa because it had a singular headcut. The gully has a north to south orientation (Figure 1a), with a broad gully headcut (17.3 m). Low sensitivities were found between 2 m and 10 m, but significant total errors occurred at 20 m, except in a westerly direction. Overall, this indicates limited sensitivity to headcut identification, assuming that users can identify headcuts within 10m accuracy.

A further sensitivity analysis compared the goodness of fit when all the gully headcuts, the main drainage channel gully headcuts, and only a single gully headcut along the main channel were used. The main channel was defined as the channel that extended the furthest upstream. See APPENDIX E.

Lastly, a sensitivity analysis was completed to test the influence of spatial resolution. The 2 m DEM was upsampled to 1 m (Castillo et al., 2014), by converting the 2 m DEM to points (points were placed at the center of each pixel), which was interpolated to create the 1 m DEM (Kriging interpolation method following the default settings according to the ArcGIS Geostatistical wizard; Environmental Systems Research Institute, Inc., 2018). The 2 m DEM was also downsampled to 4 m and 10 m, respectively, by cubic resampling. Lastly, a 20 m DEM

(GeoSmart Space, 2020a) that was available for the area was implemented as the DEM in gHAND.

4.4 RESULTS

4.4.1 Testing scalability: Gully identification in the Tsitsa

The results show that the same semi-automated workflow adequately maps permanent gullies with a gullied area between 1619 m^2, considered small-scale, to 70 246 m^2, considered large-scale (Figures 4.7, 4.8) for the native 2 m DEM. The A_u ranges between 84.5% and 94%, showing limited non-gullied areas falsely predicted as a gully. Similarly, the A_p shows that more than 80% of the gullied area is detected accurately for the small and medium-scale gullies and 75.4% for the large-scale gully. E_o, i.e., false positive rate, at these scales is low, between 4.4% and 16%, decreasing with the gully scale. The performance of gHAND for the colossus-scale gully, which is an order of magnitude larger than the large-scale gully (six times larger), is variable. E_o is low (3.1%), but this is coupled with a large E_u (48.9%) resulting in a total error of 52.1%. The low A_p of 51.1% also validates the large E_u. Limited editing to include local knowledge regarding depths and widths, improves accuracy for the colossus-scale gully to conform to those of the large-scale gully, i.e., A_p of 74.6% and E_o and E_u errors calculated as 7.8% and 25.4% respectively.

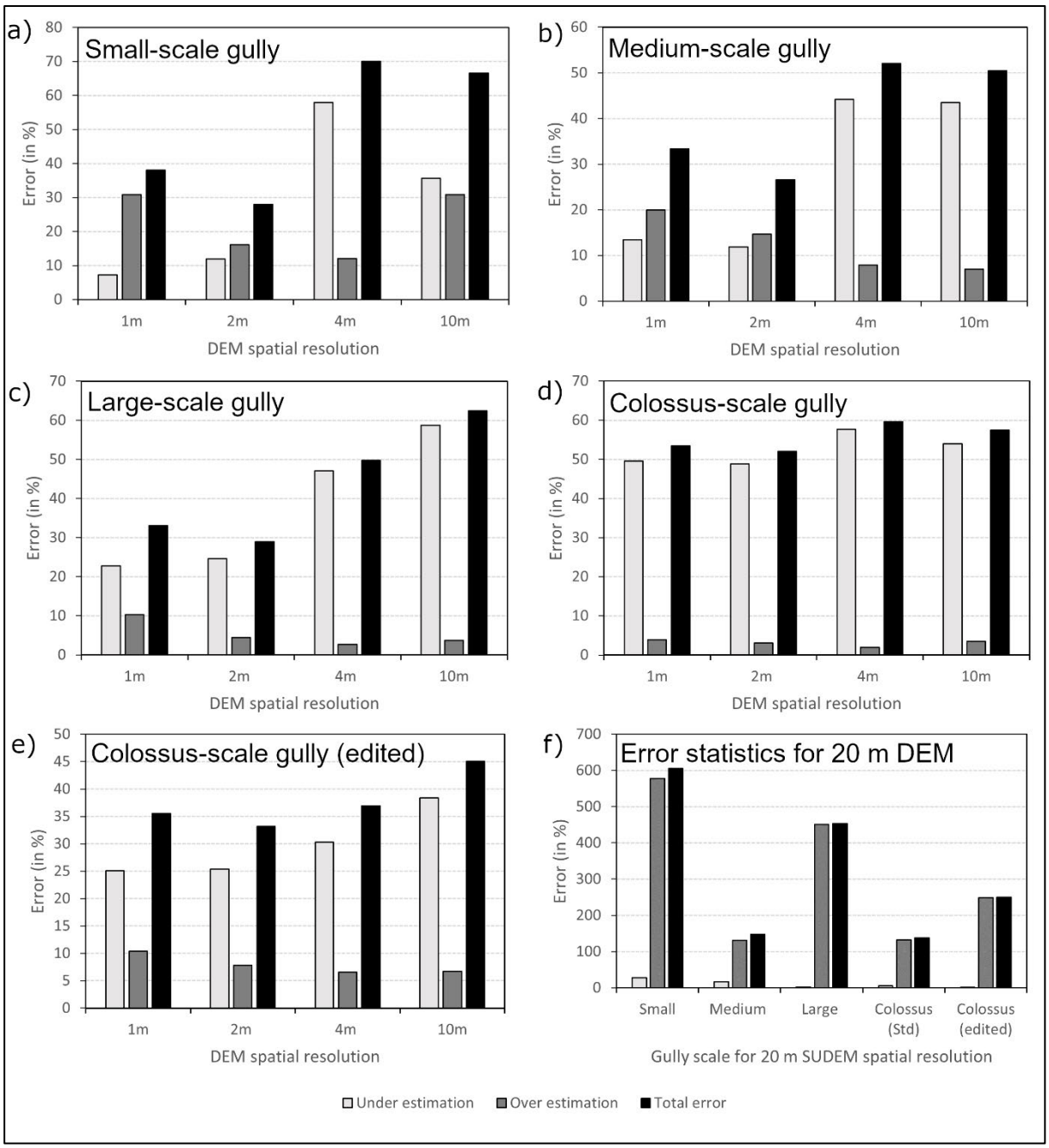

Figure 4.7 Under prediction, over prediction, and total error of the gHAND method for the native 2 m spatial resolution DEM, an up-sampled 1 m DEM, and a down-sampled 4 m and 10 m DEM for: a) a small-scale gully; b) a medium scale gully; c) a large-scale gully; d) a colossus-scale gully according to the standard gHAND; e) colossus-scale gully according to an edited gHAND; and f) the error rates for a 20 m DEM product for the different scale gullies.

Figures 4.7 and 4.8 also show areal error and accuracy results for up-sampled and down-sampled versions of the native 2 m DEM, in addition to a 20 m DEM. The correctly predicted gullied area results for the 1 m DEM and 2m DEM are similar. The difference between A_p and

E_u for the two DEMs is less than 4.6%, with the 1 m DEM having a higher accuracy for small- to large-scale gullies. The 1 m DEM, however, has higher E_o, resulting in the 2 m DEM having the lowest total areal error (10.1% for the small-scale gully, 6.8% for medium-scale gully, 4.1% for the large-scale gully, and between 1.5% and 2.3% for the colossus-scale gully). As validation, the average accuracy is also comparable between the 1 m and 2 m DEMs, with the 2 m DEM marginally outperforming the 1 m DEM due to better A_u. The performance of gHAND mostly decreases in accordance with coarsening of the DEM resolution.

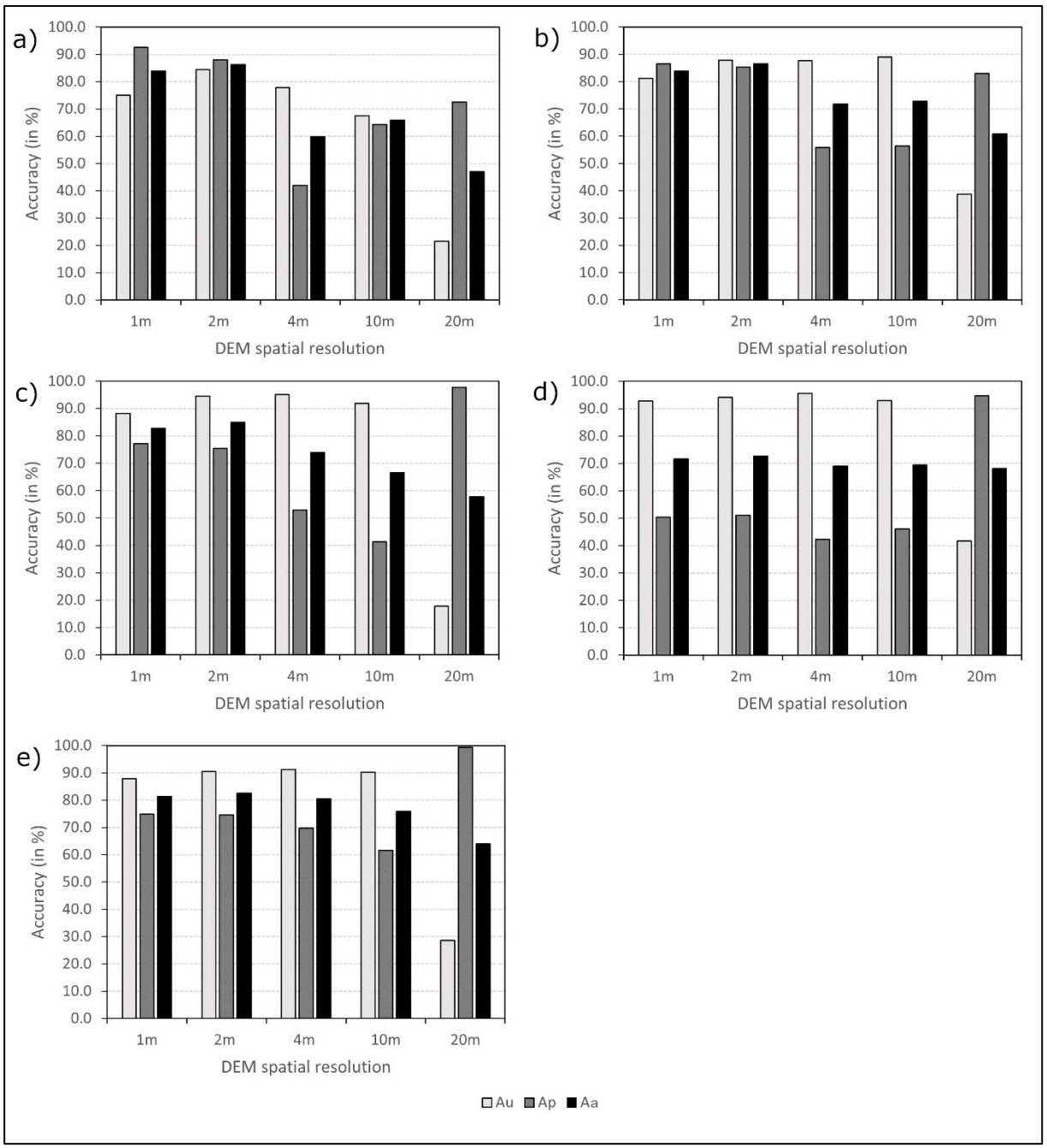

Figure 4.8 User accuracy (A_u), producer accuracy (A_p), and average accuracy (A_a) for gHAND method for the native 2 m spatial resolution DEM, an upsampled 1 m DEM, and a downsampled 4 m and 10 m DEM, and a 20 m DEM for: a) a small-scale gully; b) a medium scale gully; c) a large-scale gully; d) a colossus-scale gully according to the standard gHAND; e) colossus-scale gully according to an edited gHAND.

The total gullied area predicted by gHAND mostly correlates well with the reference dataset (Figure 4.9). Dissimilarity lower than 4% is predicted for the small- and medium-scale. The gHAND prediction has a higher error for the large- and colossus-scale, acceptable with 20.2%

for the large-scale gully, but poor for the colossus-scale gully at 45.8% dissimilarity (Figure 4.9b). However, by introducing local knowledge into the workflow, making changes to depth and widths expected, the dissimilarity for the colossus scale gully reduces to 17.5%.

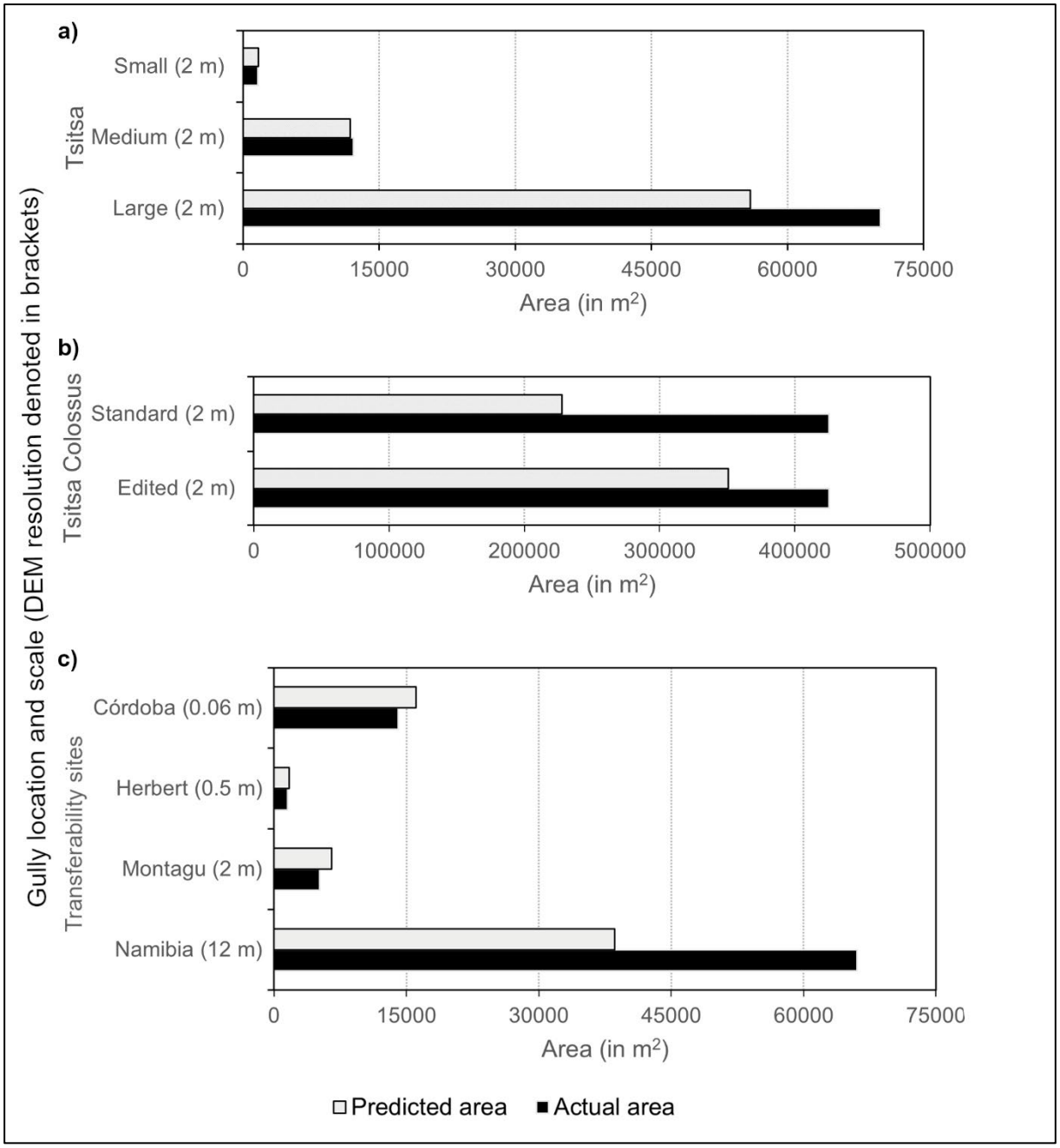

Figure 4.9 A comparison of the total areas obtained from the reference dataset and the gHAND method applied to the native DEM resolution for all the gully sites: a) Tsitsa small-, medium-, and large-scale gullies; b) colossus-scale gully (edited and non-edited gHAND); and c) at the sites where we tested the transferability of gHAND.

4.4.2 Testing transferability: Gully identification in various geo-environments

The performance of the semi-automated gHAND for gullies in different geo-environments depends on DEM resolution (Figure 4.10). The gHAND workflow performs best for the two

gullies with the highest resolution DEMs, with A_p above 95% for the 0.06 m DEM in Córdoba and the 0.5 m DEM in the Herbert catchment. E_u increase with spatial resolution, showing good results for Montagu, Córdoba, and the Herbert catchment (E_u <10.9%), but poor accuracy for the 12 m DEM used in Krumhuk (E_u =47.9%). E_o is inversely related to DEM resolution and decreases with the coarsening resolution, except for Montagu. The lowest E_o is thus recorded for Krumhuk (5.3%) and is validated by the high A_u (90.9%), which then increases the average accuracy output of gHAND. The A_u for Córdoba and the Herbert catchment is below 17.7% returning low total areal errors of 20.8% and 21.8% respectively.

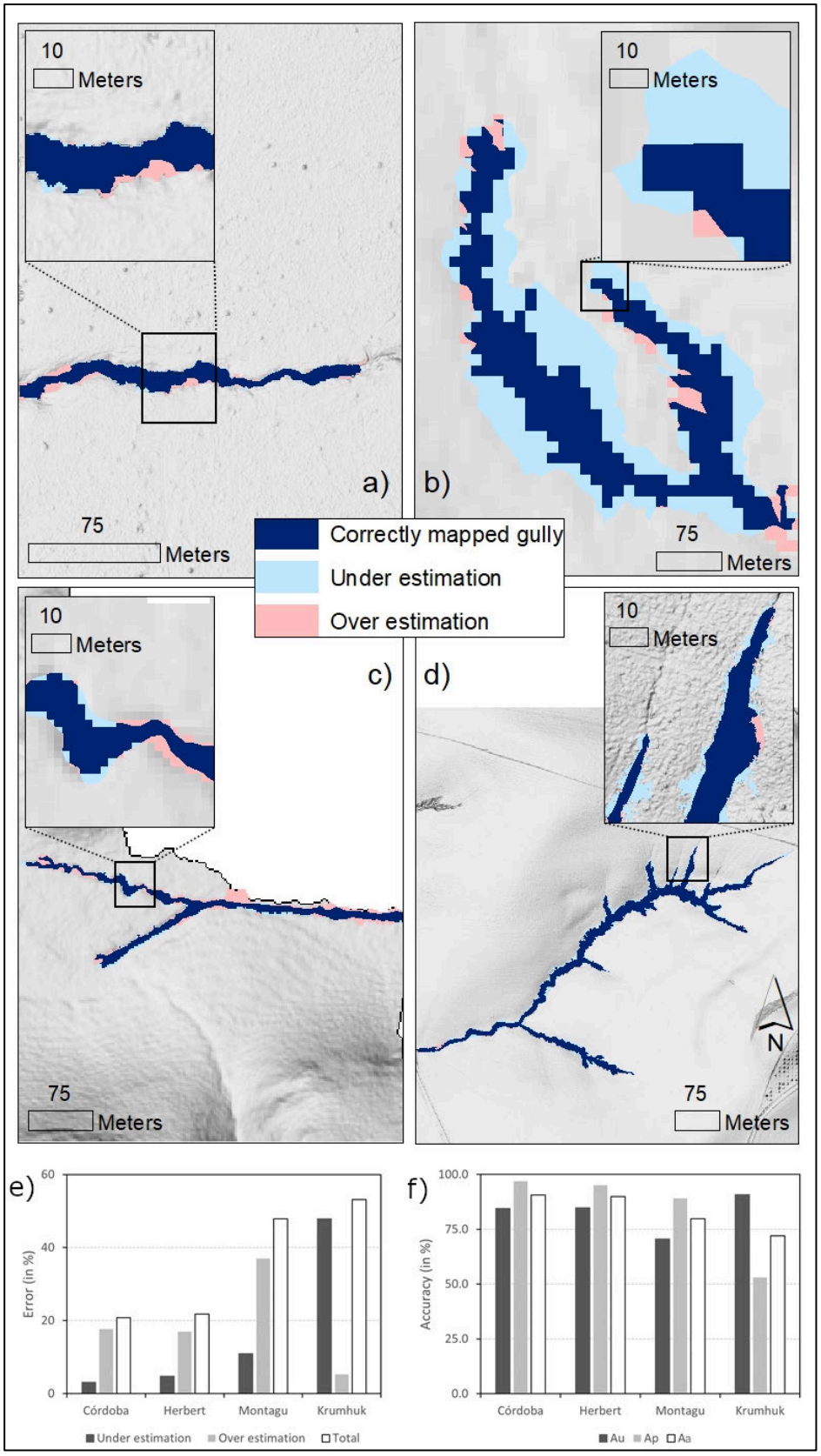

Figure 4.10 The resultant gully maps from gHAND method compared to the reference datasets, showing correctly predicted gullied area, *Eu*, *Eo* for: a) a gully in the Herbert catchment in Australia from a 0.5 m DEM;

b) a gully in Krumhuk, Namibia derived from a 12 m DEM; c) a gully in the Karoo, South Africa obtained from a 2 m DEM; and d) a gully in Córdoba, Spain from a 0.06 m DEM. Statistics regarding the results for *Eu*, *Eo*, total error, and *Au*, *Ap*, and the average thereof is given in e) and f) respectively.

4.4.3 Comparison with benchmark workflows in Namibia and Spain

At Córdoba and Krumhuk, benchmark methods were developed for the site-specific gully typology by Castillo et al. (2014) and Vallejo-Orti et al. (2019) respectively. The gHAND workflow shows comparable accuracy to the benchmark methods (Figure 4.11). At Krumhuk, three benchmark methods were implemented, namely IMR, SMPF, and MPCA (Vallejo-Orti., 2019). The MPCA method produced the most reliable results, with an A_a of 69.9%, compared to 72% achieved by gHAND. The higher A_a is influenced by the high *Au* of 90.9%. Comparing the area mapped correctly as gullied, the MCPA method had a 17.1% higher prediction accuracy. At Cordoba, gHAND underpredicts by 3.1% but due to a larger E_o (17.7%), has a larger total error (20.8%) when performance is compared to NorToM (10.8%; Castillo et al., 2014).

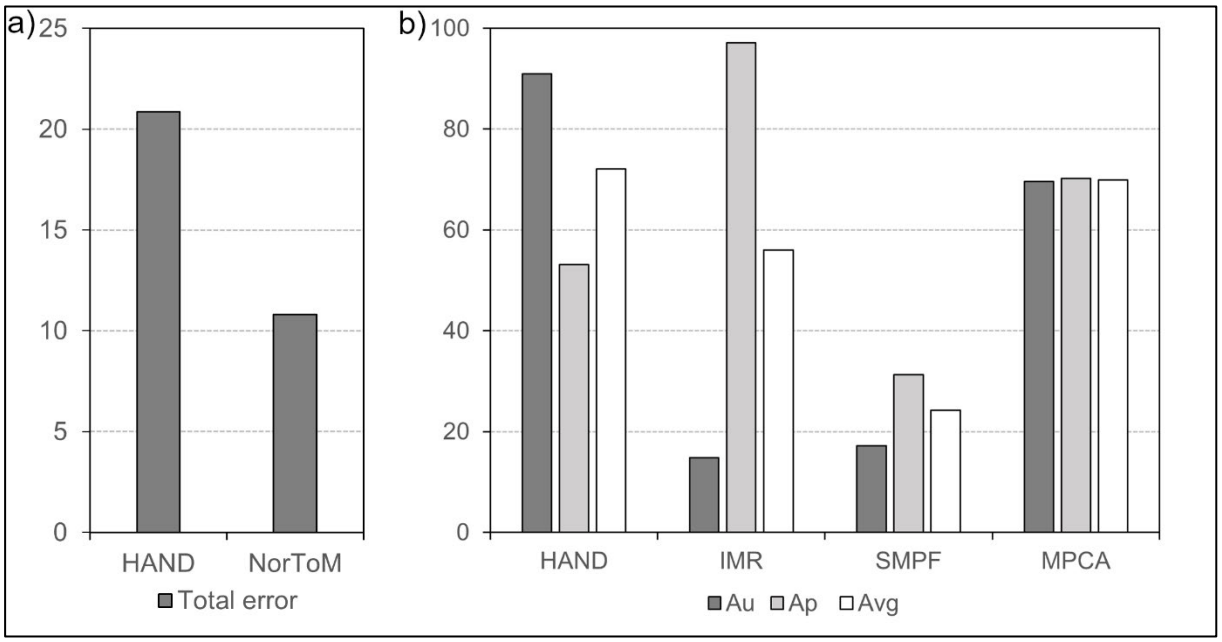

Figure 4.11 Comparison of gHAND error and accuracy statistics with benchmark methods: a) Total errors of gHAND and NorToM (Castillo et al., 2014); b) Accuracy of gHAND and three different methods implemented by Vallejo-Orti et al., 2019).

4.4.4 Parameter relationships

The accuracy statistics and DEM spatial resolution are plotted to find whether a relationship exists between the A_u and A_p variables (Figure 4.12). Accuracy statistics from the literature are included for comparison. In publications where more than one detection workflow was presented, all A_u and A_p results are included, for example, Phinzi et al. (2020) and Vallejo-Orti et al., (2019). The accuracy results from gHAND of the 20 m DEM at the Titsa sites are excluded due to the large E_o for all sites. A moderate correlation is found between the A_p and the dataset spatial resolution (R^2 =0.41; Figure 4.12b), indicating a higher correct prediction of the gullied area with a higher spatial resolution. However, no correlation is found between A_u and DEM spatial resolution (R^2 =0.01; Figure 4.12a), showing that the inclusion of false positives in the prediction is not inherent to the data resolution, but most likely has additional environmental elements. The low correlation of A_u with spatial resolution most likely contributes to the 0.24 R^2 value showing little relationship between the average accuracy and the spatial resolution of the dataset, in addition to no correlation with A_p.

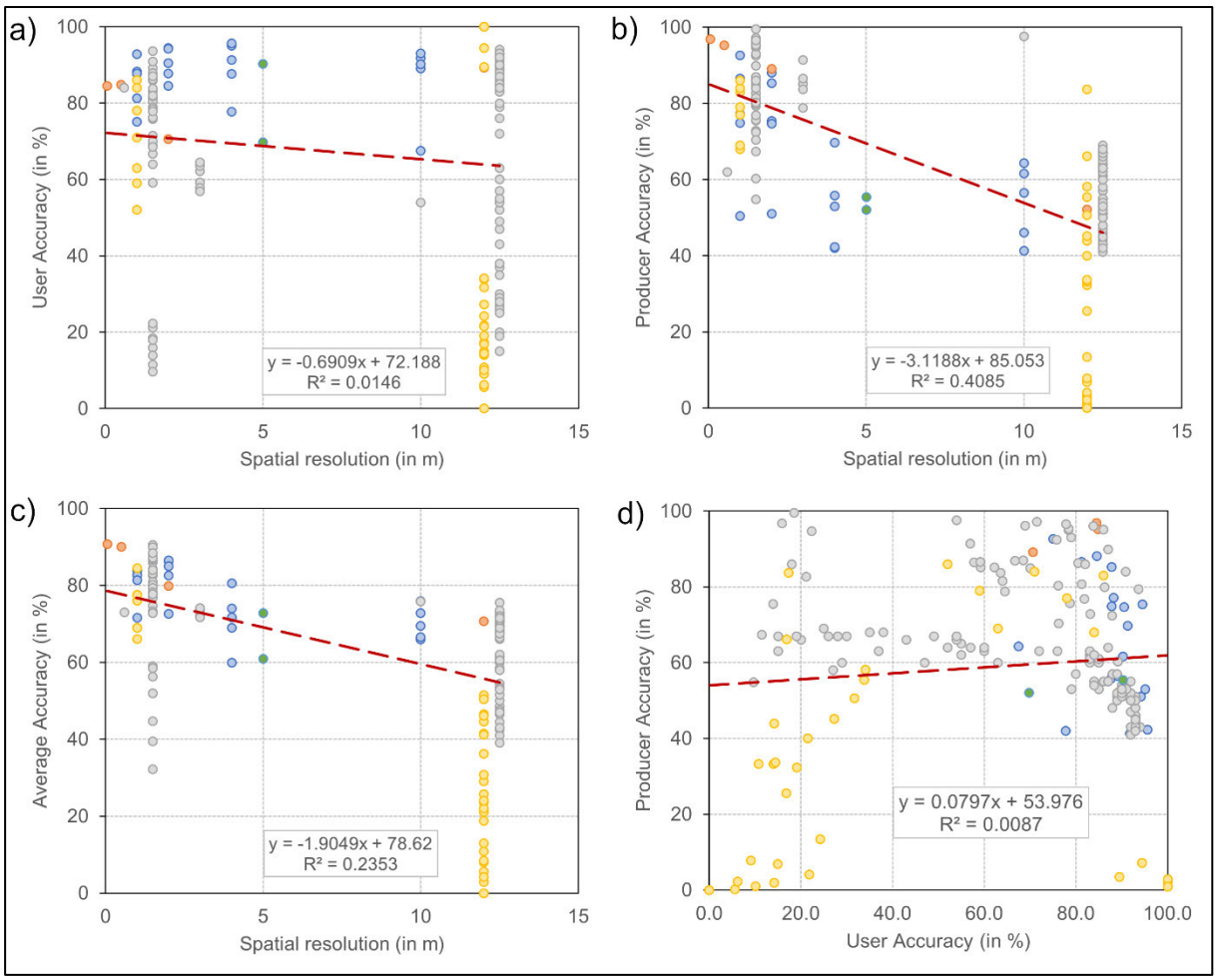

† Colour symbology according to how the predicted gullies were derived: blue denotes gullies mapped from gHAND where scalability was tested, orange is used for gullies mapped from gHAND where transferability was tested, grey for methods using spectral properties for gully detection, yellow when DEM products were used to map gullies, and green when a combination of spectral properties and DEM products were used to map gullies

Figure 4.12 Relationships between A_u, A_p, average accuracy, and spatial resolution for the gullies mapped here by the gHAND method in addition to gullies mapped by other semi-automated methods from literature: a) A_u vs spatial resolution of the DEM; b) A_p vs spatial resolution of the DEM; c) averaged accuracy vs spatial resolution of the DEM; and d) A_u vs A_p.

Although points are limited, a strong linear relationship was found with E_u and gully area (Figure 4.13a). Similarly, a strong correlation, albeit logarithmic, was found for E_o and gully area (Figure 4.13b). The edited version of gHAND, which used local knowledge, was excluded as it was deemed dissimilar due to using different threshold metrics for HAND depths. The complimentary nature of the E_u and E_o correlation with gully scale, is caused by the shrinking procedure to limit overprediction during the slope calculation.

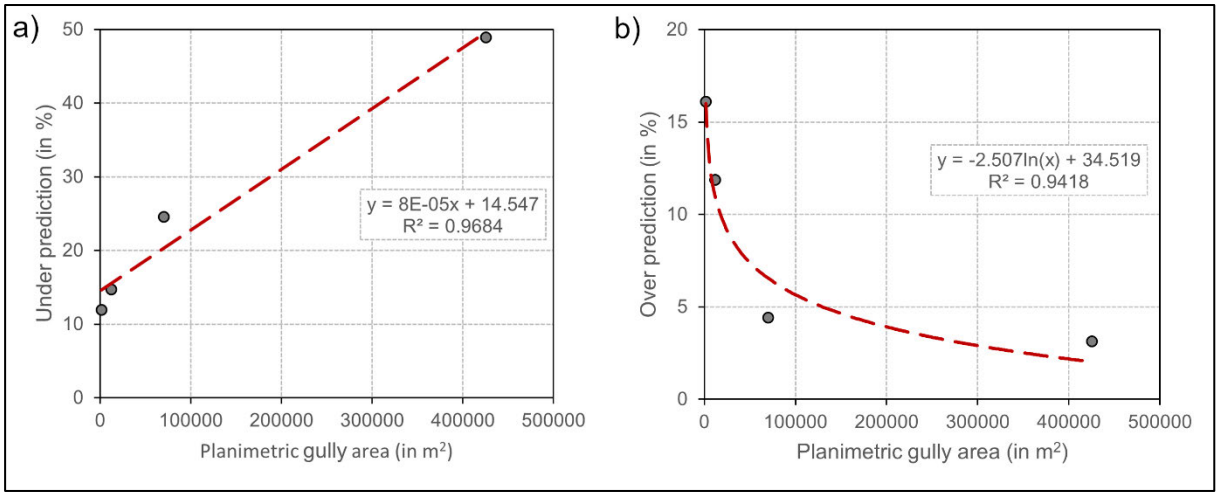

Figure 4.13 Relationship between E_u and E_o with gully area: a) E_u and gully area; and b) E_o and gully area.

4.5 DISCUSSION

4.5.1 Evaluation of gHAND

Although rigorously tested at different geomorphic scales, in different geo-environments, and differently derived DEM products, gHAND's results were encouraging, with A_u and A_p exceeding 70.6% and 51.1%, respectively. It is challenging to compare other semi-automated methods to gHAND as the reported accuracy metrics vary. However, if considering A_u and A_p, which are communicated often as an accuracy metric for remotely sensed detection, gHAND mostly performs at the upper threshold compared to other methods (Figure 12). Methods relying on spectral input alone reported A_u between 9.7% and 94% (mean of 63.4%), with A_p between 41% to 99.5% (mean of 58%) (de'Oleire-Oltmanns et al., 2014; Mararakanye & Nethengwe, 2012; Phinzi et al., 2020, 2021; Vrieling et al., 2007). When a DEM was used as the only input, A_u values between 0% and 100% (mean of 47.9%) and A_p values between 0% to 86% (mean of 40.1%) were reported (Johansen et al.,2012; Korzeniowska et al., 2018; Rijal et al., 2018; Vallejo-Orti et al., 2019). Methodologies combining topographic and spectral data as input in semi-automated detection strategies, returned A_u and A_p values from 69.8% and 52.1%, respectively (Utsumi et al., 2020). Compared with methods developed explicitly for the gully types in Krumhuk, Namibia (Vallejo-Orti et al., 2019) and Córdoba, Spain (Castillo et al., 2014), gHAND exhibited comparable accuracy (variance of 1.4% to 14.8% at Krumhuk, and 10.1% in Córdoba).

The gHAND workflow achieved the highest accuracy metrics for the gullies in the Herbert catchment, Australia and Córdoba, Spain (Au >84.5% and Ap >95.2%). This performance is likely due to lower morphological complexity and finer spatial resolution of the input DEM. In Córdoba, the agricultural gullies have clearly defined, steep-walled limits and are surface flow-dominant with little vegetative cover. Although the Herbert catchment exhibits significant tree coverage, the vegetation was removed to derive a terrain model (Geoscience Australia National Elevation Data Framework, available at http://www.ga.gov.au/elvis/), allowing distinct steep-walled limits to be detected by gHAND. It is expected that gHAND accuracy metrics will increase with fining spatial resolution, although in this case better prediction metrics were found at the Herbert catchment (0.5 m) compared to Córdoba (0.06 m). The higher accuracy at the Herbert catchment is likely due to the terrain model being free from vegetation interference and more clearly exhibiting the defined gully landform elements. Due to the performance of gHAND at Córdoba, we do not expect gHAND to suffer from detection deterioration resulting from hillslope noise (therefore the increase of false positives), as has been communicated by other studies (Dai et al., 2019; Garosi et al., 2018). Higher spatial resolution input will allow improved accuracy of predicted flow position (McMaster, 2002), increasing gully floor recognition with HAND. Additionally, a higher resolution will allow the detection of local topographic changes, expanding the aptness of gHAND to accurately identify typically steep sidewalls (as defined by Thwaites et al., 2022) as the gully boundary limit.

Conversely, as spatial resolution coarsens, gHAND prediction capability decreases. The sensitivity analysis evaluating the impact of DEM spatial resolution shows that total error by gHAND increases by order of a magnitude (for all gully scales in the Tsitsa) when the 2 m and 20 m DEM results are compared. Moreover, gHAND had the lowest accuracy at Krumhuk, Namibia, where the coarsest native DEM (12 m) was used as input. As the spatial resolution of the DEM coarsens from 2 m to 12 m, there is a general increasing trend associated with E_u of gHAND (Figure 14). Underprediction is likely a cause of a loss of local scale ruggedness that smooths the DEM resulting in fewer short steep slopes (Claessens et al., 2005; Deng et al., 2007), translating into a loss of gully wall candidates. Similarly, Dai et al. (2019) found an underprediction in the gully extent as DEM resolution coarsened, migrating downstream and becoming narrower. At Krumhuk, the gully morphology compounds the E_u effect from slope deficiency. Here gully walls are laterally eroded, lowering the main historical gully wall. The gullied landscape is transitioning towards badlands, like those described in the semi-arid

Sneeuberg region by Boardman et al. (2003), which may render a strategy founded on distinct gully morphology ill-equipped to detect it; and possibly why both the MPCA method (based on local slope detection) and gHAND performed with lower accuracy.

On the colossus scale, the unedited gHAND workflow returned low accuracy metrics with an E_u of 48.9%. Although there was an improvement of 23.5% in E_u from limited editing, we infer that the leading cause of underprediction is associated with gully complexity, which in some instances is related to the scale of the gully. The most significant contributor to E_u is caused by topographic variation of the gully floor. Due to the expansive width of the gully (up to 210 m), large zones are not identified as gully floor elements, likely due to the gully floor being higher than 0.5 m from the thalweg determined by HAND. These local highs above 0.5 m are a consequence of a gradual increase of the gully floor from the thalweg to the wall perimeter, but also from sharper terraces (similar to alluvial terraces in river morphology). These large unclassified zones result in a disassociation between the gully floor and wall candidates, producing an unsuitably narrow prediction by gHAND. Point bars and depositional bars inside the colossus gully magnified the disassociation effect. Increasing the *Low_HAND* threshold overcame this disassociation, being able to fill the smaller (non-identified areas due to being higher than 0.5 m) areas between gully floor and wall candidates, and thus not erroneously removing correctly identified wall candidates as dangles due to their small object size.

Other gully morphological properties that led to underprediction, although to a lesser extent, include meandering, piping, lateral erosion types, and human-induced geometry. The gHAND workflow predicts the active cut bank well, but underpredicts the point bar where sediment is deposited, creating a low-sloped incline above the gully thalweg. Newly connected pipes are also underpredicted, most likely due to pixel size. Similarly, gully fronts extending laterally in the form of multiple narrow, quick-deepening channels, separated by tapering interfluves are also underpredicted, likely a result of pixel resolution. Nonetheless, the gHAND workflow adequately predicts certain non-linear geometries found within the colossus gully, for example, a zone at the main headcut that is up to 210 m wide and 75 m long, whereafter it drains into two narrow channels (<12 m) around a non-gullied island. However, other non-linear gully geometries impacted by human activities from footpaths and abandoned fields (some with contour failures) are underpredicted. Castillo et al. (2014) similarly found more variance in prediction accuracy due to land-use patterns.

Although the gHAND workflow performs suitably at small to large-scale gullies, strategies could be put in place to limit underprediction at the colossus scale. One could add a process to map lower-sloped areas within proximity of 0.5 m HAND, but this would mean adding a width threshold, which could be detrimental to the ability to map different scaled gullies; setting the margin too high could map flat terrain outside the perimeter of the gully as gullied area, and threshold too small may yield no significant improvement. Another possibility, excluding widths thresholds, would be to find lower slopes between "*Low_HAND*" and areas of sharp slopes. Further testing would be required to assess the impact of such processes on accuracy metrics at various scale levels.

4.5.2 Advantages of gHAND

Implementing the gHAND workflow has several interrelated advantages. Firstly, it uses limited input; secondly, it normalises a DEM to create input variables; and lastly, it uses measurements associated with gully morphology, like those measured in-field. In terms of limited input, gHAND only requires a DEM of the study area. Moreover, we demonstrated that gHAND could be used from DEMs derived from different sources (aerial imagery, LiDAR, and satellite imagery) and spatial resolutions (although there is a decrease in accuracy metrics associated with coarsening resolution). Furthermore, detection performance was acceptable using both surface and terrain models as DEM.

Regarding the normalisation process, the DEM is normalised according to the HAND process, removing the requirement of using defined search windows. Search windows are a crucial strategy in other methods using DEMs to extract distinct gully landforms from their local terrain (Castillo et al., 2014; Eustace et al., 2011; Evans & Lindsay, 2010; Francipane et al., 2020; Johansen et al., 2012; Vallejo-Orti, 2019; Walker et al., 2020), but this strategy is scale-dependent and thus impacts the methods' scalability. Castillo et al. (2014) argue that calculating z-score statistics creates a scale-independent methodology. However, its scale dependency is evident from the array of window sizes used and the acknowledgment that "landscapes with highly contrasting gully widths might require the use of several runs with different window sizes" (Castillo et al., 2014: p2013). Contrastingly, gHAND produced a total error of <29% for gullies with a planimetric area ranging over two orders of magnitude (1619.0 m^2 up to 70246.7 m^2) without the need for editing the workflow. Additionally, due to the elevation heights being normalised along the gully thalweg, gHAND is unlikely to

experience detection decay in strongly sloped landscapes (as demonstrated in the strongly sloping Tsitsa catchment), while such decay as methods using search windows (Castillo et al., 2014).

Lastly, gHAND exploits gully morphology in quantitative measures to map gully elements: threshold values that need to be set are associated with values that would be measured in the field, unlike more obscure measurements and statistics with little physical relevance to the actual gully, especially when implementing spectral datasets (Phinzi et al., 2020, 2021; Shruthi et al., 2011; Vrieling, 2007). Using gully morphological measures in the gHAND workflow produces an easily understandable means of mapping gullies semi-automatically. Due to the mapping output of gHAND being polygons extracted from a DEM, an additional step can be added to calculate gully volumes by using the polygon output and DEM in conjunction. Additionally, and significantly, due to being based on gully morphology, the detection capability of gHAND in dissimilar geo-environments is strengthened.

4.5.3 gHAND model disadvantages and study limitations

Although implementing gHAND has several advantages, it also has limitations (Figure 4.15).

Firstly, gHAND relies on manual digitising gully headcut locations as the initial step; secondly, overprediction occurs at the deposition zones of discontinuous gullies; thirdly, underprediction is found at atypical and complex gully features (some scale-related); and lastly, accuracy metrics are strongly related to DEM quality.

The gHAND workflow requires gully headcut locations to be manually digitised to allow accurate normalisation of the DEM according to HAND. This can introduce user bias and uncertainty. However, a sensitivity analysis showed that performance was not severely affected by the exact placement of the point to implicate the headcut (APPENDIX D). Therefore, a rapid mapping process of gully headcuts should enable the successful application of gHAND. In some regions, gully headcut inventories exist, mapped to assess gully occurrence and density (Hayas et al., 2017; Vanderkerckhove, 1998). At such locations, gHAND can augment findings, but manual digitising is a prerequisite in a new study site. It would be beneficial to find a way to automate gully headcut identification, alternatively identify gully headcut susceptibility zones (such as implementing the frequently used topographic threshold concept; see Rossi et al., 2022;

Torri & Poesen, 2014) in which to search for gully headcuts to be mapped, to make regional mapping more feasible. Other semi-automated detection methods do not have this limitation (for example, Castillo et al., 2014; Mararakanye & Nethengwe, 2012; Vallejo-Orti et al., 2019; Vrieling et al., 2007; Walker et al., 2020), although spectral methodologies do require gully inventory maps to be generated for training purposes (Mararakanye & Nethengwe, 2012; Phinzi et al., 2021; Taruvinga, 2008; Vrieling et al., 2007).

For discontinuous gullies, frequently found in arid regions, gHAND produces an overprediction as the gully channel becomes shallower towards the deposition zone, ballooning larger at the flood-out. The overprediction is likely a cause of the *Low_HAND*, 0.5 m threshold. Similar limitations have been reported for discontinuous gullies. Contrastingly, gHAND underpredicts atypical features and complex gully characteristics associated with colossus-scale gullies (see section 4.5.1).

Lastly, the output accuracy of gHAND is impacted by the quality and spatial resolution of the native dataset, although this is a general constraint that needs to be addressed in all semi-automated methods that model landforms. Although there is no strong relationship between spatial resolution and accuracy metrics (Figure 4.12), previous works demonstrated that the finest resolution is not necessarily the best detection option (Dai et al., 2019; Tarolli & Tarboton, 2006). Careful consideration is therefore required to select the correct resolution to reduce noise on the hillslope (Castillo et al., 2014; Dai et al., 2019) and reduce processing time. Positively, gHAND was able to return good results for the finest scale (0.06 m) due to the detection strategy that makes use of the HAND normalised DEM, which reduces the probability of falsely mapping hillslope noise as gully elements. The accuracy metrics start to decay after 2 m as E_u propagates because spatial resolution is vital to accurately detect the gully building blocks of gHAND. Downsampling the South African data to double the native resolution, *viz*., 4 m, produced increase error rates towards 50%, although additional uncertainty was added due to the cubic resampling procedure. For the gully typology investigated, a 2 m spatial resolution or better would therefore be preferred for accurate prediction of flow path within the gully confines representing the gully floor and the identification of short steep slopes that signify gully walls (also see section 5.1). Depending on the DEM type used, large woody vegetation and human structures in proximity to the gully may lead to a false positive gully wall detection, likely to lead to overprediction. A terrain model such as the one used at the Herbert catchment,

Australia, would be preferable as an input, but gHAND produces adequate performance using surface models in Spain (agricultural environment) and South Africa (grasslands with isolated trees).

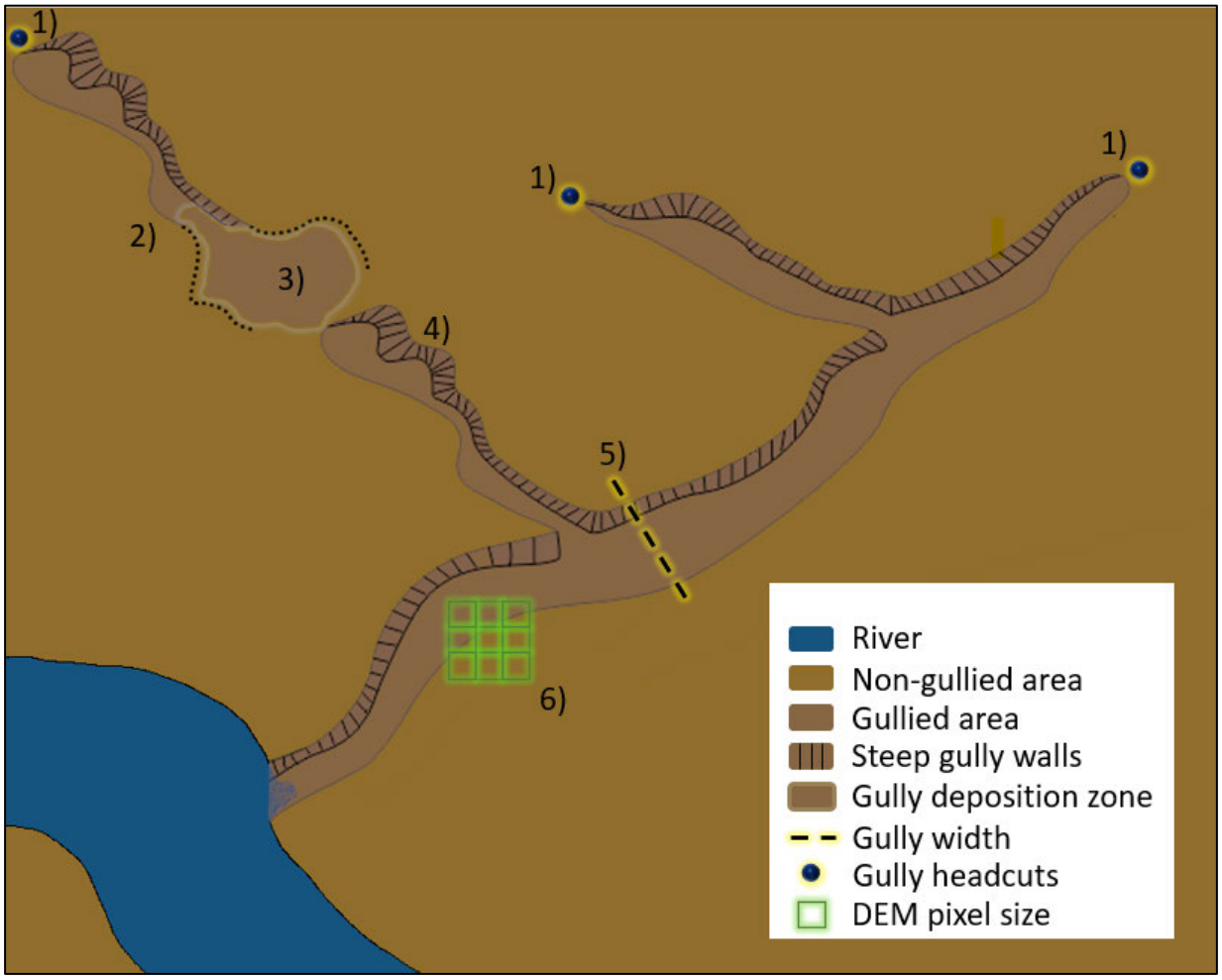

Figure 4.14 A graphical depiction of some of the limitations and problems encountered with the gHAND method: 1) requirement to manually digitise gully headcuts; 2) when mapping discontinuous gullies, especially in flat terrain, overprediction becomes evident towards the flood-out, with 3) large overprediction at the flood-out zone where the gully expires, although the gHAND prediction accuracy will increase again once it reaches the gully headcut of the successive gully chain; 4) it predicted a-typical meandering gully channels well for narrow channels, but for large channels found on the colossus-scale (where widths exceed 50 m), it underpredicted due to its inability to map the point bars correctly; 5) similarly, very wide channels were underpredicted on the colossus-scale gully; and 6) we added an iteration of shrinking to limit overprediction occurring from the way slope is derived from pixels, which resulted in a systematic increase in underprediction as the gully scale increased.

There were also some practical limitations to the study itself. gHAND was tested on an individual gully scale. Further testing should be done on catchment scales when multiple gullies are mapped. Still, initial indications suggest that accuracy remains unaffected (Olivier et al., 2022), but an effective approach to discriminate gullies from rivers is required. Strategies that can be implemented, some of which have been used in other gully-mapping methodologies, are applying contributing area (Castillo et al., 2014; Daba et al., 2003), stream order thresholds (Bartley et al., 2007; Johansen et al., 2012), or using vector overlay from existing river data (Johansen et al., 2012; Olivier et al., 2021). An alternative strategy could also be to implement a discriminatory width-depth ratio. Lastly, we are advocating for a practical solution to semi-automate the mapping of gullies, a method that can be readily applied to aid management strategies. Although we have met the aim of having a methodology that is easily understood and reliable, its current implementation is based on an object-orientated approach using proprietary software. However, we envisage that gHAND can be implemented, at comparable accuracy rates, by following a pixel-based approach since the main component is threshold-dependent. Further testing is required to confirm this.

4.6 CONCLUSION

Herein we developed a new semi-automated gully detection strategy, gHAND, based on geomorphic measurements associated with gully dimensions, which we rigorously tested for scalability and transferability. The gHAND workflow proposed had small differences in accuracy metrics compared with benchmark methods developed for region-specific gully forms. Furthermore, the error rate was similar to previous studies for typical gullies from small- to large scales. The gHAND workflow shows adaptability to map gullies at contrasting scales and geo-environments, capable of using DEMs derived from different sources with various spatial resolutions. There are limitations associated with the implementation of gHAND, most noteworthy the need to manually digitise gully headcuts. Nevertheless, gHAND shows clear potential for catchment- to regional-scale gully detection. Thus, gHAND can be implemented to map gullies, providing information regarding their location, morphology, and density for various geo-environmental regions. The extracted information can further improve our understanding of how control factors impact gullying on catchment management to regional scales. Because of the ability of the gHAND to extract specific gully features and its unbiased repeatability, we envisage that it can also be used to monitor gullies temporally. For example,

gHAND could be implemented to create long-term datasets (>15 years) regarding gully evolution when applied to DEMs retrieved at various temporal intervals, which are still limited in global gully research. This can help identify areas where active gully expansion is concerning or can assist in assessing the efficacy of any mitigation measures.

CHAPTER 5: HISTORICAL EVOLUTION OF GULLIES: IMPACT OF CLIMATE AND LAND USE

5.1 ABSTRACT

Gully erosion is a degradational process resulting in important socio-economic and environmental consequences, on-site where soil is lost and off-site where eroded soil is transported and deposited. Unsustainable human activities have been strongly associated with increased gully incidence and severity. Additionally, the severity of gully erosion is expected to be exacerbated under current climate change forecasts resulting from increased higher-intensity rainfall events. Due to the complex nature of gully erosion, stemming from a range of sub-processes and controls, the modelling capability of gully evolution, and therefore its impacts, on large geographic extents is still tenuous. Without accessibility to such models, it remains unclear how gully erosion will react to environmental change. In the absence of regional gully models, we aim to isolate climate and land use variables by selecting a range of local sites across the East-West climate gradient of South Africa. A triangulation of methods is implemented, consisting of 1) remotely analysed data to build a large temporal scale, 2) field observations and measurements to yield high-resolution process and volumetric estimates, and 3) semi-structured interviews, focus group, and participatory mapping to obtain local knowledge regarding event-based impacts on gully erosion, perceived drivers of gully expansion and initiation, local-scale manner (processes) of expansion, and to gauge the implementation and effectiveness of mitigation measures. Although it was difficult to disentangle climatic and land use variables, an approximate polynomial trend was detected from quantitative data and corroborated through qualitative methods capturing local knowledge. No clear trend was observable from land use classifications. However, similar activities within land use classes were identified as driving gully evolution. Although future gully erosion in South Africa is envisaged to increase due to increased high-intensity rainfall, rainfall variation that coincides with the high-intensity rainfall may be the more critical driver of gully erosion, especially in arid and semi-arid regions.

5.2 INTRODUCTION

Gully erosion is a geomorphic process which is considered a major environmental problem (Poesen et al., 2003; Wilkinson et al., 2023). Due to unsustainable human activities, gully erosion transcends physiographic boundaries, reaching concerning levels in various regions worldwide (Castillo & Gómez, 2016; Olivier et al., 2023a).

On a local scale, gully erosion primarily affects soil resources, consequently impacting the sustainability of agricultural practices as it lowers agricultural production due to soil losses and deteriorating soil quality; moreover, increasing farming costs (due to mitigation measures but also increasing fuel costs when having to traverse around gullies when it cannot be crossed) (Capra, 2013; Liu et al., 2013). Furthermore, infrastructure, such as roads and buildings, can be damaged by locally expanding gullies (Jahantigh & Pressarakli, 2011; Imwangana et al., 2015).

On a catchment scale, gullies increase the hillslope channel connectivity, negatively affecting water resources. Continuous gully channels act as effective routeways that promote the delivery of sediment, pesticides, and nutrients from fertilisers to river systems (Wantzen, 2006; Katz et al., 2014) and reef lagoons (Bartley et al., 2017), deteriorating water quality and habitat. Additionally, an increase in sediment delivery lowers reservoir capacity, aggravating drought effects and increasing flood risk (Fox et al., 2016; Le Roux, 2018).

Gully erosion is complex, involving a range of sub-processes, for example, vortex erosion in plunge pools, soil cracks, piping, fluting, and mass wasting (Oostwoud-Wijdenes & Bryan, 2001; Poesen, 2018). This complexity continues to be a significant obstacle in modelling ventures, limiting detailed gully assessments on larger geographic footprints (Vanmaercke et al., 2021). There currently still is no standardised, validated model that can be implemented on regional scales to assess gully evolution, soil loss, and sediment yield rates from gullying (Poesen, 2018; Vanmaercke et al*.,* 2021), in contrast to other erosion types, for example, rill and sheet erosion that can be modelled by a scientifically accepted RUSLE (Ghosal & Bhattacharya, 2020). Gully evolution analysis and soil loss determination are still primarily conducted manually, either quantitatively from conducting classical fieldwork (mainly from repeat field surveys, less often by surveys reconstructing gully erosion by dating mineral or organic material) and by examining remotely sensed imagery (mapping of gullies on historical imagery) or qualitatively from interviews or workshops (Ionita, 2006; Nyssen et al., 2006;

Grellier et al., 2012; Belayneh et al., 2020; Franco-Ramos et al., 2022; Wang et al., 2022). Due to the labour- and data-intensive nature of these manual approaches, studies typically have a small geographical footprint, yielding findings that, albeit valuable, only pertain to local significance. However, strategically selecting multiple local sites, constituting regions with contrasting physiographic conditions, could be used collectively to inform on a regional scale (Vanmaercke et al*.,* 2021).

Constructing long-term datasets (>15 years) at these multiple locations will provide insight into temporal gully perturbations for unique physiographic environments in response to gully control variables. Furthermore, gully erosion rates can be calculated, indicating gully erosion severity on a fine resolution on a large geographic extent. The long-term data will improve our understanding of gully evolution, aiding modelling developments and providing calibration datasets. In the immediate term, the long-term data could be used to identify areas where mitigation measures are more urgently required and could also inform policy and catchment management actions.

Additionally, these local sites can be selected to isolate certain control variables, which could be valuable to help understand (in the absence of adequate models) how gully networks may react to environmental change. Gullying is expected to generally increase under current climate change scenarios (Poesen et al., 2003; Marden et al., 2018) and may reactivate stable gullies, which have previously been mitigated (Meadows, 2003). Making use of a global dataset (n = 672), Vanmaercke et al. (2016), empirically demonstrated that gully headcut retreat may increase by up to 300% (Vanmaercke et al., 2016), but our understanding of how gully networks will react to climate change remains limited. Isolating climate as a control variable and investigating long-term historical perturbations may better our understanding of the impact climate change may have on gully erosion. In addition to climate change, unsustainable human practices, viz. land use (and past land-use change), have been demonstrated to impact gully erosion (Castillo & Gómez, 2016). Similarly, a RUSLE-derived model showed that ongoing land use change substantially affects rill and sheet erosion worldwide (Borrelli et al., 2017). Hence, it is reasonable to assume that future land-use change will also significantly impact gully evolution. Isolating land use as a control factor would provide insight into how these changes may affect gully networks.

Our aim is to identify several local case study sites, isolating climate and land use, to inform how changes in these drivers may influence future gully erosion. Climate is isolated by identifying several land use classes and selecting research locations across the E-W climate gradient of South Africa for each, while land use is be isolated by selecting several gullies in proximity but with contrasting land use. We implement a triangulation of methods at each site, consisting of i) creating long-term data by digitising gully features from historical aerial imagery; ii) conducting classical fieldwork to observe (in)active processes while determining volume estimates by measuring cross sections of individual gully networks; and iii) participatory mapping and interviewing landowners, -users, and -managers to learn from their local knowledge regarding gully expansion and rehabilitation efforts. Although the triangulation of these three methods is rare (Tebebu et al., 2010), we believe that the different methods complement each other by addressing the disadvantages of each unique method (Table 5.1), providing a more comprehensive analysis.

Table 5.1 Advantages and disadvantages of different methodologies.

Indirect measurements from aerial and satellite imagery
Advantages
- High temporal scale
- Inexpensive (mostly)
- Planimetric quantification
- Remote assessment of causative factors
Disadvantages
- Spatial resolution (consistency and quality)
- Misinterpretation without ground-truthing
- Decadal gaps between flight missions
- Lack of event-based and gully process observations
Direct in-field measurements and observations
Advantages
- Volumetric quantification
- High-resolution gully process observations
- High-resolution factor analysis (control and driving factors)
Disadvantages
- Low temporal resolution (mostly)
- Expensive
- Coarse geographic coverage
- Lack of event-based observations
Qualitative interaction
Advantages
- High temporal scale
- Identification of crucial gully expansion events
- Local knowledge regarding susceptibility and causative factors
- Perceived effectiveness of implemented mitigation interventions

Disadvantages
- Expensive
- Need to have trust and willingness to participate
- Precision may be low due to recollection

5.3 METHODS

5.3.1 Study Area

South Africa occupies the southern-most tip of Africa (located between 22°S to 35°S and 15°E to 33°E) and is approximately 1.22 million km^2 in extent. Soil erosion in South Africa is not a recent phenomenon, with one of the first official directives to combat soil erosion recorded in 1682 (Verster et al., 2009). King (1963) observed that gully channels are standard landscape features in the South African landscape, and the "evil" impacts of gullies and their mitigation were first discussed in the form of agricultural journals in the early 1900s (Rowntree, 2013) (see Figure 5.1 for examples of gullies found in different physiographic regions of South Africa). Although gully erosion is a complex geomorphic process, the impact of human activities to expose inherent preconditions to accelerate gullying is strongly evident in South Africa (Olivier et al., 2023a). The human influence, especially political interventions (Meadows, 2003), has likely a strong influence on the gully distribution that is skewed towards the east in South Africa (Mararakanye & Le Roux, 2012), where the inherent properties of soils are more susceptible to erosion coupled with strongly sloping terrain and higher intensity rainfall (Olivier et al., 2023a).

Figure 5.1 Examples of gullies found in South Africa: a) gully along a drainage channel in grain fields close to Riebeek Kasteel, situated in the winter rainfall region in the Fynbos biome, b) gully complex on a private game reserve in the semi-arid Karoo, c) narrow gully on rangeland in the semi-arid Karoo; d) gully complex adjacent to rehabilitation works in the Albany thicket biome in the semi-arid Karoo; e) hillslope gullies in the former homelands area in the Tsitsa catchment situated in the grassland biome; f) a shallow meandering gully in the lowveld in Limpopo in the Savanna biome (photographs a, c, d, e, and f by G. Olivier; photograph b by M. Van De Wiel).

The mean annual rainfall in South Africa is also skewed, exhibiting a strong E-W climate gradient (De Wit & Stankiewicz, 2006), generally increasing from west to east (Figure 5.2a). In the west, arid regions with a mean annual rainfall below 200mm are found, while sub-humid to humid areas that exceed a mean annual rainfall of 1000mm are located towards the east

(Schulze et al., 2006). The RDN, which can be used as a proxy for rainfall intensity, shows a good correlation to gully erosion (Vanmaercke et al., 2016). The RDN (Figure 5.2b) was calculated from 10' resolution long-term (1961–1990) climate data from New et al. (2002) by

$$RDN = \frac{MAR}{ARD} \qquad \text{Equation 5.1}$$

where RDN is Rainy Day Normal;

MAR represents the mean annual rainfall;

ARD is the number of annual rain days

The RDN mostly follows the E-W climate gradient, with the highest intensities located in a small pocket in southwestern South Africa and is more widespread in the northeastern parts.

Figure 5.2 Hydroclimate orientation of South Africa: a) mean annual rainfall (Schulze et al., 2006); b) Rainy Day Normal (derived from New et al., 2002) rainfall intensity proxy. Circles indicate the location of local scale case-study sites, coloured by dominant land-use.

The natural vegetation reflects the E-W rainfall gradient and has been classified into nine broad biomes (Mucina & Rutherford, 2006) (Figure 5.3a). In the west, situated in the winter rainfall region, the Fynbos biome consisting of shrubs and succulents is found. The succulent and Nama Karoo biomes cover much of the semi-arid to arid interior, which transitions to the Albany thicket biome that changes into the Grasslands biome in the more humid east. Gully erosion is prevalent in the Karoo and Grasslands biome, especially where grassland is degraded such as in the former homeland areas (Mararakanye & Le Roux, 2012; Olivier et al., 2023b) (Figure

5.3 Physiographic orientation of South Africa: a) Nine broad classified biomes of South Africa. Biomes in addition to azonal vegetation (Mucina & Rutherford, 2006); b) map showing lithologies and areas commonly referred to in the text (data sourced from Mucina & Rutherford, 2006; Burger, 2013; Khuthadzo, 2019; and Centre for Geographical Analysis at Stellenbosch University; c) broad soil classification (Land Type Survey Staff, 1972-2006); d) generalised rock type map of South Africa (see Olivier et al., 2023b for more classification detail).

The great escarpment (Figure 5.3b) separates South Africa into a narrow coastal region and a vast inland plateau (Moore et al., 2009), with its highest point in the western Drakensberg. The

plateau consists of a large sedimentary basin (Moore et al., 2009) with scattered mafic intrusions (Figure 5.3c). Felsic intrusions are widespread in the northeast (Van Tongeren & Mathex, 2015). The parent rock has been shown to have a strong influence on the erodibility of soils in South Africa. Soils derived from the mudstones and shales from the Beaufort Group (mid-Permain to early Triassic period), specifically the Adelaide and Tarkastad subgroups, and the Elliot Formation of the Stormberg Group (early to late Triassic period) have been shown to yield soils that are especially susceptible to gullying (Laker, 2004). These soils are often dispersive and Duplex (Figure 5.3d; see Table 5.2 for South African soil concepts and World Reference Base classification system comparison), exhibiting an abrupt texture change between surface and sub-surface horizons from its inherited clay mineralogy (Parwada and Van Tol, 2016) and silica content (Laker, 2004). The textural contrast of Duplex soils causes them to be prone to piping. The lithic Glenrosa and Mispah soils are abundant in South Africa and have been associated with erosion due to their positions on convex crests and mid-slopes (Fey, 2010a). The Red-yellow apedal soils are less prone to soil erosion due to the micro-aggregating effect of oxides, resulting in a soil with low dispersibility (Fey, 2010a).

Table 5.2 Broad South African soil classes with a short description of soil concepts.

South African soil classification	Soil concepts from Fey (2010a, 2010b)	Comparison to the World Reference base
Red-yellow apedal soils,	Mostly freely drained, Iron enrichment [residual]; uniform colour with structured B	Ferralsols and Latosols
Plinthic soils (soft B)	Soft B, iron enrichment, mottling, or some cementation	Plinthosols
Glenrosa and Mispah (Inseptic lithic soils)	Young soil on weathered rock	Cambisols and Leptosols
Duplex dominant	Permeable topsoil with marked clay enrichment resulting in contrast texture in subsoil	Stagnosols, Solonchaks and Luvisols
Undifferentiated soils	Variable soil associations	More than one soil form occurs
Ferrihumic horizon (Podzolic soil)	Diagnostic podzol B, metal humate enrichment	Podzols
Grey regic sands (Cumulic soil)	Freely drained, young soil formed on recently deposited colluvial, alluvial, or aeolian sediment	Cambisols Arenosols Fluvisols Luvisols Acrisols Lixisols
Rocky, with little soil	N/A	N/A

5.3.2 Site investigation

A selection of 19 gully sites was made to represent similar land uses across the E-W climate gradient and different land uses in the same Mean Annual Rainfall (MAR) classification (Table 5.3, 5.4). A combination of sampling techniques was used, with purposive sampling being the predominant sampling method, combined with convenience and snowballing sampling. First, the combination of climatic zones and land uses formed the sample universe, which purposefully framed the selection of gullies to serve as local case study sites (Robinson, 2014). Within each climatic zone and land use combination area, convenience sampling was applied to select gully sites where access to research participants was feasible within the available timeframe. The selection of gully sites using convenience sampling was critical to enabling the intended triangulation of methods. Convenience sampling allowed the selection of gully sites (in target regions spanning the land use-climatic region matrix) where, ideally, remotely sensed data, permissions for physical access to land, thus gully sites, and willing local research participants were available.

The snowball technique (Belayneh et al., 2020), which builds on existing social connections to recruit further research participants or sites, was implemented in areas with no previously established contacts. In some instances, gatekeepers were approached to enable access. Using gatekeepers was, for example, relevant in areas of former homelands or national parks, where it is not private individuals but social networks or local organisations that influence and sometimes control access to sites and participants. In those instances, the first author aimed to build rapport with a trusted local gatekeeper (or gatekeeper organisation), who then supported entrance into unfamiliar areas and communities. The facilitated support of gatekeepers was particularly relevant given South Africa's past and current political context and since the first author, who primarily conducted the fieldwork, is a male of white descent and a native Afrikaans speaker. Approaching local communities via locally familiar gatekeepers was deemed necessary to establish confidence in the researcher's presence and research interest in gully erosion.

Fieldwork was conducted during 29 non-consecutive days between May 2022 and July 2022, and constituted gully sites in the Western Cape, Eastern Cape, Free State, and Limpopo provinces. A triangulation of methods was designed to be implemented at each site, consisting

of 1) remote interpretation of gully sites using historical aerial imagery, 2) quantitative and observational assessments of the gully sites, and 3) a qualitative approach for gathering local knowledge of gully erosion and evolution. Ethics approval for this methodology was received from both Coventry and Stellenbosch Universities, with whom the first author has an affiliation (See APPENDIX F).

Table 5.3 Site selection.

Placename	Coordinates[†]		Province	Phase of fieldwork	Sample type[‡]	Gatekeeper	Discussion type[‡]	Participatory mapping[§]	Participants	General designation class
	X (dd)	Y (dd)								
Bergpad	20.6258	-33.7302	Western Cape	1	Convenience	Yes	Group interview	Yes (#)	5	Conservation staff
Bumpy Track	20.6259	-33.7270	Western Cape	1	Convenience	Yes	Group interview	Yes (#)	5	Conservation staff
Skietdam	20.6483	-33.7506	Western Cape	1	Convenience	Yes	Group interview	Yes (#)	5	Conservation staff
Humpsback	24.6007	-32.1449	Eastern Cape	1	Convenience	No	Group interview	Yes	2	Landowner
Rooiflip	24.581	-32.1510	Eastern Cape	1	Convenience	No	Individual interview	Yes	1	Land manager
Sakhu	28.2955	-30.8405	Eastern Cape	1	Convenience	Yes				
Trickle Main W	28.6044	-31.1399	Eastern Cape	1	Snowballing	Yes	Focus group ([§])	No	9	Community members (different age groups)
Trickle Main E	28.6354	-31.1244	Eastern Cape	1	Snowballing	Yes	Focus group ([§])	No	32	Community members (different age groups)
Contour game NS	28.3532	-28.6211	Free State	2	Convenience	No				
Contour game E-W	28.3553	-28.6186	Free State	2	Convenience	No				
Mushroom NS	28.4273	-28.5579	Free State	2	Snowballing	No				

Mushroom E-W	28.4291	-28.5557	Free State	2	Snowballing	No				
Golden 1W	28.6463	-28.5104	Free State	2	Snowballing	Yes				
Golden 1E	28.6500	-28.5099	Free State	2	Snowballing	Yes				
Golden 2	28.6865	-28.4264	Free State	2	Snowballing	Yes				
Makgo W	30.5162	-24.1621	Limpopo	2	Convenience	No	Individual interview (§)	Yes (#)	1	Land manager
Makgo E	30.5753	-24.1621	Limpopo	2	Convenience	No	Individual interview (§)	Yes (#)	1	Land manager
BushW N	30.8822	-24.3201	Limpopo	2	Convenience	No	Interview (§)	No	1	Landowner
BushW S	30.8874	-24.3259	Limpopo	2	Convenience	No	Interview (§)	No	1	Landowner

† Locations ordered according to longitude and province
‡ The sampling method here refers to the method applied after purposeful sampling was applied to define the sample universe
§ Recordings of discussion/interview were not permitted, or not possible. Handwritten notes were taken during discussions.
# Gully walk conducted, in addition to participatory mapping.

The 19 selected sites mainly exhibited sedimentary lithology and Glenrosa/ Mispah soils, with RDN varying between 5.5 and 8.7 (Table 5.4). Local slopes varied, but most sites (n = 11) have a gentle to moderate slope (<10%).

Two land uses were selected to investigate across the E-W climate gradient: 1) conservation and 2) livestock and game. Local sites for conservation land-use practices were selected in MAR classifications of 0 mm to 200 mm (Succulent Karoo biome), 400 mm to 600 mm (Savanna biome), and 800 mm to 1000 mm (Grassland biome). The livestock and game land use classification were distributed between the 200 mm to 400 mm (Nama Karoo and Albany thicket biomes, respectively), 400 mm to 600 mm (Savanna biome), and 600 mm to 800 mm (Grassland biome). Land uses that were clustered in the Grassland biome (between 600 mm and 1000 mm MAR) were used to isolate the effect of land use on gullying and consisted of livestock and game, conservation, and communal grazing in the former Homelands.

Table 5.4 Geo-environmental descriptors of the selected study sites.

Gully name	Mean annual rainfall (mm)	Rainy Day Normal	Biome	Contemporary land-use	Mitigation measures	Local slope in (%)†	Soil	Geology
Bergpad	0-200	5.5	Succulent Karoo	Conservation	Gabions	3.4	Glenrosa/ Mispah	Coarse sedimentary
Bumpy Track	0-200	5.5	Succulent Karoo	Conservation	Gabions	3.0	Glenrosa/ Mispah	Coarse sedimentary
Skietdam	0-200	5.5	Succulent Karoo	Conservation		7.8	Glenrosa/ Mispah	Coarse sedimentary
Humpsback	200-400	5.6	Albany thicket	Livestock and game	Soil bunds	18.9	Glenrosa/ Mispah	Coarse sedimentary‡
Rooiflip	200-400	6.4	Nama Karoo	Livestock and game	Contour banks	3.6	Glenrosa/ Mispah	Coarse sedimentary‡
Sakhu	8000-1000	5.9	Grassland	Communal grazing		5.9	Red-yellow apedal	Fine sedimentary‡
Trickle Main W	800-1000	5.7	Grassland	Communal grazing		17.7	Glenrosa/ Mispah	Fine sedimentary‡
Trickle Main E	800-1000	5.7	Grassland	Communal grazing	Soil bunds and contour banks (abandoned)	10.1	Duplex	Fine sedimentary‡
Contour game NS	600-800	8.1	Grassland	Game	Contour banks (abandoned)	8.5	Red-yellow apedal	Fine sedimentary‡
Contour game E-W	600-800	8.1	Grassland	Game	Contour banks (abandoned)	11.6	Red-yellow apedal	Fine sedimentary‡

Mushroom NS	600-800	8.1	Grassland	Livestock		37.5	Glenrosa/ Mispah	Fine sedimentary‡
Mushroom E-W	600-800	8.1	Grassland	Livestock	Check dam	9.1	Red-yellow apedal	Fine sedimentary‡
Golden 1W	800-1000	8.7	Grassland	Conservation	Gabions	11.8	Glenrosa/ Mispah	Fine sedimentary‡
Golden 1E	800-1000	8.7	Grassland	Conservation		14.8	Glenrosa/ Mispah	Coarse sedimentary
Golden 2	800-1000	7.7	Grassland	Conservation		13.5	Glenrosa/ Mispah	Coarse sedimentary
Makgo W	400-600	8.5	Savanna	Conservation		2.6	Glenrosa/ Mispah	Mafic igneous/ metamorphic
Makgo E	400-600	8.3	Savanna	Conservation		2.7	Glenrosa/ Mispah	Felsic igneous/ metamorphic
BushW N	400-600	8.3	Savanna	Livestock and game	Brush and stone fill	5.6	Glenrosa/ Mispah	Felsic igneous/ metamorphic
BushW S	400-600	8.3	Savanna	Livestock and game	Brush and stone fill	7.6	Glenrosa/ Mispah	Felsic igneous/ metamorphic

† A local slope was calculated using equation 5.2

‡ Local study sites overlaying the Adelaide and Tarkastad subgroups and the Elliot Formation

5.3.2.1 Remote analysis

Originally from the CD: NGI (Chief Directorate of National Geospatial Information, Department of Rural Development and Land Reform) portal (http://www.cdngiportal.co.za/cdngiportal/), historical aerial imagery was acquired from the Centre for Geographic Analysis based at Stellenbosch University. The imagery consisted of georeferenced aerial images dated between 1938 and 2007 (captured in analogue with spatial scales between 1:20000 and 1:50000) and orthorectified aerial imagery between 2008 and 2016 (digitally captured with spatial resolutions between 0.25 m to 0.50 m). Additionally, where permitted, aerial images were captured during 2022 with a Da-Jiang Innovations (DJI) Mavic 3 UAV fitted with a 4/3 CMOS Hasselblad camera. The UAV imagery was georeferenced and mosaicked using Agisoft Metashape Professional 1.8.1. Where necessary, a fine adjustment was made to the UAV imagery using the ground control points defined during the georeferencing procedure.

Gullies were manually digitised as lines at a scale of 1:3500 and as polygons at a scale of 1:1500 in QGIS 3.16.16. If gullies exhibited indistinguishable channels due to being in proximity with narrow, bare interfluves, they were lumped together when mapped as a polygon. Gully channels were approximated in areas where tree coverage obstructed visual gully channel detection. Annual linear and planimetric retreat rates were calculated by subtracting the length (in m) and area (in m^2) of subsequent images and dividing it by the number of years lapsed.

A local slope of each gully was calculated by extracting height values from a 2 m DEM (GeoSmart Space, 2022b), by:

$$S = \frac{h_{HC} - h_L}{L} \qquad \text{Equation 5.2}$$

where h_L is the elevation at the gully's outlet or deposition zone;

h_{HC} is the elevation at the gully headcut;

L is the straight-line length between h_{HC} and h_L;

The gully line feature digitised from the most recent aerial image was used to identify the point features that would represent the gully headcut and outlet or expiry point. The origin point of

the digitised line (lowest position) was regarded as the expiry point of the gully, while the main headcut was determined as the point furthest away along the digitised line feature from the point of expiry.

The point at the gully expiry or outlet was used to derive the gully catchment from a 2 m DEM (GeoSmart Space, 2022b). For discontinuous gullies, the deposition point furthest downstream was used to determine the catchment area, for example, if the deposition zone migrated upstream between 1944 and 2022, the 1944-point location was used to calculate the catchment size. The nested catchment was calculated for each discontinuous gully by subtracting the upstream gully catchments from those occurring downstream (Figure 5.4). A linear and planimetric gully density was calculated as a ratio, dividing the total gully channel length (in km) and total gullied area (m^2), respectively, by the catchment size (in km^2) (Wilkinson et al., 2018; Li et al., 2021).

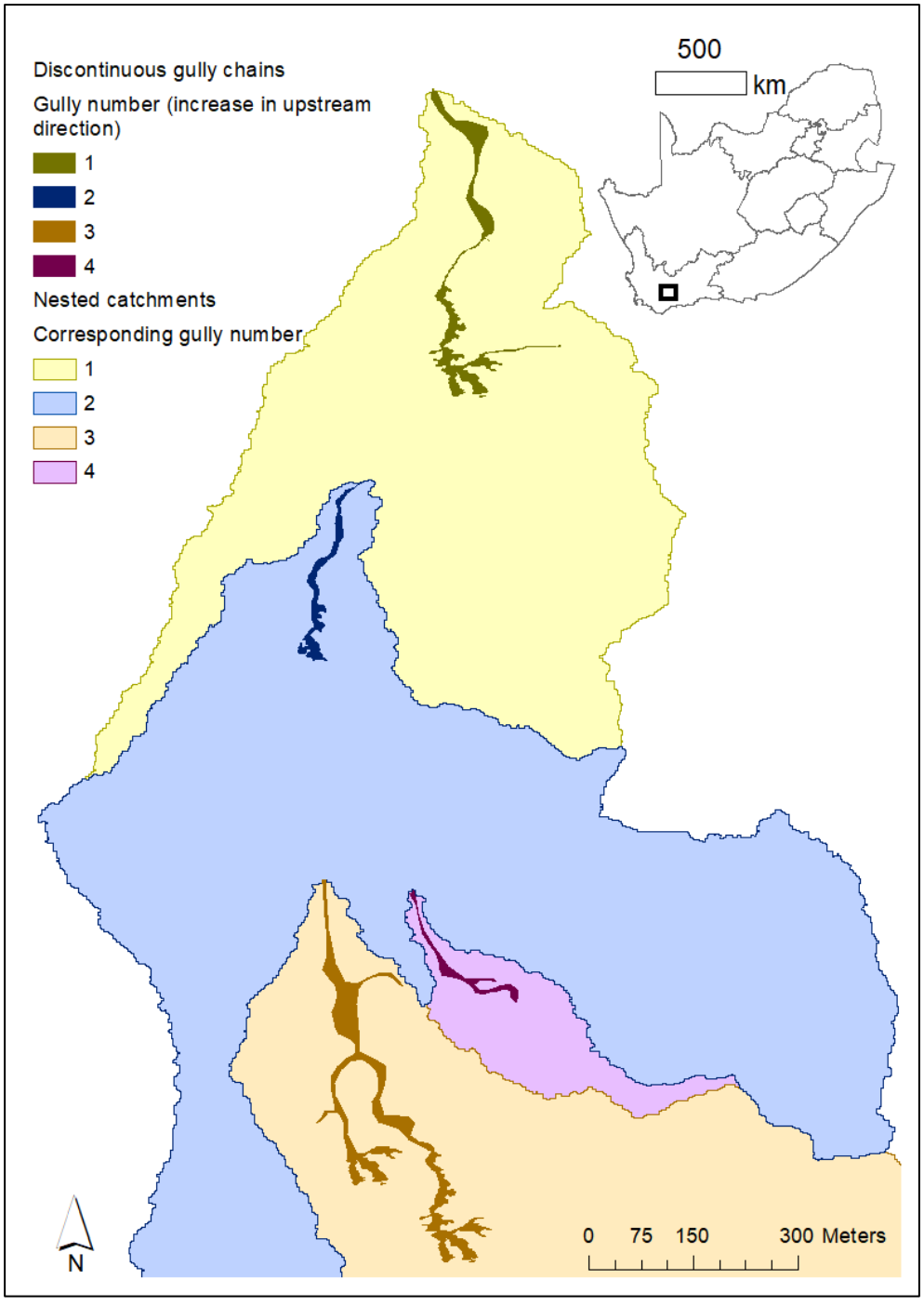

Figure 5.4 Showing how the catchment size was derived for discontinuous gully chains (gully 1 and 2 depicts the Bergpad and Bumpy Track gullies respectively; the insert shows the location in South Africa). Upper gully catchments were subtracted from the catchment furthest downstream.

The oldest and most recent imagery were used to classify the gully system (modification to the proposed classification by Thwaites et al. (2021); see Figure 5.5 for the classification metric)

according to family, position in the landscape, land-use in which it occurs, planform shape, and connectivity.

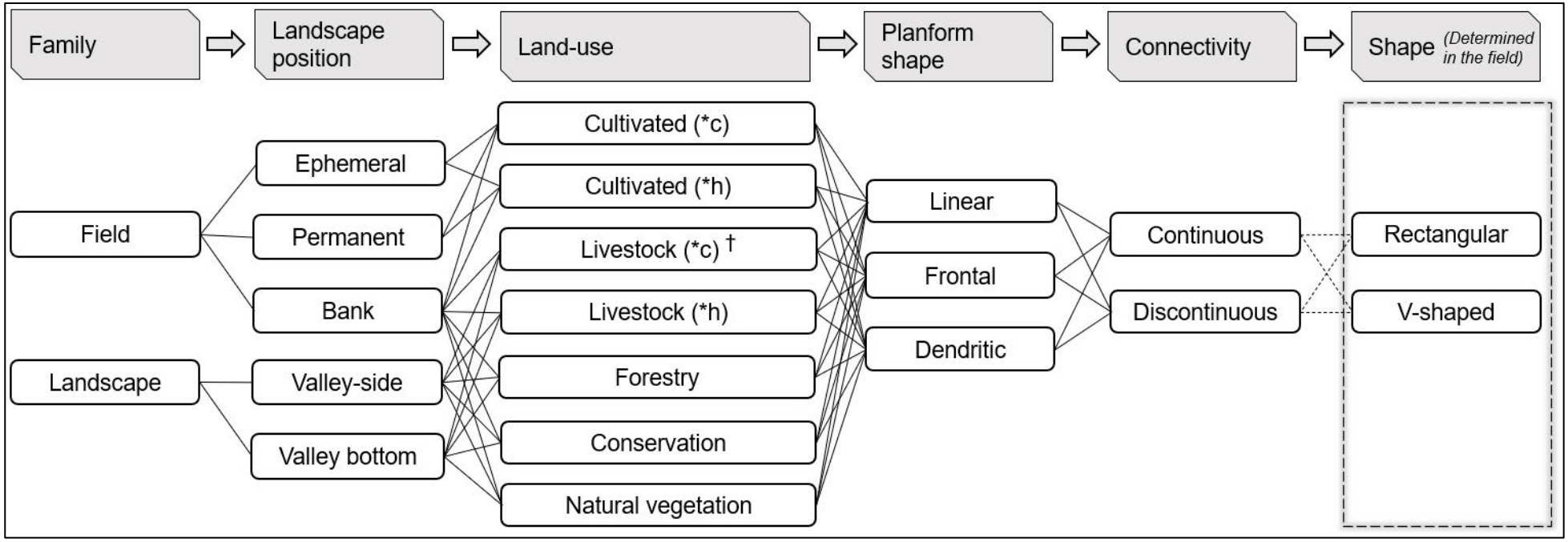

Figure 5.5 A graphical illustration of the classification system used to analyse every gully, which was modified from Thwaites et al. (2021). The classification was completed from remotely sensed imagery for the oldest and most recent image according to family, landscape position, land-use, planform shape, and connectivity, for example, *Field, permanent, cultivated (*c), dendritic, and continuous* (*c and *h denote commercial and former homelands, respectively).

.

5.3.2.2 Field measurements

Detailed cross-section measurements were taken where a distinct change in shape or size of gully channels was observed or at a maximum interval of 15% of the total gully length if channel shape variation was imperceptible (Figure 5.6). The Global Positioning System (GPS) position of each cross-section point was recorded with a Garmin eTrex Touch 35, which has an accuracy variance of 5 m. The GPS locations were supported by sketches to improve accuracy upon importing the cross-section measurement positions into a GIS environment. Pegs were used to secure a measuring tape on both banks of the gully. After affixing the measuring tape, depth measurements were taken with an extendable measurement staff at 0.5 m intervals for gullies with a width < 10 m, 1 m intervals for widths between 10 m and 20 m, and 2 m intervals when gully widths exceeded 20 m. Gully volume was estimated by summing the cross-sectional measurements by:

$$V = \sum_n L_i \left(\frac{A_{up}\, A_{down}}{2}\right) \qquad \text{Equation 5.3}$$

where V is the total volume of the gully system;

n is the number of gully segments measured;

L_i is the length of the i-th gully segment (in m);

A_{up} and A_{down} respectively, are the upstream-downstream cross-sectional areas (in m^2) of the i-th gully segment

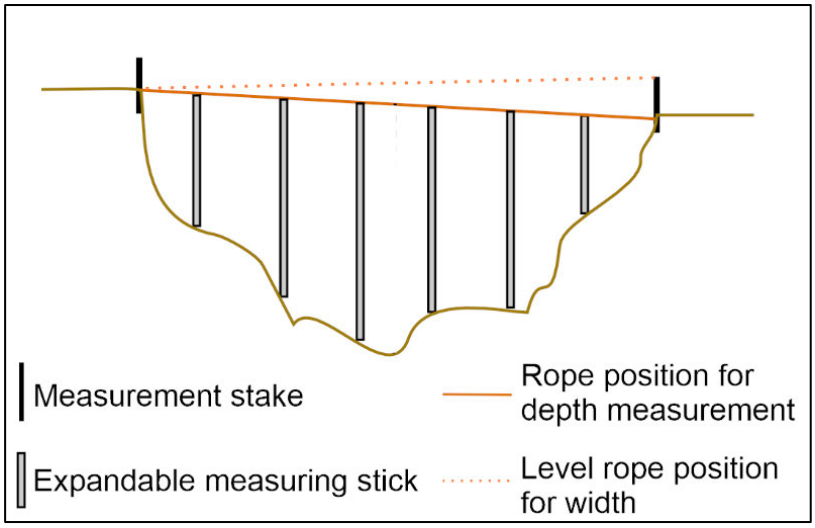

Figure 5.6 Schematic representation of cross-section measurement process.

Several gullies exhibited dimensions and shapes that would pose a high risk of injury when traversed, which made surveying at the abovementioned intervals impractical. At such gullies (for which volume will be communicated in italics), volume was related to gully shape, viz., V, U, or trapezoidal forms. Although gully cross sections are more complex than these generalised shape forms (Casalí et al., 2015), it was the only alternative available with the equipment we had available. However, approximating gully cross sections from generalised forms remains a valid and acceptable methodology (Vandekerckhove et al., 2000; Slimane et al., 2018; Fashae et al., 2022). For V-shaped gullies, the deepest position at the gully thalweg was measured, and volume was calculated as follows:

$$V = \sum_n L_i \left(\left(\left(\frac{(h_T\, W)_{up}}{2} \right) + \left(\frac{(h_T\, W)_{down}}{2} \right) \right) 0.5 \right) \qquad \text{Equation 5.4}$$

where h_T is deepest point of the gully;

W is the width for upstream and downstream positions;

n indicates the number of segments

L_i is the length of the i-th gully segment (in m);

A_{up} and A_{down} respectively, are the upstream-downstream cross-sectional areas (in m^2) of the i-th gully segment

L is the straight-line length between h_{HC} and h_L

For U- and trapezoidal-shaped gullies the volume was calculated as:

$$V = \sum_n L_i \left(\left(\left(\frac{(L_b + R_b)up}{2} W \right) + \left(\frac{(L_b + R_b)up}{2} W \right) \right) 0.5 \right) \quad \text{Equation 5.5}$$

where L_b and R_b are the depth measured at the left and right bank, respectively, for the upstream and downstream cross-sectional measurements positions.

An annual volumetric retreat rate was estimated by first calculating an average volume by dividing the volume (m^3) derived from field measurements by the most recently digitised planimetric area (m^2), and thereafter multiplying this V-A ratio with historically derived planimtric areas to allow the calculation of historic soill loss. Although the V-A ratio is likely to change, especially if the gully reaches bedrock, the method implies a linear progression where the V-A ratio remains constant, which is congruent with studies that assumes unchanging depths to estimate gully headcut retreat (Vandekerckhove et al., 2000; Grellier et al., 2012). The method does introduce uncertainty, but we believe it is a fair assumption to caluclate soil loss in the absence of validated eqautions or models, especially since Shellberg et al. (2010) demonstrated a primarily linear expansion, both in terms of areal and volumetric gully growth for their gully expansion. A soil bulk density of 1.5 g cm^{-3} , which is an average of bulk densities used in South Africa (see APPENDIX G), was used in conjunction with the derived catchments to calculate a gully erosion rate in t ha^{-1} y^{-1}. Gully erosion was classified according to the erosion rates calculated: below 1 t ha^{-1} y^{-1} was classified as stable, between 1 t ha^{-1} y^{-1} and 10 t ha^{-1} y^{-1} were classified as a medium severity, while above 10 t ha^{-1} y^{-1} were classed as high gully erosion severity.

Width-depth (W/D) ratios were calculated for each cross-section by dividing the true width (level rope line in Figure 5.6) with the average depth. Observations regarding activity and dominant erosive processes were noted at the positions of cross-sectional measurements and gully headcuts.

5.3.2.3 Semi-structured and focus group discussion

In order to gain a better understanding of local sites' historic and contemporary factors affecting gully evolution, semi-structured interviews and, where feasible, participatory mapping exercises were conducted. The specific format of interviews was adapted to local context and ranged from interviews with individual participants, to small group interviews to a larger group in a community setting. In this section, the nature of these different types of interview formats is described further.

A thematic guide was developed to serve as a generic base for interviews and focus group discussions, which could be adapted according to specific contexts in the different research sites for participatory discussions (see APPENDIX H). The themes and semi-structured questions were open-ended to allow participants to expand on themes as the discussion progressed, allowing exchanges to follow conversational flow, instead of explicitly directing specific questions to the participants (Archer, 2004; Brinkman, 2014). Themes that were introduced to entice the sharing of local knowledge included, but were not limited to, land-use history, contemporary and historical gully erosion causes and rates, mitigation works, and associated costs. In addition, for many settings, historical sequential base maps were printed and used as a tool to start the dialogue about the local area, to enable an easier spatial contextualisation of different interview points. However, there were circumstances were this was not possible due to either the lack of available historical sequential base maps or a participant-directed ad-hoc adjustment of the specific geographical focus area for interview discussions. Such field-based adaptation ensured that local knowledge about specific gully systems could be incorporated.

Participants were met where most convenient and comfortable for them, (for example, at the house of the village headmen, in a lodge, or a pre-arranged field site), and interviews and focus groups took place in a variety of settings, including outdoors or office-spaces (Figure 5.7).

Figure 5.7 Participatory discussions were held at the most convenient and comfortable location for the participants, for example, a) at the house of the village headman, or b) at lodge accommodation.

Specific interview participants at the different sites were selected due to their level of knowledge of the local areas, including the identified gully sites. In commercial and conservation land uses, semi-structured interviews took place with either individuals or smaller groups (Table 5.4). At the Bergpad, Bumpy Track, and Skietbaan gully sites, a gatekeeper provided access to the conservation team and managing director, who acted as participants. The group of interview participants all had formal training and had professional experience in conservation or ecology ranging between 8 years and 20 years. The Humpsback site is located on a 5th generation farm, and a semi-structured interview was conducted with two members of the most recent generations of farmers. At the other sites, semi-structured interviews were conducted on a one-on-one basis, and all participants, whether landowners or land managers, were involved in the activities of the respective land uses. At the conclusion of the semi-structured interviews, participants were asked if they had any concerns regarding gullies other than those preselected.

In the communal areas, the former homelands, focus groups were used to inform on past and present gully erosion. At the Sakhut, Trickle E, and Trickle W sites, the gatekeeper, and subsequently the chief and headman, selected the focus group participants based on our inquiry to conduct: "…interviews with community members of different age groups…". A discussion with a transect of community members of different age groups (and different designations, for example, headmen, herders, and collectors) can enable us to tap into historical narratives, first-hand experiences, and knowledge that was handed down by word of mouth, providing rich data in the absence of formal written organisational memory. Participants were separated into

decadal age categories (20 to 30 years old, 30 to 40 years old, >40 years old) to allow focus group discussion per age bracket. The different age groups allowed information regarding drivers and impacts to be cross-checked and any contradictions identified (similar to Nyssen et al., 2006 and Tebebu et al., 2010). Both Nyssen et al. (2006) and Tebebu et al. (2010) successfully used interviews with different age groups in communal areas to learn more about gully evolution and rates.

Discussions were held at the house of the relevant headman. At the Trickle E site, 32 participants (6 participants between 20 and 30 years old, 8 participants between 30 and 40, 18 participants >40) were present for the focus group discussions. Focus group discussions were conducted with one age group at a time but in the presence of the other age groups. At the Trickle W site, nine participants (1 participant between 20 and 30; 8 participants >40 years old) arrived for talks, and the first author facilitated one joint discussion. Discussions were more general and not specific to preselected gullies as per commercial farming and conservation sites, as the gatekeeper provided access to sites on short notice. The gatekeeper was present throughout the days of fieldwork and discussions and served as an interpreter between the isiXhosa-speaking focus group participants and the English-speaking researcher.

5.3.2.4 Participatory mapping and gully walks

Following the semi-structured interviews and focus group discussion, participants were invited to partake in a participatory mapping exercise. Participatory mapping provides a visual means for participants to share their understanding of gully erosion. Participatory mapping is an additional way to incorporate local knowledge into gully evolution drivers and to translate this knowledge into geospatial vulnerability assessments of gullies (like Sullivan-Wiley et al., 2016; Samodra et al., 2018). The participatory mapping exercise involved participants using coloured pens to map gully susceptibility on the contemporary base map, while explaining reasons for their classification. Follow-up questions were posed regarding the history of the gully to invite discussion on key events leading to gully expansion, the process of expansion, reasons for implemented mitigation measures (current and potential future installations), and the success rate thereof.

Upon conclusion of the semi-structured interviews and participatory mapping exercise, participants were invited to partake in a ‘gully walk’. Due to time constraints, “gully walk”

activities were not raised during the focus group discussions at either site. These ‘gully walks’, consisted of walking along the selected (and discussed gullies), whilst the researcher promoted further discussion to the same themes covered during the participatory mapping exercise. Results obtained from ‘gully walks’ were collectively compared to participatory maps, and adjusted if differences arose.

5.4 RESULTS

5.4.1 Local case study to introduce captured data

The Bumpy Track site will be used to illustrate the application of the triangulation of methods and the specific results it can delivered. Bumpy Track was selected because the triangulation of methods, more specifically the different qualitative methodologies (semi-structured interview, participatory mapping, and ‘gully walks’), were most comprehensively applied compared to other sites. Using Bumpy Track as an example, therefore, allows to optimally demonstrate the usefulness and impact of using the triangulation of methods. Similar data was retrieved from other sites, and a summary is provided in Table 5.6.

5.4.1.1 GIS analysis

Bumpy Track (Table 5.4) is a discontinuous landscape gully within conservational land use in the semi-arid Karoo. It is situated on the valley bottom, with an average local slope of 2.3% and forms part of several successive discontinuous gully chains (Table 5.5). In the 1944 aerial image, the linear gully appears in rangeland, with an average width of 8.4 m along its 241.9 m length. The average linear retreat since 1944 was 4.3 m y^{-1}, but the expansion was not constant over time. Between 2007 and 2010, there was a significant reduction in length (-54.6%) due to deposition shifting upstream, possibly because of extra sediment load from the gully capturing an old farm road to the east in proximity to the gully headcut (Figure 5.8, 5.9). In the subsequent imagery, the gully migrates northwards in both its deposition zone and gully headcut position, although total length increases except for the contraction between 2007 and 2010 (Figures 5.8, 5.9). The average width of the gully decreased between 1944 and 2022, notwithstanding the contemporary planimetric growth between 2010 and 2022, recorded as 71.2 m^2 y^{-1} (2.1%) and 46.4 m^2 y^{-1} (1.2%), respectively. The linear drainage density extracted from the 2022 aerial imagery is 1.9 km km^{-2} compared to 0.8 km km^{-2} in 1944. It is, however, lower than the

maximum density of 2.1 km km^{-2} recorded in 2007. The 2022 planimetric density was calculated as 12097.4 m^2 km^{-2} y^{-1}, increasing by an average of 71.3 m^2 km^{2} y^{-1}.

Table 5.5 Geomorphic changes of the Bumpy Track gully network between 1944 and 2022.

	Length in m (rate m y^{-1})	Area in m^2 (rate m^2 y^{-1})	Average width (m)	Volume in m^3 (rate m^3 y^{-1}) †	Average depth (m)	Local slope (in %)	Gully density in km/km^2 (m^2/km^2)	Classification
1944	241.9	2025.6	8.4	2009.8		1.6	0.8 (6534.2)	Landscape, valley bottom, livestock (*c), linear, discontinuous
1960	469.5 (14.2)					1.9	1.5	
2007	655.3 (4.0)					1.6	2.1	
2010	491.4 (-54.6)	3044.7 (15.4)	15.4	3020.9 (15.3)		2.9	1.6 (9821.6)	
2016	526.3 (5.8)	3471.8 (71.2)	71.2	3444.7 (70.6)		3.0	1.7 (11199.4)	
2022	573.7 (7.9)	3750.2 (46.4)	46.4	3720.9 (46.0)	1.1	2.8	1.9 (12097.4)	Landscape, valley bottom, conservation, dendritic, discontinuous, rectangular

† Volume was measured for 93.2% (3495.2 m^2) of the digitised gullied area

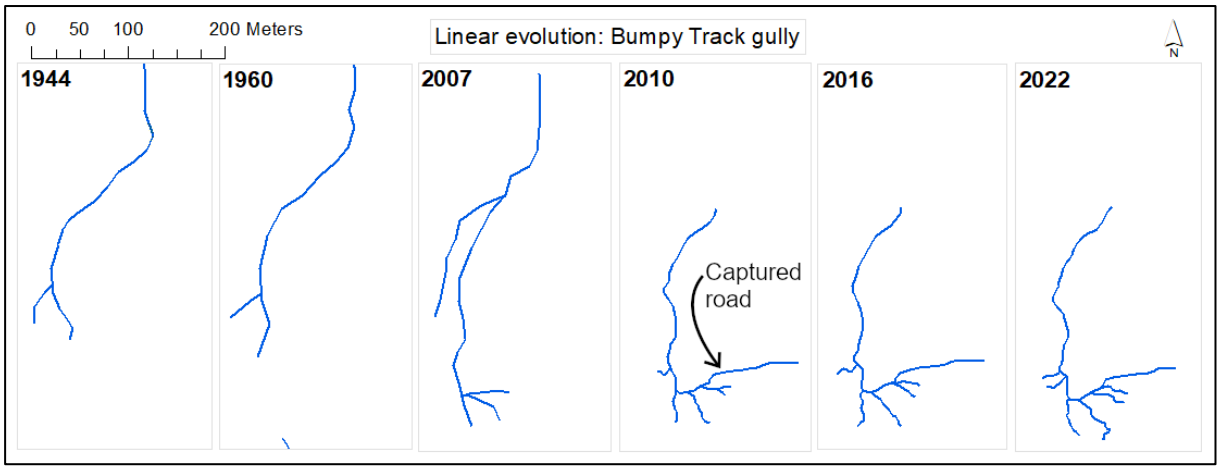

Figure 5.8 Linear gully evolution of the Bumpy Track gully network, which is under conservational land use in the semi-arid Karoo.

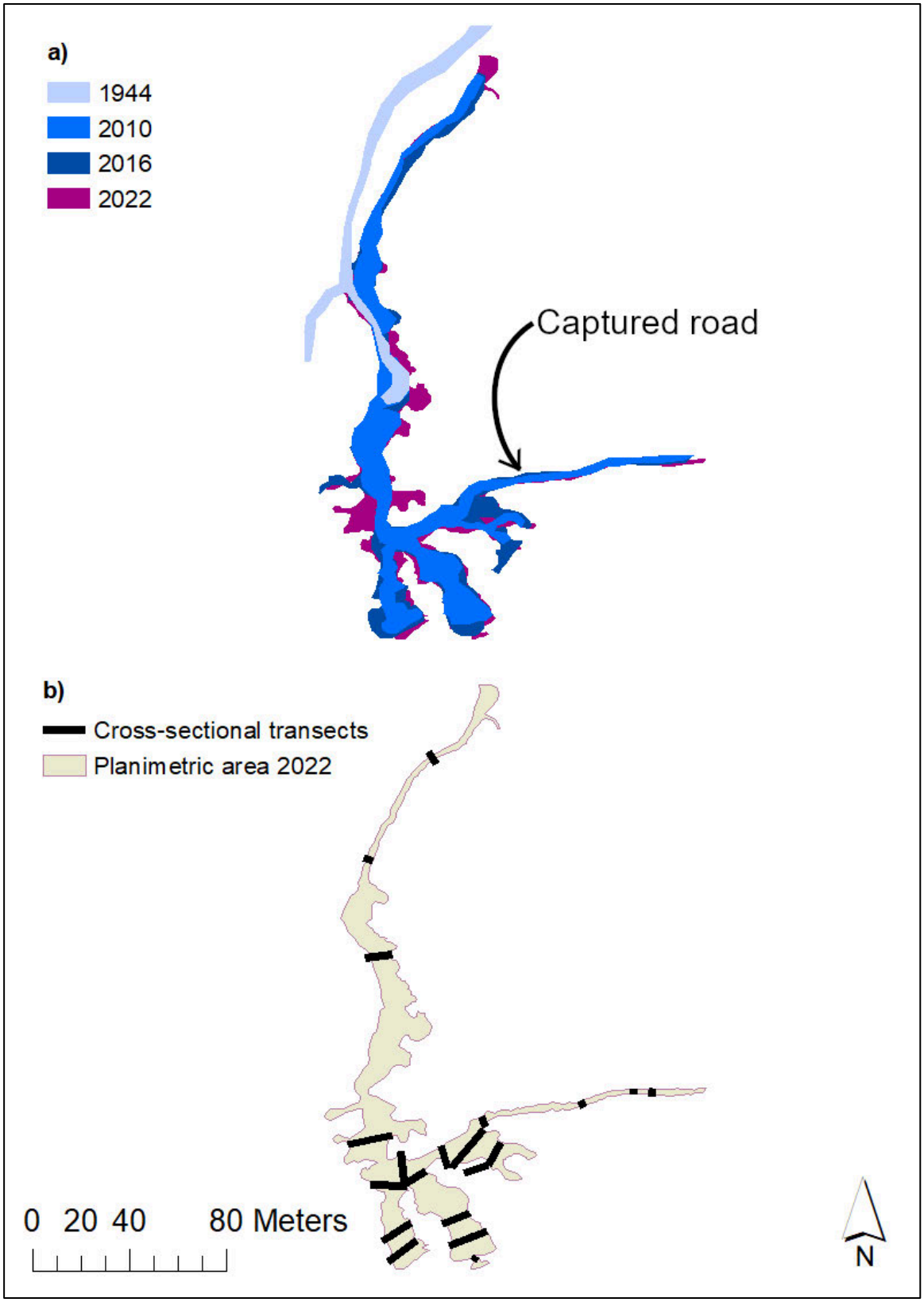

Figure 5.9 Planimetric area of the Bumpy Track gully network. a) evolutionary progression of the gully network; b) locations of cross-sectional measurements.

5.4.1.2 Field inspection

An aggregate gully area of 3495.2 m^2 (93.2%) was surveyed in the field, compared to the total gullied area of 3750.2 m^2 digitised remotely. Due to time constraints, smaller 1st order gully channels were not surveyed. Cross-sectional areas were measured at 20 transects to determine volumetric soil loss (Figure 5.8b). The total volume of soil eroded at the measured portion of the Bumpy Track gully is 3720.9 m^3, estimated to equate to an average of 21.9 m^3 y^{-1} of soil loss since 1944.

The gully channels are predominantly U-shaped, with several sections being eroded to bedrock. Overland processes are dominant at bumpy track, with no subsurface processes identified in the field. The gully is active at its headcuts, becoming less active when it peters out into a deposition zone approximately 83 m upstream of another sharp headcut. Broad lobes are being eroded on the right bank, likely from sheet flow overflowing the gully banks. Several gully headcuts are near a road, and gabions have been installed. However, the gully is eroding around and undercutting these gabions, resulting in it failing. Gully channels immediately downstream of the gabions are wide and U-shape. The gully captured the above-mentioned old farm road and had a maximum depth and cross-sectional area of 84 cm and 2.9 m^3 at the time of fieldwork.

5.4.1.3 Interviews and participatory mapping

The participants from the Bumpy track site consisted of a conservation team and the general manager, who all had tertiary education. The participants have been employed at the conservation site for up to 20 years, and therefore possess good historical local knowledge. They indicated that gully erosion was a problem in several areas of the conservation site, including threats to infrastructure at the Bumpy Track gully. Mitigation measures are implemented and consist of gabions being placed at gully headcuts. During the gully walk, we were shown several sagging gabions and new 1st order gullies channels eroding around previously installed gabions, highlighting the significant failure rate being experienced. At the time of the interview, the conservation team had a retrospective approach to gully mitigation, which they wanted to progress to a preventative strategy.

The conservation team indicated that gully erosion was an event-based process caused by high-intensity rainfall events. During the gully walk, an area that had recently eroded after a few

high-intensity rainfall events was highlighted. Gully erosion also has an anthropogenic imprint. Game stock levels are kept below the calculated carrying capacity to ensure vegetation cover can expand; however, the inherited road structure (from prior rangeland farming) that runs up and down the slope was regarded as a driver of gully erosion due to its impervious nature resulting in the accumulation of concentrated overland flow downslope. During the participatory mapping exercise, the conservation team observed that more than one area existed where roads, which used to be straight, were reconstructed around active gully headcuts (Figure 5.9) due to the gully capturing part of the road. In the participatory map, areas susceptible to gullying were shown in proximity to the existing gully headcuts, indicative of their current strategy of gabions placement specifically at gully headcuts.

Figure 5.10 Participatory map showing areas of concern regarding gully erosion in red, with additional notes in black on the most recent aerial image of the Bumpy Track gully network in the center of the image.

5.4.2 Regional gully assessment

5.4.2.1 Gully characteristics

A temporal desktop study and field survey were conducted at 19 gully sites across the E-W climate gradient of South Africa, the furthest sites being approximately 1542 km apart (Table 5.6). The aerial imagery used to construct long-term datasets varied from 1944 to 2022, with an average coverage of 57 years per site. All studied gullies were already formed by the earliest

image dates, and the date of origin was not discernable, except for the Makgo W, BushW N, and BushW S gullies in Limpopo. Following the classification system from Figure 5.5, the contemporary gullies were all landscape gullies, of which 11 were located on valley sides (Table 5.6). The planform shape was primarily dendritic (68.4%), with 89.4% of gully channels exhibiting a rectangular shape. Discontinuous gully chains were mainly found in the arid regions of South Africa and comprised 42.1% of the gully sites investigated.

Contemporary gully lengths varied between 24.6 m and 3842.9 m, with a mean of 734.0 m (Table 5.6; Figure 5.10a). Planimetric gully areas ranged between 20.9 m^2 to 83286.2 m^2 with a mean of 12503.8 m^2 (Figure 5.10b). Gully volumes were primarily calculated for specific segments of the gully network only, due to time constraints in the field (APPENDIX I). The estimated gully volumes varied between 5.3 m^3 and 72596.1 m^3, with a mean of 12009.6 m^3 (Figure 5.10c). Figure 5.10 shows the variability of the gully dimensions. It suggests that the distribution is right-skewed, with a median smaller than the average for gully length (57.4% of the mean), planimetric area (30.0% of the mean), and volume (31.0% of the mean). A significant correlation ($R^2 = 0.76$) was observed between the gully planimetric area and volume (Figure 5.11a). No significant correlation between climatic variables is evident when considering gully planimetric area and volume relationships. The average depth, a ratio of volume and planimetric area and the average width, the ratio between planimetric area and length, show little association, except for the conservation land use ($R^2 = 0.96$; Figure 5.11b). The mean annual rainfall grouping suggests that it impacts average depths and widths, with higher rainfall area plotting generally in the upper half, indicating deeper gully forms (Figure 5.11b). In contrast, lower rainfall plots towards the lower half, showing shallower gullies form in this climate.

A total of 234 gully channel transects were measured at the 19 gully sites, excluding measurements at gully headcuts and observations at discontinuous deposition zones. Gully widths varied between 0.3 m and 64 m with a mean of 9.1 m (Figure 5.10d). The maximum depth for gully channels ranged between 10 m and 6.5 cm, with a mean of 192.5 cm (Figure 5.10e). The mean WD ratio calculated from the in-field measurements was 6.8, with individual WD ratios varying between 0.5 and 37.2 (Figure 5.10f). Gully cross sections range between 0.1 m^2 and 306.5 m^2 with a mean of 19.8 m^2. Like length, planimetric area, and volume, the in-

field measurements and derived metrics had a lower median than the mean, with the boxplots further suggesting that the distribution is right skewed.

The gully catchment varied between 33 km^2 to 809 km^2 with a mean of 285 km^2. The density within these catchments ranged between 0.6 m^2 km^2 and 162.0 m^2 km^2, with a mean of 40.6. m^2 km^2. Local slopes measured at valley bottom gullies were as gentle as 0.4%, with the steepest slopes calculated for valley side gullies being 18.2%.

Table 5.6 Gully classification and morphometry.

Placename	Earliest image classification[†]	Classification changes according to contemporary image	Duration between image years (time period)	Length in m[‡] (avg. growth rate in m y^{-1})	Area in m^2 [‡] (avg. growth rate in m^2 y^{-1})	Volume in m^3 [‡] (avg. growth rate in m^3 y^{-1}) [‡§]	Local slope in % [‡] (slope change in %)	Gully catchment in km^2 [‡] (density in m^2 km^{-2})
Bergpad	Landscape, valley-bottom, **livestock (*c), linear**, discontinuous	Conservation, dendritic (rectangular)	78 (1944-2022)	336.0 (2.1)	2365.3 (18.7)	1652.8 (13.1)	1.8 (0.5)	0.5 (3292.4)
Bumpy Track	Landscape, valley-bottom, **livestock (*c), linear**, discontinuous	Conservation, dendritic (rectangular)	78 (1944-2022)	573.7 (4.3)	3750.2 (22.1)	3720.9 (21.9)	2.8 (0.8)	0.3 (12189.8)
Skietdam	Landscape, valley-side, **livestock (*c), linear, discontinuous**	Conservation, dendritic, continuous (rectangular)	72 (1944-2016)	1186.8 (8.9)	3243.0 (28.3)	1557.4 (13.8)	7.2 (2.5)	0.5 (3294.2)
Rooiflip	Landscape, valley-bottom, livestock (*c), frontal, continuous	(rectangular)	28 (1994 - 2022)	1027.6 (13.9)	32532.5 (218.2)	3383.0 (22.7)	3.6 (0.1)	0.8 (4184.0)
Humpsback	Landscape, valley-side, livestock (*c), **linear, continuous**	Frontal, discontinuous (rectangular)	77 (1945 - 2022)	421.2 (-0.2)	11743.0 (76.5)	6457.8 (42.0)	4.1 (-0.1)	0.1 (35246.3)
Sakhut	**Field**, valley-side, **cultivated (*c)**, dendritic, continuous	Landscape, livestock (*h) (rectangular)	63 (1952-2015)	1238.5 (8.4)	182286.4 (190.7)	*8776.2 (91.5)*	10.9 (3.5)	0.2 (39456.2)
Trickle Main W	**Field**, valley-side, **cultivated (*c)**, dendritic, continuous	Landscape, livestock (*h) (rectangular)	74 (1948-2022)	1675.2 (8.6)	30346.8 (211.9)	*48415.5 (338.1)*	8.0 (3.2)	0.6 (1622.3)
Trickle Main E	Landscape, valley-bottom, livestock (*h), dendritic, continuous	(V-shaped)	74 (1948-2022)	368.8 (3.7)	4959.2 (57.4)	*6527.6 (75.6)*	12.3 (6.0)	0.08 (978.5)
Contour game NS	**Field**, valley-bottom, **cultivated (*c)**, dendritic, continuous	Landscape, livestock (*c) [g] (rectangular)	46 (1969 - 2015)	777.5 (5.9)	8394.1 (130.2)	17385.9 (269.7)	0.4 (-2.6)	0.3 (51668.9)
Contour game E-W	**Field**, valley-side, **cultivated (*c)**, **linear**, continuous	Landscape, livestock (*c) [g], frontal (rectangular)	46 (1969 - 2015)	221.6 (0.6)	3039.3 (6.8)	1436.7 (3.2)	10 (1.2)	0.3 (55351.4)
Mushroom NS	Landscape, valley-side, livestock (*c), linear, discontinuous	(rectangular)	11 (2011 – 2022)	170.7 (0.0)	1022.1 (18.1)	2286.8 (40.6)	18.2 (-0.4)	0.4 (63830.7)

Mushroom E-W	Landscape, valley-side, livestock (*c), linear, discontinuous	(rectangular)	11 (2011-2022)	234.0 (0.0)	3175.0 (45.7)	4561.4 (65.6)	7.5 (0.4)	0.3 (14124.7)
Golden 2	Landscape, valley-side, **livestock (*h)**, dendritic, continuous	Conservation (rectangular)	47 (1970-2017)	3842.9 (30.3)	83286.2 (620.4)	72596.1 (540.7)	9.9 (3.4)	0.5 (162.0)
Golden 1W	Landscape, valley-side, **livestock (*c)**, dendritic, continuous	Conservation (rectangular)	55 (1962-2017)	491.9 (2.7)	7653.5 (60.3)	-	11.5 (1.3)	0.2 (46850.2)
Golden 1E	Landscape, valley-side, **livestock (*c)**, **linear**, continuous	Conservation, dendritic (rectangular)	55 (1962-2017)	859.1 (5.3)	22608.4 (242.7)	41534.4 (445.9)	6.5 (3.1)	0.5 (75999.2)
Makgo W	No gully, **natural vegetation**	Landscape, valley-bottom, conservation, dendritic, continuous (rectangular)	68 (1954-2022)	74.3 (5.3)	162.1 (11.6)	53.4 (3.8)	4.8 (1.2)	0.03 (1622.3)
Makgo E	Landscape, valley-bottom, **natural vegetation, linear**, continuous	Conservation (*c), dendritic (rectangular)	68 (1954-2022)	325.2 (3.6)	897.1 (9.5)	140.8 (1.5)	1.9 (1.3)	0.1 (978.5)
BushW N	No gully, **natural vegetation**	Landscape, valley-side, livestock (*c), dendritic, discontinuous (V-shaped)	66 (1956-2022)	96.5 (1.5)	86.3 (1.3)	16.2 (0.2)	4.1 (-)	0.1 (144.9)
BushW S	No gully, **natural vegetation**	Landscape, valley-side, livestock (*c), linear, discontinuous (rectangular)	66 (1956-2022)	24.6 (0.4)	20.9 (0.3)	5.3 (0.1)	11.7 (-)	0.03 (1622.3)

† Classification in **bold** changed between the earliest and contemporary image and only the change class type is provided in the subsequent column: "Classification changes according to contemporary image".

‡ Dimension or property measured from the most recent imagery.

§Volume calculations constrained to certain areas of the gullies only; see APPENIX H for equivalent area and the plan area to volume ratio

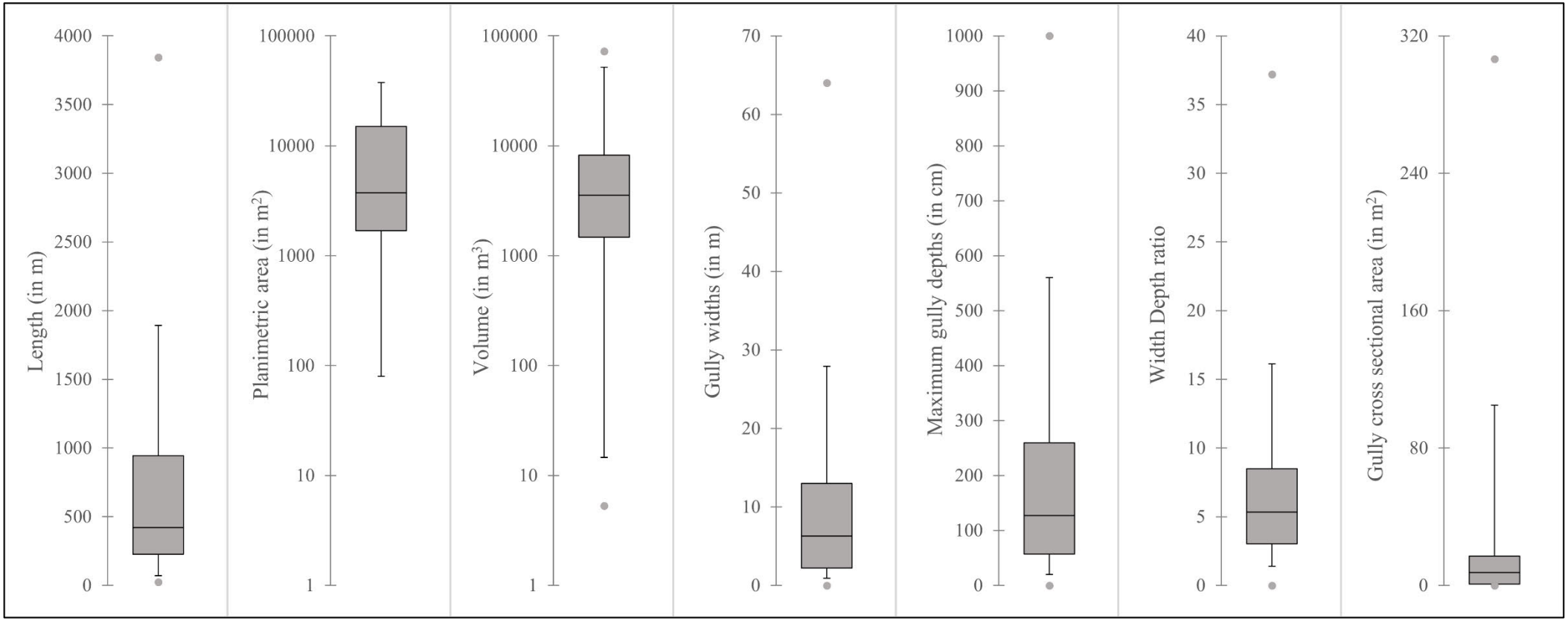

Figure 5.11 Boxplots showing the variation of gully characteristic in the study; a) length (n = 19), b) planimetric area (n = 19), and c) volume (n = 19) show variation in data for the gully network, while d) gully widths (n = 234), e) maximum gully depths (n = 234), f) width depth ratios (n = 234), and g) gully cross sections (n = 234) show variation from measurements along transects within the gully channel (therefore excluding measurements at gully headcuts).

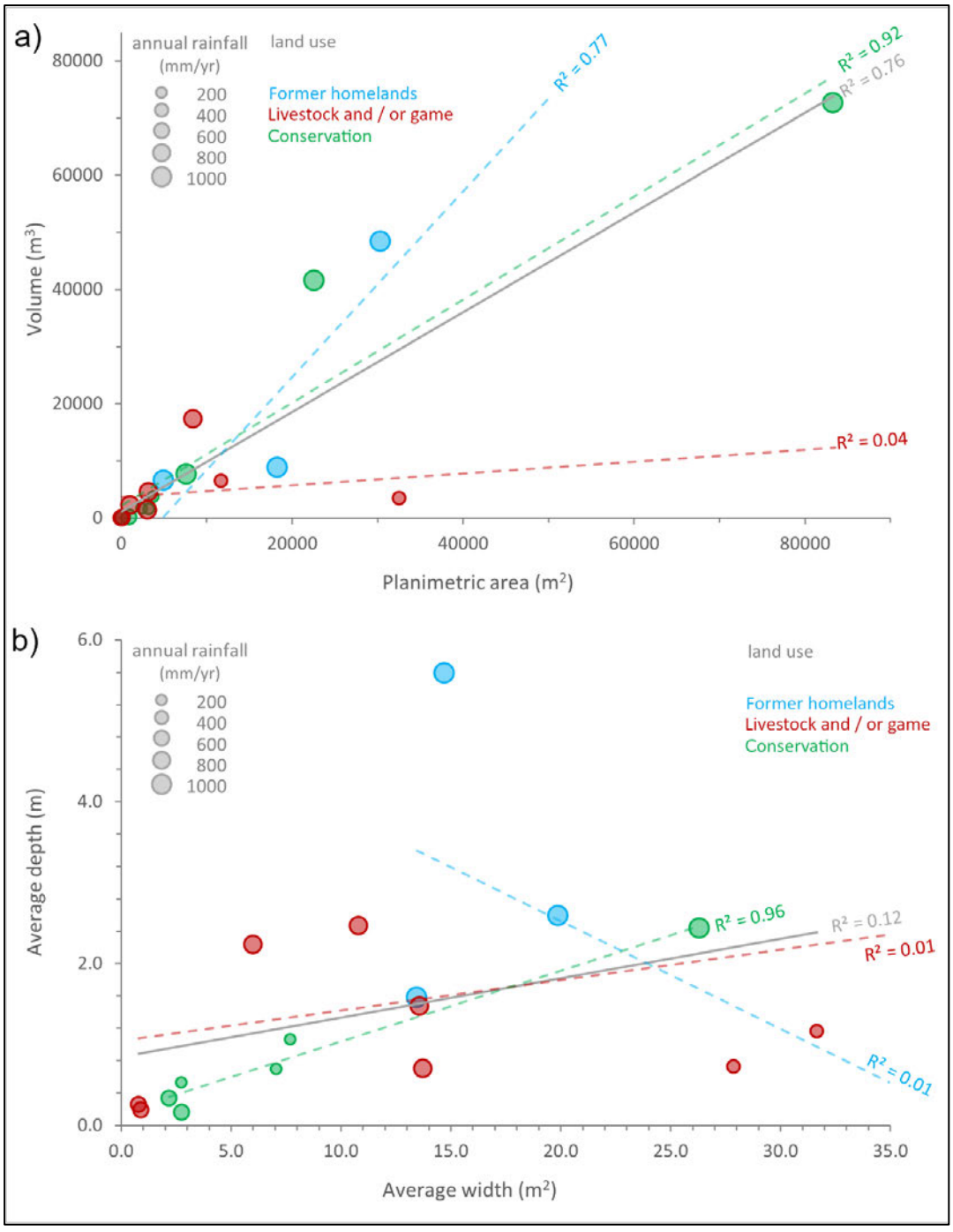

Figure 5.12 Relationship between volume and planimetric areas of the gullies with land use denoted by colour and points scaled according to Mean Annual Rainfall: a) gully volume and area relationship; and b) average gully depth (volume divided by planimetric area) and average width (planimetric area divided by length) relationship. Dashed coloured lines indicate trends for individual land uses. The solid grey trendline represents all datapoints, i.e., all land uses combined.

5.4.2.2 Gully change characteristics and severity

All the gully sites, except Mushroom NS and Mushroom E-W, which had the shortest temporal scale (11 years), showed a change in the classification metric from Figure 5.5 when comparing the oldest with the most recent imagery. Only four gully sites were initially classified as being located in natural vegetation, all of which were transformed into another land use by the most recent image. Land use changed at 14 of the 19 gully sites: At six sites livestock and/ or game land use changed to conservation, and four sites each from the cultivated and natural vegetation classes were transformed into livestock and/ or game land use. Seven linear gullies expanded into a dendritic planform shape, which is the main planform shape (68.4%).

Average linear retreat varied from a contraction of -0.2 m y^{-1} to an extension of 30.3 m y^{-1} with a mean of 5.4 m y^{-1} (Table 5.6). The average planimetric areal growth per meter linear growth ranged from 0.8 m^2 y^{-1} to 45.4 m^2 y^{-1} with a mean of 13.5 m^2 y^{-1}. The gullies that showed no linear expansion and retraction continued to exhibit an average planimetric area of up to 76.5 m^2. The mean planimetric areal retreat was 104.1 m^2 y^{-1} with a maximum rate of 620.4 m^2 y^{-1}. The ratio between the average volumetric retreat and planimetric areal growth (mean of 1.2 m^3 y^{-1}) was significantly lower than the length and areal growth. The average volumetric retreat ranged between 0.1 m^3 y^{-1} and 540.7 m^3 y^{-1}, with a mean of 108.6 m^3 y^{-1}. The average planimetric area to length ratio for growth rates is 18.8. Considering planimetric areal retreat and volumetric growth, there is a general increasing trend from west to east, which tapers off towards the northeast in Limpopo.

Average soil loss rate per unit area ranged from 0 t ha^{-1} y^{-1} to 17.0 t ha^{-1} y^{-1}, with a mean of 5.5 t ha^{-1} y^{-1} (Figure 5.12). However, the gully erosion soil loss rate was not evenly distributed across South Africa, suggesting a trend similar to areal and volumetric growth, which generally increased from west to east while tapering off towards the northeast in Limpopo. Contractions occurred at two gully sites (BushW N and BushW S), both of which were situated in Limpopo. Erosion rates were primarily stable in the Western Cape (average soil loss between 0.4 t ha^{-1} y^{-1} to 1.1 t ha^{-1} y^{-1}) and Limpopo (average soil loss variation between 0 t ha^{-1} y^{-1} to 1.7 t ha^{-1} y^{-1}). An increase in gully erosion severity to the medium and high classification occurred eastwards toward central South Africa with soil loss rates varying between 0.4 t ha^{-1} y^{-1} and 17.0 t ha^{-1} y^{-1} at the Eastern Cape and Free State sites.

Author	Location † x	y	Province	Survey method	Duration of survey (y)†	1930	1935	1940	1945	1950	1955	1960	1965	1970	1975	1980	1985	1990	1995	2000	2005	2010	2015	2020	2022	Average soil loss (t ha^{-1} y^{-1}
Olivier *et al*., 2019 [5]	18.764	-33.282	WC	Field, aerial	17 (2000-2017)																					0.0
Meadows, 2003	18.870	-33.352	WC	Aerial	61 (1938-1989)																					
Bergpad	20.626	-33.730	WC	Field, aerial	78 (1944-2022)											0.3							0.8	0.6		0.4
Bumpy Track	20.626	-33.727	WC	Field, aerial	78 (1944-2022)											0.8							3.5	2.3		1.1
Skietdam	20.648	-33.751	WC	Field, aerial	72 (1944-2016)											0.4							0.9			0.4
Schmiedel et al., 2017	19.070	-31.260	NC	Field, aerial	51 (1960-2011)																					3.0
Keay-Bright and Boardman, 200	24.545	-31.743	EC	Aerial	57 (1945-2002)																					
Rooiflip	24.581	-32.151	EC	Field, aerial	13 (2009-2022)																	0.3		0.6		0.4
Humpsback	24.601	-32.145	EC	Field, aerial	77 (1945-2022)											2.7							6.8	7.5		3.4
Favis-Mortlock *et al*., 2018 [5]	24.617	-31.617	EC	Field	16 (2001-2018)																					82.4
Marker, 1988	26.815	-32.770	EC	Aerial	38 (1949-1987)																					
Kakembo and Rowntree, 2003	27.113	-33.201	EC	Aerial	50 (1938-1988)																					
Vetter, 2007	27.490	-30.500	EC	Aerial	45 (1950-1995)																					
Dollar and Rowntree, 1995	27.870	-30.840	EC	Field, aerial	39 (1952-1991)																					
Sakhut	28.296	-30.841	EC	Field, aerial	63 (1952-2015)					5.5						6.5						3.5				6.2
Trickle Main W	28.604	-31.140	EC	Field, aerial	74 (1948-2022)											7.4						24.0		9.5		9.0
Trickle Main E	28.635	-31.124	EC	Field, aerial	74 (1948-2022)											13.6						28.3		13.2		14.8
Le Roux, 2018	28.567	-31.083	EC	Aerial	5 (2007-2012)																					
Seutloali *et al*., 2017	28.675	-31.546	EC	Aerial	26 (1984-2010)																					
Contour game NS	28.353	-28.621	FS	Field, aerial	46 (1969-2015)										9.9			14.0				6.9				12.0
Contour game EW	28.355	-28.619	FS	Field, aerial	46 (1969-2015)										2.6			-0.1				12.6				1.8
Mushroom NS	28.427	-28.558	FS	Field, aerial	11 (2011-2022)																	36.8		5.7		17.0
Mushroom EW	28.429	-28.556	FS	Field, aerial	11 (2011-2022)																	5.7		1.5		3.0
Brady, 1993	28.625	-28.533	FS	Field, aerial	32 (1952-1991)																					
Golden 2	28.646	-28.510	FS	Field, aerial	47 (1970-2017)										20.9			14.6		16.8		8.0				15.8
Golden 1E	28.650	-28.510	FS	Field, aerial	55 (1962-2017)								19.1		11.8			7.2			17.4	15.4				12.2

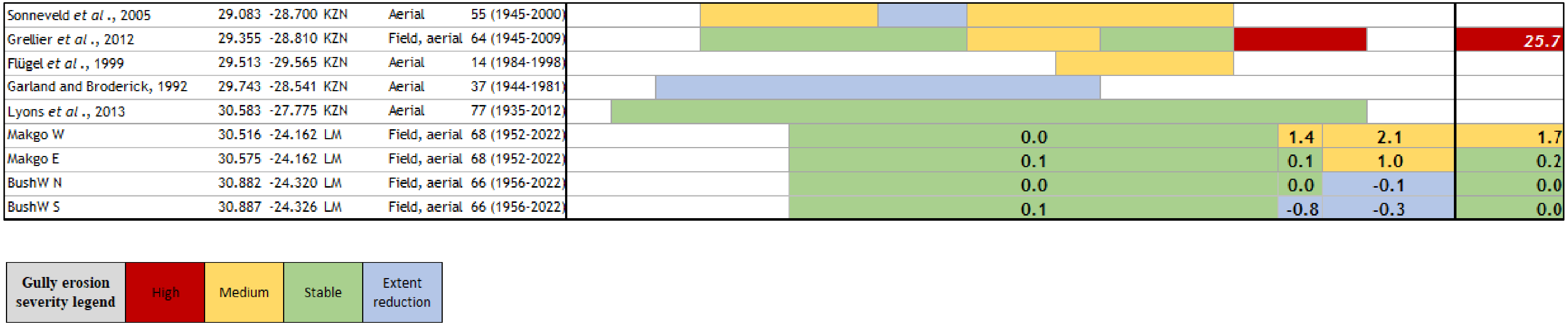

† Locations are grouped by province and then listed according to their longitude..
‡ The survey time may differ compared to Table 5.6 because areal digitising was not always conducted on the earliest image due to lack of gully wall definition.
§ These studies formed part of a longer-term project with multiple publications; only the most recent publication was listed.

Figure 5.13 Gully evolution in South Africa for medium (>5 years) and long term (>10 years) studies (after Castillo & Gómez, 2016, Figure 8 and Chapter 2, Figure 2.9). Gully erosion severity is shown in tons per hectare per year in bold, while also colour coded according to severity (soil loss rates obtained from published data extracted during the literature review of Chapter 2 are provided in a white font, while primary data is provided in black font). WC denotes Western Cape, EC Eastern Cape, FS Free State, KZN KwaZulu-Natal, and LM Limpopo.

5.4.2.3 Isolating climate

The GG2 site was excluded from the dataset used in the correlation analysis. The reason for the exclusion was due to the outlier values it produced, both in terms of dimension and erosion rates, but also due to dual land use that is still currently being employed. Although GG2 is now within the confines of a national park and thus classified as a conservation land use, subsistence grazing is still allowed at the site.

Considering all the data points, gully dimensions in terms of length, planimetric area, volume, and gully density show a poor exponential correlation with significant scatter and a low R^2 ranging between 0.02 and 0.38 (Figure 5.14). Subdividing according to land use increases the exponential correlation for conservation land use (although not for length) up to an R^2 of 0.80 (Figure 5.14b, c, d). Despite the apparent increase in R^2, the exponential model remains weak due to scatter around the trend line. No significant improvement is associated with the livestock and/ or game land use category, except for an increase in R^2 for the gully planimetric area (Figure 5.14b). Due to the lack of data points spread through MAR categories, no trend can be detected for the communal land use in former homeland areas. The lack of correlation between MAR and gully dimensions shows that there is no simplistic explanation for gully dimensions and density using MAR as the climatic variable. However, a non-linear trend is noticeable when considering all the data points. Gully dimensions fluctuate according to MAR in an approximately polynomial trend, which generally increases from 200 mm y^{-1} to 400 mm y^{-1}, whereafter it decreases to 600 mm y^{-1}, with a subsequent increase towards 1000 mm y^{-1}.

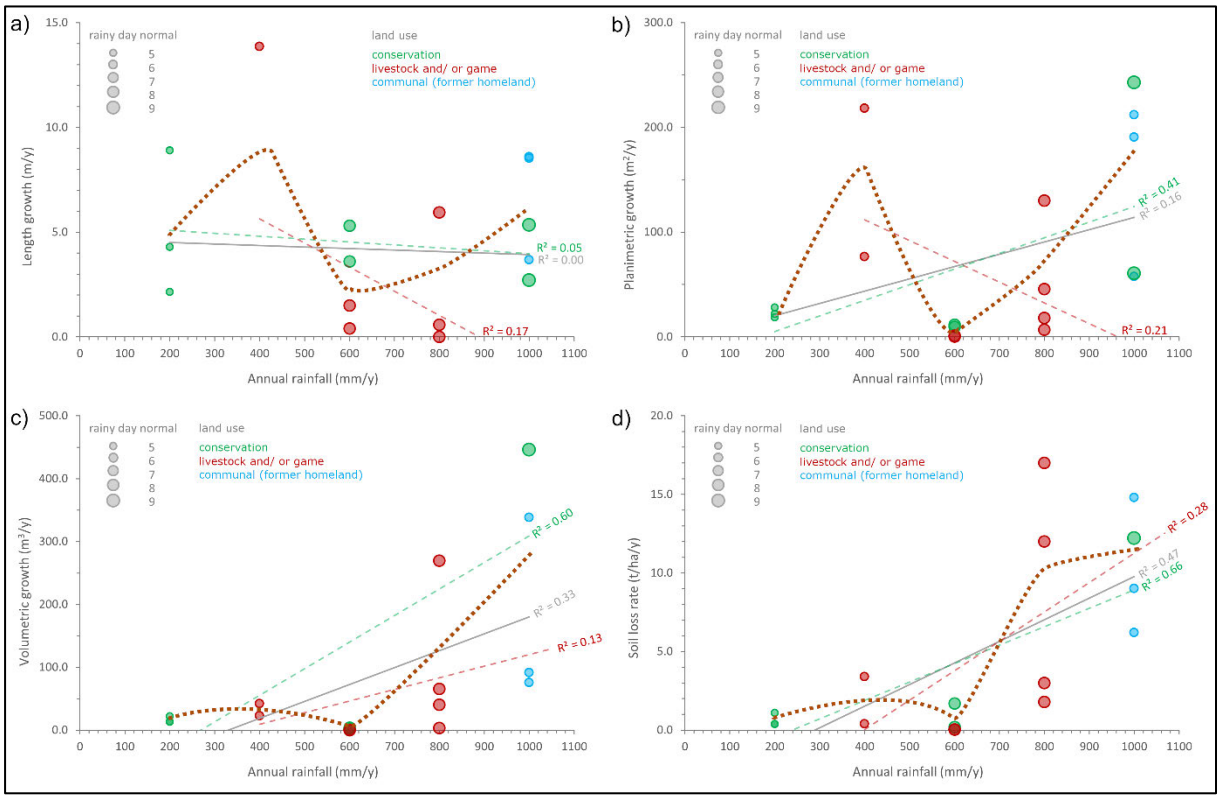

Figure 5.14 Relationships between mean annual rainfall and gully dimensions, *viz*., a) length; b) planimtric area; c) volumentric area; d) and gully density (calculated by dividing gully planimetric area (m^2) by gully catchment area (km^2)). The scatter plot markers are coloured according to land use. Trendlines are addded to show the exponential relationship between annual ainfall and all land uses (in grey), and according to specific land uses (coloured), except for communal as these are all in the same annual rainfall zone. Additionally, a brown dotted trendline are added to show the approximated polynomial trend.

Figure 5.15 shows the relationship of gully growth rates with climatic variables MAR (explanatory varibale on the x-axis) and RDN (as scaled markers). Considering all the data, a moderate exponential correlation is exhibited for volumetric growth and annual soil loss (Figure 5.15c, d). Despite the moderate R^2 between 0.33 and 0.47, the exponential model can be considered weak due to signifcant scatter around the trend line. When subdividing according to land use, the correlation of MAR remains moderate to poor for the game and/ or livestock category. Regarding the conservation land use, a stronger positive correlation is observed, explaining between 47% and 66% of variance within the data. Nevertheless, a exponential model remains weak, as is evident from the data scatter. However, a similar non-linear trend emerges for gully growth rates compared to gully dimensions (Figure 5.14), *viz*., growth rates generally increase initially up to 400 mm yr^{-1}, after which they decrease towards 600 mm yr^{-1}, followed by an increase towards 1000 mm yr^{-1}.

The markers in Figure 5.15 are scaled according to RDN. Although RDN generally increases along the E-W gradient, thus following an increase in MAR, there is significant variance in the RDN data showing no distinct trend. For RDN values between five and six, growth rates are lower for conservation land use than for the communal and livestock and/or game land uses. Livestock and/ or game and the former homelands show an average linear growth rate of 3.3 and 6.7 times and volumetric growth rates of 2.5 and 10.4 times, respectively, compared to conservation areas. Conversely, considering the same land use classification of conservation and the former homelands in the 1000 mm y^{-1} MAR classification, conservation areas generally exhibit more considerable growth and soil loss rates, although the communal areas have an RDN 1.5 times lower than the conservation land use.

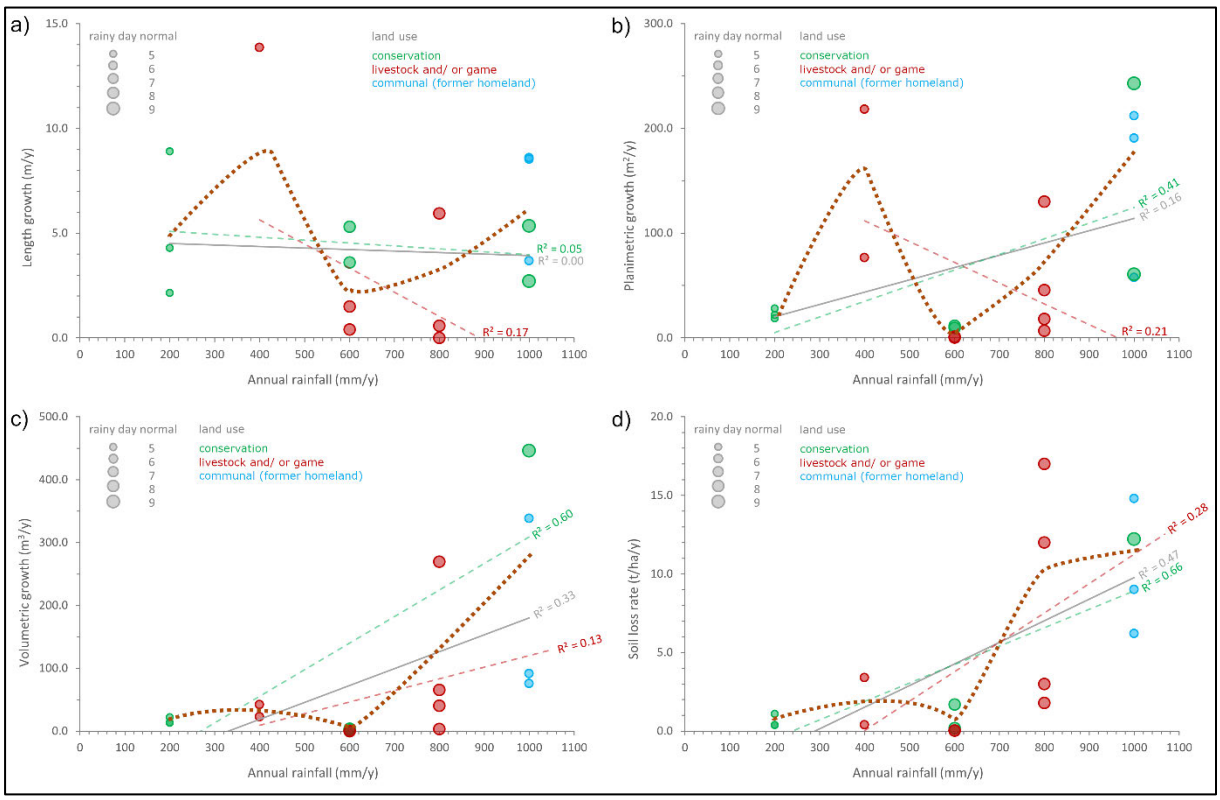

Figure 5.15 Correlation between mean annual rainfall and Rainy Day Normal with gully erosion rates consisting of: a) linear growth; b) planimetric growth; c) volumetric growth; and d) annual soil loss rate normalised to ha. The scatter plot markers are coloured according to land use and scaled according Rainy Day Normal. Trendlines are addded to show the exponential relationship between annual ainfall and all land uses (in grey), and according to specific land uses (coloured), except for communal as these are all in the same annual rainfall zone. Additionally, a brown dotted trendline are added to show the approximated polynomial trend.

Climate was identified as a driver of current and past gully erosion by participants at 64% of the gully sites where the complete triangulation of methods was implemented (Table 5.7). The climate variables associated with past and contemporary gullying are the cyclical nature of rainfall and high-intensity events. Participants from Bumpy Track and Bergpad in the lower MAR gully sites (200 mm and 400 mm) indicated that cyclicity and magnitude of rainfall function conjointly. During drought cycles, the vegetation that acts as a protective barrier reduces. When significant rainfall events occur after a drought, gully expansion or new gully formation occurs. This effect is compounded by growth sensitivity of vegetation types, which inhibits the revegetation of bare patches. At the Trickle Main E and W gully sites, gully erosion was associated with large-magnitude events only. Participants state that large volumes of water concentrate and cause large erosion scars in the lowlands. Climate change was not identified as a causative factor of past or contemporary gully initiation or expansion, but it was mentioned as a future concern, which could result in gully erosion due to the higher intensity storms forecasted.

Table 5.7 Drivers of gully erosion obtained from local knowledge of participants.

Placename	MAR zone	Climatic drivers			Land use drivers						Physical drivers	Observations by researcher
		Intense rainfall	Cyclical rainfall variance	Climate change†	Overgrazing	Animal tracks	Grazing on abandoned cultivated land	Roads	Fire	Land use change	Slope	Additional drivers observed from field work (*other notes*)
Bergpad	200	X	X	X				X				
Bumpy Track	200	X	X	X				X				
Skietdam	200	X	X	X								Kraaling (historical)
Humpsback	400	X	X		X	X		X§				
Rooiflip	400	X	X		X‡						X	
Trickle Main W	1000	X						X	X (wild)			Soil (dispersive, piping), animal tracks; *large gullies (some tributary) in proximity*
Trickle Main E	1000	X					X	X	X (wild, regime)		X	Soil (dispersive, piping), animal tracks; *large gullies (some tributary) in proximity*
Makgo W	600			X	X	X						
Makgo E	600			X	X	X						
BushW N	600									X		
BushW S	600									X		

† Climate change explicitly was not identified as a past or contemporary driver, but as a future driver of gully erosion by participants

‡ The grazing of game was specifically outlined as their patterns cannot be controlled

§ Associated with ox wagon routes at various colonial settler treks and with newly built tar roads and culverts

5.4.2.4 Isolating land use

Figures 5.14 and 5.15 show no apparent trend between land use classifications. No clear clustering of specific land uses above or below other classifications regarding dimensions or growth rates is discernable. Additionally, there is a significant scatter between the same land use classifications, some of which are in proximity, for the same MAR classification. Notably, the gully density for conservation land use and communal areas in the former homelands are comparable, although the former homelands have lower magnitude RDN values.

Although the quantitative data revealed no clear correlation with gully dimensions or growth rates, participants associated land use drivers with gully erosion at all the sites where the complete triangulation of methods was implemented (Table 5.7). Roads and overgrazing were identified as the primary drivers in the land use category. The placement of roads and the impervious surface resulting in concentrating overland flow was mainly associated with gully erosion. Additionally, road culverts were identified as driving gully erosion immediately downstream of their outlets. Overgrazing was not only associated with livestock but also specifically game farming. At the Makgo E and W gully sites, overgrazing by zebra expressly was noted as a cause of gully erosion. At the Rooiflip gully site, game in general, were regarded as a cause of gullying since their grazing patterns are challenging to manage in terms of rotation.

5.4.2.5 Mitigation measures

Efforts to mitigate expansion were observed at numerous sites (Table 5.4). In two locations, i.e., BushW N and S, this reversed the gully extent (Figure 5.13). In other locations, however, abandonment of mitigation works has yielded an increase in the severity of gully erosion (for example, Countour game NS and Trickle Main E; Figure 5.13)

Active remediation works are continually undertaken at eight sites (Table 5.4). Remediation works primarily targeted gully headcuts, inserting gabions or constructing earth walls to act as barriers. The remediation efforts align with the output from the participatory maps, on which the most prone areas to gullying were identified at the gully headcuts. However, little remediation attention is given to the inner gully channel area (except for two sites that adopted brush filling), and no attention is paid to locations upstream of the gully headcuts or walls. The timing of all remediation works is uncertain, but at Bergpad and Bumpy Track sites, the participants indicated that “most of

the work is done reactively". However, their aim is to understand gullying better to evolve into more proactive remediation strategies. Current efforts involve the implementation of gabions at gully headcuts, but a high failure rate currently exists. Due to failure, the road, which was initially straight, had to be rounded further in subsequent decades due to gully expansion underneath or around gabions.

At Humpsback, a holistic grazing strategy (high intensity, short duration) is advocated to reduce gully erosion as the participants have heard of positive experiences with this approach. Participants were also able to provide reasons and timing of remediation measures, for example, in the Karoo, a government initiative was launched in the 1950s that provided subsidies enabling the implementation of extensive anti-erosion works. Although it helped to improve the veld (open, uncultivated field), where there used to be very little vegetation, the participants indicated that they could no longer undertake or maintain such works due to the monetary costs involved.

5.5 DISCUSSION

5.5.1 Using local study sites to inform regional gully erosion

Gully erosion in South Africa is complex, with different intensities and timings regarding (re)activity (and stabilisation) (Figure 5.12). Considering the variance in intensity and timing, controls are likely to be associated with local scale events, possibly at catchment management scale, instead of being driven by a singular global or regional event. Castillo & Gómez (2016) and Olivier et al. (2023a) made a similar observation and attributed the complexity of gully evolution to various drivers, including anthropogenic and climate, which may be active on a more local scale.

Considering the baseline erosion rate between 0.01 t ha^{-1} y^{-1} and 0.64 t ha^{-1} y^{-1} (Reinwarth et al., 2019) and a sustainable erosion rate calculated between 5 t ha^{-1} y^{-1} and 10 t ha^{-1} y^{-1} (McPhee & Smithen, 1984), gully erosion generally increases in severity, from a stable rate (below baseline erosion (< 0.4 t ha^{-1} y^{-1}), eastwards towards the Grasslands biome (reaching a severity above the sustainable erosion rate; (<14.8 t ha^{-1} y^{-1}), subsequently decreasing towards the northeast in Limpopo (mainly below the baseline rate). In the semi-arid Karoo at the Rooiflip and Humpback sites (near the sites of a long-term study by Boardman et al., 2003 in the Sneeuberg), the landscape is transitioning to a more badlands topography evident from terrain in proximity to gullies (and inter-gullied area between closely spaced, parallel gullies), becoming hummocky with little

vegetation. Boardman et al. (2003) described similar badlands terrain, with an average soil loss rate of 82.4 t ha-1 y-1 (Favis-Mortlock et al., 2018) compared to our 0.4 t ha-1 y-1 to 3.4 t ha-1 y-1 measured rate. The lower rate measured does, however, conform with the outlook of Keay-Bright & Boardman (2006) and Rowntree (2014), who demonstrated that older valley bottom gullies on the Karoo have primarily stabilised since initial onset in the second quarter of the 1800's and beginning of the1900's. Despite having a lower erosion rate, it may increase if the transition to badlands continues due to gully and rill erosion at these two sites.

In the Grasslands biome, we had sites near those studies by Brady (1993), in a conservation land use, and Grellier et al. (2012), in communal grazing land use. At the Golden 1E and 2 sites (conservation land use), the erosion rate were calculated above the sustainable rate of erosion in South Africa (12.2 t ha^{-1} y^{-1} to 15.8 t ha^{-1} y^{-1}; like the outlook of Brady, (1993)). Similar gully erosion severity was calculated in the communal grazing areas in the former homelands (<14.8 t ha^{-1} y^{-1}), but not at the same soil loss severity as Grellier et al. (2012). Our data therefore contrasts findings in literature, which indicates that land in the former homelands is more degraded compared to other land uses (Hoffman & Todd, 2000; Mararakanye & Le Roux 2012). This contrast may relate to the focus on singular gullies, which in the Grasslands biome show similar erosion rate potential (Langbein & Schumm, 1958). When augmenting our rates with frequency from field observations and trends from Mararakanye and Le Roux (2012), the degradation of land from gullying in communal grazing areas can be considered significantly more severe compared to conservation land use.

Moving northeast towards the Savanna biome in Limpopo, gully erosion stabilizes, mainly exhibiting erosion rates below the baseline threshold of South Africa. The observed gully erosion trends in this study thus generally conform to a regional gully susceptibility model (Olivier et al., 2023b) and a manually derived gully map of South Africa, if one considers gully density as a surrogate for gully severity (Mararakanye & Le Roux, 2012).

Although the gullies that we investigated in the Karoo and the Grasslands biomes are primarily rectangular, soil loss rates were more severe in the Grasslands biome (above the sustainable threshold). Observations in the field showed that sub-surface processes were a dominant process driving gully erosion in the Grasslands, compared to overland flow in the more arid Karoo and Limpopo. These observations coupled with the high erosion rates suggests that gullying is more severe in areas with sub-surface erosion processes (similar deduction from Faulkner, 2013 and

articles therein), accentuating the need for mitigation measures here. Since the primary process driving gully erosion is associated with subsurface processes (Beckedahl, 1996), mitigation strategies need to be specifically adapted, as commonly applied methods to promote infiltration could reinforce sub-surface erosion in dispersive soils (Van Zijl & Ellis, 2013). Establishing vegetation that can reduce free water in the subsoil will likely be crucial to mitigating gullying. The importance of vegetative cover in mitigation works is well documented, and recent reviews have shown that establishing vegetation is critical to the successful long-term rehabilitation of gullies (Bartley et al., 2020).

Although gully erosion rates are low in the Karoo, exhibiting a stable outlook (primarily below he baseline rate), we would also argue for mitigation measures to be implemented here. Continued gullying may promote badland development, which could increase erosion by 3 orders of magnitude when considering rates from Favis-Mortlock et al. (2018). Once the landscape evolves into a badland, recovery of rangeland in the Karoo would take many decades (Dickie & Parsons, 2012) and likely require significant soil and water conservation works. Without these works, vegetation may become confined to the proximity of gully channels and its deposition zones (to some extent this is occurring at Humpsback, with tree coverage contained to gully channels), where water is rapidly directed to and subsequently evacuated from hillslope.

5.5.2 Disentangling climatic drivers

When isolating climate as a control of gully erosion, gully sites GG1 E and W, which exhibited the highest annual rainfall (MAR=1000 mm y^{-1}) and RDN (8.8), constituted larger gully dimensions and rates. However, when the other gully sites in lower MAR regions are incorporated, the correlation with RDN disappears. The lack of correlation contrasts with findings from Vanmaercke et al. (2016), who found a significant correlation ($R^2 = 0.47$) between RDN and global gully headcut retreat rates (n = 724). Since RDN is a function of MAR, variance in rainfall erosivity defined as RDN is likely to be low (Garland 1995 and Laker, 2004) due to low MAR exhibited in South Africa (91% of the country is classified as drylands; Hoffman & Todd, 2000). Considering MAR explicitly, an approximated polynomial trend becomes evident for gully dimensions and rates (Figures 5.14, 5.15). The trend shows three inclinations, with gully erosion increasing from 200 mm y^{-1} towards 400 mm y^{-1}, decreasing towards 600 mm y^{-1}, whereafter it increases again towards higher MAR of 1000 mm y^{-1}. The small gully dimensions and low growth rates in the 600 mm y^{-1} MAR class are associated with the Savanna biome, as vegetation cover likely forms a

protective barrier for soil from rainfall. This trend converges with Ohmori (1983) (in Mishra et al., 2019) and Walling & Kleo (1979) (in Thomas et al., 2018), which is attributed to vegetative cover (Walling & Kleo, 1979). At lower MAR (< 400 mm/yr), the vegetation cover is too sparse to offer protection against erosion, and at higher MAR (> 600 mm/yr) the excess rainfall can overcome the vegetation's resistance again.

This observation is supported by the qualitative data since conversations with participants suggest a similar trend. Participants in the lower and higher MAR categories specifically identified rainfall (and rainfall variance) to gullying. In the lower MAR regions (200 mm y^{-1} to 400 mm y^{-1}), participants associated gully erosion with rainfall intensity and variance. The low MAR would mask intensity in terms of RDN, and would also, especially during low rainfall periods or drought, result in vegetation decay. A high-magnitude rainfall event could trigger renewed gullying without the protective vegetative cover. In the 1000 mm y^{-1} MAR class, participants associated gully erosion with large rainfall events, not necessarily intense, but in volume, thus not associating rainfall variance as a driver. The data from participants corroborate a fluctuating polynomial trend resulting from quantitative data and indirectly links vegetation decay *via* rainfall variability to gully erosion in the lower MAR classes (Langbein & Schumm, 1958). However, the polynomial trend increases after 600 mm y^{-1}, dissimilar to Langbein & Schumm (1958). The increase in gully erosion is likely due to a lack of tree canopy cover as these sites are situated in the Grassland biome, unlike change to forested areas identified by Langbein & Schumm (1958). Additionally, land use practices may also influence the increase in vegetation removal, exposing soil vulnerability to erode due to increase in concentrated overland flow or the deterioration of soil structure due to the loss in organic matter (Laker, 2004; Frankl et al., 2019).

5.5.3 Disentangling land use drivers

Comparing the gully dimensions and rates does not deliver a clear pattern, *viz*., specific land uses do not cluster at larger dimensions or rates than others. Additionally, there is a significant spread between data points for similar land uses in the same MAR category. However, there are some contrasts (and similarities) between explicit land use activities within each category.

Roads were identified as a causal factor for gully erosion by participants from all land use categories. Roads are impervious surfaces that result in concentrated water flow. Culverts that divert concentrated water into rangelands have been demonstrated to cause gully erosion

(Beckedahl & Dardis, 1988; Seutloali et al., 2016). Mainly, culverts were associated with gullying (for example, Humpsback, Trickle W and E). However, the orientation of inherited roads was also identified as a driver of gully erosion at Bumpy Track and Bergpad. At these two conservation sites, dirt roads are orientated up and down the slope, resulting in a gully capturing a road and causing the subsequent diversion of the road as the gully expands.

Participants from livestock and/ or gaming and conservation land uses, identified overgrazing as a driver of historical and contemporary gully erosion. At Makgo W and E, overgrazing was associated with zebra populations, while likely also being affected by preferential grazing of game that cannot be managed (as acknowledged at Rooiflip). Historical overgrazing was recognized as a contributor to gully erosion along trekboer routes (Table 5.7), which is aligned with findings from different authors investigating gully erosion in the Karoo (Boardman et al., 2003; Keay-Bright & Boardman, 2007; Rowntree, 2013). At the sites where overgrazing was identified as a driver, cattle tracks were mostly identified as a contributor to gullying. Animal tracks augment gully development by compacting soil, resulting in retarded vegetative growth and an increase in concentrated overland flow, initiating gullying (Hudec et al., 2005) as new channels or perpendicular tributary channels caused by animals moving through gullies.

Contrastingly, overgrazing and cattle tracks were not identified as a driver of gully erosion in communal grazing sites, despite literature recognising the critical role that overgrazing has played in communal areas to gully erosion (Liggit & Fincham, 1989; Dollar & Rowntree, 1995; Le Roux & Sumner 2012; Mararakanye & Le Roux, 2012; Grellier et al., 2012; Ebhuoma et al., 2023). Instead, participants from the Trickle E site indicated that livestock numbers were appropriate, and that erosion was caused when communal graziers moved livestock to the lower valley when cultivation stopped. Gullies would therefore initiate on these discarded fields, subsequently retreating up slope. Abandoned cultivated lands in communal areas have been linked with gully erosion (Kakembo & Rowntree, 2003). A combination of overgrazing, some of which occurred on abandoned cultivated lands, would have led to severe gullying since Trickle E and W are both situated in an area where the soil is prone to erosion due to its duplex and dispersive properties (observation in the field; soil derived from mudstones and shales of lithologies demonstrated to be susceptible to gully erosion (Laker, 2004). Overgrazing reduces vegetation, thus removing its protective “barrier” in addition to its organic matter, exposing its inherent vulnerability to erosion from rainfall (Laker, 2004). Le Roux et al. (2022) maintained that overgrazing was a factor that

led to the formation of the largest reported gully in literature, which is in proximity to the Trickle E and W sites, due to its small upslope drainage area. Pathways, both in terms of human and livestock were also observed as augmenting gully erosion. It is also worth noting that even though lithology and soil have been identified as a critical driver of erosion in South Africa (Rienks et al., 2000; Laker, 2004; Olivier et al., 2023a), no participants identified either as a driver. Participants not naming soil as an underlying factor could be due to a potential lack of awareness of variance in soil susceptibilities across sites, due to challenges around identifying specific types of soils as problems soils, or because soils were not perceived as a main driver of gully erosion.

Due to the impact of gully erosion, present and past mitigation works were located at gully sites of all land uses to stabilize gullying. However, the soil and water conservation works were at different states when visiting gully sites during fieldwork. At the conservation land use sites, mitigation works were ongoing.

Current active mitigation works at the conservation sites (Bergpad and Bumpy Track sites), and the Rooiflip site (livestock and/ or game) focus on the gully headcut. The focus of their efforts conforms to their susceptibility maps created during the participatory mapping exercises, but also due to road infrastructure being threatened by gully headcut retreat at Bergpad and Bumpy Track. The gabions (Bumpy Track and Bergpad) and retaining walls (Skietdam) implemented had a high failure rate, as was evident from sagging gabions and gullies eroding around the installed measures. Although gully severity is likely perceived more severe where incision and soil loss scars originate, compared to areas flow accumulation upstream of the headcut or at gully walls, effectiveness of mitigation measures would likely increase if strategies included applying measures to the hillslope, upstream of gully headcuts, and within gully channels to trap sediment (as per Bartley et al., 2020 and Frankl et al., 2021; BushW N and S also showed gully extent reductions due to brushfill barriers along gully channels). Observed mitigation works in the Karoo currently solely relies on structural works, but long-term efficacy has been closely related to the revegetation of gullies (Bartley et al., 2020). However, reestablishing vegetation in the Karoo sites (Bumpy Track, Bergpad, and Skietbaan) are tenuous as demonstrated by Keay-Bright & Boardman (2007). Further strategies should therefore be sought to achieve revegetation within and in proximity of gully channels in the semi-arid Karoo, to reduce gullying and deter terrain evolving into badlands.

Although active mitigation is ongoing at certain sites (as per above), the cessation thereof has also occurred due to monetary and staffing shortcomings (Humpsback site), apprehension to tackle gully erosion (Trickle W and E sites) or being determined irrelevant due to land use change (Contour NS and E-W sites). The non-maintenance of soil and conservation work (such as at Humpsback, Trickle W and E, Contour NS and E-W sites) has been identified as a driver of gully erosion and land degradation (Kakembo & Rowntree, 2003; Vetter et al., 2007; Bosino et al., 2021), and it, therefore, could become an important future driver of gully erosion in South Africa. Meadows (2003) and Wilkinson et al. (2023) demonstrated and discussed how gully erosion was reduced due to the application of governmental aid. However, without these funding structures, the maintenance of mitigation measures can become unsustainable (Schmiedel et al., 2017).

Participants from the communal grazing land use (Trickle E and W) indicated their willingness to partake in and maintain any mitigation efforts but were apprehensive about initiating measures as they were unsure what strategies to implement. Subsurface processes were observed in the field, indicating that commonly applied procedures, such as check dams that slow water and promote infiltration may exacerbate gullying (Van Zijl & Ellis, 2013), except if additional measures are taken such as the installation of inert geomembranes (Frankl et al., 2016). Subsidies would likely be needed to rehabilitate gullies in the communal grazing areas successfully, but we would argue that these subsidies should be supplemented by knowledgeable persons facilitating mitigation efforts, who are able to blend their experience in mitigation works with learning from and applying local knowledge. Using community-based approaches and including local knowledge will yield better trust relationships and deliver strategies that would be readily acceptable, enhancing cooperative activeness in measures and, thus, long-term success (Peterson et al., 2018). Additionally, learning from previous failures and successes and providing insight into the usefulness of local vegetation species would increase the likelihood of successfully reducing gully erosion.

5.5.4 Environmental change implications

Although numerous sites were selected across the E-W climate gradient of South Africa, the dataset remains limited, influencing the ability to disentangle the role of land use and climate more exhaustively. More sites are required to confirm trends and draw more rigorous conclusions. Nonetheless, even with this limited dataset, we can provide some insight into the potential impact of environmental change on gully erosion in South Africa.

Regarding climate change, gully erosion is expected to increase due to increased rainfall erosivity. Current climate change scenarios for South Africa predict similar MAR but with fewer and more intense rainfall events. Our data shows no clear relationship between RDN and gully erosion across the sample sites. We could assume that this increase in intensity on its own may not considerably influence gully erosion. However, the dual effect of an increase in rainfall intensity with rainfall variability is likely to intensify gully erosion. Rainfall variability has been demonstrated to induce gullying in South Africa, with heavy rainfall after drought being identified as an important driver both in the academic literature (Dollar & Rowntree, 1995; Sonneveld et al., 2005), as well as by participants in semi-arid Karoo. Since 1920, there has been a tendency towards cyclical droughts (Malherbe et al., 2016), which will leave soil susceptible to gully erosion if intense rainfall returns after vegetation decay. The cyclical droughts are associated with El Niño Southern Oscillation (ENSO) (Anderson et al., 2021), and although the extent to which climate change impacts ENSO is still being debated, specific models using high CO_2 scenarios predict an increase in ENSO, which could exacerbate gully erosion further (Yeh et al., 2009; Singh et al., 2022).

The Karoo and Grasslands biomes will likely be significantly impacted in these scenarios. The Karoo is an area where vegetation survival is already tenuous (Midgley et al., 2008). Under drier scenarios, vegetation cover will be weakened, inducing gully erosion. Additionally, gully mitigation from reintroducing vegetation is unlikely due to the harsh Karoo climatic conditions (Keay-Bright & Boardman, 2007). Climate variability in the Grasslands can contribute to succulent and bush encroachment (Midgley et al., 20008), which has been associated with the degradation of grasslands (Belayneh & Tessema, 2017). Although the Savanna biome showed stable gully conditions at our sites, if bush and succulent encroachment leads to weakened grass cover, susceptible soils could be left vulnerable to more intense rainfall, increasing gully incidence and severity (Grellier et al., 2012). The impact may be most significant in the communal grazing areas of the former homelands, where grasslands are already degraded, and large gully systems are already found close to each other. These gullies may rapidly expand, in addition to form further tributaries, if the soil is exposed to rainfall.

Regarding land use, gully erosion has been associated with past land use changes, intensification of farming, and land tenure (Castillo & Gómez, 2016; Olivier et al., 2023a). Although severely degraded land is commonly associated with communal land tenure in the former homelands (Hoffman & Todd, 2000; Kakembo & Rowntree, 2003; Vetter et al., 2006; Mararakanye &

Sumner, 2017), no significant trend is apparent in our data points. Notably, gully dimensions and growth rates are comparable for conservation and communal land use in former homelands for similar climatic variables (Figure 5.13, 5.14, 5.15). However, this may be related to sample selection (see section 5.4.4). One could argue that if RDN in the communal gully sites (RDN of 5.7 to 5.9; 1000 mm y^{-1} MAR) increases to the same category of the conservation land use (RDN of 8.8; 1000 mm y^{-1} MAR), it might translate into an increase in severity since RDN may seemingly impact gully erosion in higher MAR regions. Therefore, an easy deduction could be that conservation land use converted to communal grazing or inherited land reform farms may increase gullying with current climate change forecasts predicting higher intensity rainfall events. Care should, however, be taken with such assumptions since if managed adequately by local traditional institutions, communal grazing can be successful, especially in catchments with less prone preconditions (identified by Watson, 2000), as demonstrated by Bennett et al. (2012).

A more acceptable deduction could be that the cessation of maintenance of soil and water conservation works could yield severe gully erosion. At the Contour NS gully site (livestock and/ or game), land use has changed from crops to game farming, resulting in the maintenance of the ploughed contours becoming unnecessary. Since the change, contours have been breached, and gully erosion increased in severity (Figure 5.12), while the adjacent field, which is still under crop with contour banks being maintained, has seen no gullies evolving. Olivier et al. (2019) and Bosino et al (2021) also observed the increase in gully erosion due to the non-maintenance of ploughed contour banks. Similarly, participants at the (communal) Sakhut gully site indicated severe gully erosion started once fields under crops (with contour banks) were abandoned. Land abandonment, particularly in South Africa, has been strongly associated with gully erosion (Kakembo & Rowntree, 2003; Vetter, 2007). Once the abandoned land becomes severely eroded, natural vegetative regrowth that could yield a more stable phase of erosion, is tenuous (Kakembo and Rowntree, 2003), except if appropriate long-term management strategies such as the removal of herbivores, are adhered to (Palmer & Bennett, 2013). Land use changes from arable lands to other land use may induce gully erosion or increase, if associated soil and conservation works are not managed adequately.

Even in land use change to conservation areas, gully erosion remains stubborn, for example, Bergpad and Bumpy Track sites in the Karoo where gullies are continuing to breach gabions situated at gully headcuts damaging roads, or at GG1 E in the Grassland biome where gabions in

the lower main gully section have had negligible impact on the expansion of upper tributaries and the establishment of new channels. The continuing erosion may be part of inherited problems from earlier land uses, but it can also be a sign of a particular lag time between effective land management change and gully stabilization. Therefore, land use changes to a conservation-orientated approach that aims to rehabilitate and mitigate gully erosion using small-scale adaptations may not necessarily have an immediate impact on gully evolution, and long-term strategies, monitoring, and maintenance remain critical.

5.5.5 Limitations and future recommendations

Due to time constraints and increased travel costs after COVID-19, fieldwork at gully sites was limited, resulting in a relatively small sample size, especially for gully sites within the communal grazing land use, which are all situated in the Eastern Cape. Additional research is required to increase sites across the E-W climate gradient (including arable land uses) to disentangle the climate and land use drivers more rigorously. Additionally, the improved spread of sites could be used to ascertain whether current mitigation strategies will be efficient in a changing climate and land use.

With the current data points, it remains challenging to disentangle land use and climatic drivers of gully erosion from variables completely. Soils and the lithology from which they are derived were not identified by any participants as a driver of gully erosion but have nonetheless been shown to be a critical driver thereof in South Africa (Rienks et al., 2000; Laker, 2004; Le Roux & Sumner, 2012; Olivier et al., 2023a). Palmer and Bennett (2013) illustrate the impact of different lithologies on land degradation by showing contrasting degradation severity in two adjacent catchments under the same communal tenure management regimes for >70 years. Soils derived from mudrock and shales in the Karoo basin, especially the Elliot formation and the Adelaide and Tarkastad subgroups, are prone to erosion due to their textural and dispersive properties (Laker, 2004). Subsurface erosion is often reported in these soils, resulting in large gully formations near each other (Le Roux et al., 2022). Piping subsequently causes gullies to extend linearly and laterally (Brady, 1993), form perpendicular tributary gully channels due to collapsed pipes (Le Roux et al., 2022), and form discontinuous gully channels that are parallel to the established gully (Beckedahl & Dardis, 1988; Figure 5.1e).

Due to the aim of this research to conduct research in many study sites to cover the different landuse/climate combinations, only limited time could be spent at each site. Consequently, the relatively short time per site, there were challenges around building trust relationships. In sites where no previous connections existed, gatekeepers were identified. This was particularly relevant in the context of game reserves and communal rangeland areas. For example, one gatekeeper, a non-governmental organization (NGO) aiding the local community with managing rangeland and resources, was approached to facilitate fieldwork in the Tsitsa catchment. Due to the continued presence of the NGO in the community, the hope was also that mistrust would be alleviated.

To a certain extent, this was achieved as headmen and community members conversed about gully erosion issues. However, the decision of focus groups not consenting to audio recordings likely indicates a level of remaining apprehension by the participants. It is also important to acknowledge that the NGO staff also helped with translations, and their presence during the focus group discussions may have influenced responses since the NGO is actively involved with managing conservation efforts within the community. The NGO determined access to gully sites, mostly focusing on sites that were easy to access, i.e., that were convenient to reach. The authors' pre-identified sites were deemed inaccessible due to damage to gravel roads. The "convenience" sample, limited time to conduct measurements, and difficulty climbing into the gullies resulted in the non-measurement of the more extensive gullies, which are prominent in the area. The "convenience" sample was compared to the most extensive gullies in the conservation land use in the same MAR classification, which may add uncertainty with regards to resultant interpretations. Adding additional gully sites at both locations would improve characteristic representation.

Gatekeepers, however, also facilitated additional beneficial outcomes. In the Karoo, a conservation team allowed gully walks at our preselected sites, ensuring our safekeeping from predatory animals that preside there. After semi-structured interviews, we were invited to inspect additional gullies that were deemed of concern and different typologies. Although time constraints did not allow quantification, our measurement technique was demonstrated, hopefully resulting in future community-based participatory research collaborations.

In the Free State, no gatekeepers were used to facilitate access to gully sites nor participants. The additional absence of prior acquaintances led to land access problems. None of the preselected sites were visited, and sites were found via a contact made at the accommodation (previously a farmer in the area) and a few "cold calls". The time spent finding suitable sites led to fewer sites

being visited and allowed less time per gully site. The combined impact of searching for sites and having less time per gully site led to a loss of capability to complete the triangulation of methods. Due to the relatively ad-hoc nature of identifying possible sites, there was not enough time to prepare base maps that were crucial to the participatory discussion and mapping, and landowners could not plan their time to partake in qualitative assessment.

Recommendations for future research are to include more gully sites, most essentially to add cultivated sites across the E-W climate gradient, but also adding more sites in communal grazing areas which experience a different MAR, with similar management strategies. We would also recommend having a longer lead-up time, potentially being in communication prior to arrival in the field, or spending more time on-site, allowing us to build a stronger relationship and trust. An additional benefit of being in dialogue with participants prior arrival, would be that gully sites can be formally selected prior arrival (whether identified by the researcher, the participants due to the gully posing problems and being of concern, or a combination), ensuring that base maps are printed and ready for use upon arrival at sites. In our experience, having the base maps was crucial to having good discussions and completing the triangulation of methods as described in the methodology section. Enabling participants to identify gully sites may prove beneficial as it they may identify prominent gullies that are of concern (potentially more representative of the gully typologies in the area) and provide better discussion. An additional step that could be investigated could be how to limit time (while still maintaining accuracy) to conduct gully measurements, in our case with a measuring tape and staff. It could be useful to spend more time discussing gully erosion with participants, while measuring gullies in field quickly (even if this leads to more processing time post-field work), for example, with UAV photogrammetric or structure for motion techniques (see Hout et al., 2020; Koci et al., 2017).

5.6 CONCLUSION

Gully erosion is a severe land degradation process with substantial on- and off-site impacts. Although gully erosion is expected to increase due to climate change, little is known about how environmental change will impact gully networks. We selected various gully sites across the E-W climate gradient of South Africa to use local sites to inform on gully erosion regionally, but also to isolate climate and land use to identify how changes to these drivers may induce gullying or alter severity.

Local findings agree with regional assessments of gully erosion and previous studies in similar areas. Gully erosion is stable in the west, becoming more prevalent and severe towards central South Africa. Although our dataset is limited, initial deductions regarding climate and land use change can be made. The rainfall intensity increases from climate change may not increase gullying as a sole driver, but when in conjunction with an increase in rainfall variability, and hence possibly more frequent drought scenarios, gully erosion would be exacerbated. The Karoo and Grasslands biomes may be most affected by this cyclical drought-induced gullying.

Land use change was more difficult to disentangle from our dataset due to the scatter variance from livestock and/ or game land use. However, land use change from arable lands to livestock-orientated land use points toward an increase in gully erosion, especially if anti-erosion works are not maintained. Currently, the former homeland areas show some of the highest gully erosion dimensions and rates, suggesting that a change from another land use to communal grazing may promote gully erosion if land capability is not accounted for and proper support systems and communal management structures are lacking.

Further research into environmental change is required, and this study could be enhanced by adding more sites across the E-W gradient, especially arable lands.

CHAPTER 6: CONCLUDING REMARKS

6.1 INTRODUCTION

Gully erosion represents a type of water-driven land degradation that manifests both on-site through the erosion of soil and off-site through the transportation of soil and often detrimental substances like pesticides downstream within the catchment area (Valentin et al., 2005; Shellberg, 2016). Given prevailing climate change projections, a heightened occurrence of gully erosion is expected concur with the predicted increase in high intensity rainfall events, leading to escalating environmental, socio-economic, and sustainability challenges.

The need exists to identify appropriate mitigation measures that would tolerate more intense rainfall events. Additionally, improving approaches to gully erosion modelling can provide a better understanding of how gully networks on catchment to regional scales may evolve in future under different climate conditions. However, our modelling capability is still lacking predictive accuracy (Poesen, 2018). Furthermore, collecting data on the location and activity of gullies would significantly enhance our capacity to comprehend the influence of various controlling factors on gully formation. This, in turn, would bolster our capability to construct accurate gully models and pinpoint effective mitigation strategies. Implementing new remote sensing technologies will be essential, especially on regional scales and long-time-series (> 15 years), as it would highlight the varying interaction of control factors with gully erosion in contrasting environments (Vanmaercke et al., 2021). Augmenting remote sensing studies with detailed field data, such as identifying dominant processes, time of expansion, and susceptibility towards gullying, remains important and could address gaps in the remotely sensed datasets (Castillo & Gómez, 2016).

Given all of the above, a general aim was consequently established to conduct gully analysis on a regional scale (in this study a national scale), with the focus on developing methods for regional assessments and using quantitative and qualitative methodologies to address the impact of environmental change on gullying. This has led to the following research questions:

1. What is the current level of scientific understanding regarding gully erosion in South Africa, along with the spatial scope of the areas under study?

2. Is it possible to model gully erosion susceptibility on a regional scale, with limited data availability, which can also be validated at the same scale?

3. Would it be possible to develop a gully detection strategy that is built on limited data input and easily understandable metrics, but remains scalable and transferable to enable use by practitioners?

4. How will gully erosion react to environmental change?

5. What is the land-user and landowner perceptions of gully erosion, and how does it align with findings from remotely sensed data and field observations?

Five research objectives were set to answer these questions:

1. Use local study sites to inform on gully erosion over large geographic extents.

2. Synthesise gully erosion works in South Africa to intersect views to allow a better understanding of the current state of research in South Africa and to identify broader and local knowledge gaps.

3. Obtain regional datasets regarding gully control factors, to develop and produce a gully susceptibility model for South Africa.

4. Develop and implement a semi-automatic detection method for South Africa and test it at different geomorphic scales and geo-environments.

5. Identify sites across the E-W climate gradient of South Africa to isolate land use and climate as drivers of gully erosion, to assess gullying quantitatively and qualitatively to identify possible environmental change impacts.

This concluding chapter will firstly investigate how well the research questions were addressed by the objectives (Section 6.2), then secondly, highlight the novelty and contribution to the gully erosion body of knowledge (Section 6.3), thirdly note the limitations of the study (Section 6.4), and lastly, provide recommendations for future research (Section 6.5).

6.2 A SYNTHESIS AND REFLECTIVE ASSESSMENT

6.2.1 What is the current level of scientific understanding regarding gully erosion in South Africa, along with the spatial scope of the areas under study?

Google Scholar and Scopus were used as search engines to retrieve works on gully erosion in South Africa to review gully erosion systematically for South Africa (Objective 2; Chapter 2, 3). The database of published research was divided into separate sections: 1) DONGA papers, for all work that explicitly investigated gully erosion, viz., being the (or part of) primary aim, 2) EXTERRA papers, which addressed a broader scope but provided relevant contextual information.

Local case study sites were identified (n =60; x, y coordinates were used as input for Objective 2 and 3; Chapter 2, 3) to inform on gully controls and the severity thereof (Objective 1). Additionally, the study aims were separated in categories relating to study type, and methodologies were captured to analyse the frequency and evolution of study types since 1988. Lastly, the academic background of the first author was noted, to assess in which academic domain gully erosion studies were primarily being conducted, and whether this background impacts on the factors hypothesised to influence gullying.

Study sites were sparse, primarily clustered in particular areas, for example, the Sneeuberg, Tsitsa, and Swartland. However, some inferences regarding gully erosion could be derived regionally (Objective 1). Gullies were found at various stages of evolution and exhibited different temporal timings regarding stabilising and (re)activating. Western South Africa shows a stabilising trend, with gully extent reductions noted in the Swartland. In the central Karoo, gullies were found to be mostly stabilising. However, badlands associated with gullies continued to produce significantly higher soil loss (> 123 t ha^{-1} y^{-1}) than the sustainable soil tolerance of 5 t ha^{-1} y^{-1} to 10 t ha^{-1} y^{-1} and a natural baseline calculated as 0.01 t ha^{-1} y^{-1} to 0.64 t ha^{-1} y^{-1}. Towards the central parts of South Africa, in the Free State and the eastern parts of the Eastern Cape, gullying continued to be active. In the Tsitsa, in the former homelands, gullying remains severely active, plotting in the upper quartile compared to global data. In terms of the Free State, the active gully erosion processes were identified in proximity to the Drakensberg, which exhibits a contrasting topography compared to the central to western Free State, which has a significantly flatter topography (Mararakanye & Le Roux, 2012). Further eastwards, towards KwaZulu-Natal, gullies were found to be stable, and in some instances, show a reduction in planimetric extent (Chapter 5). Although there is an interplay

between control factors involved in gullying in South Africa, the impact of human activities to accelerate gully erosion cannot be overlooked and is a primary cause driving gully erosion.

Newer technologies are being merged with gully erosion research, with nearly 60% of investigations using remotely sensed data. Similar to the insights provided by Laker (2004), most gully erosion studies are still being investigated by researchers situated within the geography domain, although findings regarding causes of gullying seem not to be influenced by academic background. Investigations into c*ausal factors, processes, and impacts* remain dominant, although most studies are short-term (< 5 years). Studies about the quantification of soil loss remain scarce, with ten sites located in only three prominent locations, viz., semi-arid Mediterranean climate (n = 2; located in the winter rainfall season in the Fynbos biome, in the Swartland and Namakwaland, respectively), Sneeuberg (n =5; all in proximity found in the Nama Karoo biome with a very late summer rainfall season), and close to Potshini (n = 3, all in proximity found in the Grassland biome exhibiting a Mid-summer rainfall season).

6.2.2 Is it possible to model gully erosion susceptibility on a regional scale, with limited datasets?

Yes.

The local case study sites identified in South Africa (n = 60, through achieving Objective 2 in Chapter 2) were used as training data points to model gully susceptibility on a regional scale; in this case, it can be termed a national scale (Objectives 1 and 3; Chapter 3). A frequency ratio statistic was used to train points, thus correlating control variables with gullying. In the literature, five broad categories were found to be the main control factors of gullying (as identified for Objective 2 in Chapter 2): topography, soil, geology, climate, and anthropogenic activities. Seven datasets were used to represent these categories: slope for topography, general soil classes to represent soil, generalised rock type for geology, aridity and RDN (a rainfall intensity proxy that has shown good correlation with gully headcut retreat in Vanmaercke et al., 2016) to constitute climate, and lastly, land-use/-cover to represent contemporary anthropogenic activities, and historical agricultural zonal map to provide a historical component to anthropogenic activities. Gully activity for each local case study site was classified according to stable (1), active (1.5), and very active (2) and used as a scaled multiplier for the correlated variable statistics. A weighted overlay procedure was conducted with the conditioned control factor maps, according to a weight

obtained by aggregating causal control variables hypothesised to induce gullying in South Africa (obtained during Objective 2; Chapter 2). The output was quantitatively validated using a published dataset consisting of 163019 manually mapped gullies (Mararakanye & Le Roux, 2012). Additionally, a 1 km^2 tessellation coverage grid was created for South Africa, from which digitising gullies retrieved primary data for nine randomly selected tessellated polygons.

According to the gully susceptibility output, 1.8% of South Africa is classified as very highly susceptible to gullying, and 12.0% is highly susceptible. Gully susceptibility is, however, not evenly spread across South Africa and exhibits a general increasing trend from the western parts of the country towards the east, towards KwaZulu-Natal. The Eastern Cape and KwaZulu-Natal had the highest gully susceptibility. Although a large portion of the Northern Cape is classified as the Karoo, which had considerable proportions of moderate susceptibility, this region is predicted to have the lowest susceptibility to gullying. Regarding validation, the model performed better in areas where the study site was located, with poorer performance in understudied regions. Still, the model performed better than a random classification model. For 160952 gullies from the Mararakanye & Le Roux (2012) dataset (2067 gullies were omitted due to being in "No Data" areas), 79.8% were mapped with a moderate to very high susceptibility when implementing a zonal average for each gully. A general increasing trend was observed for gully density with increasing susceptibility in the tessellated polygons.

6.2.3 Would it be possible to develop a gully detection strategy that is built on limited data input and easily understandable metrics, but remains scalable and transferable to enable use by practitioners?

Yes.

A gully is a distinct landform, typically an elongated linear feature that exhibits an active headcut and short steep slopes, bordering a gully floor that has a similar slope to the terrain in which it is located. A DEM is thus ideally suited for extracting gullies through its morphology. A workflow that combined traditional raster-based processes with object-based image analysis was followed, using a DEM as the sole input to semi-automate the mapping of gully features (Objective 4; Chapter 4).

The foundation of the workflow rests upon using HAND to normalise the DEM along the thalweg of the gully channel (which is assigned a zero value). The normalised DEM enables more accessible threshold settings, as thresholds take on similar values to depth measurements in the field, while it also helps to detect short steep slopes without having to calculate statistics from size-defined moving windows. The gHAND workflow was rigorously tested on gullies exhibiting different geomorphic scales in the Tsitsa catchment of South Africa, using a 2 m DEM (Objective 1; Chapter 4). Additionally, the transferability of gHAND was assessed by implementing it in contrasting geo-environments spanning three continents where DEMs of different source origins and spatial resolutions had to be used as input (Objective 1; Chapter 4).

The gHAND workflow returned accuracy metrics similar to those in published literature, albeit towards the upper accuracy range. In terms of scalability, the gHAND workflow predicted >75.4% of the gullied area correctly for small- (planimetric area of 1619 m^2) to large-scale (planimetric area of 70246 m^2) gullies. The gHAND workflow produced an over-estimation error of <16.1% in conjunction with the correctly mapped gully area at a small- to large-scale geomorphic range. At the colossus scale (planimetric area of 425404 m^2), detection decay did occur due to landform complexity and scale. Regarding transferability, gHAND performed similarly to benchmark methods developed explicitly for the gullies found in the study areas (variance between 1.4% to 14.8%; user and producer accuracies above 84.5% and 70.6%.). The performance of gHAND mainly improved with spatial resolution and accuracy of the DEM.

6.2.4 How will gully erosion react to environmental change?

Local case study sites (n = 19) were selected across the E-W climate gradient of South Africa to inform on gully erosion severity on a regional scale (Objective 1; Chapter 5), in addition to isolating climatic and regional drivers of gullying (Objective 5; Chapter 5). Regarding informing about gully erosion on a regional scale, findings converge with regional assessments of South Africa (for example, Mararakanye & Le Roux, 2012, De Geeter et al., 2022; Olivier et al., 2023b). In addition, similar timings and gully rates were found compared to other studies that were in proximity to the 19 selected sites. Regarding current severity, there is a generally increasing trend towards the eastern Grasslands.

Although central South Africa is currently the primary concern regarding gully erosion, increasing rainfall intensity and possible different timings may reactivate currently stable gullies in South

Africa (Meadows, 2003). Chapter 5 tries to isolate rainfall as a driver of gullying in South Africa to assess how climate change may impact its evolution. Unlike Vanmaercke et al. (2016), who found a close correlation with RDN, this study's data aligned more with MAR than RDN at the 19 sites under investigation. Thus, the empirical model Vanmaercke et al. (2016) established with RDN and used to show high expected gully retreat rates globally under climate change prediction is likely an unsuitable model for South African conditions. Instead, rainfall variability, as suggested by Laker (2004), and cyclical droughts that are often associated with ENSO (Malherbe et al., 2016), may be the dominant driver of gullying. Intense rainfall events post-drought could rapidly expand gullying. According to the MAR trend, areas likely to experience an increase in gully severity will be the Karoo, where MAR between 0 mm y^{-1} to 400 mm y^{-1} is received, and the Grasslands biome, where rainfall upwards of 600 mm y^{-1} is experienced. If climate change increases the frequency of ENSO events (Yeh et al., 2009; Singh et al., 2022), gully erosion severity will be exacerbated even more.

It was challenging to disentangle the impact of land use change on future gully erosion from our 19 sites, especially since arable areas were unaccounted for. However, from interviews at the Sakhut site and temporal analysis from the Contour game NS site, it is evident that changing arable land to livestock and/ or game land uses, whether commercial or communal, may have adverse gully erosion implications. The impact of gully erosion may be more severe if the arable fields had erosion mitigation works (such as contour banks) that are not maintained after the land use change has occurred.

Gully erosion is prevalent in the former homeland areas, as found in this study but also in previous works (Hoffman & Todd, 2000; Vetter et al., 2006; Mararakanye & Sumner, 2017), and an easily admissible deduction could be that any land use change to communal land tenure will aggravate gully erosion. However, a whole suite of control factors and political policies need to be accounted for to explain the eroded landscape in the former homelands, and more data points are required to assess how a land use change to communal tenure or peasant small-hold farming may influence gully erosion in future areas. Furthermore, there has been evidence of the (cost) effectiveness of erosion control measures in such communal land use settings (Morokong & Blignaut, 2019).

6.2.5 What is the land-user and landowner perceptions of gully erosion, and how does it align with findings from remotely sensed data and fieldwork observations?

Of the 19 gully sites, semi-structured interviews with local land users and/or landowners were conducted at 14 sites, gully walks were made at seven locations, and participatory mapping exercises were carried out at four sites. Gully erosion was considered a problem at all sites, except at the BushW N, BushW S, and Humpback gully sites. Results from the temporal and fieldwork analyses are in agreement with the participant assessment at the two BushW sites, calculating 0 t ha^{-1} y^{-1} soil loss from gullying.

At the Karoo sites, except for Humpsback, participants from the conservation and livestock and / or game land use sites indicated concern for gullying. Indeed, active gully processes were observed at these sites, although the soil loss thresholds were below the sustainability thresholds for South Africa. From a sustainability perspective, there is disagreement between the primary data retrieved and the landowner's perception. However, at Bergpad and Bumpy Track, the gullies are threatening infrastructure. With the aid of the participants, the temporal aerial images were used in conjunction with the gully walk to identify an old road now captured by a gully. Subsequent road renewals were made to round the gully. Gabion installation to mitigate gullying and protect roads are unsuccessful. In this sense, gully erosion is a major problem, and their perception is thus accurate, albeit not in an environmentally sustainability sense (Chapter 2). At Rooiflip, measurements were focused upstream on renewed gullies, as the measurement means were inadequate to capture downstream gully elements where it is transitioning into a badlands-type landscape. The participant perception is therefore vindicated by Boardman et al. (2010), whose sites were also in the Sneeuberg area, and found gullies to be mostly stable, but badlands to have a soil loss of up to 123 t ha^{-1} y^{-1} (Favis-Mortlock et al., 2018). Perceptions of the landowner/ -user participants regarding severity mainly aligned with findings from remotely sensed data and field measurements and observations in all land uses. Participant perceptions regarding gully erosion drivers varied, with overgrazing and cattle tracks (or pathways in general) not being perceived as a driver of gully erosion in the communal grazing areas of the former homelands despite indications from previous literature and field observations (regarding tracks) that it has been critical to the removal of vegetation which would have enhanced gullying. Other factors such as fires (wild and regime), intense rainfall, and steep slopes were recognised as drivers gully erosion due to it resulting in an increase in concentrated flow; livestock could have been overlooked due to its importance in

communal areas (both socially and economically), although this would require further analysis especially regarding stock quantities and management structures. Contrastingly, the causes of gully erosion from conservation areas and commercial livestock and/ or game land uses mainly aligned with field deductions.

In a few sites, mitigation measures were in place and actively maintained, with new strategies implemented. The placement of mitigation measures was aligned with the participatory maps, in which concerns of gullying were marked at gully headcuts in all instances. Mitigation measures included reducing water flow or protecting the soil at gully headcuts. All the methods consisted of earthen works or gabion installations. Although Frankl et al. (2021) and Bartley et al. (2020) showed that establishing vegetation is critical to gully mitigation, it has yet to be used as a strategy, or at least not at any of the 19 investigated sites. It must be acknowledged that some of these sites are situated in the Karoo. In this area, rainfall variability makes it very unlikely for new vegetation to sprout in badland and gullied areas (Keay-Bright & Boardman, 2007). Additionally, gullies are widening more than they are retreating, which may be disconcerting given the strategies implemented.

At five sites, participants indicated they are somewhat embarrassed regarding the gullied extent on their land (rather than the gullies being problematic as such). At two of these sites, soil loss from gullying was below the reported maximum baseline erosion threshold of 0.64 t ha^{-1} y^{-1}, showing that reflections may be hyper-critical. As Wilkinson et al. (2023) stated, the socio-economic impact on regional communities, including land managers feelings of humiliation due to being labelled poor land managers, should be addressed, and in South Africa this need would be valuable to pursue.

6.3 NOVELTY AND CONTRIBUTION TO CURRENT STATE OF SCIENCE

This thesis is written in manuscript style. Each chapter contributes a novel approach and is thus contributing to broader gully erosion research. However, holistically, the body of work can potentially be regarded as a novel perspective on how to tackle the investigation of gully erosion on a regional scale.

Regarding the individual chapters, in Chapter 3, a gully erosion susceptibility model was developed. A weighted overlay procedure was linked with frequency ratio statistics. Neither of

these methods is new and has been used previously to model gully susceptibility (Rahmati et al., 2016; Arabameri et al., 2018, 2019; Domazetović et al., 2019; Makaya et al., 2019). However, modelling gully erosion susceptibility at a regional scale, including the validation thereof, remains scarce (De Geeter et al., 2023). The reason for the smaller geographic footprints could be data related, although a significant reason could be the requirement of a gully inventory. The gully inventory is often divided into a training dataset and a test or validation set, for example, a 70 to 30 split whereby 70% percent of digitised gullies are used for training and the remaining 30% for validation, as employed by Arabimeri et al. (2018). Although applying a gully susceptibility model to such a large geographic extent is rare, novelty is primarily associated with using literature as a directive to model it. Firstly, case studies were identified in the literature to use its location to correlate gully control variables, and secondly, literature learning was used to feed input into the model. Although the validation at regional scale is complex, and no one validation technique is perfect, a triple validation process was implemented, which used an existing published dataset in two different ways (generating gully susceptibility statistics for each gully and testing against random) and generated primary data from randomly selected tessellation grid. The model performed adequately and aligns with other metrics employed to inform on degradation and erosion susceptibility, viz., RUSLE-derived soil erosion risk map (Le Roux et al., 2008) a degradation assessment based on interviews and workshops (Hoffman & Todd, 2000), and a continental-scale gully erosion risk map calculated for Africa (De Geeter et al., 2023).

In Chapter 4, a semi-automated gully mapping strategy was developed. Finding gully occurrence and monitoring gullies in susceptible areas on regional scales may yield higher learning potential when compared to conducting studies on a local scale only. Although manual mapping was used in the past, gully inventories showing gully occurrence on regional scales are rare (Le Roux and Mararakanye, 2012) and are unlikely to be repeated. Even if repeated, comparing the datasets will have inherent uncertainties due to user interpretations and bias when manually digitising (Vanmaercke et al., 2021). Semi-automated methods can eliminate these uncertainties whilst they also enable rapidly mapping gullies at larger geographic scales. Numerous semi-automated methods have been proposed, primarily using topographic data (Brecheisen and Richter, 2021; Castillo et al., 2014), spectral data (d'Oleire-Oltmanns et al., 2014; Vrieling et al., 2007), or a combination of the aforementioned (Shruthi et al., 2011). For a semi-automated detection technique to be applied on a regional scale, it needs to be transferable, i.e., it needs to successfully map gullies in different geo-environmental conditions, and scalable, viz., it is able to map gullies

at different scales. Rarely are any of these methods, irrespective of data input, tested outside the region of development. A possible explanation could be associated with detection issues when applied at different geomorphic gully scales or transferring to a different geo-environment. Methods using spectral data as input will likely hinder transferability due to the difference in vegetation cover and mosaic of cover types found within a gully. Methods using topographic information may experience accuracy decay when applied to different geomorphic scales, as they often use the detection of local topographic differences calculated from moving windows. The gHAND method is novel, as it uses a normalised DEM, according to HAND, which allows threshold inputs like those measured in the field. Importantly, the normalisation of the DEM provides a way to detect gully landform elements without needing a search window. Additionally, contrasting to previously published methods, the method was rigorously tested on gullies with different geomorphic scales and gullies located in dissimilar geo-environments. The developed method, gHAND, performed in the upper threshold of accuracy metrics when compared to published methods, for gullies with a planimetric area ranging from 1530.1 m^2 and 70246 m^2 (user and producer accuracies above 84.5% and 70.6% respectively). Additionally, gHAND provided similar performance (variance between 1.4% to 14.8%) compared to two benchmark methods (also in contrasting geo-environments in Spain and Namibia), that were explicitly developed for the gully types found at these locations.

A triangulation of methods (combining remotely sensed data, fieldwork consisting of observations and measurements, and interviews) was employed in Chapter 5 to investigate gully erosion. Other researchers investigating gullying on local scales have used a combination of the methods. However, the application of all three techniques for the same case study site remains limited (Wen et al., 2021). The study applies the rarely used triangulation of methods in South Africa. Still, its primary novelty is associated with the regional imprint focussed on attempting better to understand the impact of environmental change on gully erosion. Numerous sites were selected across the E-W climate gradient of South Africa to isolate climate and land use. The climate was isolated by selecting study locations with similar land uses in different climatic zones, whilst land use was isolated by selecting sites with contrasting land uses in relative proximity in the same climate zone.

Regarding the current dialogue on gully erosion internationally, there is a purpose of advancing gully erosion research by implementing newer technologies, especially for regional work (Vanmaercke et al., 2021, De Geeter et al., 2022). However, the need remains to extract reliable

fieldwork data to complement these technologies (Castillo & Gómez, 2016). Intertwining the findings from both approaches will ultimately yield a better understanding of how gully evolution is affected by control variables (Poesen, 2018), improving the aspiration to model gully erosion, which is still lacking, with modelling output being able to be calibrated and validated. Another aspect currently being debated in gully erosion research is to make research findings more impactful (Wilkinson et al., 2023). Results need to be of high quality to inform land managers how to mitigate gullying and to deploy strategies against gullying on an institutional level in land policies.

This study speaks to both described current topics. As individual elements, in Chapters 3 and 4, GIS capacity is implemented to assess gully erosion regionally (to identify susceptibility in Chapter 3 and potentially to map gully features semi-automatically in Chapter 4). In Chapter 5, local case studies are investigated in different geo-environments. The methodologies implemented are coherent, enhancing practicality, and the thesis workflow could be applied as a framework to investigate gully erosion regionally. The framework consists of, firstly, generating a gully susceptibility map on a regional scale. Secondly, using the susceptibility map constrains a semi-automated technique to determine critical areas. Lastly, collect in-depth field data to establish primary control variables and identify and implement rehabilitation methods.

6.4 LIMITATIONS OF THE STUDY

The here-presented study has several limitations which are being presented and discussed below. For the review process for Chapter 2, searches were limited to Google Scholar and Scopus. The search results may therefore have missed white papers and governmental research institutional reports. Furthermore, if the word “gully” was not in the title or keywords of a publication, as it may have had a different primary focus, for example, connectivity or sediment yield, it may have been overlooked.

Regarding modelling in Chapters 3 and 4, uncertainties were introduced due to the spatial resolution of datasets. Additionally, both models were dependent on manual user input; in the susceptibility model, gullies had to be identified and manually mapped, and for the detection, gully headcuts had to be manually digitised as a point feature. Although the gHAND workflow was tested on different geomorphic scales and in geo-environments, it was still conducted on an individual gully scale, as it is in the initial stages of development.

The fieldwork required for the triangulation of methods in Chapter 5 was pushed back during the project due to COVID-19, resulting in a much more limited time for conducting field analyses. In areas with known contacts, time was sufficient to visit the planned sites and work accordingly. Building relationships was complicated in regions where known contacts were absent, having a knock-on effect on land access. Site accessibility challenges forced the shifting of gully investigative locations on short notice, hence not allowing the temporal analysis to be conducted before visiting the site. Therefore, sometimes it was not possible to bring historical maps for interviews. In some cases, landowners were too busy to participate in the interview process. Additionally, the lack of drivability of some roads resulted in specifically pre-selected sites to being inaccessible, especially in the study area near Nqanqarhu, where maybe a Volkswagen Polo was not the vehicle of choice… The consequences of time pressure and access consequentially impacted sample size and distribution, making it difficult to thus far deconvolute the separate workings of climate and land use to determine the primary cause of gullying at each local study site.

In the field, measurement equipment failed! Or at least at a few places, but "'n boer maak 'n plan". Although testing the differential GPS prior to fieldwork showed it was functioning, it failed on the first day of fieldwork, possibly due to an internal battery failure. The positions of gully volume measurements were constrained by the use of a backup Garmin Etrex GPS, which has a more considerable accuracy error variance. GPS measurements were used in conjunction with field sketches to ensure accurate placement in a GIS environment. The dimensions of the large gullies, especially towards central South Africa, were underestimated, making it difficult, precarious, and time-consuming to make depth measurements with an extendable measurement staff.

In terms of scope, the initial intention was to conclude with modelling individual gullies, using the temporal data gained from Chapter 5 as calibration data to model environmental change. Unfortunately, interruptions from COVID-19 did not allow to complete this step within the timeframe of this thesis.

6.5 FUTURE RESEARCH RECOMMENDATIONS

The study started with a systematic review of the literature on gully erosion in South Africa. The review was focused on different terminology used for gullies in South Africa and was coupled with the country name in Google Scholar and Scopus. Fifty-three gully-specific publications were

retrieved from the search. As the literature was intersected, knowledge gaps were identified. Two geomorphic processes were identified that need further attention from South Africa. Firstly, the focus in South Africa has been on larger permanent gullies, with no research being published on ephemeral gully erosion. However, the smaller gullies on agricultural fields have been identified as a significant source of soil loss (Poesen et al., 2003). Secondly, in South Africa, piping has been noted to contribute to gullying (Le Roux et al., 2022), but works with piping as the primary focus remain scarce (Beckedahl, 1996). The sub-surface process has been demonstrated to play a significant role in initiating gully erosion processes (Bernatek-Jakiel & Poesen, 2018). These two geomorphic processes, i.e., ephemeral gully erosion and piping, need further research attention in South Africa.

Although 53 gully-specific publications were found, their geographic location remains nucleated to particular research areas, with numerous publications reporting updated findings from the original sites, for example, in the Sneeuberg (Boardman et al., 2003; Keay-Bright & Boardman, 2007; Boardman et al., 2015; Favis-Mortlock et al., 2018). A national gully inventory map was created by Mararakanye & Le Roux (2012), which has undoubtedly been an enormous and impressive achievement and remains essential. Still, this dataset is static and was conducted on a scale at which only large gullies would have been identified. To better gauge the extent of gully erosion in South Africa, more sites are required in areas not previously investigated and potentially not yet identified by the gully inventory map.

After study sites have been expanded to areas previously understudied, findings captured from these sites can be implemented towards the further development of the susceptibility map (introduced in Chapter 3) and deconvoluting the effects of climate and land use on gullying (Chapter 5). Regarding the susceptibility model, additional data points and their findings can be incorporated, which should improve modelling output by reducing uncertainties in areas where there are currently no study sites. There are also more immediate approaches in which the model could be further developed, viz., data-mining additional gully attributes such as morphology, connectivity, or mitigation measures, to incorporate into the model, and using a zonal approach to correlate gully control variables, instead of a singular point at the gully headcut. These additions should be tested to see whether it substantially improves the current susceptibility model.

The spatial resolution of datasets introduces uncertainties in the susceptibility model (Chapter 3) and the detection model (Chapter 4). Finer resolution datasets exist, although not at the regional

scale or at the local study sites that were investigated. Nevertheless, implementing finer resolution datasets into both these models should be investigated further. Findings from the gHAND method indicated that accuracy metrics improve with spatial resolution, and it would be worth testing to see if the 1 m DEM, derived from a similar method as the DEMSA-2, would yield higher detection accuracy. The gHAND model should also be expanded to map larger geographic footprints, such as on a catchment scale or in an area identified as highly susceptible.

The sensitivity of the susceptibility model (Chapter 3) towards climate and land use/ cover should be tested. Once completed, it could be useful to model different environmental change conditions to see how it would impact gully susceptibility on a regional scale. Moreover, it is critical to predict gully evolution and its associated expansion and soil loss, especially under environmental change conditions. Roberts et al. (2022) indicated that efforts to model gully erosion are still in their infancy, and long-term data is required in contrasting environments (such as Chapter 5) to be able to predict better how environmental change will exert change on gully erosion. Gully evolution models, such as CAESAR or SIBERIA, could yield insightful findings if calibrated to long-term datasets (as established in Chapter 5; and can potentially be furthered by the sequential use of gHAND in Chapter 4).

6.6 CONCLUSION

The general aim of this study was to investigate gully erosion on a regional scale and to develop and use tools to assess current severity, and to inform on possible future scenarios under environmental change conditions. The work hinges on two major novel elements. Firstly, local case studies were implemented to inform on regional gully erosion. Secondly, a scaled approach to investigate gully erosion was identified for regional gully analysis.

In the first instance, a gully susceptibility map was produced for South Africa using local case studies from the literature. Similarly, primary data was retrieved from a triangulation of methods at local case study sites across the E-W climate gradient of South Africa. Findings from the susceptibility map and the primary field data converge and agree with other regional assessments of South Africa.

A scaled approach for regional gully assessment was identified in the second instance. Although not part of the primary aim or objectives of this study, the sequence of work could provide a helpful

guideline for future regional works on gullying, which remains challenging. As an initial step, a gully susceptibility model could be used to identify areas of concern, where a detection strategy could be implemented to map actual gully extents, which are constrained to the areas of interest. The detected gullies could be used to identify representative gullies in areas of concern in which more expensive (time and labour costs) fieldwork could be initiated. Fieldwork can then use field measurement, observations, and interviews to inform on processes, severity, and implications.

Currently, in South Africa, gully erosion severity increases eastwards towards the Grassland biome. Although climate change is envisioned to affect gully erosion in South Africa, it cannot be attributed to rainfall intensity increases alone. Rainfall variability, which is closely associated with ENSO cycles and could increase in frequency due to climate change, will drive gullying in conjunction with intense rainfall after sustained periods of low rainfall. Gully erosion could become more severe in central South Africa, where it is more prevalent, but it could also reactivate stable gullies that have been mitigated. Continued work is required to investigate further the extent to which gully erosion will be exacerbated. Establishing models that can predict extent changes and identify areas of soil loss and deposition from gullying is critical to address concerns regarding increased gully erosion severity in South Africa.

REFERENCES

Abdulfatai IA, Okunlola IA, Akande WG, Momoh LO & Ibrahim KO 2014. Review of gully erosion in Nigeria: Causes, impacts and possible solutions. *Journal of Geosciences and Geomatics* 2(3), 125-129.

Abuzied SM & Pradhan B 2021. Hydro-geomorphic assessment of erosion intensity and sediment yield initiated debris-flow hazards at Wadi Dahab Watershed, Egypt. *Georisk: Assessment and Management of Risk for Engineered Systems and Geohazards 15*(3), 221-246.

Anderson RL, Rowntree KM & Le Roux JL 2021. An interrogation of research on the influence of rainfall on gully erosion. *Catena* 2016, 105482.

Arabameri A, Asadi Nalivan O, Chandra Pal S, Chakrabortty R, Saha A, Lee S, Pradhan B & Tien Bui D 2020. Novel machine learning approaches for modelling the gully erosion susceptibility. *Remote Sensing* 12(17), 2833.

Arabameri A, Pradhan B & Lombardo L 2019. Comparative assessment using boosted regression trees, binary logistic regression, frequency ratio and numerical risk factor for gully erosion susceptibility modelling. *Catena 183*, 104223.

Arabameri A, Pradhan B, Rezaei K & Conoscenti C 2019. Gully erosion susceptibility mapping using GIS-based multi-criteria decision analysis techniques. *Catena* 180, 282-297.

Arabameri A, Rezaei K, Pourghasemi HR, Lee S & Yamani M 2018. GIS-based gully erosion susceptibility mapping: a comparison among three data-driven models and AHP knowledge-based technique. *Environmental earth sciences 77*, 1-22.

Archer ER 2004. Beyond the "climate versus grazing" impasse: using remote sensing to investigate the effects of grazing system choice on vegetation cover in the eastern Karoo. *Journal of Arid Environments 57*(3), 381-408.

Avakoudjo J, Kouelo FA, Kindomihou VM, Akponikpe PI, Azontonde, AH, Sinsin BA, Akplo, TM & Agonvinon MS 2020. Water Erosion in the Donga Soils in Subhumid Zone in West Africa. *Journal of Environmental Protection* 11(12), 1073-1088.

Azedou A, Lahssini S, Khattabi A, Meliho M & Rifai N 2021. A Methodological Comparison of Three Models for Gully Erosion Susceptibility Mapping in the Rural Municipality of El Faid, Morocco). *Sustainability* 13(2), 682.

Bartley R, Hawdon A, Post DA & Roth CH 2007. A sediment budget for a grazed semi-arid catchment in the Burdekin basin, Australia. G*eomorphology* 87(4), 302-321.

Bartley R, Henderson A, Prosser IP, Hughes AO, McKergo L, Lu H, Brodie J, Bainbridge Z & Roth CH 2003. Patterns of erosion and sediment and nutrient transport in the Herbert River catchment, Queensland Consultancy Report, CSIRO Land and Water.

Bartley R, Poesen J, Wilkinson S & Vanmaercke M 2020. A review of the magnitude and response times for sediment yield reductions following the rehabilitation of gullied landscapes. *Earth Surface Processes and Landforms* 45(13), 3250-3279.

Bartley R, Poesen J, Wilkinson S & Vanmaercke M 2020. A review of the magnitude and response times for sediment yield reductions following the rehabilitation of gullied landscapes. *Earth Surface Processes and Landforms 45*(13), 3250-3279.

Bartley, R, Hawdon, A, Henderson, A, Wilkinson, S, Goodwin, N, Abbott, B & Telfer, D 2017. Quantifying the effectiveness of gully remediation on off-site water quality: preliminary results from demonstration sites in the Burdekin catchment. *NESP Project 2*(4).

Beckedahl H & Dardis G 1988. The role of artificial drainage in the development of soil pipes and gullies: Some examples from Transkei, southern Africa. In: Dardis G, Moon BP (eds) *Geomorphological studies in Southern Africa*, Rotterdam: AA Balkema, 229–246.

Beckedahl H 1996. *Subsurface soil erosion phenomena in Transkei and Southern KwaZulu-Natal, South Africa*, PhD thesis, University of Natal.

Belayneh A & Tessema ZK 2017. Mechanisms of bush encroachment and its inter-connection with rangeland degradation in semi-arid African ecosystems: a review. *Journal of Arid Land* 9, 299-312.

Belayneh M, Yirgu T & Tsegaye D 2020. Current extent, temporal trends, and rates of gully erosion in the Gumara watershed, Northwestern Ethiopia. *Global Ecology and Conservation 24*, 01255.

Bell FG & Maud RR 1994. Dispersive soils: a review from a South African perspective. *Quarterly Journal of Engineering Geology and Hydrogeology 27*(3), 195-210.

Bennett SJ, Casalí J, Robinson KM & Kadavy KC 2000. Characteristics of actively eroding ephemeral gullies in an experimental channel. *Transactions of the ASAE* 43(3), 641-649.

Bennett JE, Palmer AR & Blackett MA 2012. Range degradation and land tenure change: insights from a 'released' communal area of Eastern Cape Province, South Africa. *Land Degradation and Development* 23(6), 557-568.

Bennett, SJ & Wells, RR 2019. Gully erosion processes, disciplinary fragmentation, and technological innovation. *Earth surface processes and landforms*, 44(1), 46-53.

Bennetto M 2019. Presentation at International Symposium on Gully Erosion Symposium, July 2019.

Bergsma E, Charman P, Gibbons F, Hurni H, Moldenhauer WC & Panichapong S 1996. *Terminology for soil erosion and conservation*. ISSS: ITC: ISRIC.

Bernatek-Jakiel A & Poesen J 2018. Subsurface erosion by soil piping: significance and research needs. *Earth-Science Reviews* 185, 1107-1128.

Bernini A, Bosino A, Botha GA & Maerker M 2021. Evaluation of Gully Erosion Susceptibility Using a Maximum Entropy Model in the Upper Mkhomazi River Basin in South Africa. *ISPRS International Journal of Geo-Information* 10(11), 729.

Blaschke, T, Hay, GJ, Kelly, M, Lang, S, Hofmann, P, Addink, E, Feitosa, RQ, Van der Meer, F, Van der Werff, H, Van Coillie, F & Tiede, D 2014. Geographic object-based image analysis–towards a new paradigm. *ISPRS Journal of Photogrammetry and Remote Sensing* 87, 180-191.

Boardman J & Foster I 2008. Badland and gully erosion in the Karoo, *South Africa Journal of Soil and Water Conservation* 63(4), 121A-125A.

Boardman J 2014. How old are the gullies (dongas) of the Sneeuberg uplands, Eastern Karoo, South Africa? *Catena* 113, 79-85.

Boardman J, Favis-Mortlock D & Foster I 2015. A 13-year record of erosion on badland sites in the Karoo, South Africa. *Earth Surface Processes and Landforms* 40, 1964–1981. Available from: http://dxdoiorg/101002/esp3775.

Boardman J, Favis-Mortlock D & Foster I 2015. A 13-year record of erosion on badland sites in the Karoo, South Africa. *Earth Surface Processes and Landforms 40*(14), 1964-1981.

Boardman J, Foster I, Rowntree K, Mighall T & Gates J 2010. Environmental stress and landscape recovery in a semi-arid area, the Karoo, South Africa *Scottish Geographical Journal* 126, 64–75. Available from: http://dxdoiorg/101080/14702541003711038.

Boardman J, Foster ID, Rowntree KM, Favis-Mortlock DT, Mol L, Suich H & Gaynor D 2017. Long-term studies of land degradation in the Sneeuberg uplands, eastern Karoo, South Africa: a synthesis. *Geomorphology 285*, 106-120.

Boardman J, Parsons AJ, Holland R, Holmes PJ & Washington R 2003. Development of badlands and gullies in the Sneeuberg, Great Karoo, South Africa. *Catena* 50 165–184. Available from: http://dxdoiorg/101016/S0341-8162(02)00144-3.

Bocco G & Oliva FG 1992. Researching gully erosion in Mexico *Journal of soil and water conservation* 47, 365–367.

Bocco G 1991. Gully erosion: processes and models. *Progress in physical geography* 15(4), 392-406.

Borrelli P, Robinson DA, Fleischer LR, Lugato E, Ballabio C, Alewell C, Meusburger K, Modugno S, Schütt B, Ferro V & Bagarello V 2017. An assessment of the global impact of 21st century land use change on soil erosion. *Nature communications* 8(1), 2013.

Bosino A, Bernini A, Botha GA, Bonacina G, Pellegrini L, Omran A, Hochschild V, Sommer C & Maerker M 2021. Geomorphology of the upper Mkhomazi River basin, KwaZulu-Natal, South Africa, with emphasis on late Pleistocene colluvial deposits. *Journal of Maps* 17(3), 5-16.

Botha GA, Wintle AG & Vogel JC 1994. Episodic late quaternary palaeogully erosion in northern KwaZulu-Natal, South Africa. *Catena* 23, 327–340. http://dxdoiorg/101016/0341-8162(94)90076-0.

Bouramtane T, Hilal H, Rezende-Filho AT, Bouramtane K, Barbiero L, Abraham S, Valles V, Kacimi I, Sanhaji H, Torres-Rondon L & de Castro DD 2022. Mapping gully erosion variability and susceptibility using remote sensing, multivariate statistical analysis, and machine learning in South Mato Grosso, Brazil. *Geosciences 12*(6), 235.

Brady HM 1993. *An investigation into the nature of gully erosion at Golden Gate Highlands National Park.* MSc thesis, University of Natal.

Brecheisen ZS & Richter DD 2021. Gully-erosion estimation and terrain reconstruction using analyses of microtopographic roughness and LiDAR. *Catena* 202, 105264.

Brooks A, Spencer J & Knight J 2007. Alluvial gully erosion in Australia's tropical rivers: a conceptual model as a basis for a remote sensing mapping procedure. In Proceedings of the 5th Australian Stream Management Conference, Albury, Australia, 21-25 May 2007, 43-48.

Brooks AP, Shellberg JG, Knight J & Spencer J 2009. Alluvial gully erosion: an example from the Mitchell fluvial megafan, Queensland, Australia. *Earth Surface Processes and Landforms* 34(14), 1951-1969.

Brice JB 1966. Erosion and deposition in the loess-mantled Great Plains, Medecine Creek drainage basin, Nebraska. *US Geological Survey Professional Paper* 352H, 235–339.

Bufalo LJ & Nahon D 1992. Erosional processes of Mediterranean badlands - a new erosivity index for predicting sediment yield from gully erosion. *Geoderma* 52: 133–147. Available from: http://dxdoiorg/101016/0016-7061(92)90079-M.

Burger M 2013. *Geology of South Africa-1:1,000,000 – chronostratigraphic* Council for Geoscience. Available from: http://wwwgeoscienceorgza/ [Accessed 14 February 2021].

Capra A 2013. Ephemeral gully and gully erosion in cultivated land: A review *Drainage Basins and Catchment Management*, Lannon E (ed) Hauppauge, NY: Nova Science Publishers, Inc, 109-141.

Carvalho Junior O, Guimaraes R, Freitas L, Gomes-Loebmann D, Gomes RA, Martins E & Montgomery DR 2010. Urbanization impacts upon catchment hydrology and gully development using multi-temporal digital elevation data analysis. *Earth Surface Processes and Landforms* 35(5), 611-617.

Casalí J, Loizu J, Campo MA, De Santisteban LM & Álvarez-Mozos J 2006. Accuracy of methods for field assessment of rill and ephemeral gully erosion. *Catena* 67(2), 128-138.

Castillo C & Gómez JA 2016. A century of gully erosion research: Urgency, complexity and study approaches. *Earth-Science Reviews* 160, 300–319. Available from: http://dxdoiorg/101016/jearscirev201607009.

Castillo C, Taguas EV, Zarco-Tejada P, James MR & Gómez JA 2014. The normalized topographic method: an automated procedure for gully mapping using GIS. *Earth Surface Processes and Landforms* 39(15), 2002-2015.

Castillo VM, Gomez-Plaza A & Martınez-Mena M 2003. The role of antecedent soil water content in the runoff response of semiarid catchments: a simulation approach. *Journal of Hydrology* 284(1-4), 114-130.

Cerqueira H, Roxo MJ, Calvo-Cases A 2022. *Agricultural Policy triggers Land Degradation in the dry Mediterranean Southern Alentejo, Portugal (1986-2021)* (No ICG2022-292). Copernicus Meetings.

Chaplot V & Mutema M 2022. Impact of overgrazing on diffuse and concentrated erosion: case study in the sloping lands of South Africa. *Hydrology* 9(7), 121.

Chaplot V 2013. Impact of terrain attributes, parent material and soil types on gully erosion. *Geomorphology* 186, 1–11. Available from: http://dxdoiorg/101016/jgeomorph201210031.

Chaplot V, et al. 2011. Rainfall simulation to identify the storm-scale mechanisms of gully bank retreat. *Agricultural Water Management* 98, 1704–1710. Available from: http://dxdoiorg/101016/jagwat201005016.

Claessens L, Heuvelink GBM, Schoorl JM & Veldkamp A 2005. DEM resolution effects on shallow landslide hazard and soil redistribution modelling. *Earth Surface Processes and Landf*orms 30(4), 461-477.

Clark VR, Barker NP & Mucina L 2011. The Great Escarpment of southern Africa: a new frontier for biodiversity exploration. *Biodiversity and Conservation 20*, 2543-2561.

Cobban DA & Weaver AVB 1993. A preliminary investigation of the gully features in the Tsolwana game reserve, Ciskei. *Southern Africa South African Geographical Journal* 75, 14–21. Available from: http://dxdoiorg/101080/0372624519939713557.

Collison AJC 2001. The cycle of instability: stress release and fissure flow as controls on gully head retreat. *Hydrological Processes* 15(1), 3-12.

Compton JS, Herbert CT, Hoffman MT, Schneider RR & Stuut JB 2010. A tenfold increase in the Orange River mean Holocene mud flux: Implications for soil erosion in South Africa. *Holocene* 20, 115–122. Available from: http://dxdoiorg/101177/0959683609348860.

Congalton RG 1991. A review of assessing the accuracy of classifications of remotely sensed data. *Remote Sensing of Environment* 37(1), 35-46.

Conoscenti C, Angileri S, Cappadonia C, Rotigliano E, Agnesi V & Märker M 2014. Gully erosion susceptibility assessment by means of GIS-based logistic regression: A case of Sicily (Italy). *Geomorphology* 204, 399-411.

Council for Scientific and Industrial Research 2021. *Climate Indicators: Aridity*. Available from: http://stepsaorg/climate_arid ityhtml [Accessed 18 August 2021].

Cowie AL, Orr BJ, Sanchez VM, Chasek P, Crossman ND, Erlewein A, Louwagie G, Maron M, Metternicht GI, Minelli S & Tengberg AE 2018. Land in balance: The scientific conceptual framework for Land Degradation Neutrality. *Environmental Science & Policy* 79, 25-35.

Crosby CT, Smithen AA & McPhee PJ 1981. The role of soil loss equations in estimating sediment production. In *Proceedings of the Workshop on the Effect of Rural Land Use and Catchment Management on Water Resources*, H Maaren, ed. TR 113, Department of Water Affairs: Pretoria; 188– 213.

Crouch RJ 1990. Rates and mechanisms of discontinuous gully erosion in a red-brown earth catchment, New South Wales. Australia *Earth Surface Processes and Landforms* 15, 277 282.

d'Oleire-Oltmanns S, Marzolff I, Tiede D & Blaschke T 2014. Detection of gully-affected areas by applying object-based image analysis (OBIA) in the region of Taroudannt, Morocco. *Remote Sens*ing 6(9), 8287-8309.

Daba S, Rieger W & Strauss P 2003. Assessment of gully erosion in eastern Ethiopia using photogrammetric techniques. *Catena* 50(2-4), 273-291.

Dai W, Yang X, Na J, Li J, Brus D, Xiong L, Tang G & Huang X 2019. Effects of DEM resolution on the accuracy of gully maps in loess hilly areas. *Catena* 177, 114-125.

Dardis G & Beckedahl H 1988. Gully formation in Archean rocks at Saddleback Pass, Barberton Mountain. In: Dardis G & Moon BP, eds. *Geomorphological studies in Southern Africa*, Rotterdam: AA Balkema, 285–298.

Dardis G & Beckedahl HR 1991. The role of rock properties in the development of bedrock-incised rills and gullies: Example from Southern Africa. *Geojournal* 23, 35-40.

De Baets, S, Poesen J, Reubens B, Wemans K, De Baerdemaeker J & Muys B 2008. Root tensile strength and root distribution of typical Mediterranean plant species and their contribution to soil shear strength. *Plant and soil* 305, 207-226.

De Geeter S, Verstraeten G, Poesen J, Campforts B & Vanmaercke M 2023. A data driven gully head susceptibility map of Africa at 30 m resolution. *Environmental Research* 224, 115573.

De Wit M & Stankiewicz J 2006. Changes in surface water supply across Africa with predicted climate change. *Science* 311, 1917–1921. Available from: http://dxdoiorg/101126/science1119929.

Deng Y, Wilson JP & Bauer BO 2007. DEM resolution dependencies of terrain attributes across a landscape. *International Journal of Geographical Information Science* 21(2), 187-213.

Department of Environment, Forestry, & Fisheries 2021. The South African National Land Cover 2018. Available from: https://egis.environment.gov.za/sa_national_land_cover_datasets [Accessed 1 January 2021].

Department of Environment, Forestry, & Fisheries 2016. *Land Cover 2013-2014, 35 classes*. Available from: https://egisenvironmentgovza/data_egis/data_download/current [Accessed 1 June 2021].

Department of Rural Development & Land Reform 2022. Chief Directorate National Geo-Information portal. Available from: http://www.cdngiportal.co.za/cdngiportal/ [Accessed: 20 December 2022].

Dewitte O, Daoudi M, Bosco C & Van Den Eeckhaut M 2015. Predicting the susceptibility to gully initiation in data-poor regions. *Geomorphology* 228, 101-115.

Dickie JA & Parsons AJ 2012. Eco-geomorphological processes within grasslands, shrublands and badlands in the semi-arid Karoo, South Africa. *Land degradation and development* 23(6), 534-547.

D'Oleire-Oltmanns S, Marzolff I, Peter KD & Ries JB 2012. Unmanned aerial vehicle (UAV) for monitoring soil erosion in Morocco *Remote Sensing* 4(11), 3390-3416.

Dollar ESJ & Rowntree KM 1995. Hydroclimatic trends, sediment sources and geomorphic response in the Bell River catchment, Eastern Cape Drakensberg. *South Africa South African Geographical Journal* 77, 21–32. Available from: http://dxdoiorg/101080/0373624519959713585.

Domazetović F, Šiljeg A, Lončar N & Marić I 2019. Development of automated multicriteria GIS analysis of gully erosion susceptibility. *Applied geography* 112, 102083.

Dotterweich M, Ivester AH, Hanson PR, Larsen D & Dye DH 2014. Natural and human-induced prehistoric and historical soil erosion and landscape development in Southwestern Tennessee, USA. *Anthropocene* 8, 6-24.

Douglas-Mankin KR, Roy SK, Sheshukov AY, Biswas A, Gharabaghi B, Binns A, Rudra R, Shrestha NK & Daggupati P 2020. A comprehensive review of ephemeral gully erosion models. *Catena* 195, 104901.

Du Plessis C, Van Zijl G, Van Tol J & Manyevere A 2020. Machine learning digital soil mapping to inform gully erosion mitigation measures in the Eastern Cape, South Africa. *Geoderma* 368, 114287.

Dube F, Nhapi I, Murwira A, Gumindoga W, Goldin J & Mashauri DA 2014. Potential of weight of evidence modelling for gully erosion hazard assessment. In *Mbire District–Zimbabwe Physics and Chemistry of the Earth, Parts A/B/C*, 67, 145-152.

Ebhuoma O, Gebreslasie M, Ebhuoma E, Leonard L, Silas Ngetar N & Zamisa B 2023. Farmers' perception of soil erosion and degradation and their effects on rural livelihoods in KwaMaye Community, KwaZulu-Natal, South Africa. *Journal of Asian and African Studies* 58(8), 1405-1421.

Eekhout JP & de Vente J 2022. Global impact of climate change on soil erosion and potential for adaptation through soil conservation. *Earth-Science Reviews 226*, 103921.

European Commission, Directorate-General for Environment 2021a. *EU Soil Strategy for 2030 Reaping the benefits of healthy soils for people, food, nature and climate Publications Office of the European Union*. Available from: https://eur-lexeuropaeu/legal-content/EN/TXT/PDF/?uri=CELEX:52021DC0699 [Accessed: 18 August 2023].

European Commission, Directorate-General for Environment 2021b. *EU biodiversity strategy for 2030: bringing nature back into our lives Publications Office of the European Union*. Available from: https://dataeuropaeu/doi/102779/677548 [Accessed: 18 August 2023].

Eustace AH, Pringle MJ & Denham RJ 2011. A risk map for gully locations in central Queensland, Australia. *European Journal of Soil Science* 62(3), 431-441.

Evans M & Lindsay J 2010. High resolution quantification of gully erosion in upland peatlands at the landscape scale. *Earth Surface Processes and Landforms* 35(8), 876-886.

Fashae O, Obateru R, Olusola A & Dragovich D 2022. Factors controlling gully morphology on the quartzite ridges of Ibadan, Nigeria. *Catena 212*, 106127.

Faulkner H 2006. Piping hazard on collapsible and dispersive soils in Europe. *Soil erosion in Europe* 537-562.

Faulkner H 2013. Badlands in marl lithologies: a field guide to soil dispersion, subsurface erosion and piping-origin gullies. *Catena* 106, 42-53.

Favis-Mortlock D, Boardman J, Foster I & Greenwood P 2018. 'Local gradient' and between-site variability of erosion rate on badlands in the Karoo, South Africa. *Earth Surface Processes and Landforms* 43, 871–883. Available from: http://dxdoiorg/101002/esp4293.

Fey M 2010a. *Soils of South Africa.* Cambridge University Press.

Fey M 2010b. A short guide to the soils of South Africa, their distribution and correlation with World Reference Base soil groups. In *Proceedings 19th World Congress of Soil Science, Soil Solutions for a Changing World*, Brisbane, Australia, 1-6 August 2010, 32-35.

Flügel WA, Märker M, Moretti S & Rodolfi G 1999. Soil erosion hazard assessment in the Mkomazi river catchment (KwaZulu/Natal - South Africa) by using aerial photo interpretation. *Zentralblatt für Geologie und Paläontologie* 1, 641–653.

Flügel WA, Märker M, Moretti S, Rodolfi G & Sidrochuk A 2003. Integrating geographical information systems, remote sensing, ground truthing and modelling approaches for regional erosion classification of semi-arid catchments in South Africa. *Hydrological Processes* 17, 929–942. Available from: http://dxdoiorg/101002/hyp1171.

Foster GR 1986. Understanding Ephemeral Gully Erosion Soil Conservation: Assessing the National Research Inventory, National Research Council, Board on Agriculture 2. In *Board on agriculture 2*, National Academy Press Washington, DC.

Fox GA, Sheshukov A, Cruse R, Kolar RL, Guertault L, Gesch KR & Dutnell RC 2016. Reservoir sedimentation and upstream sediment sources: perspectives and future research needs on streambank and gully erosion. *Environmental management 57*, 945-955.

Fox RC & Rowntree KM 2001. Redistribution, Restitution and Reform: Prospects for the Land in the Eastern Cape Province, South Africa. In Conacher AJ, ed. *Land Degradation: The GeoJournal Library, vol 58*, Dordrecht: Springer, 167-186. Available from: https://doiorg/101007/978-94-017-2033-5_11.

Francipane A, Cipolla G, Maltese A, La Loggia G & Noto LV 2020. Using very high resolution (VHR) imagery within a GEOBIA framework for gully mapping: an application to the Calhoun Critical Zone Observatory. *Journal of Hydroinformatics* 22(1), 219-234.

Franco-Ramos O, Ballesteros-Cánovas JA, Terrazas T, Stoffel M, Vázquez-Selem L & Cerano-Paredes J 2022. Reconstruction of gully erosion based on exposed tree roots in a recent landform of Paricutin Volcano, Mexico. *Earth Surface Processes and Landforms* 47(3), 742-755.

Frankl A, Deckers J, Moulaert L, Van Damme A, Haile M, Poesen J & Nyssen J 2016. Integrated solutions for combating gully erosion in areas prone to soil piping: innovations from the drylands of Northern Ethiopia. *Land Degradation and Development* 27(8), 1797-1804.

Frankl A, Nyssen J, Adgo E, Wassie A & Scull P 2019. Can woody vegetation in valley bottoms protect from gully erosion? Insights using remote sensing data (1938–2016) from subhumid NW Ethiopia. *Regional Environmental Change* 19, 2055-2068.

Frankl A, Nyssen J, Vanmaercke M & Poesen J 2021. Gully prevention and control: Techniques, failures and effectiveness. *Earth Surface Processes and Landforms* 46(1), 220-238.

Fullen MA & Catt JA 2004. Soil Erosion. In: Goudie A, ed. *Encyclopaedia of Geomorphology*, Vol. 1. London: Routledge, 977–981.

Galang MA, Markewitz D, Morris LA & Bussell P 2007. Land use change and gully erosion in the Piedmont region of South Carolina. *Journal of Soil and Water Conservation 62*(3), 122-129.

Garland G & Broderick D 1992. Changes in the extent of erosion in the Tugela catchment, 1944–1981. *South African Geographical Journal* 74, 45–48.

Garland GG, Hoffman MT & Todd S 2000. Soil degradation. In Hoffman MT, Todd S, Ntshona Z and Turner S, eds. *A National Review of Land Degradation in South Africa,* Pretoria, South Africa: South African National Biodiversity Institute, 69-107.

Garosi Y, Sheklabadi M, Conoscenti C, Pourghasemi HR & Van Oost K 2019. Assessing the performance of GIS-based machine learning models with different accuracy measures for determining susceptibility to gully erosion. *Science of the Total Environment* 664, 1117-1132.

Garosi Y, Sheklabadi M, Pourghasemi HR, Besalatpour AA, Conoscenti C & Van Oost K 2018. Comparison of differences in resolution and sources of controlling factors for gully erosion susceptibility mapping. *Geoderma* 330, 65-78.

Garousi-Nejad I, Tarboton DG, Aboutalebi M & Torres-Rua AF 2019. Terrain analysis enhancements to the height above nearest drainage flood inundation mapping method. *Water Resources Research* 55(10), 7983-8009.

Geoscience Australia, 2012. Australian and Region Surface Geology [Online]. Commonwealth of Australia. Available from: http://maps.ga.gov.au/interactive-maps/#/theme/minerals/map/geology [Accessed: 1 February 2023].

GeoSmart Space (2020a) Stellenbosch University Digital Elevation Model (SUDEM) Stellenbosch, GeoSmart Space Pty Ltd. Available from: https://geosmartspace/products/sudemhtml [Accessed: 2 October 2020].

GeoSmart Space (2020b) 2 m Digital Elevation Model of South Africa (DEMSA) Stellenbosch, GeoSmart Space Pty Ltd. Available from: https://geosmartspace/products/sudemhtml [Accessed: 2 October 2020].

Ghosal K & Das Bhattacharya S 2020. A review of RUSLE model. *Journal of the Indian Society of Remote Sensing 48*, 689-707.

GI Metternicht, S Minelli, AE Tengberg, S Walter, & S Welton 2017. *Scientific Conceptual Framework for Land Degradation Neutrality A Report of the Science-Policy Interface United Nations Convention to Combat Desertification (UNCCD)*, Bonn, Germany.

Gómez-Gutiérrez Á, Conoscenti C, Angileri SE, Rotigliano E & Schnabel S 2015. Using topographical attributes to evaluate gully erosion proneness (susceptibility) in two mediterranean basins: Advantages and limitations. *Natural Hazards* 79(1), 291-314.

Grab S & Knight J 2015. *Landscapes and landforms of South Africa*. Cham: Springer International Publishing.

Grellier S, Kemp J, Janeau JL, Florsch N, Ward D, Barot S, Podwojewski P, Lorentz S & Valentin C 2012. The indirect impact of encroaching trees on gully extension: A 64year study in a sub-humid grassland of South Africa. *Catena* 98, 110–119. Available from: http://dxdoiorg/101016/jcatena201207002.

Grenfell SE, Grenfell MC, Rowntree KM & Ellery WN 2014. Fluvial connectivity and climate: A comparison of channel pattern and process in two climatically contrasting fluvial sedimentary systems in South Africa. *Geomorphology* 205, 142–154. Available from: http://dxdoiorg/101016/jgeomorph201205010.

Grenfell SE, Rowntree KM & Grenfell MC 2012. Morphodynamics of a gully and floodout system in the Sneeuberg Mountains of the semi-arid Karoo, South Africa: Implications for local landscape connectivity. *Catena*, *89*(1), 8-21.

Guo M, Lou Y, Chen Z, Wang W, Feng L & Zhang X 2021. The proportion of jet flow and on-wall flow and its effects on soil loss and plunge pool morphology during gully headcut erosion. *Journal of Hydrology 598*, 126220.

Hagerty DJ 1991. Piping/sapping erosion. I: Basic considerations. *Journal of Hydraulic Engineering* 117(8), 991-1008.

Hamdani N & Baali A 2019. Height Above Nearest Drainage (HAND) model coupled with lineament mapping for delineating groundwater potential areas (GPA). *Groundwater for Sustainable Development* 9, 100256.

Hancock GR & Willgoose GR 2021. Predicting gully erosion using landform evolution models: Insights from mining landforms. *Earth Surface Processes and Landforms* 46(15), 3271-3290.

Hanvey PM & Dardis G 1991. Soil Erosion on a sub-tropical coastal dune complex, Transkei, Southern Africa. *GeoJournal* 23, 41–48.

Hassen G & Bantider A 2020. Assessment of drivers and dynamics of gully erosion in case of Tabota Koromo and Koromo Danshe watersheds, South Central Ethiopia. *Geoenvironmental Disasters*. *7*, 1-13.

Hauge C 1977. Soil erosion definitions. *California Geology* 30, 202–203.

Hayas A, Poesen J, Vanwalleghem T 2017. Rainfall and vegetation effects on temporal variation of topographic thresholds for gully initiation in Mediterranean cropland and olive groves. *Land Degradadation and Development* 28 (8), 2540–2552.

Hayas A, Vanwalleghem T, Laguna A, Peña A & Giráldez JV 2017. Reconstructing long-term gully dynamics in Mediterranean agricultural areas. *Hydrology and Earth System Sciences 21*(1), 235-249.

Hoffman MT & Todd S 2000. A national review of land degradation in South Africa: the influence of biophysical and socio-economic factors. *Journal of Southern African Studies 26*(4), 743-758.

Hoffman MT, & Ashwell A 2001. *Nature Divided: Land degradation in South Africa.* Lansdowne, SA: University of Cape Town Press.

Holmes P & Boardman J 2018. *Southern African landscapes and environmental change.* Oxford: Routledge.

Holmes P & Meadows M 2012. *Southern African geomorphology: Recent trends and new directions.* Bloemfontein: Sun Media.

Hosseinalizadeh M, Kariminejad N, Chen W, Pourghasemi HR, Alinejad M, Behbahani AM & Tiefenbacher JP 2019. Gully headcut susceptibility modeling using functional trees, naïve Bayes tree, and random forest models. *Geoderma* 342, 1-11.

Hout R, Maleval V, Mahe G, Rouvellac E, Crouzevialle R & Cerbelaud F 2020. UAV and LiDAR data in the service of bank gully erosion measurement in Rambla de Algeciras lakeshore. *Water* 12(10), 2748.

Hudec PP, Simpson F, Akpokodje EG, Umenweke MO 2005. Anthropogenic contribution to gully initiation and propagation in southeastern Nigeria. *Reviews in Engineering Geology* 16,149-158.

Imeson AC & Kwaad FJPM 1980. Gully types and gully prediction. *Geografisch Tijdschrift*, 14(5), 430- 441.

Imwangana FM, Vandecasteele I, Trefois P, Ozer P & Moeyersons J 2015. The origin and control of mega-gullies in Kinshasa (DR Congo). *Catena 125*, 38-49.

Ionita I 2006. Gully development in the Moldavian Plateau of Romania. *Catena 68*(2-3), 133-140.

Ionita I, Niacsu L, Petrovici G & Blebea-Apostu AM 2015. Gully development in eastern Romania: a case study from Falciu Hills. *Natural Hazards 79*, 113-138.

Ireland HA, Eargle DH & Sharpe CFS 1939. *Principles of gully erosion in the Piedmont of South Carolina* (No. 633). US Department of Agriculture.

Jahantigh M & Pessarakli M 2011. Causes and effects of gully erosion on agricultural lands and the environment. *Communications in soil science and plant analysis 42*(18), 2250-2255.

Johansen K, Taihei S, Tindall D & Phinn, S 2012. Object-based monitoring of gully extent and volume in north Australia using LiDAR data. In *Proceedings of the 4th GEOBIA* 25.

Johnson JM, Munasinghe D, Eyelade D, Cohen S 2019. An integrated evaluation of the national water model (NWM)–Height above nearest drainage (HAND) flood mapping methodology. *Natural Hazards and Earth System Sciences* 19(11), 2405-2420.

Johnson MR, Anhauesser CR, Thomas RJ 2006. *The Geology of South Africa.* Geological Society of South Africa.

Kakembo V & Rowntree KM 2003. The relationship between land use and soil erosion in the communal lands near Peddie town, Eastern Cape, South Africa. *Land Degradation and Development* 14, 39–49. Available from: http://dxdoiorg/101002/ldr509.

Kakembo V, Xanga WW & Rowntree K 2009. Topographic thresholds in gully development on the hillslopes of communal areas in Ngqushwa Local Municipality, Eastern Cape, South Africa. *Geomorphology* 110 188–194. Available from: http://dxdoiorg/101016/jgeomorph200904006.

Kariminejad N, Hosseinalizadeh M, Pourghasemi HR, Bernatek-Jakiel A & Alinejad M 2019. GIS-based susceptibility assessment of the occurrence of gully headcuts and pipe collapses in a semi-arid environment: Golestan Province, NE Iran. *Land Degradation and Development* 30(18), 2211-2225.

Karydas C & Jiang B 2020. Scale optimization in topographic and hydrographic feature mapping using fractal analysis. *ISPRS International Journal of Geo-Information* 9(11), 631.

Katz HA, Daniels JM & Ryan S 2014. Slope-area thresholds of road-induced gully erosion and consequent hillslope–channel interactions. *Earth surface processes and landforms* 39(3), 285-295.

Keay-Bright J & Boardman J 2006. Changes in the distribution of degraded land over time in the central Karoo, South Africa. *Catena* 67, 1–14. Available from: http://dxdoiorg/101016/jcatena200512003.

Keay-Bright J & Boardman J 2009. Evidence from field-based studies of rates of soil erosion on degraded land in the central Karoo, South Africa. *Geomorphology* 103, 455–465. Available from: 101016/jgeomorph200807011.

Keay-Bright, J & Boardman, J, 2007. The influence of land management on soil erosion in the Sneeuberg Mountains, Central Karoo, South Africa. *Land degradation and development 18*(4), 423-439.King C, Baghdadi N, Lecomte V & Cerdan O 2005. The application of remote-sensing data to monitoring and modelling of soil erosion. *Catena* 62(2-3), 79-93.

Khuthadzo M 2019. Agricultural regions Environmental Systems Research Institute. Available from: https://agisndaagricza/portal/home/itemhtml?id=cb4bdf81ae2f4fbc819d057e8bd644ff [Accessed: 2 October 2021].

King LC 1963. *South African scenery.* Edinburgh, UK: Oliver and Boyd Ltd.

Kirkby MJ & Bracken LJ 2009. Gully processes and gully dynamics. *Earth Surface Processes and Landforms* 34, 1841–1851. Available from: https://doiorg/101002/esp1866.

Knighton D 1998. *Fluvial Forms and Processes – A New Perspective*. Hodder Education: London.

Koci J, Leon JX, Jarihani B, Sidle, RC, Wilkinson SN & Bartley R 2017. Strengths and limitations of UAV and Ground-based Structure from Motion photogrammetry in a gullied Savanna catchment. *ISPRS International Journal of Geo-Information* 6(11), 328.

Koci J, Sidle RC, Jarihani B & Cashman MJ 2020. Linking hydrological connectivity to gully erosion in savanna rangelands tributary to the Great Barrier Reef using structure-from-motion photogrammetry. *Land Degradation and Development 31*(1), 20-36.

Korzeniowska K, Pfeifer N & Landtwing S 2018. Mapping gullies, dunes, lava fields, landslides via surface roughness. *Geomorphology* 301, 53-67.

Kuhn CES, Reis FAGV, Zarfl C & Grathwohl P 2023. Ravines and gullies, a review about impact valuation. *Natural Hazards 117*(1), 597-624.

Laker MC 2004. Advances in soil erosion, soil conservation, land suitability evaluation and land use planning research in South Africa, 1978-2003. *South African Journal of Plant and Soil* 21(5), 345-368.

Land Type Survey Staff 1972 - 2006 *Land types of South Africa: Digital map (1:250 000 scale) and soil inventory datasets* ARC-Institute for Soil, Climate and Water, Pretoria.

Langbein WB, Schumm SA. 1958. Yield of sediment in relation to mean annual precipitation. *Transactions American Geophysical Union*, 39, 1076-1084.

Larue JP 2005. The status of ravine-like incisions in the dry valleys of the Pays de Thelle (Paris basin, France). *Geomorphology* 68(3-4), 242-256.

Le Roux J, Morake L, van der Waal B, Leigh Anderson R & Hedding DW 2022. Intra-gully mapping of the largest documented gully network in South Africa using UAV photogrammetry: Implications for restoration strategies. *Progress in Physical Geography: Earth and Environment*, 46(5), 772-789.

Le Roux J, Morgenthal T, Malherbe J 2008. Water erosion prediction at a national scale for South Africa. *Water SA* 34, 305–314.

Le Roux J, Van der Waal B 2020. Gully erosion susceptibility modelling to support avoided degradation planning South African Geographical Journal, 102(3), 406-420.

Le Roux JJ & Sumner PD 2012. Factors controlling gully development: Comparing continuous and discontinuous gullies. *Land Degradation and Development* 23, 440–449. Available from: http://dxdoiorg/101002/ldr1083.

Le Roux JJ & Sumner PD 2013. Water erosion risk assessment in South Africa: a proposed methodological framework. *Geografiska Annaler: Series A, Physical Geography* 95, 323–336.

Le Roux JJ 2018. Sediment yield potential in South Africa's only large river network without a Dam: Implications for Water Resource Management. *Land Degradation and Development* 29, 765–775. Available from: http://dxdoiorg/101002/ldr2753.

Lesschen JP, Cammeraat LH & Nieman T 2008. Erosion and terrace failure due to agricultural land abandonment in a semi-arid environment. *Earth Surface Processes and Landforms* 33(10), 1574-1584.

Li M, Li T, Zhu L, Meadow ME, Zhu W & Zhang S 2021. Effect of land use change on gully erosion density in the black soil region of Northeast China from 1965 to 2015: a case study of the Kedong County. *Frontiers in Environmental Science 9*, 652933.

Liggit B & Fincham RJ 1989. Gully erosion: The neglected dimension in soil erosion research. *South African Journal of Science* 85(1), 18.

Liu Q, Wang Y, Zhang J & Chen, Y 2013. Filling gullies to create farmland on the Loess Plateau. *Environmental Science Technology* 47(14), 7589-7590.

Liu YY, Maidment DR, Tarboton DG, Zheng X, Yildirim A, Sazib NS & Wang S 2016. A CyberGIS approach to generating high-resolution height above nearest drainage (HAND) raster for national flood mapping. *The Third International Conference on CyberGIS and Geospatial Data Science*. Urbana, Illinois, July 24-26. Available from: http://dx.doi.org/10.13140/RG.2.2.24234.41925/1.

Lucà F, Conforti M & Robustelli G 2011. Comparison of GIS-based gullying susceptibility mapping using bivariate and multivariate statistics: Northern Calabria, South Italy. *Geomorphology* 134(3-4), 297-308.

Lyons R, Tooth S & Duller GA 2013. Chronology and controls of donga (gully) formation in the upper Blood River catchment, KwaZulu-Natal, South Africa: Evidence for a climatic driver of erosion. *Holocene* 23, 1875–1887. Available from: http://dxdoiorg/101177/0959683613508157.

Maier WD, Barnes SJ & Groves DI 2013. The Bushveld Complex, South Africa: formation of platinum– palladium, chrome-and vanadium-rich layers via hydrodynamic sorting of a mobilized cumulate slurry in a large, relatively slowly cooling, subsiding magma chamber. *Mineralium Deposita* 48(1), 1-56.

Makaya N, Dube T, Seutloali K, Shoko C, Mutanga O & Masocha M 2019a. Geospatial assessment of soil erosion vulnerability in the upper uMgeni catchment in KwaZulu Natal, South Africa. *Physics and Chemistry of the Earth* 112, 50–57. Available from: https://doiorg/101016/jpce201902012.

Makaya NP, Mutanga O, Kiala Z, Dube T & Seutloali KE 2019b. Assessing the potential of Sentinel-2 MSI sensor in detecting and mapping the spatial distribution of gullies in a communal grazing landscape. *Physics and Chemistry of the Earth.* 112, 66–74. Available from: https://doiorg/101016/jpce201902001.

Malherbe J, Dieppois B, Maluleke P, Van Staden M & Pillay DL 2016. South African droughts and decadal variability. *Natural Hazards* 80, 657-681.

Manjoro M, Rowntree K, Kakembo V & Foster I 2012. Gully fan morphodynamics in a small catchment in the Eastern Cape, South Africa. *Land Degradation and Development* 23, 569–576. Available from: http://dxdoiorg/101002/ldr2174.

Manjoro M, Rowntree K, Kakembo V, Foster I & Collins AL 2017. Use of sediment source fingerprinting to assess the role of subsurface erosion in the supply of fine sediment in a degraded catchment in the Eastern Cape, South Africa. *Journal of Environmental Management* 194, 27–41. Available from: http://dxdoiorg/101016/jjenvman201607019.

Mararakanye N & Le Roux JJ 2012. Gully location mapping at a national scale for South Africa. *South African Geographical Journal* 94, 208–218. Available from: http://dxdoiorg/101080/037362452012742786.

Mararakanye N & Nethengwe NS 2012. Gully features extraction using remote sensing techniques. *South African Journal of Geomatics* 1, 109–118. Available from: http://dxdoiorg/104314/sajgv1i2.

Mararakanye N & Sumner PD 2017. Gully erosion: A comparison of contributing factors in two catchments in South Africa. *Geomorphology* 288, 99–110. Available from: http://dxdoiorg/101016/jgeomorph201703029.

Mararakanye N 2015. *A comparative study of gully erosion contributing factors in two tertiary catchments in Mpumalanga, South Africa.* MSc thesis, University of Pretoria.

Marden M, Fuller IC, Herzig A & Betts HD 2018. Badass gullies: Fluvio-mass-movement gully complexes in New Zealand's East Coast region, and potential for remediation. *Geomorphology* 307, 12-23.

Marker M 1988. Soil erosion in catchment near Alice, Ciskei, southern Africa. In Dardis G, Moon BP, eds. *Geomorphological studies in Southern Africa* Rotterdam: AA Balkema, 267–276.

Martínez Casasnovas JA & Poch RM 1998. Estado de conservación de los suelos de la cuenca del embalse de Joaquín Costa. *Limnetica* 14, 83–91.

Martínez-Casasnovas JA, Antón-Fernández C & Ramos MC 2003. Sediment production in large gullies of the Mediterranean area (NE Spain) from high-resolution digital elevation models

and geographical information systems analysis. *Earth Surface Processes and Landforms* 28 (5), 443-456.

Maugnard A, Cordonnier H, Degre A, Demarcin P, Pineux N & Bielders CL 2014. Uncertainty assessment of ephemeral gully identification, characteristics and topographic threshold when using aerial photographs in agricultural settings. *Earth Surface Processes and Landforms* 39(10), 1319-1330.

McMaster KJ 2002. Effects of digital elevation model resolution on derived stream network positions. *Water Resources Research* 38(4), 13-1.

McPhee PJ & Smithen AA 1984. Application of the USLE in the Republic of South Africa. *Agricultural Engineering South Africa* 18, 5–13.

Meadows ME 2003. Soil erosion in the Swartland, Western Cape Province, South Africa: implications of past and present policy and practice. *Environmental Science and Policy 6*(1), 17-28.

Midgley G Rutherford MC & Bond WJ 2008. *The heat is on: impacts of climate change on plant diversity in South Africa.* South African National Biodiversity Institute.

Miguez-Macho G, Fan Y & Dominguez F 2020. *Advances in groundwater representation at the subgrid scale in Land Surface Models: an approach based on HAND (height above nearest drainage)*. In AGU Fall Meeting Abstracts (Vol 2020, H201-03).

Mishra AK, Placzek C & Jones R 2019. Coupled influence of precipitation and vegetation on millennial-scale erosion rates derived from 10Be. *PloS one* 14(1), e0211325.

Moeyersons J, Makanzu Imwangana F, Dewitte O 2015. Site-and rainfall-specific runoff coefficients and critical rainfall for mega-gully development in Kinshasa (DR Congo). *Natural Hazards* 79(1), 203- 233.

Moon BP & Dardis GF, eds. 1988. *Geomorphology of Southern Africa.*

Moore A, Blenkinsop T & Cotterill F 2009. Southern African topography and erosion history: plumes or plate tectonics? *Terra Nova* 21(4), 310-315.

Morel A 1998. *Soil erosion and land degradation in the Swartland and Sandveld, Western Cape Province, South Africa: A re-evaluation.* MSc thesis, University of Cape Town.

Morokong T & Blignaut JN 2019. Benefits and costs analysis of soil erosion control using rock pack structures: The case of Mutale Local Municipality, Limpopo Province, South Africa. *Land Use Policy* 83, 512-522.

Mucina L & Rutherford MC 2006. *The vegetation of South Africa, Lesotho and Swaziland Strelitzia 19*. South African National Biodiversity Institute: Pretoria, South Africa, Memoirs of the Botanical Survey of South Africa.

National Soil Survey Handbook 2008. *National Soil Survey Handbook*. Washington, DC: Natural Resources Conservation Service, US Department of Agriculture.

Ndomba PM, Mtalo F & Killingtveit A 2009. Estimating gully erosion contribution to large catchment sediment yield rate in Tanzania. *Physics and Chemistry of the Earth, Parts A/B/C* 34(13-16), 741-748.

Neville D, Sampson BE & Sampson CG 1994. The frontier wagon track system in the Seacow river valley, North-Eastern Cape. *The South African Archaeological Bulletin*, 49(160), 65-72.

New M, Lister D, Hulme M & Makin I 2002. A high-resolution data set of surface climate over global land areas. *Climate Research* 21, 1–25. Available from: http://dxdoiorg/103354/cr021001.

Nhu VH, Janizadeh S, Avand M, Chen W, Farzin M, Omidvar E, Shirzadi A, Shahabi H, J Clague J, Jaafari A & Mansoorypoor F 2020. GIS-based gully erosion susceptibility mapping: A comparison of computational ensemble data mining models. *Applied Sciences* 10(6), 2039.

Nir N, Knitter D, Hardt J & Schütt B 2021. Human movement and gully erosion: Investigating feedback mechanisms using Frequency Ratio and Least Cost Path analysis in Tigray, Ethiopia. *PloS one* 16(2), 0245248.

Nir N, Stahlschmidt M, Busch R, Lüthgens C, Schütt B & Hardt J 2022. Footpaths: Pedogenic and geomorphological long-term effects of human trampling. *Catena 215*, 106312.

Nobre AD, Cuartas LA, Hodnett M, Rennó CD, Rodrigues G, Silveira A & Saleska S 2011. Height Above the Nearest Drainage–a hydrologically relevant new terrain model. *Journal of Hydrology* 404(1-2), 13-29.

Nordström K 1988. *Gully erosion in the Lesotho lowlands A geomorphological study of the interactions between intrinsic and extrinsic variables*. Uppsala University.

Nyssen J, Poesen J, Veyret-Picot M, Moeyersons J, Haile M, Deckers J, Dewit J, Naudts J, Teka K & Govers G 2006. Assessment of gully erosion rates through interviews and measurements: a case study from Northern Ethiopia. *Earth Surface Processes and Landforms* 31(2), 167-185.

Ohmori H 1983. Erosion rates and their relation to vegetation from viewpoint of world-wide distribution. *Bulletin of the Department of Geography*, University of Tokyo, 15, 77-91.

Olivier G 2013. Gully erosion in the Sandspruit catchment, Western Cape, with a focus on the discontinuous split gully system at Malansdam. MSc Thesis, Stellenbosch University.

Olivier G, de Clercq WP & Helmschrot J 2016. A GIS based gully classifications approach that reflects on origination and process for the Western Cape Province, South Africa. *Zentralblatt für Geologie und Paläontologie* Teil I, 55–73. Available from: http://dxdoiorg/101127/zgpI/2016/0055-0073.

Olivier G, de Clercq WP & Helmschrot J 2018. Are large classical gully systems inactive remnants of the past? A field-based case study investigating sediment movement. In Revermann R, Krewenka KM, Schmiedel U, Olwoch JM, Helmschrot J, Jürgens N, eds. *Climate change and adaptive land management in southern Africa – assessments, changes, challenges, and solutions Biodiversity and Ecology 6.* Göttingen and Windhoek: Klaus Hess Publishers, 146–154. Available from: http://dxdoiorg/107809/b-e00317.

Olivier G, de Clercq WP & Helmschrot J 2019. *The impact of contour banks on hillslope hydrology and gully erosion A field-scale case study in the Swartland, South Africa.* 8th International Symposium on Gully Erosion 22 July 2019, Townsville, Australia.

Olivier G, Van De Wiel M & de Clercq WP 2021. *Semi-automated detection of gully slivers from a Digital Surface Model in rough agricultural terrain*. In EGU General Assembly Conference Abstracts (EGU21-5747).

Olivier G, Van De Wiel M & de Clercq WP 2022. *Giving gully detection a HAND*. Copernicus Meetings (No ICG2022-102).

Olivier G, Van De Wiel M & de Clercq WP 2023a. Intersecting views of gully erosion in South Africa. *Earth Surface Processes and Landforms* 48(1), 119-142.

Olivier G, Van De Wiel M & de Clercq WP 2023b. Predicting gully erosion susceptibility in South Africa by integrating literature directives with regional spatial data. *Earth Surface Processes and Landforms* 48(14), 2661-2681.

Oostwoud Wijdenes DJ & Bryan R 2001. Gully-head erosion processes on a semi-arid valley floor in Kenya: a case study into temporal variation and sediment budgeting. *Earth Surface Processes and Landforms* 26(9), 911-933.

Oostwoud Wijdenes, DJO, Poesen J, Vandekerckhove L, Nachtergaele J & De Baerdemaeker J 1999. Gully-head morphology and implications for gully development on abandoned fields in a semi-arid environment, Sierra de Gata, southeast Spain. *Earth Surface Processes and Landforms* 24(7), 585-603.

Orr HG, Wilby RL, Hedger MM & Brown I 2008. Climate change in the uplands: a UK perspective on safeguarding regulatory ecosystem services. *Climate Research*, 37(1), 77-98.

Palmer AR & Bennett JE 2013. Degradation of communal rangelands in South Africa: towards an improved understanding to inform policy. *African Journal of Range and Forage Science*, 30(1-2), 57-63.

Panter B & Ruwanza S 2019. Spekboom (Portulacaria afra) planting in degraded thickets improves soil properties and vegetation diversity. *Ecological Restoration* 37(2), 76-80.

Parkner T, Page M, Marden M & Marutani T 2007. Gully systems under undisturbed indigenous forest, East Coast region, New Zealand. *Geomorphology* 84(3-4), 241-253.

Parkner T, Page MJ, Marutani T & Trustrum NA 2006. Development and controlling factors of gullies and gully complexes, East Coast, New Zealand. *Earth Surface Processes and Landforms* 31(2), 187- 199.

Parwada C & Van Tol J 2016. The nature of soil erosion and possible conservation strategies in Ntabelanga area, Eastern Cape Province, South Africa. *Acta Agriculturae Scandinavica, Section B—Soil and Plant Science* 66(6), 544-552.

Pathak P, Wani, SP & Sudi R 2006. *Gully control in SAT Watersheds*. ICRISAT, 2.

Patton PC & Schumm SA 1975. Gully erosion, Northwestern Colorado: a threshold phenomenon. *Geology* 3(2), 88-90.

Peñuela A, Hayas A, Infante-Amate J, Ruiz-Montes P, Temme A, Reimann T, Peña-Acevedo A & Vanwalleghem T 2023. A multi-millennial reconstruction of gully erosion in two contrasting Mediterranean catchments. *Catena* 220, 106709.

Phinzi K & Ngetar NS 2017. Mapping soil erosion in a Quaternary catchment in Eastern Cape using geographic information system and remote sensing. *South African Journal of Geomatics* 6(1), 11-29. Available from: http://dxdoiorg/104314/sajgv6i12.

Phinzi K, Abriha D & Szabó S 2021. Classification efficacy using k-fold cross-validation and bootstrapping resampling techniques on the example of mapping complex gully systems. *Remote Sensing* 13(15), 2980.

Phinzi K, Abriha D, Bertalan L, Holb I & Szabó S 2020. Machine learning for gully feature extraction based on a pan-sharpened multispectral image: Multiclass vs Binary approach. *ISPRS International Journal of Geo-Information* 9(4), 252.

Piest, R.F., Bradford, J.M. and Spomer, R.G., 1975. Mechanisms of erosion. In *Present and Prospective Technology for Predicting Sediment Yield and Sources: Proceedings of the Sediment-Yield Workshop*, USDA Sedimentation Laboratory, 162.

Planchon O & Darboux F 2002. A fast, simple and versatile algorithm to fill the depressions of digital elevation models. *Catena* 46(2), 159–176.

Podwojewski P, Janeau JL, Caquineau S & Hughes J 2020. Mechanisms of lateral and linear extension of gullies (dongas) in a subhumid grassland of South Africa. *Earth Surface Processes and Landforms* 45(13), 3202-3215.

Poesen J 2018. Soil erosion in the Anthropocene: Research needs. *Earth Surface Processes and Landforms* 43(1), 64-84.

Poesen J, Nachtergaele J, Verstraeten G & Valentin C 2003. Gully erosion and environmental change: importance and research needs. *Catena* 50, 91–133. Available from: http://dxdoiorg/101016/S0341-8162(02)00143-1.

Poesen J, Nachtergaele J, Verstraeten G & Valentin C 2003. Gully erosion and environmental change: importance and research needs. *Catena* 50(2-4), 91-133.

Poesen JW, Vandaele K & Van Wesemael B 1996. Contribution of gully erosion to sediment production on cultivated lands and rangelands. In *IAHS Publications-Series of Proceedings and Reports-Intern Assoc Hydrological Sciences* 236, 251-266.

Pourghasemi HR, Sadhasivam N, Kariminejad N & Collins AL 2020. Gully erosion spatial modelling: Role of machine learning algorithms in selection of the best controlling factors and modelling process. *Geoscience Frontiers* 11(6), 2207-2219.

Prah KK 1989. Land degradation and class struggle in rural Lesotho. In *Ecology and Politics: Environmental Stress and Security in Africa*. Hiort af Ornas A, Mohamed Salih MA, eds. Motala: Motala Grafiska, Sweden, 117-129.

Pretorius SN, Weepener HL, Le Roux JJ, Sumner PD 2017. SWAT and OBIA based sediment yield analysis in the Tsitsa Catchment of the Eastern Cape Province, South Africa. In *Proceedings of Centenary Conference of the Society of South African Geographers*: Stellenbosch, South Africa, September 2016, 25-28.

Pulley S, Ellery WN, Lagesse JV, Schlegel PK & McNamara SJ 2018. Gully erosion as a mechanism for wetland formation: An examination of two contrasting landscapes. *Land Degradation and Development* 29(6), 1756-1767.

Rahmati O, Haghizadeh A, Pourghasemi HR & Noormohamadi F 2016. Gully erosion susceptibility mapping: the role of GIS-based bivariate statistical models and their comparison. *Natural Hazards* 82(2), 1231-1258.

Rahmati O, Kalantari Z, Ferreira CS, Chen W, Soleimanpour SM, Kapović-Solomun M, Seifollahi-Aghmiuni S, Ghajarnia N & Kazemabady NK 2022. Contribution of physical and anthropogenic factors to gully erosion initiation. *Catena* 210, 105925.

Rahmati O, Tahmasebipour N, Haghizadeh A, Pourghasemi HR & Feizizadeh B 2017. Evaluation of different machine learning models for predicting and mapping the susceptibility of gully erosion. *Geomorphology* 298, 118-137.

Ramezanpour H, Esmaeilnejad L & Akbarzadeh A 2010. Influence of soil physical and mineralogical properties on erosion variations in Marlylands of Southern Guilan Province, Iran. *International Journal of physical sciences* 5(4), 365-378.

Reinwarth B, Petersen R & Baade J 2019. Inferring mean rates of sediment yield and catchment erosion from reservoir siltation in the Kruger National Park, South Africa: An uncertainty assessment. *Geomorphology* 324, 1-13.

Rennó CD, Nobre AD, Cuartas LA, Soares JV, Hodnett MG & Tomasella J 2008. HAND, a new terrain descriptor using SRTM-DEM: Mapping terra-firme rainforest environments in Amazonia. *Remote Sensing of Environment* 112(9), 3469-3481.

Rey F & Labonne S 2015. Resprout and survival of willow (Salix) cuttings on bioengineering structures in actively eroding gullies in marls in a mountainous Mediterranean climate: a large-scale experiment in the Francon catchment (Southern Alps, France). *Environmental management* 56(4), 971-983.

Rey F 2003. Influence of vegetation distribution on sediment yield in forested marly gullies. *Catena* 50(2-4), 549-562.

Rienks SM, Botha GA & Hughes JC 2000. Some physical and chemical properties of sediments exposed in a gully (donga) in northern KwaZulu-Natal, South Africa and their relationship to the erodibility of the colluvial layers. *Catena* 39, 11–31. Available from: http://dxdoiorg/101016/S0341-8162(99)00082-X.

Ries JB & Marzolff I 2003. Monitoring of gully erosion in the Central Ebro Basin by large-scale aerial photography taken from a remotely controlled blimp. *Catena* 50(2-4), 309-328.

Rijal S, Wang G, Woodford PB, Howard HR, Hutchinson JS, Hutchinson S, Schoof J, Oyana TJ, Li R & Park LO 2018. Detection of gullies in Fort Riley military installation using LiDAR derived high resolution DEM. *Journal of Terramechanics* 77, 15-22.

Roberts ME, Burrows RM, Thwaites RN & Hamilton DP 2022. Modelling classical gullies–A review. *Geomorphology* 407, 108216.

Rong L, Duan X, Zhang G, Gu Z & Feng D 2019. Impacts of tillage practices on ephemeral gully erosion in a dry-hot valley region in southwestern China. *Soil and tillage Research* 187, 72-84.

Rossi M, Torri D & Santi EJNH 2015. Bias in topographic thresholds for gully heads. *Natural Hazards 79*(1), 51-69.

Rossi M, Torri D, De Geeter S, Cremer C, Poesen J 2022. Topographic thresholds for gully head formation in badlands. *Earth Surface Processes and Landforms* 47(15), 3558-3587.

Rowntree KM & Foster ID 2012. A reconstruction of historical changes in sediment sources, sediment transfer and sediment yield for a small, semi-arid Karoo catchment, South Africa. *Zeitschrift fur Geomorphologie, Supplementary Issues* 56, 87-100.

Rowntree KM 2013. The evil of sluits: A re-assessment of soil erosion in the Karoo of South Africa as portrayed in century-old sources. *Journal of Environmental Management* 130, 98–105. Available from: http://dxdoiorg/101016/jjenvman201308041.

Ruecker G, Schad P, Alcubilla MM & Ferrer C 1998. Natural regeneration of degraded soils and site changes on abandoned agricultural terraces in Mediterranean Spain. *Land Degradation & Development* 9(2), 179-188.

Saha S, Roy J, Arabameri A, Blaschke T & Tien Bui D 2020. Machine learning-based gully erosion susceptibility mapping: A case study of Eastern India. *Sensors* 20(5), 1313.

Samodra G, Chen G, Sartohadi J & Kasama K 2018. Generating landslide inventory by participatory mapping: an example in Purwosari Area, Yogyakarta, Java. *Geomorphology* 306, 306-313.

Sartori M, Philippidis G, Ferrari E, Borrelli P, Lugato E, Montanarella L & Panagos P 2019. A linkage between the biophysical and the economic: Assessing the global market impacts of soil erosion. *Land use policy* 86, 299-312.

Schmiedel U, Kruspe M, Kayser L & Oettlé N 2017. The ecological and financial impact of soil erosion and its control - A case study from the semiarid Northern Cape Province, South Africa. *Land Degradation and Development* 28, 74–82. Available from: http://doiwileycom/101002/ldr2513.

Schoener G & Stone MC 2019. Impact of antecedent soil moisture on runoff from a semiarid catchment. *Journal of Hydrology* 569, 627-636.

Schulze RE, Lynch SD & Maharaj M 2006. Annual Precipitation. In: Schulze RE, Ed. *South African Atlas of Climatology and Agrohydrology*, Water Research Commission, Pretoria, RSA, WRC Report 1489/1/06, Section 62.

Schulze RE, Maharaj M (2006) Rainfall seasonality In: Schulze RE, Ed. *South African Atlas of Climatology and Agrohydrology*, Water Research Commission, Pretoria, RSA, WRC Report 1489/1/06, Section 62.

Schumm SA, Harvey MD & Watson CC 1984. *Incised Channels: Morphology, Dynamics and Control*. Littleton, CO: Water Resources Publications.

Setargie TA, Tsunekawa A, Haregeweyn N, Tsubo M, Fenta AA, Berihun ML, Sultan D, Yibeltal M, Ebabu K, Nzioki B & Meshesha TM 2023. Random Forest–based gully erosion susceptibility assessment across different agro-ecologies of the Upper Blue Nile basin, Ethiopia. G*eomorphology*, 431, 108671.

Seutloali KE, Beckedahl HR, Dube T & Sibanda M 2016. An assessment of gully erosion along major armoured roads in south-eastern region of South Africa: a remote sensing and GIS approach. *Geocarto International* 31(2), 225-239.

Seutloali KE, Beckedahl, HR, Dube T & Sibanda M 2016. An assessment of gully erosion along major armoured roads in south-eastern region of South Africa: a remote sensing and GIS approach. *Geocarto International* 31(2), 225-239.

Seutloali KE, Dube T & Mutanga O 2017. Assessing and mapping the severity of soil erosion using the 30-m Landsat multispectral satellite data in the former South African homelands of Transkei. *Physics and Chemistry of the Earth, Parts A/B/C* 100, 296-304.

Shackleton CM 1993. Are the communal grazing lands in need of saving? *Development Southern Africa* 10(1), 65-78.

Shellberg JG 2021. Agricultural development risks increasing gully erosion and cumulative sediment yields from headwater streams in Great Barrier Reef catchments. *Land Degradation and Development* 32(3), 1555-1569.

Shellberg JG & Brooks A 2012. *Alluvial Guly Erosion: A Dominant Erosion Process Across Tropical Northern Australia*. Charles Darwin University.

Shellberg JG, Brooks AP, Spencer J, Knight J & Pietsch T 2010. Alluvial gully erosion rates and processes in Northern Queensland: an example from the Mitchell River fluvial megafan. In *Produced for The Caring for Our Country (CfoC) Initiative*. Australian Rivers Institute, Griffiths University.

Shellberg JG, Spencer J, Brooks AP & Pietsch TJ 2016. Degradation of the Mitchell River fluvial megafan by alluvial gully erosion increased by post-European land use change, Queensland, Australia. *Geomorphology* 266, 105-120.

Shit PK & Maiti RK 2012. Mechanism of gully-head retreat-a study at Ganganir Danga, Paschim Medinipur, West Bengal. *Ethiopian Journal of Environmental Studies and Management* 5(4), 332-342.

Shit PK, Paira R, Bhunia G & Maiti R 2015. Modeling of potential gully erosion hazard using geo-spatial technology at Garbheta block, West Bengal in India. *Modeling Earth Systems and Environment* 1,1-16.

Shruthi RB, Kerle N & Jetten V 2011. Object-based gully feature extraction using high spatial resolution imagery. *Geomorphology* 134(3-4), 260-268.

Shulze RE, Maharaj M, Warburton ML, Gers CJ, Horan MJC, Kunz RP & Clark DJ 2007. *South African Atlas of Climatology and Agrohydrology.* Water Research Commission, Pretoria, RSA, WRC Report 1489/1/06.

Sidle RC, Jarihani B, Kaka SI, Koci J & Al-Shaibani A 2019. Hydrogeomorphic processes affecting dryland gully erosion: Implications for modelling. *Progress in Physical Geography: Earth and Environment* 43(1), 46-64.

Sidorchuk A 1999. Dynamic and static models of gully erosion. *Catena* 37, 401–41.

Simon A, Curini A, Darby SE & Langendoen EJ 2000. Bank and near-bank processes in an incised channel. *Geomorphology* 35(3-4), 193-217.

Singh J, Ashfaq M, Skinner CB, Anderson WB, Mishra V & Singh D 2022. Enhanced risk of concurrent regional droughts with increased ENSO variability and warming. *Nature Climate Change 12*(2), 163-170.

Slimane AB, Raclot D, Rebai H, Le Bissonnais Y, Planchon O & Bouksila, F 2018. Combining field monitoring and aerial imagery to evaluate the role of gully erosion in a Mediterranean catchment (Tunisia). *Catena* 170, 73-83.

Soeder DJ & Borglum SJ 2019. *The fossil fuel revolution: Shale gas and tight oil.* Elsevier.

Sonneveld MPW, Everson TM & Veldkamp A 2005. Multi-scale analysis of soil erosion dynamics in Kwazulu-Natal, South Africa. *Land Degradation and Development* 16, 287–301. Available from: http://dxdoiorg/101002/ldr653.

Stankoviansky M 2003. Historical evolution of permanent gullies in the Myjava Hill Land, Slovakia. *Catena* 51(3-4), 223-239.

Steudel T, Bugan R, Kipka H, Pfennig B, Fink M, de Clercq W, Flügel WA & Helmschrot J 2015. Implementing contour bank farming practices into the J2000 model to improve hydrological and erosion modelling in semi-arid Western Cape Province of South Africa. *Hydrology Research* 46(2), 192-211.

Stöcker C, Eltner A & Karrasch P 2015. Measuring gullies by synergetic application of UAV and close range photogrammetry—A case study from Andalusia, Spain. *Catena* 132, 1-11.

Sullivan-Wiley KA 2016. *Risk reduction and development in a multi-hazard landscape: A case study of eastern Uganda*, PhD thesis, Boston University.

Summerfield MA 2014. *Global geomorphology.* Routledge.

Sumner ME 1957. *The physical and chemical properties of Tall Grass Veld soils of Natal in relation to their erodibility.* MSc Thesis, University of Natal.

Sun L, Liu YF, Wang X, Liu Y & Wu GL 2022. Soil nutrient loss by gully erosion on sloping alpine steppe in the northern Qinghai-Tibetan Plateau. *Catena* 208, 105763.

Stratton SJ 2021. Population research: convenience sampling strategies. *Prehospital and disaster Medicine* 36(4), 373-374.

Svoray T & Markovitch H 2009. Catchment scale analysis of the effect of topography, tillage direction and unpaved roads on ephemeral gully incision. *Earth Surface Processes and Landforms* 34(14), 1970-1984.

Talbot WJ 1947. *Swartland and Sandveld: A survey of land utilization and soil erosion in the western lowland of the Cape province.* Oxford, UK: Oxford University Press.

Tarolli P & Tarboton DG 2006. A new method for determination of most likely landslide initiation points and the evaluation of digital terrain model scale in terrain stability mapping. *Hydrology and Earth System Sciences* 10(5), 663-677.

Taruvinga K 2008. Gully mapping using remote sensing: Case study in KwaZulu-Natal, South Africa. MSc, University of Waterloo.

Tebebu TY, Abiy AZ, Zegeye AD, Dahlke HE, Easton ZM, Tilahun SA, Collick AS, Kidnau S, Moges S, Dadgari F & Steenhuis TS 2010. Surface and subsurface flow effect on permanent gully formation and upland erosion near Lake Tana in the northern highlands of Ethiopia. *Hydrology and Earth System Sciences* 14(11), 2207-2217.

Temme AJAM, Baartman JEM, Botha GA, Veldkamp A, Jongmans AG & Wallinga J 2008. Climate controls on late Pleistocene landscape evolution of the Okhombe valley, KwaZulu-Natal, South Africa. *Geomorphology* 99(1-4), 280-295.

Thomas J, Joseph S & Thrivikramji KP 2018. Estimation of soil erosion in a rain shadow river basin in the southern Western Ghats, India using RUSLE and transport limited sediment delivery function. *International Soil and Water Conservation Research* 6(2), 111-122.

Thwaites RN 1986. A Technique for local soil erosion survey. *South African Geographical Journal* 68, 67–76. Available from: http://dxdoiorg/101080/03736245198610559722.

Thwaites RN, Brooks AP, Pietsch TJ & Spencer JR 2022. What type of gully is that? The need for a classification of gullies. *Earth Surface Processes and Landforms 47*(1), 109-128.

Tobler WR 1987. Measuring Spatial Resolution. In *Proceedings, International Workshop on Geographical Information Systems*, Beijing, China, 25-28 May 1987, 42-47.

Tooth S, Brandt D, Hancox PJ & McCarthy TS 2004. Geological controls on alluvial river behaviour: A comparative study of three rivers on the South African Highveld. *Journal of African Earth Sciences* 38, 79–97. Available from: http://dxdoiorg/101016/jjafrearsci200308003.

Torri D & Poesen J 2014. A review of topographic threshold conditions for gully head development in different environments. *Earth-Science Reviews* 130, 73–85. Available from: http://dxdoiorg/101016/jearscirev201312006.

Trimble Germany GmbH 2023. *Trimble Documentation eCognition Developer 9 User Guide*. Trimble Germany GmbH: Munich, Germany.

Trimble S 1999. Decreased rates of alluvial sediment storage in the Coon Creek Basin, Wisconsin, 1975–93. *Science* 285, 1244–1246.

United Nations 2015. *Transforming our World: The 2030 agenda for sustainable development* A/RES/70/1. Available from: at:https://sdgsunorg/sites/default/files/publications/21252030%20Agenda%20for%20Sustainable%20Development%20webpdf.

Utsumi AG, Pissarra TCT, Rosalen DL, Martins Filho MV & Rotta LHS 2020. Gully mapping using geographic object-based image analysis: A case study at catchment scale in the Brazilian Cerrado. *Remote Sensing Applications: Society and Environment* 20, 100399.

Valentin C, Poesen J & Li Y 2005. Gully erosion: Impacts, factors and control. *Catena* 63, 132–153.

Vallejo-Orti M, Negussie K, Corral-Pazos-de-Provens E, Höfle B & Bubenzer O 2019. Comparison of three algorithms for the evaluation of TanDEM-X data for gully detection in Krumhuk farm (Namibia). *Remote Sensing* 11(11), 1327.

Van Tongeren JA & Mathez EA 2015. On the relationship between the Bushveld Complex and its felsic roof rocks, part 2: the immediate roof. *Contributions to Mineralogy and Petrology* 170(5), 1-17.

Van Zijl GM & Ellis F 2013. Emphasising the soil factor in geomorphological studies of gully erosion: a case study in Maphutseng, Lesotho. *South African Geographical Journal* 95(2), 205-16.

Van Zijl GM 2010. *An investigation of the soil properties controlling gully erosion in a sub-catchment in Maphutseng, Lesotho*. MSc Thesis, Stellenbosch University.

Van Zyl AJ 2007. A knowledge gap analysis on multi-scale predictive ability for agriculturally derived sediments under South African conditions. *Water Science and Technology* 55, 107–114.

Vandekerckhove L, Poesen J, Oostwoud Wijdenes D, Nachtergaele J, Kosmas C, Roxo MJ & De Figueiredo T 2000. Thresholds for gully initiation and sedimentation in Mediterranean Europe. *Earth Surface Processes and Landforms 25*(11), 1201-1220.

Vandekerckhove L, Poesen J, Oostwoud Wijdenes, D & De Figueiredo T 1998. Topographical thresholds for ephemeral gully initiation in intensively cultivated areas of the Mediterranean. *Catena* 33 (3–4), 271–292.

Vandekerckhove L, Poesen J, Wijdenes DO, Gyssels G, Beuselinck L & De Luna E 2000. Characteristics and controlling factors of bank gullies in two semi-arid Mediterranean environments. *Geomorphology* 33(1-2), 37-58.

Vanmaercke M, et al. 2016. How fast do gully headcuts retreat? *Earth-Science Reviews* 154, 336–355. Available from: http://dxdoiorg/101016/jearscirev201601009.

Vanmaercke M, et al. 2021. Measuring, modelling and managing gully erosion at large scales: A state of the art. *Earth-Science Reviews*, 103637.

Vanmaercke M, Panagos P, Vanwalleghem T, Hayas A, Foerster S, Borrelli P, Rossi M, Torri D, Casali J, Borselli L & Vigiak O 2021. Measuring, modelling and managing gully erosion at large scales: A state of the art. *Earth-Science Reviews* 218, 103637.

Verster E, Du Plessis W, Fuggle RF & Schloms BHA 2009. Soil. In Strydom HA, King ND, Fuggle RF, Rabie MA, eds. *Environmental Management in RSA*, 313-342 Cape Town: Juta.

Vetter S 2007. Soil erosion in the Herschel district of South Africa: changes over time, physical correlates and land users' perceptions. *African Journal of Range and Forage Science* 24, 77–86. Available from: http://dxdoiorg/102989/AJRFS20072424158.

Vetter S, Goqwana WM, Bond WJ & Trollope WW 2006. Effects of land tenure, geology and topography on vegetation and soils of two grassland types in South Africa. *African Journal of Range and Forage Science* 23(1), 13-27.

Vrieling A, Rodrigues SC, Bartholomeus H & Sterk G 2007. Automatic identification of erosion gullies with ASTER imagery in the Brazilian Cerrados. *International Journal of Remote Sensing* 28(12), 2723-2738.

Waldner F, Hansen MC, Potapov PV, Löw F, Newby T, Ferreira S & Defourny P 2017. National-scale cropland mapping based on spectral-temporal features and outdated land cover information. *PloS one* 12(8), 0181911.

Walker SJ, Wilkinson SN, van Dijk AI & Hairsine PB 2020. A multi-resolution method to map and identify locations of future gully and channel incision. *Geomorphology*, 358, 107115.

Walling DE & Kleo A 1979. Sediment yields of rivers in areas of low precipitation: a global view. In: IAHS (ed). *The Hydrology of Areas of Low Precipitation*. Wallingford: *IAHS Publication*, 479-493.

Wang R, Sun H, Yang J, Zhang S, Fu H, Wang N & Liu Q 2022. Quantitative evaluation of gully erosion using multitemporal UAV data in the southern black soil region of Northeast China: A case study. *Remote Sensing* 14(6), 1479.

Wang R, Zhang S, Pu L, Yang J, Yang C, Chen J, Guan C, Wang Q, Chen D, Fu B & Sang X 2016. Gully erosion mapping and monitoring at multiple scales based on multi-source remote sensing data of the Sancha River Catchment, Northeast China. *ISPRS International Journal of Geo-Information* 5(11), 200.

Wantzen KM 2006. Physical pollution: effects of gully erosion on benthic invertebrates in a tropical clear-water stream. *Aquatic Conservation: Marine and Freshwater Ecosystems* 16(7), 733-749.

Watson HK 2000. Land reform implications of the distribution of badlands in the Mfolozi catchment, KwaZulu-Natal. *South African Geographical Journal* 82(3), 143-148.

Watson HK, Ramokgopa R 1997. Factors influencing the distribution of gully erosion in Kwazulu Natal's Mfolozi catchment—land reform implications. *South African Geographical Journal* 79, 27-34. Available from: http://dxdoiorg/101080/0373624519979713619.

Weaver A 1988. Changes in land use and soil erosion in South African and Ciskeian portions of the Yellowwoods drainage basin between 1975 and 1984. *Earth-Science Reviews* 25(5-6), 501-507.

Wells NA, Andriamihaja B & Rakotovololona HS 1991. Patterns of development of lavaka, Madagascar's unusual gullies. *Earth Surface Processes and Landforms* 16(3), 189-206.

Wells RR, Momm HG, Bennett SJ, Gesch KR, Dabney SM, Cruse R & Wilson GV 2016. A measurement method for rill and ephemeral gully erosion assessments. *Soil Science Society of America Journal*, 80(1), 203-214.

Wen Y, Kasielke T, Li H, Zepp H & Zhang B 2021. A case-study on history and rates of gully erosion in Northeast China. *Land Degradation and Development* 32(15), 4254-4266.

Wen Y, Kasielke T, Li H, Zhang B & Zepp H 2021. May agricultural terraces induce gully erosion? A case study from the Black Soil Region of Northeast China. *Science of the Total Environment* 750, 141715.

Wilkinson S, Hairsine PB, Bartley R, Brooks A, Pietsch T, Hawdon A & Shephard B 2022. *Gully and Stream Bank Toolbox A technical guide for gully and stream bank erosion control programs in Great Barrier Reef catchments.* Reef Trust, 112.

Wilkinson SN, Bartley R, Hairsine PB, Bui EN, Gregory L & Henderson AE 2015. *Managing gully erosion as an efficient approach to improving water quality in the Great Barrier Reef lagoon*. Report to the Department of the Environment.

Wilkinson SN, Kinsey-Henderson AE, Hawdon AA, Hairsine PB, Bartley R & Baker B 2018. Grazing impacts on gully dynamics indicate approaches for gully erosion control in northeast Australia. *Earth Surface Processes and Landforms* 43(8), 1711-1725.

Wilkinson SN, Rutherfurd ID, Brooks AP & Bartley R 2023. Achieving change through gully erosion research. *Earth Surface Processes and Landforms.*

Wilson GV, Wells R, Kuhnle R, Fox G & Nieber J 2018. Sediment detachment and transport processes associated with internal erosion of soil pipes. *Earth Surface Processes and Landforms* 43(1), 45-63.

Wu Y, Zheng Q, Zhang Y, Liu B, Cheng H & Wang Y 2008. Development of gullies and sediment production in the black soil region of northeastern China. *Geomorphology* 101(4), 683-691.

Xu J, Li H, Liu X, Hu W, Yang Q, Hao Y, Zhen H & Zhang X 2019. Gully erosion induced by snowmelt in Northeast China: A case study. *Sustainability* 11(7), 2088.

Xu M, Li Q & Wilson G 2016. Degradation of soil physicochemical quality by ephemeral gully erosion on sloping cropland of the hilly Loess Plateau, China. *Soil and Tillage Research* 155, 9-18.

Yang S, Guan Y, Zhao C, Zhang C, Bai J & Chen K 2019. Determining the influence of catchment area on intensity of gully erosion using high-resolution aerial imagery: A 40-year case study from the Loess Plateau, northern China. *Geoderma* 347, 90-102.

Yeh SW, Kug JS, Dewitte B, Kwon MH, Kirtman BP & Jin FF 2009. El Niño in a changing climate. *Nature* 461(7263), 511-514.

Yibeltal M, Tsunekawa A, Haregeweyn N, Adgo E, Meshesha DT, Masunaga T, Tsubo M, Billi P, Ebabu K & Liyew Berihun M 2021. Effect of subsurface water level on gully headcut retreat in tropical highlands of Ethiopia. *Earth Surface Processes and Landforms* 46(6), 1209-1222.

Yitbarek TW, Belliethathan S & Stringer LC 2012. The onsite cost of gully erosion and cost-benefit of gully rehabilitation: A case study in Ethiopia. *Land Degradation and Development* 23(2), 157-166.

Zabihi M, Mirchooli F, Motevalli A, Darvishan AK, Pourghasemi HR, Zakeri MA & Sadighi F 2018. Spatial modelling of gully erosion in Mazandaran Province, northern Iran. *Catena* 161, 1-13.

Zhang Y, Wu Y, Liu B, Zheng Q & Yin J 2007. Characteristics and factors controlling the development of ephemeral gullies in cultivated catchments of black soil region, Northeast China. *Soil and Tillage Research* 96(1-2), 28-41.

Zhao J, Van Oost K, Chen L & Govers G 2016. Moderate topsoil erosion rates constrain the magnitude of the erosion-induced carbon sink and agricultural productivity losses on the Chinese Loess Plateau. *Biogeosciences* 13(16), 4735-4750.

Zucca C, Canu A & Della Peruta R 2006. Effects of land use and landscape on spatial distribution and morphological features of gullies in an agropastoral area in Sardinia (Italy). *Catena* 68(2-3), 87-95.

APPENDICES

APPENDIX A: The generalised geology reclassification used to produce the gully susceptibility map of South Africa

Lithostratigrophy	Parent	Description	Generalized classification
		Alluvium, sand, calcrete	Coarse sedimentary
		Amphibolite, serpentinite, talc, schist, diorite, gabbro, pyroxenite	Mafic igneous/ metamorphic
		Biotite trondhjemite gneiss	Felsic igneous/ metamorphic
		Diabase	Mafic igneous/ metamorphic
		Dunite, harzburgite, pyroxenite, metagabbro, serpentinite, amphibolite, lava	Mafic igneous/ metamorphic
		Granite dyke	Felsic igneous/ metamorphic
		Granite, gneiss	Felsic igneous/ metamorphic
		Hornblendite	Mafic igneous/ metamorphic
		Leucocratic biotite granite	Mafic igneous/ metamorphic
		Potassic granite, gneiss	Felsic igneous/ metamorphic
		Pyroxenite	Mafic igneous/ metamorphic
		Syenite, syenite dyke	Felsic igneous/ metamorphic

		Ultrabasic rocks	Mafic igneous/ metamorphic
		Undifferentiated granite and gneiss	Felsic igneous/ metamorphic
		Water	Water
ACHAB	*	Gneiss, granite, calc-silicate rocks, quartzite, amphibolite	Felsic igneous/ metamorphic
ADELAIDE	BEAUFORT	Mudrock, subordinate sandstone	Coarse sedimentary
ALGOA	*	Calcareous sandstone, clastic limestone, conglomerate, coquinite	Coarse sedimentary
ALLANRIDGE	VENTERSDORP	Andesitic lavas, tuffs	Felsic igneous/ metamorphic
ALLDAYS GNEISS	BEIT BRIDGE	Grey, medium-grained, migmatitic, tonalitic-trondhjemitic gneiss	Felsic igneous/ metamorphic
ALMA	NYLSTROOM	Felspathic and lithic sandstone, subordinate conglomerate and mudrock (mainly siltstone)	Coarse sedimentary
AMSTERDAM	*	Dacite (tuffs), rhyolite	Felsic igneous/ metamorphic
AREB GNEISS	*	Quartz-biotite-feldspar augen gneiss	Felsic igneous/ metamorphic
ASBESTOS HILLS	GHAAP	Banded iron-formation, jaspilite, riebeckite-amphibolite	Mafic igneous/ metamorphic
ASSEGAAI	*	Mafic to ultramafic schists, metabasalt, metasediments (schists, banded iron-formation, quartzites, calc-silicate rocks)	Mafic igneous/ metamorphic
AUGRABIES GRANITE/GNEISS	*	Medium- to coarse-grained, foliated biotite-hornblende granite	Felsic igneous/ metamorphic
BADEROUKWE GRANITE	VORSTER	Homogeneous, coarse-grained, tonalitic biotite-muscovite granite	Felsic igneous/ metamorphic
BAK RIVER GRANITE	EENDOORN	Biotite-rich, garnetiferous granite gneiss (intrusive)	Felsic igneous/ metamorphic

BANDELIERKOP	*	Pelitic gneisses, mafic gneisses, ultramafic rocks (serpentinised pyroxenites, peridotite), all with banded iron-formation lenses.	Mafic igneous/ metamorphic
BANKE GRANODIORITE	SPEKTAKEL	Very coarse-grained megacrystic granite	Felsic igneous/ metamorphic
BANKS VLEI GNEISS	*	Biotite gneiss, augen gneiss, quartz-feldspar gneiss	Felsic igneous/ metamorphic
BAVIAANSKRANZ GRANITE	*	Alkali granite	Felsic igneous/ metamorphic
BERG RIVER	SWARTLAND	Mica and quartz schist, greywacke, thin limestone units	Fine sedimentary
BETADAM GABBRONORITE	*	Dark grey gabbronorite forming irregular vein-like intrusions as well as plutons	Mafic igneous/ metamorphic
BETHESDA	AREACHAP	Biotite-rich and pelitic gneisses, muscovite-biotite schist, subordinate amphibolite and calc-silicate rocks	Felsic igneous/ metamorphic
BIDOUW	BOKKEVELD	Three shale units separated by two sandstone units	Fine sedimentary
BIERKRAAL MAGNETITE GABBRO	RUSTENBURG LAYERED	Magnetite gabbro with layers of magnetitite and anorthosite	Mafic igneous/ metamorphic
BIESIESFONTEIN GRANITE	*	Homogeneous, medium- to coarse-grained biotite and biotite-hornblende granite	Felsic igneous/ metamorphic
BIESJE POORT	KORANNALAND	Quartzite, quartz-feldspar gneiss, calc-silicate rocks, kinzigite, subordinate marble, amphibolite and aluminous gneiss	Fine sedimentary
BITTERFONTEIN	KAMIESBERG	Quartzite, quartz-sericite schist, cordierite-sillimanite-garnet gneiss, biotite schist and gneiss, amphibolite	Fine sedimentary
BLACK REEF	TRANSVAAL	Quartzite, subordinate conglomerate and shale	Fine sedimentary
BLAUWBOSCH GRANITE	*	Medium-grained, porphyritic, unfoliated syeno-granite occurring as several small stocks	Felsic igneous/ metamorphic
BLOEMPOORT	TRANSVAAL	Mudrock, siltstone, arenite, andesitic lava, limestone/dolomite	Fine sedimentary

BLOUBERG	*	Coarse-grained sandstone (feldspathic in places), "grit", conglomerate	Coarse sedimentary
BOEGOEBERG DAM	OLIFANTSHOEK	Greenstone, quartz-chlorite-epidote schist, subgreywacke, conglomerate	Mafic igneous/ metamorphic
BOESMANSKOP SYENITE	*	Syenite	Felsic igneous/ metamorphic
BOKKEVELD	CAPE	Mudrock, sandstone	Fine sedimentary
BOTHAVILLE	VENTERSDORP	Conglomerate, "grit", quartzite, subgreywacke, shale lenses	Coarse sedimentary
BRAKWATER METAMORPHIC	*	Biotite and quartz-feldspar gneisses (including augen gneiss)	Felsic igneous/ metamorphic
BRANDKOP	VANRHYNSDORP	Mudrocks, sandstone, minor conglomerate	Fine sedimentary
BRANDWACHT	BOLAND	Greywacke, pelite, conglomerate, volcanic rocks	Coarse sedimentary
BREDASDORP	*	Limestone, sandstone, conglomerate	Carbonate
BRIDGETOWN	MALMESBURY	Greenstone with dolomite and chert lenses	Mafic igneous/ metamorphic
BRULKOLK	*	Medium-grained biotite (?) gneiss, calc-silicate rocks with lenses and layers of muscovite schist, limestone, conglomerate and amphibolite	Felsic igneous/ metamorphic
BRULSAND	VOLOP	Grey and white quartzite, subordinate shale	Coarse sedimentary
BUFFELS RIVER	COLLINGHAM	Siliceous shale, thin yellow-weathering tuff (K-bentonite) layers, subordinate siltstone and thin cherty beds	Fine sedimentary
BUFFELSFONTEIN	TRANSVAAL	Acid and basic volcanic rocks and subordinate sedimentary rocks	Mafic igneous/ metamorphic
BUFFELSKLOOF	UITENHAGE	Conglomerate, subordinate sandstone, siltstone and mudstone	Coarse sedimentary
BUFFELSKRAAL	*	Pyroxenite, carbonatite	Mafic igneous/ metamorphic
BUHLENI GNEISS	*	Granitoid gneiss (intrusive)	Felsic igneous/ metamorphic

BULAI GNEISS	BEIT BRIDGE	Porphyroblastic biotite gneiss (tonalitic)	Felsic igneous/ metamorphic
BUMBENI	*	Conglomerate, sandstone, siltstone, basaltic lava, ash-flow tuff, rhyolite, syenite, minor granite	Coarse sedimentary
CAMPBELL RAND	GHAAP	Dolomite/limestone (generally stromatolitic), subordinate chert, minor quartzite, shale and banded iron-formation	Carbonate
CANGO CAVES	*	Sandstone, shale, limestone, conglomerate lenses	Coarse sedimentary
CERES	BOKKEVELD	Three sandstone and three shale units	Coarse sedimentary
CLARENS	KAROO	Fine-grained sandstone, siltstone	Coarse sedimentary
CLEREMONT	KRANSBERG	Very coarse-grained, white sandstone with fine-grained, purple, micaceous sandstone at the base	Coarse sedimentary
CNYDAS	KEIMOES	Unfoliated, equigranular leucocratic and mesocratic granites, granodiorite, charnockite	Felsic igneous/ metamorphic
COLSTON GRANITE	KEIMOES	Weakly foliated, coarse-grained, grey biotite granite	Felsic igneous/ metamorphic
COMMONDALE	*	Mafic and ultramafic metavolcanic rocks (amphibolite, tremolite-actinolite schist, talc-magnesite schist, serpentinite) and subordinate metasedimentary rocks (iron-formation, fuchsitic quartzite, metapelite)	Mafic igneous/ metamorphic
CONCORDIA GRANITE	SPEKTAKEL	Poorly foliated leucogranite	Felsic igneous/ metamorphic
CONSTANTIA	*	Pink, leucocratic gneiss, grey augen gneiss, various granites, syenite, pyroxenite	Felsic igneous/ metamorphic
CUNNING MOOR TONALITE	*	Grey, medium-grained, equigranular tonalite	Felsic igneous/ metamorphic
CURRIES CAMP GNEISS	*	Coarse-grained to megacrystic quartz-feldspar gneiss (intrusive)	Felsic igneous/ metamorphic
DABERAS GRANODIORITE	EENDOORN	Medium- to coarse-grained charnockitic granodiorite with numerous inclusions	Felsic igneous/ metamorphic

DAGBREEK	VAALKOPPIES	Quartz-muscovite schist, quartzite, subordinate gneiss and amphibolite	Fine sedimentary
DALMEIN GRANODIORITE	*	Medium- to coarse-grained, generally porphyritic (K-feldspar phenocrysts) granite/granodiorite	Felsic igneous/ metamorphic
DAMWAL	ROOIBERG	Rhyolite with subordinate pyroclastic rocks and minor sandstone	Felsic igneous/ metamorphic
DARLING BATHOLITH	CAPE GRANITE	Granite, granodiorite	Felsic igneous/ metamorphic
DASPOORT	PRETORIA	Quartzite with minor shale and siltstone	Coarse sedimentary
DE BAKKEN GRANITE	*	Light grey, foliated, coarse-grained, porphyritic biotite granite	Felsic igneous/ metamorphic
DE HOOP	ORANGE RIVER	Predominantly calc-alkaline, acid and intermediate metavolcanic rocks and quartzitic metasediments	Felsic igneous/ metamorphic
DE KRAALEN	*	Banded iron-formation, calc-silicate gneiss, komatiitic meta-volcanic rocks, quartzite	Felsic igneous/ metamorphic
DE KRUIS	*	Calc-silicate rocks, quartz-feldspar gneiss	Felsic igneous/ metamorphic
DENNILTON	*	Gneiss, acid lava, tuff, granulitic schist	Felsic igneous/ metamorphic
DIMANE GRANITE	*	Pink, medium- to coarse-grained granite	Felsic igneous/ metamorphic
DOMINION	*	Basaltic andesite, acid lava (quartz-feldspar porphyry), subordinate quartzite	Mafic igneous/ metamorphic
DONKIEBOUD GRANITE	EENDOORN	Biotite-rich granite gneiss (intrusive), garnetiferous and/or megacrystic in places	Felsic igneous/ metamorphic
DOORNFONTEIN	MARYDALE	Amphibolite, banded iron-formation, greenstone, quartzite, limestone/dolomite	Mafic igneous/ metamorphic
DRAGHOENDER GRANITE/GNEISS	*	Light grey, coarse-grained, gneissic, biotite, biotite-muscovite and muscovite-biotite granites	Felsic igneous/ metamorphic

DRAKENSBERG	KAROO	Basaltic lava, with minor sandstone, tuff and agglomerate in the lower part of the succession in places	Mafic igneous/ metamorphic
DRAKENSBERG	KAROO	Fine-grained sandstone	Fine sedimentary
DRO ├ïBOOM	*	Gneisses, subordinate quartzite, calc-silicate rocks and amphibolites	Felsic igneous/ metamorphic
DSJATE	RUSTENBURG LAYERED	Gabbro, norite, anorthosite	Mafic igneous/ metamorphic
DUITSCHLAND	CHUNIESPOORT	Dolomite/limestone (+ chert), shale, subordinate quartzite, conglomerate and diamictite	Carbonate
DULLSTROOM	PRETORIA	Basaltic andesite, minor felsite, pyroclastic rocks, arenite and hornfels	Mafic igneous/ metamorphic
DWAALGEES GRANITE	KEIMOES	Red-brown-weathering, coarse-grained, moderately foliated, adamellitic granite	Felsic igneous/ metamorphic
DWAALHEUWEL	PRETORIA	Quartzitic sandstone, mudrock and (in the west) conglomerate	Coarse sedimentary
DWARS RIVER	RUSTENBURG LAYERED	Pyroxenite, norite, anorthosite, chromitite	Mafic igneous/ metamorphic
DWARSFONTEIN	*	Pyroxenite, gabbro, anorthosite	Mafic igneous/ metamorphic
DWYKA	KAROO	Diamictite (polymictic clasts, set in a poorly sorted, fine-grained matrix) with varved shale, mudstone with dropstones and fluvioglacial gravel common in the north	Fine sedimentary
DYASONS KLIP GNEISS	*	Brown-weathering porphyroblastic to megacrystic gneiss (intrusive)	Felsic igneous/ metamorphic
ECCA	KAROO	Sandstone, shale	Coarse sedimentary
ECCA	KAROO	Shale, carbonaceous shale	Fine sedimentary
ECCA	KAROO	Shale, with sandstone-rich units present towards the basin margins in the south, west and northeast and coal seams in the northeast	Fine sedimentary

EIERDOPPAN	AREACHAP	Conglomerate, schist	Coarse sedimentary
ELLIOT	KAROO	Red and greenish grey mudstone, subordinate sandstone	Fine sedimentary
ELSIE SE GORRA GRANITE	KEIMOES	Grey, medium-grained, well-foliated granite	Felsic igneous/ metamorphic
EMAKWEZINI	BEAUFORT	Mudrock, sandstone, minor coal seams	Fine sedimentary
EMPANGENI METAMORPHIC	*	Granoblastite, gneiss, pyroxenite, amphibolite	Felsic igneous/ metamorphic
ENON	UITENHAGE	Conglomerate, subordinate lenticular sandstones and claystones	Coarse sedimentary
ENTABENI GRANITE	*	Muscovite-biotite granite	Felsic igneous/ metamorphic
FIG TREE	BARBERTON	Greywacke, mudrock, pyroclastic rocks, lava, chert	Coarse sedimentary
FISH RIVER	NAMA	Red sandstone/quartzite, interbedded red siltstone and shale	Coarse sedimentary
FLAMINKBERG	VANRHYNSDORP	Coarse sandstone, granulestone, minor mudrock and conglomerate	Coarse sedimentary
FORT BROWN	ECCA	Rhythmite, mudrock, minor sandstone	Fine sedimentary
FRANSCHHOEK	MALMESBURY	Quartzite, conglomerate, slate	Coarse sedimentary
FRIERSDALE CHARNOCKITE	KEIMOES	Dark-weathering, fine- to medium-grained, inequigranular (locally porphyritic) charnockitic adamellite	Fine sedimentary
FUNDUDZI	SOUTPANSBERG	Sandstone (locally quartzitic), subordinate conglomerate, basaltic lava, tuff, shale and siltstone	Coarse sedimentary
GABORONE GRANITE	*	Rapakivi granite, leucogranite, granophyre, microgranite	Felsic igneous/ metamorphic
GAIS	GROOTDERM	Dolomitic marble	Carbonate
GAMAGARA	OLIFANTSHOEK	Shale, quartzite, minor conglomerate	Fine sedimentary
GAMTOOS	*	Limestone, phyllite, arenite, conglomerate	Carbonate
GANNAKOURIEP	*	Basic dyke swarm (amphibolitic diabase/hornblende diorite)	Mafic igneous/ metamorphic

GARIEP	*	Quartzite, limestone, dolomite, diamictite, schist, phylite	Coarse sedimentary
GARIEP	*	Schist, phyllite, arenite, dolomite, limestone, diamictite, lava, pyroclastic rocks, conglomerate	Fine sedimentary
GEMSBOKBULT GRANITE	KEIMOES	Grey, medium-grained, poorly foliated granite, porphyritic in places	Felsic igneous/ metamorphic
GEORGE BATHOLITH	CAPE GRANITE	Gneissic granite and granodiorite	Felsic igneous/ metamorphic
GESELSKAPBANK	*	Melanocratic cordierite-sillimanite gneiss with subordinate layers of mafic granulite and gneiss, marble, calc-silicate rock and migmatitic gneiss	Felsic igneous/ metamorphic
GHAAP	TRANSVAAL	Shale, sandstone, andesite, dolomite	Coarse sedimentary
GIF BERG GRANITE	KEIMOES	Dark grey, unfoliated, fine- to medium-grained, granophyric, porphyritic granite	Felsic igneous/ metamorphic
GIYANI	*	Ultramafic chlorite-amphibole-talc-serpentine-rich rocks and subordinate amphibolites, acid igneous rocks and sedimentary rocks	Mafic igneous/ metamorphic
GLADKOP	*	Grey gneiss, weathering reddish-brown in places	Felsic igneous/ metamorphic
GLENMORE GRANITE	*	Coarse-grained, foliated, porphyritic biotite-garnet granite	Felsic igneous/ metamorphic
GLENOVER CARBONATITE	*	Plug of biotite pyroxenites and carbonatites	Carbonate
GLENTIG	TRANSVAAL	Red and purple argillaceous rocks, fine- to medium-grained sandstone and altered lava overlain by conglomerate and grey quartz-feldspar porphyry	Fine sedimentary
GODWAN	TRANSVAAL	Amygdaloidal intermediate lava, tuff, quartzite (generally feldspathic), shale, conglomerate (at base)	Coarse sedimentary
GOEDE HOOP	KORANNALAND	Quartzite, quartz-muscovite schist, conglomerate lenses	Coarse sedimentary

GOEDGENOEG	PLATBERG	Greenish grey porphyritic and subordinate non-porphyritic mafic lava	Mafic igneous/ metamorphic
GORAAP	*	Granite	Felsic igneous/ metamorphic
GOUDINI	*	Tuff, volcanic breccia, metacarbonatite	Coarse sedimentary
GOUDPLAATS-HOUT RIVER GNEISS	*	Leucocratic, strongly migmatised biotite gneiss and greyish, weakly migmatised biotite gneiss; minor leucogneiss and dark grey biotite gneiss	Felsic igneous/ metamorphic
GOUSKOP GRANITE	KEIMOES	Leucocratic, medium-grained, weakly foliated granite	Felsic igneous/ metamorphic
GOVERNMENT	WEST RAND	Quartzite, shale, minor/subordinate conglomerate	Coarse sedimentary
GRAHAMSTOWN	*	Silcrete	Coarse sedimentary
GRAPPIES	*	Quartz-feldspar gneiss, calc-silicate rocks, amphibolite	Felsic igneous/ metamorphic
GRAVELOTTE	*	Mafic lavas, various chlorite schists, quartzites, conglomerates, "grits", porphyritic tuffs, banded iron-formation, ultramafic lavas	Mafic igneous/ metamorphic
GRAVELOTTE	*	Mafic lavas, various chlorite schists, quartzites, conglomerates, grits, porphyritic tuffs, banded iron-formation, ultramafic lavas	Mafic igneous/ metamorphic
GREYTON PLUTON	CAPE GRANITE	Granite	Felsic igneous/ metamorphic
GROBLERSHOOP	BRULPAN	Schist, subordinate quartzite and metalava (greenstone)	Fine sedimentary
GROENEFONTEIN	CANGO CAVES	Fine-grained quartz wacke, mudrock, subordinate limestone and medium- to coarse-grained arenite	Fine sedimentary
GROOTDERM	GARIEP	Metavolcanic rocks (chlorite schist, subordinate amphibolite, minor ultramafic rocks), minor dolomitic marble	Mafic igneous/ metamorphic

GUMBU	BEIT BRIDGE	Calc-silicate rocks and marble, together with leucogneisses and subordinate pink hornblende granitoid gneiss, metaquartzite and amphibolite	Carbonate	
HAIB	ORANGE RIVER	Andesitic lava, acid porphyry, volcaniclastic rocks	Mafic	igneous/ metamorphic
HALAMBU GNEISS	*	Fine- to medium-grained, granodioritic to granitic gneiss	Felsic	igneous/ metamorphic
HALFWAY HOUSE GRANITE	*	Granodiorite (porphyritic in places), gneiss, migmatite	Felsic	igneous/ metamorphic
HARMONY GRANITE	*	Light grey, coarse-grained (porphyritic in places), tonalitic, biotite-muscovite granite	Felsic	igneous/ metamorphic
HARTEBEEST PAN GRANITE	KEIMOES	Grey, fine- to medium-grained, well foliated granite, grading into augen gneiss in places	Felsic	igneous/ metamorphic
HARTLEY	OLIFANTSHOEK	Basalt/basaltic andesite, tuff, quartzite, minor conglomerate	Mafic	igneous/ metamorphic
HERMANUS PLUTON	CAPE GRANITE	Granite	Felsic	igneous/ metamorphic
HLAGOTHI	*	Harzburgite, olivine websterite, wehrlite, olivine gabbronorite, pyroxenite, gabbro, leucogabbro	Mafic	igneous/ metamorphic
HLOBANE	*	Metagabbro, serpentinite, talc schist	Mafic	igneous/ metamorphic
HOLGAT	PORT NOLLOTH	Greywacke, schist, arkose, conglomerate, impersistent limestone and quartzite	Fine sedimentary	
HOM	BUSHMANLAND	Leucocratic (light grey) biotite gneiss with intercalations of calc-silicate rocks, mafic gneiss, and a quartzite-schist association	Felsic	igneous/ metamorphic
HOOGOOR	*	Reddish-brown weathering, fine- to medium-grained quartzo-felspathic gneisses, nodular in places, with lenses of calc-silicate rock, quartzite, schist and amphibolite	Felsic	igneous/ metamorphic

HOSPITAL HILL	WEST RAND	Subequal shale and quartzite, minor conglomerate	Fine sedimentary
HOUTENBEK	PRETORIA	Hornfels, quartzite, carbonate and chert	Coarse sedimentary
HUGOMOND GRANITE	*	Grey, coarse-grained, occasionally porphyritic biotitic granite	Felsic igneous/ metamorphic
HUMBERDALE GRANITE	*	Medium- to coarse-grained, pinkish grey, foliated, felspar-porphyritic biotite granite	Felsic igneous/ metamorphic
INLANDSEE LEUCOGRANOFELS/GNEISS	*	Leucocratic quartzo-feldspathic gneiss	Felsic igneous/ metamorphic
IRRIGASIE	KAROO	Predominantly red mudstone containing one or more sandstone units towards the base	Fine sedimentary
JACOMYNS PAN	*	Schist, gneiss, calc-silicate rocks, amphibolite	Fine sedimentary
JANNELSEPAN	AREACHAP	Amphibolite, amphibole gneiss, subordinate biotite, quartz-feldspar and pelitic gneisses, calc-silicate rocks and mica schist.	Mafic igneous/ metamorphic
JEPPESTOWN	WEST RAND	Shale, quartzite, subordinate lava, minor conglomerate	Fine sedimentary
JEROME GRANITE	*	Generally pink, fine- to medium-grained hornblende-biotite granite	Felsic igneous/ metamorphic
JOHANNESBURG	CENTRAL RAND	Quartzite, subordinate conglomerate, shale and amygdaloidal lava	Coarse sedimentary
JOZINI	LEBOMBO	Acid lavas (rhyolites with some dacites), minor tuffs	Fine sedimentary
KAAIMANS	*	Quartzite, schist, phyllite	Coarse sedimentary
KAAP VALLEY TONALITE	*	Medium- to coarse-grained, homogeneous hornblende and hornblende -biotite tonalite	Felsic igneous/ metamorphic
KABIS GRANITE	LITTLE NAMAQUALAND	Porphyritic rapakivi granite, granodiorite	Felsic igneous/ metamorphic
KABOOM	*	White to light grey quartzite, subordinate schist	Coarse sedimentary

KAFFIRSKRAAL	*	Micronorite, magnetite dunite, magnetite websterite, magnetite wehrlite, magnetite clinopyroxenite, magnetitite, feldspathic pyroxenite, norite, gabbro	Mafic igneous/ metamorphic
KAKAMAS SUID GNEISS	*	Grey augen gneiss (intrusive)	Felsic igneous/ metamorphic
KALAHARI	*	Superficial deposits comprising gravels, clays, sandstone, silcrete, calcrete and aeolian sand	Coarse sedimentary
KALKWERF GNEISS	*	Red-brown, coarse-grained granite gneiss	Felsic igneous/ metamorphic
KAMEEL PUTS	*	Quartz-feldspar and biotite gneiss, amphibolite, lenses of conglomerate, calc-silicate rocks, marble and quartzite	Felsic igneous/ metamorphic
KAMEELDOORNS	PLATBERG	Shale, conglomerate, greywacke	Coarse sedimentary
KAMIESKROON GNEISS	*	Granitic gneisses with thin metapelites and quartzite	Felsic igneous/ metamorphic
KANONEILAND GRANITE	KEIMOES	Medium- to coarse-grained, moderately foliated, mesocratic granite with scattered phenocrysts	Felsic igneous/ metamorphic
KANYE	*	Rhyolite, dacite, andesite	Felsic igneous/ metamorphic
KAROO	*	Granulestone, sandstone, conglomerate, siltstone	Coarse sedimentary
KAROO	*	Sandstone, conglomerate, shale, mudstone,coal	Coarse sedimentary
KAROO	*	Sandstone, shale, coal	Coarse sedimentary
KAROO	*	Sandstone, siltstone, mudstone, shale	Coarse sedimentary
KAROO	*	Shale, sandstone, mudstone, coal	Fine sedimentary
KAROO DOLERITE	*	Network of dolerite sills, sheets and dykes, mainly intrusive into the Karoo Supergroup	Mafic igneous/ metamorphic
KEBOES GRANITE	KEIMOES	Medium-grained, moderately foliated, porphyritic granite	Felsic igneous/ metamorphic
KEES ZYN DOORNS SYENITE	*	Syenite/syenogranite	Felsic igneous/ metamorphic

KHURISBERG	BUSHMANLAND	Quartzites, schists	Coarse sedimentary
KINKELBOS	*	Silt, sand, calc-tufa, minor gravel	Felsic igneous/ metamorphic
KIRKWOOD	UITENHAGE	Variegated (reddish-brown and greenish) silty mudstone and sandstone, subordinate grey shale and sandstone	Fine sedimentary
KLEINBEGIN	KEIMOES	Medium- to coarse-grained, weakly foliated granites	Felsic igneous/ metamorphic
KLIP BAKKEN GNEISS	*	Coarse-grained to megacrystic quartz-feldspar gneiss (intrusive)	Felsic igneous/ metamorphic
KLIP KOPPIES GRANITE	KEIMOES	Grey, poorly foliated, fine- to medium-grained, porphyritic granite	Felsic igneous/ metamorphic
KLIPHEUWEL	*	Conglomerate, sandstone, mudrock	Coarse sedimentary
KLIPHOEK GRANITE	SPEKTAKEL	Coarse-grained, porphyroblastic granite	Felsic igneous/ metamorphic
KLIPPLAAT	SWARTLAND	Quartz schist, mica schist	Fine sedimentary
KLIPRAND CHARNOCKITE	LITTLE NAMAQUALAND	Charnockite, charno-enderbite, subordinate pyroxene monzonite and monzonorite	Felsic igneous/ metamorphic
KLIPRIVIERSBERG	VENTERSDORP	Tholeiitic basalt	Mafic igneous/ metamorphic
KNERSVLAKTE	VANRHYNSDORP	Mudrock, siltstone, sandstone, conglomerate	Fine sedimentary
KOEDOESRAND	*	Quartzite, conglomerate	Coarse sedimentary
KOEGAS	GHAAP	Mudrock, quartzite (quartz wacke), jaspilite, iron-formation, dolomite	Fine sedimentary
KOELMANSKOP METAMORPHIC	HARTBEES RIVER	Biotite gneiss, leucogneiss, subordinate kinzigite	Felsic igneous/ metamorphic
KOMATIPOORT	*	Granophyric gabbro, olivine gabbro, feldspathic gabbro, granophyre	Mafic igneous/ metamorphic
KONKYP GNEISS	LITTLE NAMAQUALAND	Grey, foliated (gneissic) biotite granite with large K-feldspar megacrysts	Felsic igneous/ metamorphic

KOOKFONTEIN	ECCA	Shale, siltstone, subordinate sandstone	Fine sedimentary
KORAS	*	Basic and acid lava, volcaniclastic rocks, sandstone, conglomerate	Mafic igneous/ metamorphic
KORINGKOPPIES	*	Layered, plug-like body composed by pyroxenite and serpentinite	Mafic igneous/ metamorphic
KORRIDOR	*	Alaskite, pegmatite	Felsic igneous/ metamorphic
KOTONGWENI TONALITE	*	Coarse-grained tonalite	Felsic igneous/ metamorphic
KRAAIPAN	*	Banded iron-formation, jaspilite, lava (amphibolite)	Fine sedimentary
KRANSBERG	WATERBERG	Sandstone, subordinate conglomerate, siltstone and shale	Coarse sedimentary
KRUIDFONTEIN CARBONATITE	*	Carbonatite, basalt, trachyte, andesite, rhyolite, volcanic breccia, agglomerate, ignimbrite, tuff	Carbonate
KUBOOS BATHOLITH	KUBOOS-BREMEN	Biotite granite	Felsic igneous/ metamorphic
KUIBIS	NAMA	Quartzite	Coarse sedimentary
KUILS RIVER BATHOLITH	CAPE GRANITE	Granite	Felsic igneous/ metamorphic
KWAGGASNEK	ROOIBERG	Massive, generally red, porphyritic felsite, minor pyroclastic rocks and sandstone/quartzite	Felsic igneous/ metamorphic
KWANOUS	VANRHYNSDORP	Limestone, calcareous shale	Carbonate
KWARRIEHOEK	MAKECKAAN	Feldspathic arenite, arkose, wacke, conglomerate	Coarse sedimentary
KWETTA GRANITE	*	Coarse-grained, porphyritic granite/granodiorite displaying rapakivi texture	Felsic igneous/ metamorphic
LAKENVALEI	PRETORIA	Quartzite, feldspathic quartzite, arkose	Coarse sedimentary
LANGE KOLK	*	Medium-grained, equigranular, porphyritic biotite gneiss, coarse-grained (megaporphyritic) and fine-grained quartz-feldspar gneiss	Felsic igneous/ metamorphic

LAT RIVER GRANITE	*	Light grey, medium-grained, equigranular, unfoliated biotite granite	Felsic igneous/ metamorphic
LEBOWA GRANITE	BUSHVELD	Granite	Felsic igneous/ metamorphic
LEERKRANS	WILGENHOUTSDRIF	Basic and acid volcanic rocks, schist	Mafic igneous/ metamorphic
LEEUWPOORT	PRETORIA	Quartzite and shale	Coarse sedimentary
LEKKERSMAAK GRANITE	VORSTER	Grey, medium-grained (porphyritic in places), granodioritic biotite-muscovite granite	Felsic igneous/ metamorphic
LETABA	LEBOMBO	Basic volcanic rocks (tholeiites, picrite basalts and nephelinites)	Mafic igneous/ metamorphic
LEYDSDORP	GRAVELOTTE	Mafic metalavas (tholeiitic) with interbedded banded iron-formation, quartz-chlorite schist and quartz porphyry	Mafic igneous/ metamorphic
LIEFDOOD GRANITE	KEIMOES	Light grey, fine- to medium-grained, weakly foliated granite	Felsic igneous/ metamorphic
LISBON	KAROO	Red mudstone and siltstone, minor sandstone	Fine sedimentary
LOSBERG	*	Harzburgite, norite, gabbro, granophyre	Mafic igneous/ metamorphic
LOSKOP	TRANSVAAL	Mudrock, sandstone, conglomerate, volcanic rocks	Fine sedimentary
LOUISVALE GRANITE	KEIMOES	Light grey, moderately to well foliated biotite granite	Felsic igneous/ metamorphic
LUNSKLIP GRANITE	MASHASHANE	Pink, medium- to coarse-grained, hornblende-biotite granite	Felsic igneous/ metamorphic
LUTZPUTS GNEISS	*	Sillimanite- and garnet-bearing granitic gneiss	Felsic igneous/ metamorphic
MABILIGWE	SOUTPANSBERG	Sandstone/quartzite (locally conglomeratic), subordinate tuff and shale, basal conglomerate	Coarse sedimentary
MACALA	*	Pyroxenite, gabbro, hornblendite, talc schist, serpentinite	Mafic igneous/ metamorphic

MACHADODORP	SILVERTON	Tuff and agglomerate overlain by pillow basalt	Coarse sedimentary
MADIAPALA SYENITE	BEIT BRIDGE	Syenite (metasyenite)	Felsic igneous/ metamorphic
MAGALIESBERG	PRETORIA	Quartzite, minor shale;	Coarse sedimentary
MAHLONGWA GRANITE	*	Pink, very coarse-grained, megacrystic granite	Felsic igneous/ metamorphic
MAKATINI	ZULULAND	Sandstone, siltstone, conglomerate	Coarse sedimentary
MAKGANYENE	POSTMASBURG	Diamictite, subordinate sandstone, carbonate rock, jaspilite, mudrock, chert and conglomerate	Fine sedimentary
MAKHUTSWI GNEISS	*	Homogeneous, light grey (leucocratic) medium-grained granodioritic/tonalitic biotite gneiss	Felsic igneous/ metamorphic
MAKWASSIE	PLATBERG	Acid lavas (mainly quartz porphyry), ash flows, subordinate sediments	Felsic igneous/ metamorphic
MALALA DRIFT GNEISS	BEIT BRIDGE	Leucogneiss with metaquartzite, hornblende granitoid gneiss, amphibolite, metapelite and calc-silicate rocks	Coarse sedimentary
MALMANI	CHUNIESPOORT	Dolomite, subordinate chert, minor carbonaceous shale, limestone and quartzite	Carbonate
MALVERNIA	*	Basal conglomerate overlain by sandstone with occasional pebbles and subordinate marl and limestone	Coarse sedimentary
MAMBULU	*	Almost circular intrusive body, comprising mainly medium-grained gabbro and subordinate norite	Mafic igneous/ metamorphic
MAPUMULO	*	Heterogenous layered paragneisses and migmatites with a wide compositional range	Felsic igneous/ metamorphic
MAPUTALAND	*	Calcarenite, clayey sand, red and grey dune sand, limestone, conglomerate	Carbonate
MARANDA GRANITE	*	Leucocratic, massive, medium-grained muscovite granite	Felsic igneous/ metamorphic

MARGATE GRANITE	*	Gneissose leucogranites and leucocharnockites, characteristically garnetiferous	Felsic igneous/ metamorphic
MASHISHIMALE	*	Biotite- and biotite-hornblende granites	Felsic igneous/ metamorphic
MATLABAS	WATERBERG	Granulestone, conglomerate, sandstone	Coarse sedimentary
MATLABAS	WATERBERG	Sandstone, mudstone	Coarse sedimentary
MATLALA GRANITE	*	Grey to pink, fine- to coarse-grained (porphyritic in places), granodioritic biotite granite	Felsic igneous/ metamorphic
MATOK GRANITE	*	Pink to grey, coarse-grained, porphyritic biotite (in places hornblende) granite/granodiorite and subordinate charnockitic rocks (enderbite and charno-enderbite)	Felsic igneous/ metamorphic
MATSAP	VOLOP	Brown and subordinate grey quartzites	Coarse sedimentary
MBOTYI	*	Breccia/conglomerate, greenish sandstone	Coarse sedimentary
MEINHARDSKRAAL GRANITE	*	Pink to red, fine- to medium-grained biotite granite, minor grey granite and granophyre	Felsic igneous/ metamorphic
MESKLIP GNEISS	LITTLE NAMAQUALAND	Mesocratic, coarse-grained, augen biotite gneiss	Felsic igneous/ metamorphic
MESSINA	BEIT BRIDGE	Meta-anorthosite, metaleucogabbro, metagrabbo, metapyroxenite	Mafic igneous/ metamorphic
MFONGOSI	*	Schist, subordinate amphibolite, quartzite and iron-formation	Fine sedimentary
MKOMAZI GNEISS	*	Coarse-grained, megacrystic, granitic biotite-garnet augen gneiss	Felsic igneous/ metamorphic
MKONDENI DIORITE	*	Medium-grained, biotite-bearing dioritic rocks	Felsic igneous/ metamorphic
MLALAZI	*	Serpentinite, ultramafic schist, metagabbro, minor gneiss and amphibolite	Mafic igneous/ metamorphic
MNGAZANA	*	Conglomerate, sandstone, siltstone, limestone	Coarse sedimentary

MODDERFONTEIN GRANITE/GNEISS	LITTLE NAMAQUALAND	Augen biotite granite	Felsic igneous/ metamorphic
MODDERGAT GNEISS	*	Biotite gneisses (including coarse-grained augen gneiss), calc-silicate lenses	Felsic igneous/ metamorphic
MODIPE	*	Basic (and ultrabasic?) intrusive rocks (gabbro, etc.)	Mafic igneous/ metamorphic
MOLENDRAAI MAGNETITE GABBRO	RUSTENBURG LAYERED	Magnetite gabbro with magnetitite layers	Mafic igneous/ metamorphic
MOLETSI GRANITE	*	Grey to pink, medium-grained porphyritic or coarse-grained granodioritic biotite granite	Felsic igneous/ metamorphic
MOLTENO	KAROO	Alternating sandstone (pebbly in places), olive mudstone and dark grey shale (containing plant remains) with coal seams and thin conglomerates in places	Coarse sedimentary
MOODIES	BARBERTON	Sandstone/quartzite, shale, conglomerate, minor jaspilite	Coarse sedimentary
MOORREESBURG	SWARTLAND	Greywacke, phyllite, schist, limestone	Coarse sedimentary
MOSITA GRANITE	*	Pinkish, coarse-grained, porphyritic granite	Felsic igneous/ metamorphic
MOUNT DOWE	BEIT BRIDGE	Metaquartzite, leucogneiss, pink biotite-hornblende granitoid gneiss	Felsic igneous/ metamorphic
MOVENE	LEBOMBO	Basaltic and subordinate rhyolitic lavas	Mafic igneous/ metamorphic
MOZAAN	PONGOLA	Shale, quartzite, minor lava	Fine sedimentary
MPAGENI GRANITE	*	Pink, coarse-grained, porphyritic, potassic granite	Felsic igneous/ metamorphic
MPILO	BUMBENI	Trachybasaltic and trachyandesitic lavas	Mafic igneous/ metamorphic
MPULUZI GRANITE	*	Medium- to coarse-grained quartz monzonite	Felsic igneous/ metamorphic

MSIKABA	*	White, coarse-grained, siliceous quartz arenite (pebbly in places)	Coarse sedimentary
MSWATI GRANITE	*	Coarse-grained, generally porphyritic granite	Felsic igneous/ metamorphic
MULATI	GRAVELOTTE	Mafic and ultramafic lavas, felsic tuffs	Mafic igneous/ metamorphic
MZAMBA	*	Mudrock, sandstone, shelly limestone, basal conglomerate (with fossil logs)	Fine sedimentary
MZIMKULU	*	Marbles and metapelitic, metabasic and calc-silicate paragneisses	Felsic igneous/ metamorphic
MZIMLILO GRANITE	*	Medium- to coarse-grained, leucocratic, typically mesocrystic granite gneiss	Felsic igneous/ metamorphic
MZINENE	ZULULAND	Siltstone with shelly and concretionary layers	Fine sedimentary
MZUMBE GRANITOID	*	Layered, medium- to coarse-grained, grey, gneissic quartz diorite, tonalite, trondhjemite and granodiorite	Felsic igneous/ metamorphic
NAAB	*	Grey-weathering , coarse-grained, megacrystic granite with idiomorphic k-feldspar megacrysts; dark-grey-weathering, medium-grained granodioritic granite	Felsic igneous/ metamorphic
NABABEEP GNEISS	LITTLE NAMAQUALAND	Intrusive, grey (brown-weathering) augen gneiss (biotite granite)	Felsic igneous/ metamorphic
NAKANAS	BUSHMANLAND	Micaceous almandine-staurolite-kyanite schist, quartzite	Coarse sedimentary
NARDOUW	TABLE MOUNTAIN	Quartzitic sandstone, minor shale	Coarse sedimentary
NATAL	*	Generally reddish, feldspathic and micaceous sandstone with subordinate quartz arenite, mudrock, granulestone and conglomerate	Coarse sedimentary
NEDERHORST	PRETORIA	Shale/hornfels and minor carbonate rocks overlain in the south by argillaceous quartzite and arkose	Fine sedimentary
NEILERS DRIFT GRANITE	KEIMOES	Weakly foliated, slightly porphyritic biotite granite	Felsic igneous/ metamorphic

NELSPRUIT	*	Coarse-grained, porphyritic granodiorite/adamellite, grading into granodioritic gneiss and migmatite	Felsic igneous/ metamorphic
NGOYE	*	Alkaline to peralkaline granitoid gneisses	Felsic igneous/ metamorphic
NGWANE GNEISS	*	Tonalite gneiss	Felsic igneous/ metamorphic
NONDWENI	*	Metavolcanic rocks (mainly komatiitic basalt and andesite), minor chert	Mafic igneous/ metamorphic
NOOITGEDACHT CARBONATITE	*	Plug (and dykes?) of carbonatite and minor nepheline syenite	Carbonate
NORREE	MALMESBURY	Phyllite, greywacke quartzite, limestone, dolomite, "grit	Felsic igneous/ metamorphic
NOUDAP GNEISS	*	Biotite-hornblende augen gneiss	Felsic igneous/ metamorphic
NOUZEES	*	Olivine gabbro and gabbro	Mafic igneous/ metamorphic
NSUZE	PONGOLA	Lavas (mostly basaltic), quartzites	Mafic igneous/ metamorphic
NTABENE	KAROO	Fine- to coarse-grained sandstone (granuly in places), subordinate mudrock	Coarse sedimentary
NTINGWE	*	Conglomerate and breccia, mudrock, limestone	Coarse sedimentary
NUMEES	PORT NOLLOTH	Massive diamictite and minor ferruginous metasedimentary rocks	Fine sedimentary
NUWEFONTEIN GRANITE	SPEKTAKEL	Pink-weathering, medium-grained, hornblende-bearing granite	Felsic igneous/ metamorphic
NYOKA	KAROO	Red mudrock and interbedded sandstones	Fine sedimentary
NZHELELE	SOUTPANSBERG	Quartzitic sandstone, shale (generally red), tuff, lavas	Coarse sedimentary
NZIMANE GRANITE	*	Coarse-grained, porphyritic biotite granite/granodiorite, fine- to medium-grained granite.	Felsic igneous/ metamorphic

OLIFANTSHOEK	*	Quarzite, limestone, shale, andesite	Coarse sedimentary
ONGELUK	POSTMASBURG	Andesitic and basaltic lava with abundant pillows, minor jasper	Mafic igneous/ metamorphic
ONVERWACHT	BARBERTON	Ultramafic to felsic lavas, pyroclastic rocks	Mafic igneous/ metamorphic
ORANJEMUND	GARIEP	Quartz-feldspar gneiss (metamorphosed greywacke or feldspathic quartzite), quartz-chlorite-sericite schists (partly metabasalts?)	Felsic igneous/ metamorphic
ORIBI GORGE GRANITOID	*	A number of plutons comprising very coarse-grained, porphyritic rapakivi granite and charnockite	Felsic igneous/ metamorphic
PAARDEBERG GRANITE	CAPE GRANITE	Unfoliated, fine-grained, equigranular, leucocratic granite in the Malmesbury Batholith	Felsic igneous/ metamorphic
PAARL PLUTON	CAPE GRANITE	Granite	Felsic igneous/ metamorphic
PALALA GRANITE	*	Biotite granite	Felsic igneous/ metamorphic
PALMIETFONTEIN GRANITE	*	Stock-like bodies of unfoliated, light grey to light brown, medium-grained muscovite granite	Felsic igneous/ metamorphic
PENGE	CHUNIESPOORT	Iron-formation	Carbonate
PHALABORWA	*	Pyroxenite, syenite, pegmatoids, carbonatite	Mafic igneous/ metamorphic
PIENAARS RIVER	*	Syenite, nepheline syenite, trachyandesite, tuff, breccia, carbonatite	Felsic igneous/ metamorphic
PIETERMARITZBURG	ECCA	Shale with thin siltstones and sandstones in the uppermost part	Fine sedimentary
PIETERSBURG	*	Ultramafic and mafic lava, quartzite, conglomerate, chlorite schist	Mafic igneous/ metamorphic
PIKETBERG	BOLAND	Phyllitic shale, greywacke, subordinate limestone	Felsic igneous/ metamorphic

PILANESBERG	*	Foyaite	Felsic igneous/ metamorphic
PILANESBERG	*	Lava	Mafic igneous/ metamorphic
PILANESBERG	*	Syenite	Felsic igneous/ metamorphic
PLATBERG	VENTERSDORP	Lava (mainly andesite and quartz porphyry), shale, quartzite, conglomerate	Felsic igneous/ metamorphic
POLIESBERG	*	Calc-silicate rocks, subordinate amphibolite and gneiss	Carbonate
POMPEY GRANITE	VORSTER	Light grey, medium-grained, granodioritic/adamellitic biotite-muscovite granite	Felsic igneous/ metamorphic
PORTERVILLE	BOLAND	Phyllitic shale, greywacke, limestone, arenite	Fine sedimentary
PRETORIA	TRANSVAAL	Andesite, conglomerate	Coarse sedimentary
PRETORIA	TRANSVAAL	Pebbly quartzite, feldspathic quarzite, micaceous shale, quartzite, hornfels	Coarse sedimentary
PRETORIA	TRANSVAAL	Quartzite, siltstone, conglomerate, shale	Coarse sedimentary
PRETORIA	TRANSVAAL	Quartzite, siltstone, conglomerate, shale, andesite	Coarse sedimentary
PRETORIA	TRANSVAAL	Quarzite, mudstone, siltstone	Coarse sedimentary
PRETORIA	TRANSVAAL	Shale, quartzite, conglomerate, breccia, diamictite	Fine sedimentary
PRIESKASPOORT	MARYDALE	Conglomerate and subgreywacke overlain by lava and tuff	Coarse sedimentary
PRINCE ALBERT	ECCA	Dark-grey mudrock	Fine sedimentary
PRYNNSBERG	BRULPAN	Muscovite quartzite, schist	Fine sedimentary
PYPKLIP GRANITE	KEIMOES	Brown-weathering, medium- to coarse-grained, moderately foliated biotite granite, porphyritic in places	Felsic igneous/ metamorphic
PYRAMID GABBRO-NORITE	RUSTENBURG LAYERED	Gabbro and norite with interlayered anorthosite	Mafic igneous/ metamorphic
RASHOOP GRANOPHYRE	BUSHVELD	Homogenous granophyre (predominant), granophyric granite, granophyre porphyry, pseudogranophyre	Felsic igneous/ metamorphic

RATEL DRAAI	AREACHAP	Kinzigite	Felsic igneous/ metamorphic
RAYTON	PRETORIA	Quartzite, shale, subordinate subgreywacke	Fine sedimentary
RICHTERSVELD	*	Syenite, granite	Felsic igneous/ metamorphic
RIEMVASMAAK GNEISS	*	Pink-weathering granular or augen quartz-feldspar gneiss	Felsic igneous/ metamorphic
RIETBERG GRANITE	SPEKTAKEL	Non-foliated, porphyritic, biotite-bearing granite	Felsic igneous/ metamorphic
RIETFONTEIN	*	Olivine gabbro, alkali granite, wehrlite, troctolite, picrogabbro	Mafic igneous/ metamorphic
RIETGAT	PLATBERG	Andesite to dacitic lava, minor conglomerate, greywacke and shale	Felsic igneous/ metamorphic
RINKHALSKOP	ROOIBERG	Arenite, wacke, diamictite, volcanic breccia, andesitic lava	Coarse sedimentary
ROBERTSON PLUTON	CAPE GRANITE	Granite	Felsic igneous/ metamorphic
ROK OPTEL GRANITE	KEIMOES	Medium- to coarse-grained, weakly foliated, porphyritic biotite granites	Felsic igneous/ metamorphic
ROODEKRAAL	*	Andesite, diorite, albitite	Mafic igneous/ metamorphic
ROOIBERG	TRANSVAAL	Felsite, basaltic andesite (lower part), minor shale and agglomerate	Felsic igneous/ metamorphic
ROOIPUTS GRANOPHYRE	*	Grey, medium-grained, unfoliated granophyre	Felsic igneous/ metamorphic
ROOIWATER	*	Gabbroic rocks, diorite	Mafic igneous/ metamorphic
ROOSSENEKAL	RUSTENBURG LAYERED	Olivine diorite, magnetite gabbro, gabbronorite	Mafic igneous/ metamorphic
ROSYNTJIEBERG	ORANGE RIVER	Quartzite, ferruginous quartzite, schist, metavolcanic rocks	Coarse sedimentary

RUBBERVALE	GRAVELOTTE	Felsic to mafic lavas and tuffs	Mafic igneous/ metamorphic
RUST DE WINTER	TRANSVAAL	Sandstone, conglomerate, minor shale and rhyolite	Coarse sedimentary
RUSTENBURG LAYERED	BUSHVELD	Bronzite, harzburgite, norite	Mafic igneous/ metamorphic
RUSTENBURG LAYERED	BUSHVELD	Gabbro, norite	Mafic igneous/ metamorphic
SABIE SANDS GRANOPHYRE	*	Granophyric quartz gabbro	Mafic igneous/ metamorphic
SALDANHA BATHOLITH	CAPE GRANITE	Granite, quartz-monzonite, quartz-porphyry	Felsic igneous/ metamorphic
SALIE SLOOT	MAKECKAAN	Claystone, siltstone	Fine sedimentary
SALISBURY KOP GRANITE	*	Medium- to coarse-grained, generally porphyritic (K-feldspar phenocrysts) granite/granodiorite	Felsic igneous/ metamorphic
SAND RIVER GNEISS	*	Grey migmatitic and leucocratic hypersthene-bearing gneisses	Felsic igneous/ metamorphic
SANDNOUTE	*	Pelitic gneiss, schist, quartzite, garnetiferous gneiss, amphibole gneiss	Felsic igneous/ metamorphic
SANDVELD	*	Calcareous sand/sandstone, gravel, limestone, phosphorite, silt, clay	Coarse sedimentary
SCHELM HOEK	ALGOA	Unconsolidated calcareous sand (coasted dunes), minor palaeosols	Coarse sedimentary
SCHIEL ALKALINE	*	Syenite, quartz syenite and subordinate hornblende granite, phoscorite and gabbro	Felsic igneous/ metamorphic
SCHILPADNEST	RUSTENBURG LAYERED	Pyroxenite, leuconorite, anorthosite, chromitite	Mafic igneous/ metamorphic
SCHMIDTSDRIF	GHAAP	Shale, dolomite	Mafic igneous/ metamorphic

SCHRIKKLOOF	ROOIBERG	Fine-grained, flow-banded, porphyritic and spherulitic felsite	Mafic igneous/ metamorphic
SCHUITDRIFT GNEISS	*	Well-foliated, biotite-hornblende augen gneiss	Felsic igneous/ metamorphic
SCHURWEDRAAI	*	Alkali granite	Mafic igneous/ metamorphic
SCHWARZRAND	NAMA	Shale, quartzite, limestone	Fine sedimentary
SELONS RIVER	ROOIBERG	Red porphyritic rhyolite	Felsic igneous/ metamorphic
SEZELA	*	Pink and grey, medium- to coarse-grained, subequigranular syenitoids (quartz monzonite, monzonite, syenite, quartz syenite, granite)	Felsic igneous/ metamorphic
SHAMIRIRI GRANITE	*	Grey, massive, medium- to coarse-grained, porphyritic, generally granodioritic biotite granite	Felsic igneous/ metamorphic
SHIRINDI GRANITE	*	Grey, leucocratic, medium-grained, tonalitic, hornblende-biotite granite	Felsic igneous/ metamorphic
SILVERTON	PRETORIA	Shale, minor limestone/dolomite, basalt and tuff	Fine sedimentary
SITHILO SERPENTINITE-TALC	*	Serpentinite, talc schist	Mafic igneous/ metamorphic
SKALKSEPUT GRANITE	*	Light grey, weakly foliated, medium- to coarse-grained, homogeneous porphyritic biotite-muscovite granite	Felsic igneous/ metamorphic
SKEERHOK GRANITE	KEIMOES	Yellowish-weathering, medium-grained granite	Felsic igneous/ metamorphic
SKOORSTEENBERG	ECCA	Mudrock and siltstone with up to five prominent sandstone units	Fine sedimentary
SMELTERSKOP	PRETORIA	Feldspathic quartzite, andesitic lava	Coarse sedimentary
SMITSKRAAL GRANITE	*	Cluster of small bodies of pink, coarse-grained biotite granite	Felsic igneous/ metamorphic

SOLITUDE	KAROO	Grey, purple (in upper part) and green mudrock, subordinate siltstone and sandstone	Fine sedimentary
SOUT RIVER	*	Fine- to medium-grained biotite gneiss, muscovite gneiss and sillimanite-bearing gneisses	Felsic igneous/ metamorphic
SOUTPANSBERG	*	Basalt, tuff, sandstone, conglomerate	Mafic igneous/ metamorphic
SOUTPUTS	*	Siliceous calc-silicate rocks with lenses and layers of amphibolite, quartzite and conglomerate	Carbonate
SPIOENKOP	*	Quartzite, quartz-sericite schist, paragneiss, subordinate amphibolite and metagabbro	Coarse sedimentary
SPITSKOP	*	Ijolite, nepheline syenite, pyroxenite, carbonatite, fenite	Felsic igneous/ metamorphic
SPRIGG	AREACHAP	Quartz-feldspar-biotite-muscovite schist, subordinate garnet-sillimanite-biotite gneiss, quartzite and conglomerate	Fine sedimentary
ST LUCIA	ZULULAND	Fossiliferous glauconitic siltstone and fine-grained sandstone, conglomeratic towards the base	Fine sedimentary
STALHOEK	*	Leucocratic biotite gneiss, quartz-feldspar gneiss	Felsic igneous/ metamorphic
STAVOREN GRANOPHYRE	RASHOOP GRANOPHYRE	Pyroxenite, gabbro, anorthosite	Mafic igneous/ metamorphic
STAYT	SOUTPANSBERG	Basalt overlain by shale and capped by quartzite and conglomerate	Mafic igneous/ metamorphic
STEENKAMPSBERG	PRETORIA	Quartzite, minor shale	Fine sedimentary
STELLENBOSCH BATHOLITH	CAPE GRANITE	Granite	Felsic igneous/ metamorphic
STINKFONTEIN	PORT NOLLOTH	Carbonate-free succession (feldspathic and subordinate quartz arenites, subordinate quartz-mica schist, minor metavolcanic rocks and conglomerate)	Felsic igneous/ metamorphic

STOLZENFELS ENDERBITE	*	Poorly foliated, fine- to coarse-grained charnockite	Felsic igneous/ metamorphic
STRANDVELD	BREDASDORP	Unconsolidated dune sand	Coarse sedimentary
STRAUSSBURG GRANITE	KEIMOES	Grey, coarse-grained, inequigranular, moderately foliated biotite granite with numerous xenoliths	Felsic igneous/ metamorphic
STRUBENKOP	PRETORIA	Shale, subordinate siltstone, minor quartzite	Fine sedimentary
STYGER KRAAL SYENITE	SPEKTAKEL	Porphyritic biotite syenite	Felsic igneous/ metamorphic
SULTANAOORD	VAALKOPPIES	Massive quartzite, subordinate phyllite	Coarse sedimentary
SUNDAYS RIVER	UITENHAGE	Grey shale, siltstone and sandstone	Fine sedimentary
SUTHERLAND	*	Volcanic breccia, tuff, trachyte, carbonatite, melilite basalt	Coarse sedimentary
SUURBERG	*	Basaltic lava, tuff, breccia/conglomerate, minor sandstone and mudrock	Mafic igneous/ metamorphic
SWAERSHOEK	NYLSTROOM	Medium- to coarse-grained sandstone (pebbly in places), conglomerate, trachytic lava, quartz porphyry	Fine sedimentary
SWANARTZ GNEISS	*	Porphyroblastic biotite gneiss	Felsic igneous/ metamorphic
SWARTBANK GRANITE	KUBOOS-BREMEN	Coarse-grained, porphyritic granite/granodiorite	Felsic igneous/ metamorphic
T'OUBEP	*	Biotite granite, granodiorite, tonalite	Felsic igneous/ metamorphic
TABLE MOUNTAIN	CAPE	Quartzitic sandstone	Coarse sedimentary
TABLE MOUNTAIN	CAPE	Quarzitic sandstone, shale	Coarse sedimentary
TARKASTAD	BEAUFORT	Red and greenish-grey mudstone, fine- to medium-grained sandstone	Fine sedimentary
TATASBERG	KUBOOS-BREMEN	Granite, syenite, nepheline syenite	Felsic igneous/ metamorphic
THOLE	*	Harzburgite, pyroxenite, gabbronorite	Mafic igneous/ metamorphic

TIERBERG	ECCA	Grey shale with interbedded siltstones in the upper part	Fine sedimentary
TIMBAVATI GABBRO	*	Gabbro, olivine gabbro, quartz gabbro	Mafic igneous/ metamorphic
TRAKA	BOKKEVELD	Shale, siltstone, minor sandstone	Fine sedimentary
TSAWELA GNEISS	*	Mesocratic hornblende-biotite tonalite gneiss	Felsic igneous/ metamorphic
TSHOKWANE GRANOPHYRE	*	Sill-like bodies and dykes of granophyre	Mafic igneous/ metamorphic
TUGELA	*	Amphibolite, gneiss, schist, metapelite, quartzite, marble	Mafic igneous/ metamorphic
TUGELA RAND LAYERED	*	Well-layered association of medium-grained mafic and ultramafic rocks (wehrlite, gabbronorite, clinopyroxenite, bronzitite, iherzolite, troctolite, serpentinite, websterite and up to 1% chromitite)	Mafic igneous/ metamorphic
TUINS GRANITE	*	Granite	Felsic igneous/ metamorphic
TURFFONTEIN	CENTRAL RAND	Quartzite, conglomerate	Coarse sedimentary
TURFLOOP GRANITE	*	Grey to pink, medium- to coarse-grained, adamellitic/granodioritic biotite granite	Felsic igneous/ metamorphic
TWEERIVIER CARBONATITE	*	Carbonatite, fenite, gabbro	Carbonate
TYGERBERG	MALMESBURY	Shale, greywacke, quartzite, minor volcanic rocks	Fine sedimentary
UITDRAAI	BRULPAN	Grey quartzite, subordinate quartz-sericite schist	Fine sedimentary
UITLOOP GRANITE	MASHASHANE	Reddish, fine- to coarse-grained biotite granite	Felsic igneous/ metamorphic
USUSHWANA	*	Quartz gabbro, ferrogabbro, granodiorite, microgranite	Mafic igneous/ metamorphic
UTRECHT GRANITE	*	Pink, fine-grained, granodioritic biotite granite	Felsic igneous/ metamorphic

VAALFONTEIN GNEISS	*	Fine- to very coarse-grained, megacrystic gneisses	Felsic igneous/ metamorphic
VAALHOEK GRANITE	*	Grey-weathering, foliated, fine- to medium-grained, porphyritic granite and dark-weathering, coarse-grained, porphyritic biotite granite	Felsic igneous/ metamorphic
VAALPUTS GRANITE	KEIMOES	Grey, well-foliated, medium-grained, locally porphyritic adamellitic granite with abundant xenoliths	Felsic igneous/ metamorphic
VAALWATER	KRANSBERG	Fine- to medium-grained, feldspathic sandstone, siltstone, shale	Coarse sedimentary
VAN WYKS PAN	AREACHAP	Grey, medium-grained, granoblastic quartz-feldspar gneiss with lenses of amphibolite, calc-silicate rocks and metapelite	Felsic igneous/ metamorphic
VERMONT	PRETORIA	Metamorphosed mudstone and shale with minor quartzite, dolomite and chert	Fine sedimentary
VILLA NORA GABBRO-ANORTHOSITE	RUSTENBURG LAYERED	Magnetite gabbro, anorthosite, magnetitite	Mafic igneous/ metamorphic
VIOOLSDRIF	*	Granodiorite, adamellite, leucogranite, tonalite, diorite, minor basic to ultrabasic rocks	Felsic igneous/ metamorphic
VLAKFONTEIN	RUSTENBURG LAYERED	Pyroxenite, harzburgite, norite	Mafic igneous/ metamorphic
VO ├ïLWATER	POSTMASBURG	Dolomite, jasper, iron-formation, chert, minor lava	Carbonate
VOLKSRUST	ECCA	Mudrock	Fine sedimentary
VREDENBURG BATHOLITH	CAPE GRANITE	Coarse-grained, porphyritic granite (monzogranite / quartz monzonite)	Felsic igneous/ metamorphic
VRYBURG	TRANSVAAL	Quartzitic sandstone, mudrock, andesitic/basaltic lava, siltstone, clastic dolomite/limestone, minor conglomerate, tuff and chert	Coarse sedimentary
VRYHEID	ECCA	Fine- to coarse-grained sandstone, shale, coal seams	Coarse sedimentary

VYFBEKER METAMORPHIC	HARTBEES RIVER	Migmatitic rocks (biotite gneiss, leucogneiss, pelitic gneiss, subordinate amphibolite), calc-silicate rocks, marble and quartzite	Felsic igneous/ metamorphic
WACHTEENBEETJE	TRANSVAAL	Mudrock, siltstone, quartz arenite, subordinate conglomerate/diamictite, minor dolomite and andesitic lava	Fine sedimentary
WATERFORD	ECCA	Sandstone, rhythmite, shale, mudstone - wave ripple marks and slumping common	Coarse sedimentary
WATERKOP	*	Syenite, granite, mangerite, jotunite	Felsic igneous/ metamorphic
WELLINGTON PLUTON	CAPE GRANITE	Granite	Felsic igneous/ metamorphic
WHITEHILL	ECCA	Black (white-weathering) carbonaceous shale	Carbonate
WILGE RIVER	WATERBERG	Reddish-brown and purple, medium- to coarse-grained sandstone, subordinate conglomerate, minor shale	Coarse sedimentary
WILLIE GRANITE	VORSTER	Grey, medium-grained, porphyritic, granodioritic muscovite-biotite granite	Felsic igneous/ metamorphic
WITTEBERG	CAPE	Quartzitic sandstone, siltstone, shale	Coarse sedimentary
WITTEBERG	CAPE	Shale, sandstone, diamictite	Fine sedimentary
WITWATER GNEISS	KOELMANSKOP METAMORPHIC	Fine- to coarse-grained, garnetiferous, mica-poor leucogneiss, pegmatitic in places	Felsic igneous/ metamorphic
WITWATERSRAND	*	Quartzite, shale, conglomerate, minor lava and diamictite	Coarse sedimentary
WOLKBERG	TRANSVAAL	Shale, quartzite, arkose, subgreywacke, conglomerate, basalt, pyroclastic rocks	Fine sedimentary
WYLLIE'S POORT	SOUTPANSBERG	Reddish or brown, medium- to coarse-grained sandstone and quartzite, minor conglomerate, basaltic lava and tuff	Coarse sedimentary
YZERFONTEIN GABBRO-MONZONITE	*	Diorite, subordinate gabbro	Mafic igneous/ metamorphic

ZEEKOEBAART	*	Andesite, dacite, tuff, minor sedimentary rocks	Mafic igneous/ metamorphic
ZOETVELD	RUSTENBURG LAYERED	Pyroxenite, harzburgite, chromitite	Mafic igneous/ metamorphic
ZONDERHUIS	WILGENHOUTSDRIF	Quartzite, phyllite, schist, dolomite, conglomerate	Coarse sedimentary

APPENDIX B: 60 gully location mapped as (x, y) points (the gully sites are in Figure 3.2)**.**

Number	Author	X	Y	Activity
1	Dardis & Beckedahl, 1988a (p.285)	31.07182	-25.84610	Active
2	Dardis & Beckedahl, 1988b (p.229)	28.53119	-31.53818	Active
3		28.75878	-31.83928	Active
4		28.53887	-31.55820	Active
5	Liggit & Fincham, 1989	31.26781	-28.38352	Partial
6	Dardis & Beckedahl, 1991	28.23660	-31.40072	Partial
7		28.23868	-31.41382	Partial
8		28.25327	-31.42495	Active
9		Same as Dardis & Beckedahl, 1988		
10	Brady, 1993	28.64230	-28.50091	Active
11		28.65046	-28.50981	Active
12		28.64628	-28.51043	Active
13		28.63124	-28.51365	Active
14		28.63223	-28.50505	Active
15		28.57113	-28.51311	Active
16	Cobban & Weaver, 1993	26.46489	-32.16477	Partial
17	Botha et al., 1994	30.67223	-28.10009	Active
18		30.75912	-28.28318	Partial
19		30.33657	-28.20789	Partial
20		30.61845	-28.33242	Partial
21		30.15580	-28.92662	Active
22		30.55436	-28.32055	Active
23		30.65650	-28.16592	Active
24		31.18878	-27.57998	Active
25	Watson and Ramokgopa, 1996	30.70131	-28.14847	Partial
26	Morel, 1998	18.85977	-33.43191	Stable
27	Flügel et al., 1999	29.65809	-29.61719	Partial
28	Rienks et al., 2000	Same as Botha et al., 2017		
29	Boardman et al., 2003	24.56623	-31.68465	Active
30	Meadows, 2003	Same as Morel, 1998		
31	Keay-Bright & Boardman, 2006	Same as Boardman et al., 2003		
32	Keay-Bright & Boardman, 2007	Same as Boardman et al., 2003		
33	Boardman and Foster, 2008	Same as Boardman et al., 2003		
34	Taruvinga, 2008	30.16959	-27.95631	Partial
35		30.43018	-27.82492	Partial
36	Kakembo et al., 2009	27.15653	-33.28940	Active
37	Keay-Bright & Boardman, 2009	27.14388	-33.24617	Active
38		24.55989	-31.67026	Active
39		24.55932	-31.70398	Active
40		Same as Boardman et al., 2003		
41		24.57329	-31.69169	Active

42	Boardman et al., 2010	24.57461	-31.70750	Partial
43	Mararakanye & Le Roux, 2012	Excluded: Entire South Africa		
44	Le Roux & Sumner, 2012	28.56804	-31.14369	Partial
45	Manjoro et al., 2012	Same as Kakembo et al., 2009		
46	Grellier et al., 2012	29.35933	-28.81063	Active
47	Grenfell et al., 2012	24.69691	-31.76056	Active
48		24.69147	-31.75677	Active
49	Mararakanye & Nethengwe, 2012	29.12813	-23.89722	Partial
50	Lyons et al., 2013	30.59531	-27.76757	Stable
51		30.59081	-27.77918	Stable
52		30.59513	-27.78721	Stable
53	Rowntree, 2013	Excluded: Regional, entire Karoo. No specific mention of gully, except Sneeuberg where Boardman et al., 2003 (and works thereafter) investigated gullies and badlands		
54	Olivier, 2013	18.75478	-33.28241	Partial
55	Boardman, 2014	Same as Boardman et al., 2003		
56	Boardman et al., 2015	Same as Keay-Bright & Boardman, 2009		
57	Mararakanye, 2015	30.92164	-26.08615	Partial
58		30.76604	-26.33253	Partial
59	Seutloali et al., 2016	28.30021	-31.85522	Active
60	Olivier et al., 2016	Same as Olivier, 2013		
61	Boardman et al., 2017	Same as Boardman et al., 2003		
62	Schmiedel et al., 2017	19.06550	-31.26012	Active
63	Mararakanye & Sumner, 2017	Same as Mararakanye, 2015		
64	Manjoro et al., 2017	Same as Kakembo et al., 2009		
65	Phinzi and Ngetar, 2017	28.81753	-30.76780	Active
66	Phinzi et al. 2020	29.44203	-30.74453	Active
67	Phinzi et al. 2020	29.43531	-30.74741	Acive
68	Phinzi et al. 2020	29.43870	-30.72633	Partial
69	Pulley et al., 2018	24.34657	-31.79155	Partial
70	Olivier et al., 2018	Same as Olivier, 2013		
71	Favis-Mortlock et al*., 2018*	Same as Keay-Bright & Boardman, 2009		
72	Makaya et al., 2019	29.06824	-28.74644	Active
73	Du Plessis et al., 2020	Same as Le Roux & Sumner, 2012		
74	Podwojewski et al., 2020	Same as Grellier et al., 2012		
75	Le Roux and De Waal, 2020	28.66412	-31.23373	Active
76	Le Roux et al., 2022	Same as Le Roux and De Waal, 2020		
77	Olivier et al., 2022	Same as Le Roux and De Waal, 2020		
78		20.60997	-33.68124	Active
79		28.47364	-31.19358	Partial
80		28.46648	-31.19113	Active
81		28.78835	-31.20160	Active
82	Omran et al., 2022	29.64460	-29.61714	Active

APPENDIX C: Accuracy dependency on scale factor.

	Scale factor						
	2	3	4	5	6	7	8
Correctly mapped as gully (in %)	83.2	85.3	90.3	85.4	86.6	87.2	87.2
Under estimation (in %)	16.8	14.7	9.7	14.6	13.4	12.8	12.8
Over estimation (in %)	12.2	11.9	11.5	11.2	11.3	11.7	11.6

APPENDIX D: Testing the sensitivity of gHAND for a small-scale gully with a north to south orientation by shifting the digitised gully headcut location; 2 m, 5 m, 10 m, and 20 m in the four cardinal directions: b) northerly direction, c) easterly direction, d) southerly direction, and e) westerly direction The accuracy statistics was calculated along the thalweg for a distance of 25 m from the digitised gully headcut to amplify distortion.

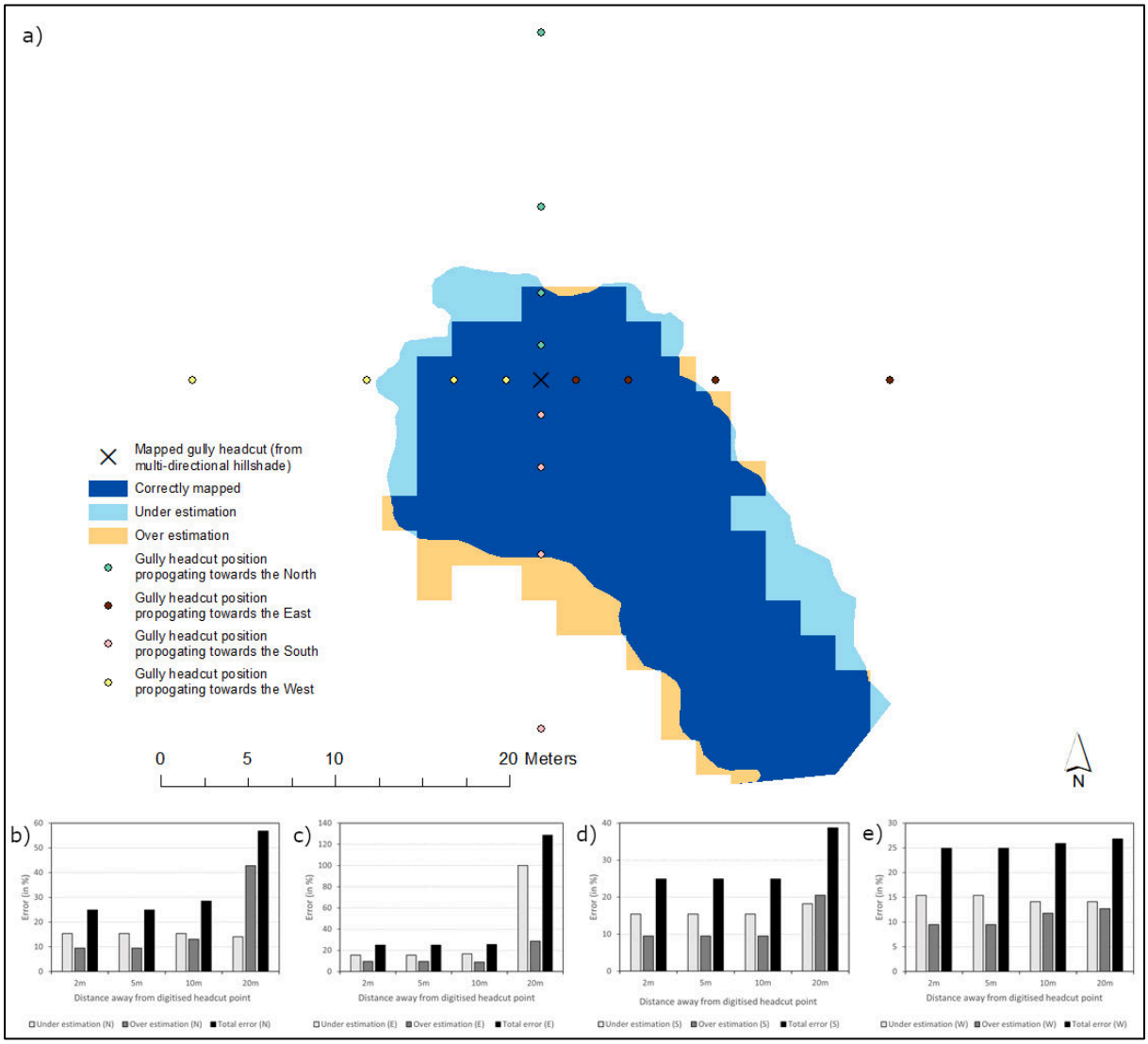

APPENDIX E: Sensitivity of gHAND to varying levels of gully tributary digitisation for a a) medium-scale gully, b) a large-scale gully, and the c) colossus-scale gully for the standard gHAND and d) edited gHAND.

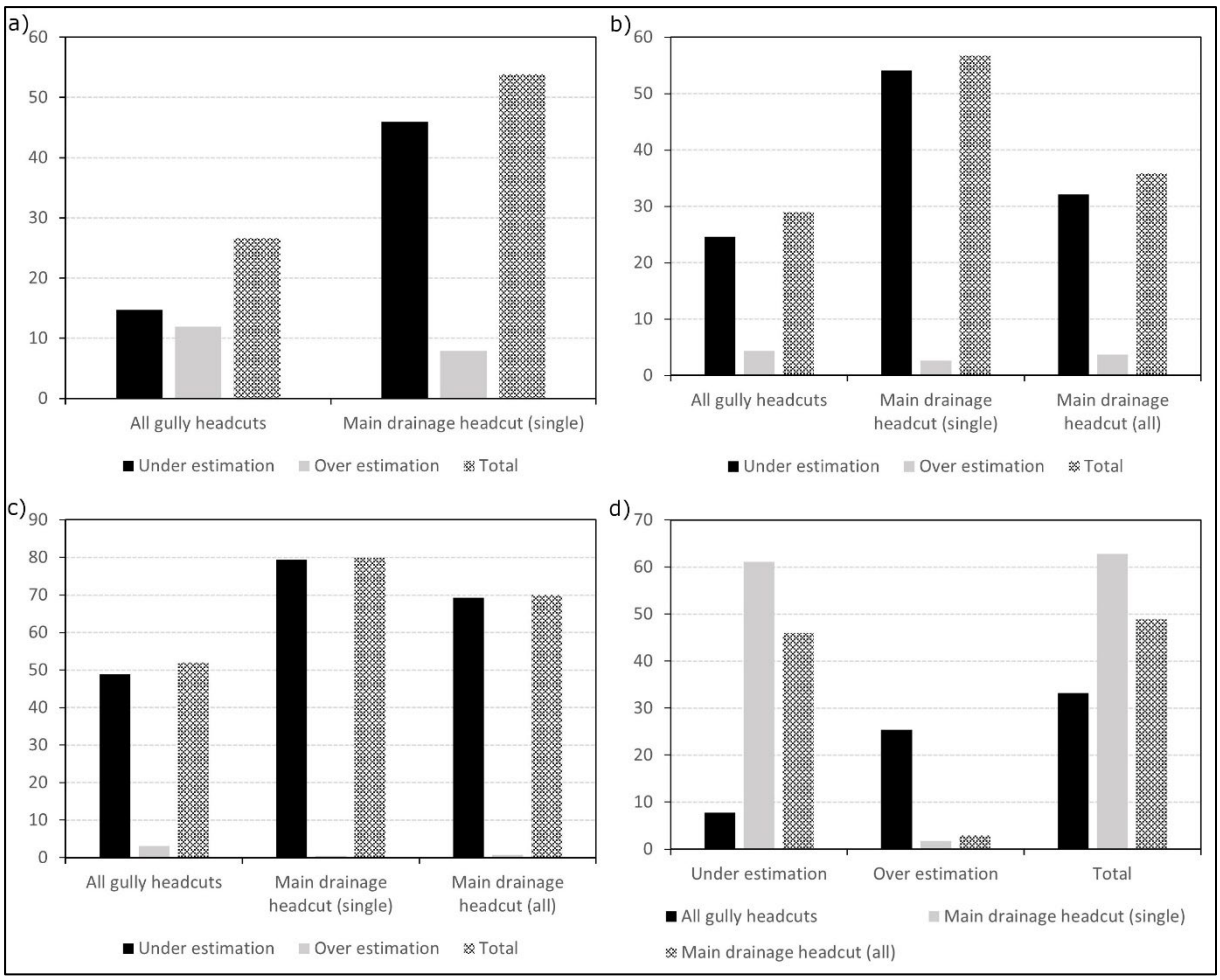

APPENDIX F

Coventry University

Certificate of Ethical Approval

Applicant:

George Olivier

Project Title:

Gully dynamics evolution under environment change pressures

This is to certify that the above named applicant has completed the Coventry University Ethical Approval process and their project has been confirmed and approved as Medium Risk

Date of approval:

24 January 2020

Project Reference Number:

P94729

Stellenbosch UNIVERSITY IYUNIVESITHI UNIVERSITEIT

forward together
sonke siya phambili
saam vorentoe

CONFIRMATION OF RESEARCH ETHICS APPROVAL

REC: SBER - Annual Progress Report

5 July 2023

Project number: 11763

Project Title: Gully dynamics evolution under environment change pressures

Dear Mr G Olivier

Identified supervisor(s) and/or co-investigator(s):

Dr WP De Clercq

Your REC: SBER - Annual Progress Report submitted on 12/06/2023 12:25 was reviewed and approved by the Social, Behavioural and Education Research Ethics Committee (REC: SBE).

This approval is only valid until the end of the protocol approval period:

Protocol approval date (Humanities)	Protocol expiration date (Humanities)
5 July 2023	4 July 2024

GENERAL COMMENTS PERTAINING TO THIS PROJECT:

INVESTIGATOR RESPONSIBILITIES

1. Please take note of the General Investigator Responsibilities attached to this letter.
2. Always use your project ID number (11763) in all correspondence with the REC: SBE concerning your project.
3. Please note that the REC has the prerogative to ask further questions, seek additional information, and monitor the conduct of your research and the consent process, where required.

List of documents approved by the REC: SBE:

Document Type	File Name	Date	Version
Informed Consent Form	G Olivier - e consent_FINAL	24/11/2019	Final
Research Protocol/Proposal	Proposal	10/10/2022	Final

If you have any questions or need further help, please contact the REC administrative officer, Mr Aden Williams at aden@sun.ac.za

Sincerely,

Mrs Clarissa Robertson (cgraham@sun.ac.za)

Secretariat: Social, Behavioral and Education Research Ethics Committee (REC: SBE)

APPENDIX G: Soil bulk densities used in South Africa.

T ha-1 y-1	Used for average	Authors
1.7 g cm^{-3}	1.7	Boardman and Foster, 2008
1.5-1.9 g cm^{-3} (1.7 used)	1.7	Keay-Bright & Boardman, 2009
1.35 g cm^{-3}	1.35	Chaplot et al., 2011
1.4 g cm^{-3}	1.4	Grellier et al., 2012
0.92 - 1.55 g cm^{-3}	1.23	Chaplot, 2013
1.7 g cm^{-3}	1.7	Boardman et al., 2015
1.7 g cm^{-3}	1.7	Boardman et al., 2017
1.5 g cm^{-3}	1.5	Schmiedel et al., 2017
1.2 g cm^{-3}	1.3	Flügel et al., 2003
1.6 Mg m^{-3}	1.6	Le Roux, 2018
AVERAGE	**1.5**	

APPENDIX H: Interview structure and foundation of questions posed for semi-structured interview and gully walk.

INTERVIE-W GUIDELINE

Gully dynamics evolution under environment change pressures. Although the guide is divided into 2 parts, the sequence needs to be adapted to best suit the local participants. If no gully walk or participatory mapping are possible, try and introduce some of the prompts of Part 1 into Part 2.

Part 1: Gully walk (Participatory mapping and discussion)

This discussion guide provides short questions that should be incorporated into discussion during the participatory mapping exercise. Questions should be selected to enable a naturally flowing discussion. An indication is given when description from answers should be mapped (MAP) – the MAP questions should be repeated at each gully site that is visited.

Background basics/ *Follow-up probes*:

Can you please tell me your name, surname, age, and how long you have been on the land (whether farming, as a ranger, or herder, etc.)?

Can you tell me about the history of the farm, national park, land, property?

Is it a family farm?

How many generations?

How long has it been a national park?

How large is the farm, national park, land, property?

What do you currently farm with?

Have you always farmed with this?

Why did you change?

What did you previously farm with?

What did previous family members/ owners farm with?

Do you share the land with other famers?

What was the land used for before it became a national park?

Do you have any problems with erosion?

I selected this gully which I would like to discuss further during a walk to find out more regarding activity, age, and mitigation.

Are there any other gullies of concern, and if so would you like to go there to discuss and map it as well?

Erosion specific questions at the site/ *Follow-up probes*:

What problems does this erosion feature cause on a day-to-day basis?

Have you tried to control erosion here – MAP

How?

Has it been successful?

Has this gully channel always been here?

Can you remember any changes? – MAP

What changes?

Are these changes mostly rapid or slow?

Did it grow larger?

How did it grow?

Can you remember any events that caused sudden growth?

Can we try to create an historical map relating to some of these events – where was the boundary before and after these events?

Can you remember any past boundaries with approximate dates?

Do you have any concerns about areas next to the gully that might start to erode? – MAP (try to classify prone areas from 1-3; 3 being most prone and 1 least).

Which specific areas do you think is prone to further erosion?

Are any of these areas you indicated more sensitive to erosion than others?

Why do you think it is prone to erosion?

What do you think is causing the erosion now?

What do you think caused the erosion in the past?

Do you have any dams close to the erosion feature? – MAP

Have you experienced any negative effects such as siltation, etc. at the dam?

Do you think this gully caused any negative effects?

Did it influence soil?

Is there less vegetation?

Part 2: Semi-structured interview

Follow-up on any themes that is deemed necessary after the completion of the participatory mapping exercise.

Themes	Questions/ *Follow-up probes*
Background	Has there been a change in the intensity of farming methods? - *When?* - *Why?* - *Has there been a loss in productivity?* - *What fallow/ resting periods do you allow?* What type of tillage methods do you employ?
Evolution	Do you think these gullies are still active? - *What evidence do you see that suggests that it is active/ inactive?* - ***If ACTIVE*** - *Is it growing?* - *How is it growing?* - *At what tempo is change occurring?* - *Can you remember gullies being stable or less active in the past?* - ***If INACTIVE*** - *When did it stabilise?* - *Can you remember active gully erosion in the past?*
Impact	How does gully erosion influence your daily tasks? How has gully erosion effected your farm, national park, land, property?

	- *Has soil quality become poorer?* - *Has there been a reduction in vegetation?* - *Is the water holding capacity of your dam becoming less?* - Is river quality become poorer? Has gully erosion had any negative effect on productivity?
Driving factors	Where does gully erosion occur on your farm, national park, land, property? - *Do gullies occur in similar areas?* - *Can you describe the different areas where gully erosion occurs?* Why do you think gully erosion occurs in these areas? - *Is it a natural process?* - *Is it human-induced?* - *Does it have to do with environmental elements such as slope, rainfall?* We mentioned the speed of gully erosion earlier. Have you experienced any significant changes in the speed of gully erosion? - *Can you associate these changes in tempo with any specific events?* Have you observed any rainfall patterns particularly affecting gully erosion? - *How?* - *Have you observed differing erosion rates with different rainfall intensities?*

	- *Have you observed differing erosion rates with different quantities of continuous daily rainfall?* Provide climate change estimates for the region. Do you think climate change will impact gully erosion? - *How?* Have you witnessed a change in gully erosion with the introduction of new farming techniques/ technologies? - *Why do you think this occurred?* Have you witnessed a change in gully erosion with the change in crop/ stock? - *Why do you think this occurred?* Have you witnessed a change in gully erosion with the change from farming to national park? - *Why do you think this occurred?*
Rehabilitation	Gullies occupy a small part of the landscape. Do you think it is necessary to rehabilitate or control gully erosion? - *Why?* Have you employed any methods to control gully erosion? - *How effective was your control measures?* - *Any lessons learned from your experience?* Are there any rehabilitation or control measures that you would not deem acceptable, for example, earthworks, fencing off areas, increasing fallow periods, change tillage, reduce stock, etc.?

	- *Why?*
Knowledge	How does s/he know what s/he knows? E.g., observation, 'passed down' knowledge/ storytelling, exchange with other farmers, specialist/expert advice/ journals/ government programmes?
Cost	Can you provide an estimate of cost, time and monetary, directly caused by gully erosion?

That concludes the interview that I wanted to conduct. Is there anything else you would like to add?

Note and respond to any additions.

Thank you very much for taking the time to conduct this interview. I think it was very valuable, providing an excellent dimension to understanding the soil erosion problem in South Africa. Would you be interested in receiving any information regarding results and findings? If so, which format would be most suitable.

Note response and indicate whether the participant would like to receive further information regarding the research.

APPENDIX I: Equivalent area used for volume measurements and the area: volume ratio used to calculate historical volumes.

Placename	Total gully area (in m^2	Area used for volume measurements (in m^2)	Volume (in m^3)	Volume area ratio
Bergpad	2365.3	2365.3	1652.8	0.7
Bumpy Track	3750.2	3495.2	3720.9	1.1
Skietdam	3243.0	2959.9	1577.4	0.5
Rooiflip	32532.5	2912.9	3383.0	1.2
Humpsback	11743.0	8937.4	6457.8	0.7
Sakhu	18286.4	1571.4	8776.2	5.6
Trickle Main W	30346.8	18693.6	48415.5	2.6
Trickle Main E	4959.2	4140.9	6527.6	1.6
Contour game NS	8394.1	7042.5	17385.9	2.5
Contour game E-W	3039.3	2046.3	1436.7	0.7
Mushroom NS	1022.1	1022.1	2286.8	2.2
Mushroom E-W	3175.0	3088.4	4561.4	1.5
Golden 2	83286.2	27949.4	72596.1	2.6
Golden 1W	7653.5	-	-	-
Golden 1E	22608.4	17085.0	41534.4	2.4
Makgo W	162.1	160.4	53.4	0.3
Makgo E	897.1	861.6	140.8	0.2
BushW N	86.3	86.3	16.2	0.2
BushW S	20.9	29.9	5.3	0.3